

Recognition in the Domain of Molecular Chirality: from Noncovalent Interactions to Separation of Enantiomers

Paola Peluso,^a Bezhan Chankvetadze^{b*}

^a *Istituto di Chimica Biomolecolare ICB, CNR, Sede secondaria di Sassari, Traversa La Crucca 3, Regione Balduca, Li Punti, I-07100 Sassari, Italy*

^b *Institute of Physical and Analytical Chemistry, School of Exact and Natural Sciences, Tbilisi State University, Chavchavadze Ave 3, 0179 Tbilisi, Georgia*

* Email: jpba_bezhan@yahoo.com; bezhan.chankvetadze@tsu.ge

ABSTRACT: It is not a coincidence that both chirality and noncovalent interactions are ubiquitous in nature and man-made molecular systems. Noncovalent interactivity between chiral molecules underlies enantioselective recognition as a fundamental phenomenon regulating life and human activities. Thus, noncovalent interactions represent the narrative thread of a fascinating story which goes across several disciplines of medical, chemical, physical, biological and other natural sciences. This review has been conceived with the awareness that a modern attitude to molecular chirality and its consequences needs to be founded on multidisciplinary approaches to disclose the molecular bases of essential enantioselective phenomena in the domain of chemical, physical, and life sciences. With the primary aim of discussing this topic in an integrating way, a comprehensive pool of rational and systematic multidisciplinary information is provided, which concerns fundamentals of chirality, description of noncovalent interactions and their implications in enantioselective processes occurring in different contexts. A specific focus is devoted to enantioselection in chromatography and electromigration techniques due to their unique feature as “multistep” processes. A second motivation for writing this review is to make a clear statement about the state of the art, the tools we have at disposal, and what is still missing to fully understand mechanisms underlying enantioselective recognition.

CONTENTS

1.	Introduction	4
2.	Chirality and chiral entities	8
2.1	A historical overview	8
2.2	The language of molecular chirality and stereochemistry	18
2.3	Chiral elements and stereochemical descriptors	25
3.	Noncovalent interactions: history, features, and trends	30
3.1	From chemical bond to chemical bonding: a unifying view	32
3.2	Classification of noncovalent interactions: limitations and current proposals	34
3.3	A historical overview: from van der Waals description to current theory	44
3.3.1	Dispersive forces	45
3.3.2	Hydrophobic effect	47
3.3.3	From hydrogen bond to σ - and π -hole interactions	48
3.4	Molecular modelling and experiments: a synergistic and necessary interplay	57
3.4.1	Van der Waals radius	59
3.4.2	Methods, functionals and basis sets	63
3.4.3	Computational energetic measures	66
3.4.4	Computational treatment of large systems	73
3.4.5	Accuracy of calculations and uncertainty quantification	77
3.4.6	Experimental techniques and strategies for exploring noncovalent forces	79
4.	Trends in enantioselective recognition in natural and man-made systems	86
4.1	Intramolecular noncovalent interactions in enantioselective recognition	93
4.2	Biological enantioselective recognition	99
4.2.1	Enantioselective drug action	99
4.2.2	Enantioselective transformations in nature	105
4.3	Enantioselective recognition in classical asymmetric synthesis	109
4.3.1	Enzyme-based enantioselective processes	109
4.3.2	Enantioselective metal-based catalysis and organocatalysis	117
4.4	Enantioselective recognition in separation science: non-chromatographic methods	127
4.4.1	Enantioselective adsorption and permeation	127
4.4.2	Crystallization	136
4.5	Enantioselective recognition in chemical sensing	142

4.5.1	Enantioselective sensing	142
4.5.2	Chiral analysis by NMR spectroscopy	146
4.6	Induced conformational chirality	150
4.7	Symmetry-breaking and absolute asymmetric synthesis	155
5.	Trends in enantioselective recognition in separation science:	
	chromatographic methods	159
5.1	Major instrumental techniques applied to separation of enantiomers	159
5.1.1	Gas chromatography	162
5.1.2	High-performance liquid chromatography	169
5.1.2.1	Chiral stationary phases	170
5.1.2.2	Mobile phases	187
5.1.3	Supercritical fluid chromatography	197
5.1.4	Capillary electrophoresis	199
5.1.4.1	Capillary electrophoresis vs. pressure-driven techniques	200
5.1.4.2	Advantages and disadvantages of CEKC for studying enantioselective intermolecular recognition	204
5.1.4.3	Chiral selectors in capillary electrokinetic chromatography	205
5.1.5	Capillary electrochromatography	209
5.2	Enantiorecognition mechanisms	212
5.2.1	Profiling noncovalent interactions and enantiorecognition models	212
5.2.1.1	Nuclear magnetic resonance studies	213
5.2.1.2	Other experimental techniques	225
5.2.1.3	Adsorption studies on selector-selectand interactions	231
5.2.1.4	Computation-based modelling of enantioseparation processes and selector-selectand interactions	237
5.2.2	Thermodynamics of enantioseparation processes	251
6.	Concluding remarks	259
	Acronyms and abbreviations	261
	References	266
	Author Information, Biographies, Graphical Abstract	383

1. Introduction

Chirality is an important property of nature, producing and regulating fundamental phenomena in living matter.^{1,2} Over time molecular chirality and related concepts such as symmetry, asymmetry, handedness, symmetry breaking, parity violation, and enantio recognition have had a growing impact on science, going beyond the boundaries of chemistry, and with crucial implications in life sciences, agriculture, food and environmental sciences, materials sciences, and several other fields.³⁻⁵ In our world, asymmetry has been found from the nuclear level to the level of living beings.⁶ Circularly polarized light has been found in Orion Nebula, also showing the existence of asymmetry at astronomical level.^{6,7} Some questions such as asymmetry at atomic and sub-atomic scales,^{8,9} the origins of biomolecular asymmetry,^{1,10} and the search for asymmetry as a signature of extraterrestrial life in our solar system¹¹ are still open, and matter of animated scientific, philosophical, epistemic, and semantic discussions.¹²⁻¹⁹

As commented by Cintas, the term chirality summarizes a long pathway initiated not by scientists pragmatically but by philosophers, mathematicians, and artists, who speculated on mirrors and their effects, wondering about the reality of inaccessible universes.²⁰ The word chirality is derived from the Greek $\chi\epsilon\iota\rho$ (hand), and the first observations of humans, which may be considered a rough approach to the awareness of the concept of chirality, were related to handedness.²¹ Hand dominance is a tendency to use one hand rather than the other for certain activities that require the use of only one hand. Human hands are architecturally symmetrical, but they are not superimposable, one hand being the mirror-image of the other hand (Figure 1). Consequently, humans tend to perform various manual activities more frequently with one hand rather than the other. Plato, a right-hander, said that the dominance of hand skills was learned, while left-handed Aristotle in *Metaphysics* claimed that people were naturally right-handed or left-handed.²²

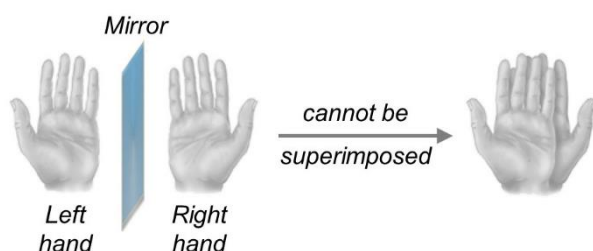


Figure 1. A left hand and a right hand as mirror-images.

In the second half of the 18th century, in the frame of a philosophical discussion about the nature of space,^{23,24} Immanuel Kant wrote that “*sie können nicht kongruieren*” (they are not congruent),²⁵ and called hands *incongruent counterparts*, referring to the property of handedness.²⁴

In the mid of 19th century, Pasteur observed the spontaneous resolution of racemic sodium ammonium tartrate tetrahydrate into enantiomorphous crystals. He separated the two types of crystals

by picking the different crystals apart with a tweezer,²⁶ as a matter of fact achieving the first enantioseparation process manually. Moreover, he reported that the *dextro* form of ammonium tartrate was faster destroyed by the mold *Penicillium glaucum* than the *levo* isomer.^{27,28} This observation led Pasteur to the recognition of the role stereochemistry plays in the basic mechanisms of life, generating a fundamental relationship between molecular chirality and living matter. Particularly, life is essentially constructed using L-amino acids as building blocks and, consequently, it is governed by *homochirality*. On this basis, it appears evident that chiral molecules recognize other chiral molecules through suitable mechanisms, recognition being not a mere binding but a binding with a purpose, as declared by Lehn in his Nobel lecture.²⁹

How a homochiral preference occurred in the primordial era, namely the origin of biomolecular homochirality,³⁰⁻³⁵ remains a challenging question, but with a huge scientific, cultural, and economic impact on science and society, being strictly related to the capability of science to manage chirality, its potential and consequences at different length scales.

The spatial array of atoms in a molecule may be as important as the chemical nature of the atoms themselves. This feature determines the key role of molecular chirality. A basic glossary,^{36,37} which is useful to introduce the language of molecular chirality, highlights as chemists coined specific words to distinguish and identify different types of spatial arrays, their chemo-physical properties and consequences in chemical and biochemical sciences. *Isomers* (from the Greek: ἴσος, meaning equal, same, and μέρος, meaning part) are chemical species that have the same number and kind of atoms but differ in physical and/or chemical properties due to a difference in structure in terms of constitution, configuration and/or conformation. *Constitution* describes the nature of the atoms and their connectivity in a molecule. *Conformation* and *configuration* define the spatial array of atoms in a molecule. Conformation refers to the spatial array of atoms in molecules of given constitution and configuration, which can be changed by rotation around single bonds. Differently, configuration refers to the spatial array that define *stereoisomers*, namely isomers of identical constitution but differing in the arrangement of their atoms in space, disregarding any conformational variation. One of the two molecular species that are mirror images of each other, and not superimposable, is defined as *enantiomer*,³⁸ whereas *racemate* is a solid, liquid, gaseous, or in solution composite of equimolar quantities of two enantiomeric species. Diastereoisomers are stereoisomers not related as mirror-images, differing in chemical and physical properties. The *absolute configuration* describes the spatial arrangement of the atoms in a chiral molecule by using either stereochemical descriptors (such as *R* and *S*, *L* and *D*, *P* and *M*, Δ and Λ) or cartesian coordinates in order to distinguish a given array from its mirror-image.

At molecular level, the enantiomeric forms of a chiral compound possess the same chemo-physical properties, therefore the preparation of a single enantiomer by synthetic and resolution procedures still remains rather challenging. In general, two major approaches can be used to obtain pure enantiomers or enantiomerically enriched mixtures, namely enantioselective asymmetric synthesis to obtain preferentially one enantiomer³⁹⁻⁴¹ or the resolution of a racemic mixture.^{42,43} In all cases, the induction of enantiomer imbalance at both synthetic and resolution levels requires the presence of a chiral environment which may be produced by a chiral auxiliary, catalyst, selector or medium. As a consequence of advances in stereoselective synthesis and enantioselective chromatography, in the 1990s drug-regulatory authorities began to recognize the importance of molecular chirality in drug action. Thalidomide story is the most tragic reminder of the importance of chirality for humanity. Indeed, left-handed thalidomide is pharmacologically active as a powerful tranquilizer, while the right-handed enantiomer proved to disrupt fetal development causing phocomelia and other congenital malformations. In the early 1960s, both enantiomers were present in the manufactured drug, with catastrophic consequences.⁴⁴

Even if a number of stereoselective synthetic processes have been applied to the production of enantiomerically pure chiral compounds, so far few have proven to be suitable for large-scale production.⁴⁵⁻⁴⁸ Consequently, separation-based techniques continue to be widely used by analytical, pharmaceutical, supramolecular, clinical and synthetic organic chemists in their daily practice.^{45,49-52} Given this context and the importance of chirality, scientists have spent research efforts not only for developing methods to separate enantiomers, but also for comprehending the mechanisms which govern the enantio-recognition processes.⁵³⁻⁵⁹

Atoms and molecules may associate (*binding*) and recognize (*recognition*) themselves through intra- and intermolecular noncovalent interactions.^{29,60} The structural features of the interacting parts and the properties of the medium determine the effect of the mutual perturbation occurring between two molecular species and, consequently, the properties of the resulting noncovalent interaction. On this basis, different types of noncovalent forces have been identified over time, namely ionic interactions, hydrogen bonding (HB), σ - and π -hole bonds, π - π stacking, anion- and cation- π , dipole-dipole, hydrophobic, steric repulsive, and van der Waals (vdW) interactions. . Noncovalent interactions proved to originate and regulate formation, properties, functions and applications of supramolecular complexes, assemblies and clusters in gas, liquid and solid phase, allowing for various applications in the field of supramolecular chemistry. . In the last decades, huge progresses in the comprehension^{61,62} and measurement of noncovalent interactions^{63,64} have allowed for achieving a deeper knowledge of nature and functions noncovalent interactions have. Significant advancements in crystal engineering,⁶⁵ analytical methods^{63,64} and computational chemistry^{61,66-68}

have contributed to disclose the importance of noncovalent forces in chemistry, physics, and biology. As a result, the International Union of Pure and Applied Chemistry (IUPAC) issued focused recommendations on HB,⁶⁹ halogen (XB),⁷⁰ and chalcogen (ChB)⁷¹ bonds. More recent advancements in this field have allowed science to deeply revise the cartography of noncovalent interactions, identifying new types of noncovalent contacts such as icosagen, triel, tetrel, pnictogen, aerogen, spondium and π -hole bonds.⁷²⁻⁷⁴

In enantioselective recognition, intermolecular noncovalent interactions can be considered as the Pasteur's tweezers that nature uses to let enantioselective recognition to occur at molecular level, representing the basis for enantioselective drug action (including absorption, transport and distribution in the living body, metabolism, pharmacokinetics, pharmacodynamics and excretion),^{75,76} enantioselective homogenous and heterogenous catalysis,⁷⁷⁻⁷⁹ enantioselective transformation of chiral agrochemicals, pharmaceuticals and other compounds in nature (soil and aquatic systems),⁸⁰ enantioselective sensing,^{81,82} diastereomeric crystallization,^{83,84} enzymatic catalytic transformation and resolution,⁸⁵ and all enantioseparation techniques.⁵⁴⁻⁵⁹ In other words, noncovalent interactions underlie all enantioselective recognition processes occurring at molecular level, representing a unifying *fil rouge* which goes across several disciplines of chemical, physical, biological, medical, and other natural sciences.

In particular, in enantioseparation science, noncovalent interactions constitute the basic tools of the process by which chiral *selector* (CS) (the agent which discriminates between two enantiomers of a chiral compound) and *selectand* (each enantiomer which is recognized) interact with each other to result the enantiomer distinction and physical separation.^{53,54,56,59} Exerting this function, noncovalent interactions also underlie sensing of diastereotopic signals through spectroscopic techniques such as nuclear magnetic resonance (NMR) spectroscopy. It is interesting to note that, often, the development of enantioseparation science occurred parallel to the advancements in understanding enantioselective recognition mechanisms of biological processes. For instance, in keeping with the pioneering works of Fischer,⁸⁶ and Easson and Stedman on biological enantioselectivity,⁸⁷ Dalgliesh invoked the three-point interaction to explain the enantioselective separation of amino acids achieved by chromatography on cellulose paper.⁸⁸

The organization of this review reflects the awareness of chemists that a modern attitude to molecular chirality and its consequences needs to be founded on multidisciplinary approaches to disclose the molecular bases of important phenomena in the domain of chemical, physical, and life sciences. With the primary aim of stimulating the interest of the reader and inducing applications of novel methodologies and approaches, a comprehensive pool of rational and systematic multidisciplinary information is organized as follows: *a*) fundamentals of chirality focusing on the

development of the concept over time, terminology, conventions and descriptors used to represent this property and its molecular consequences (section 2); *b*) description of noncovalent interactions, current classifications, and theoretical and experimental tools available for their understanding and profiling (section 3); *c*) implications of noncovalent interactions in enantioselective processes occurring in different contexts (section 4), discussing this topic in an integrating way; *d*) owing to the recognized importance of the chromatographic technology for analysis and production of enantiomerically enriched and pure chiral compounds, section 5 focuses on the main chromatographic and electromigration techniques available to separate enantiomers, on related enantioselective mechanisms, and on function of noncovalent interactions in this field.

Regrettably, benchmark procedures and focused guidelines for computational treatment of enantioselection at molecular level are still missing, the roots of this shortcoming originating, likely, either from the fact that nature, treatment, and quantification of noncovalent interactions themselves continues to be matter of animated and stimulating discussions, and from the limited number of experimental data, available for large systems, to be used as benchmark to check the accuracy of calculations. In this regard, a second aim of this review is to define the state of the art, current advancement, limits and flaws of the tools we have at disposal to fully understand mechanisms underlying enantioselective recognition.

2. Chirality and chiral entities

2.1 A historical overview

The historical roots of molecular chirality dates back to the mid of 19th century, when Pasteur's studies on molecular dissymmetry and biological enantioselectivity laid the bases for the development of the chemistry of chiral compounds.^{20,25,89,90} At that time, the only known physical phenomenon to explore molecular structure was optical activity. In 1847, Pasteur begun his studies on crystallography and optical activity of the natural tartaric acid and related molecules. In the course of this work, he developed the concept of molecular chirality, even if he never used the terms chirality and chiral in his reports.⁹¹ Although the molecular structure of tartaric acid was unknown at that time, natural tartaric acid was recognized as optically active and dextrorotatory in solution. Observing the crystals of tartaric acid, Pasteur noted that its salts showed small surfaces called *hemihedral facets* as modifications of some edges of the crystals.^{92,93} These facets reduced the symmetry of the fundamental crystal form producing a non-symmetrical external morphology. Actually, the phenomenon of hemihedrism had been already observed in quartz crystals by the French mineralogist Haüy in 1801.⁹⁴ While *holohedral crystals* had high symmetry (for instance, the external morphology of many α -quartz crystals is a symmetrical hexagonal prism belonging to the symmetry point group

D_{6h}) (Figure 2),⁹⁵ in *hemihedral crystals* Haüy observed additional facets degrading its symmetry. Such crystals could exist as right- and left-handed non-superimposable forms (Figure 3).

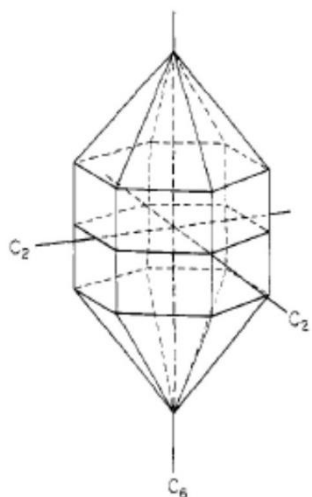


Figure 2. Holohedral hexagonal quartz crystal, symmetry point group D_{6h} . Reproduced with permission from ref. 95. Copyright 1980 American Chemical Society.

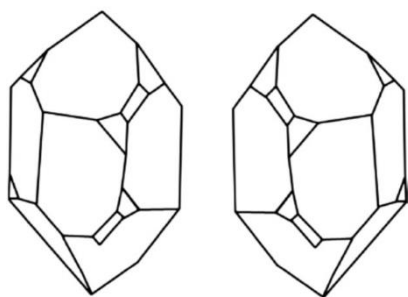


Figure 3. Hemihedral crystals of α -quartz.

Pasteur also studied a second compound, *paratartaric acid* or *racemic acid* (in current nomenclature, it is called racemic tartaric acid) (Figure 4), and some of its salts. This compound had the same elemental composition, chemical and physical properties as natural tartaric acid, whereas it did not show optical rotation. This acid was defined and considered a structural isomer of the natural tartaric acid.

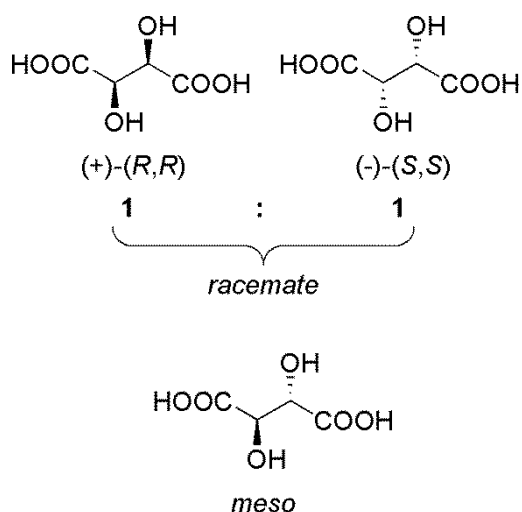


Figure 4. The stereoisomeric forms of 2,3-dihydroxybutanedioic acid (tartaric acid).

As Pasteur examined crystals of sodium ammonium paratartrate, he identified two distinct crystal types which were present in a 1:1 ratio.²⁶ Although he defined these crystal forms simply “dissymmetric”, as a matter of fact he observed crystals as not superimposable mirror-image (enantiomorphous) forms of each other (Figure 5). Carrying out a rough enantioseparation process at macroscopic level, Pasteur separated the two different forms of the sodium ammonium paratartrate crystals by using tweezers, finding that both substances were optically active in solution, with observed rotations featured by almost equal absolute magnitude and opposite direction. Pasteur then obtained the two free acids observing for these forms the same features of the paratartrate salts in terms of optical rotation. Indeed, one of the form was dextrorotatory, and identical to natural (+)-tartaric acid, whereas the other form was levorotatory, again with optical rotation almost equal in absolute magnitude and opposite in direction. These observations led Pasteur to conclude that the molecules of these acids were dissymmetric, a term he likely used with the meaning of chiral, and that paratartronic acid was a 1:1 mixture of the two forms.

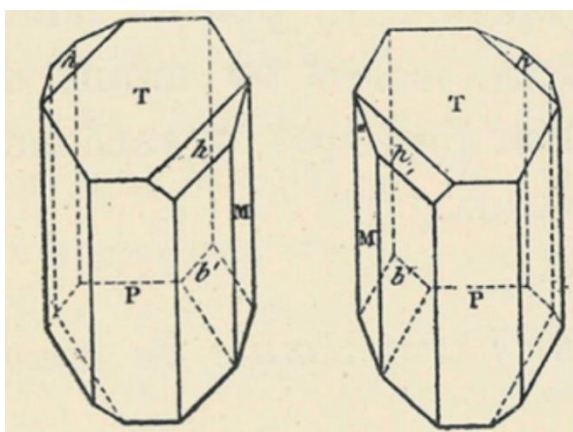


Figure 5. Sodium ammonium paratartrate enantiomorphous crystals. Reproduced with permission from ref. 91. Copyright 2019 John Wiley & Sons.

Over time, biography and scientific activity of Pasteur have been the object of several reviews and commentaries which have also analyzed the genesis of his seminal work.^{91,96-103} It is worth noting that only a small minority of racemates provides conglomerate crystallization, crystallizing as mirror-image crystals, each formed by only one enantiomer. On this basis, Gal has recently observed that Pasteur had the good fortune that sodium ammonium paratartrate is just one of the molecules that provide conglomerate crystallization.¹⁰² On the other hand, although tartrates had been studied by other scientists, molecular chirality was not discovered. In this regard, Pasteur himself stated in a lecture at the University of Lille in 1854, “*Dans les champs de l’observation le hasard ne favorise que les esprits préparés* (In the fields of observation chance favors only the prepared mind)”.

However, it is definitely true that, historically, the bases of stereochemistry lie on the discovery of plane-polarized light and, as mentioned above, on the observation of hemihedrism of crystals.¹⁰⁴ On the other hand, the roots of the discovery of molecular chirality itself were laid in early 19th century when, in particular in France, exceptional advancements of crystallography, optics, and chemistry paved the way to a new attitude toward the study of molecules and their properties.²⁵ In 1808, the French physicist Malus discovered polarized light,¹⁰⁵ and in 1811 Arago discovered optical rotation by analyzing slices of hemihedral quartz crystals.¹⁰⁶ Paratartaric acid had been discovered in 1819. Despite the fact that it was thought as isomeric with tartaric acid, the nature of this relationship was not understood at the time.¹⁰² In the 1820s, Herschel suggested that molecular asymmetry was the cause of optical rotation in solution.¹⁰⁰ However, more than others, Biot carried out an important and pioneering work in the field of optical activity. In his first studies in 1812, he followed the observations of Arago, discovering that a quartz plate, cut at right angles to its crystal axis, rotates the plane of polarized light through an angle proportional to the thickness of the plate.¹⁰⁷ Later, over a period of several decades, he observed that other natural compounds such as sucrose, oil of turpentine, camphor, and tartaric acid, rotated polarized light in solution, either in the liquid or gas phase.¹⁰⁸⁻¹¹⁰ Biot recognized that optical rotation produced by quartz is a property of the crystal, observed only in the solid state and dependent on the direction in which the crystal is viewed. Meanwhile, he noticed that in organic substances optical rotation was a property of the individual molecules, therefore observed in solid, liquid, and gas phase, and in solution. However, Biot missed either the conglomerate crystallization of sodium ammonium paratartrate, and hemihedrism and dissymmetry in the crystals of the tartaric acid/paratartaric acid-related substances. de la Provostaye investigated the crystals of natural tartaric acid, paratartaric acid, and several of their salts,¹¹¹ but he did not report the chirality of tartrate crystals. Hankel also studied the crystals of tartrates,¹¹² but without any comment on their chirality. Interestingly, in 1844 the crystallographer Mitscherlich had observed that the sodium ammonium (+)-tartrate was optically active, whereas the paratartrate was

not, even if the two species were identical in chemical composition, crystalline form, and other physical properties.¹¹³ However, also in this case the conglomerate composition of sodium ammonium paratartrate and the stereochemical relationship between its crystals were not recognized. Pasteur apparently knew this literature which, likely, had a key role to discover molecular chirality⁹² and, perhaps for this reason, some criticism has been moved to his work.¹⁰³ On the other hand, Pasteur deduced that molecular chirality could be the result of a specific three-dimensional arrangement of the atoms within the molecules.¹¹⁴ Later, the tetrahedral asymmetric carbon atom, which is the first explanation for molecular chirality, emerged in 1874 with the studies of Van't Hoff¹¹⁵ and Le Bel,¹¹⁶ twenty five years after the publication of Pasteur's observation on sodium ammonium paratartrate crystals.

Following the first studies on tartaric acid, Pasteur also recognized and discovered *a*) the thermal interconversion of the tartaric acid enantiomers, *b*) the *meso*-form of tartaric acid, relating its optical inactivity to its inherent achiral molecular structure (Pasteur referred to *meso*-tartaric acid as *inactive tartaric acid*) (Figure 4), *c*) chiral diastereoisomerism,¹¹⁷ *d*) the resolution of racemates via diastereomeric crystallization, and *e*) importantly, that molecular chirality was a sign of life.¹¹⁷

After the isolation of both enantiomers of tartaric acid by Pasteur, in 1851 Chautard isolated (–)-camphor from a natural source, and consequently found the second example of known enantiomer pair,¹¹⁸ the (+)-camphor being known at that time.

In 1857, Pasteur discovered *biological enantioselectivity* when he examined the microbial metabolism of racemic tartaric acid.^{27,119,120} In disagreement with Liebig's theory of fermentation,^{121,122} Pasteur's explanation¹²⁰ for the observed enantioselectivity in the tartrate fermentation laid the conceptual bases for all enantiorecognition models developed later. Indeed, he hypothesized that microorganism contained optically active compounds, as constituents, which were involved in the utilization of the tartrate molecules as nutrients. On this basis, Pasteur introduced the basic principle that two enantiomers can interact differently with a third chiral molecule. Indeed, he noticed that the optically active constituent of the microorganism does not relate equally well to (+)- and (–)-tartrate molecules. As a matter of fact, this was the first enunciation of that principle which remains the basis of enantioselectivity, perhaps envisaging that the relationship which we today call diastereomerism is the key requirement for enantiorecognition.

After the studies of Pasteur, two general questions were tackled by scientists: *a*) stereoselectivity in enzymatic reactions and metabolic processes, and enzyme-catalyzed transformations of molecules, and *b*) stereoselectivity in the physiological, pharmacological, or toxicological activity of chiral compounds.¹⁰¹

Emil Fischer demonstrated that the microbial fermentation and other enzymatic reactions of sugars displayed considerable stereoselectivity, observing both diastereoselectivity and enantioselectivity in the action of enzymes on sugars.^{86,123} In his studies, he demonstrated that natural sugars such as glucose, fructose, and galactose were readily fermented by yeast, whereas their “*optical antipodes*” remained unchanged. Concerning diastereoselectivity, he observed that invertin hydrolyzed α -methyl-D-glucoside but not its epimer β -methyl-D-glucoside, whereas emulsin hydrolyzed β -methyl-D-glucoside but not α -methyl-D-glucoside.⁸⁶ Importantly, Fischer also noticed that fermentation originated from the action of enzymes within microorganisms. Thus, his studies on the stereoselectivity of enzyme action allowed him to propose the *lock-and-key model*,⁸⁶ emphasizing that the process depended on the geometric complementarity between enzyme and substrate.

In 1886, Piutti reported for the first time on the *enantioselectivity at biological receptors*, discovering D-asparagine and observing that this enantiomer tasted intensively sweet, whereas the known L-asparagine had no taste.^{124,125} Actually, the receptor concept was introduced later, in the 20th century, independently by Ehrlich¹²⁶ and Langley.¹²⁷

Cushny gave an important contribution to the fields of enantioselectivity in pharmacology and biology with his studies of enzyme action. In particular, he reported the first unambiguous example of enantioselectivity in a pharmacological process, demonstrating that (–)-hyoscyamine was more potent than the (+)-enantiomer against the mydriasis in the cat, and salivary secretion in the dog, whereas (+)-hyoscyamine was the more potent enantiomer in central nervous system (CNS)-excitatory effects.¹²⁸ Cushny also observed for the enantiomers of epinephrine (Figure 6) different ability to increase blood pressure, the (–)-(R)-form being more potent than (+)-(S)-epinephrine.¹²⁹

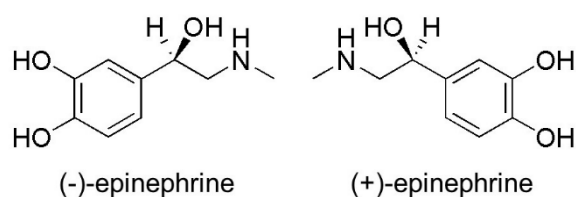


Figure 6. Structures of epinephrine enantiomers.

Following these first studies demonstrating the enantioselectivity in biological activity of chiral compounds, scientists began to explore possible mechanisms underlying this phenomenon. In 1933, Easson and Stedman proposed a fundamental model to explain enantioselective pharmacological action (Figure 7), laying the basis for the theoretical understanding of the stereochemical differences in pharmacological activity.⁸⁷

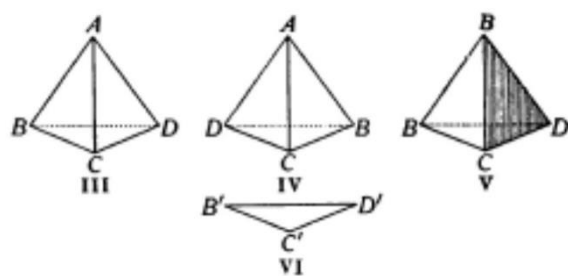


Figure 7. The Easson-Stedman model as proposed originally. As reported in Ref. 87: “*III and IV represent, in the conventional manner, two enantiomorphs, while VI depicts diagrammatically the surface of the specific receptor in the tissues. For the drug molecule to produce a maximum physiological effect it must, according to the above postulate, become attached to the receptor in such a manner that the groups B, C and D in the drug coincide respectively with B', C' and D' in the receptor. Such coincidence can only occur with one of the enantiomorphs (III), and this consequently represents the more active form of the drug. Let it now be supposed that the dissymmetry of III is abolished by replacing the group A by a second group B. The resultant molecule, represented by V, retains unchanged that part of the structure of III, i.e. the base BCD of the tetrahedron, which is concerned with its attachment to the specific receptor and must therefore be considered capable, despite the absence of molecular dissymmetry, of exerting its physiological activity with an intensity numerically equal to that of III, except in so far as this activity is changed by modifications in such of its properties as are not directly concerned with its attachment to the receptor. It will be noted that V possesses a second face, shaded in the diagram, containing the groups BCD. This face, however, corresponds with the base of IV and, like this, cannot be brought into coincidence with the receptor.*”

Reproduced with permission from ref. 87. Copyright 1933 Portland Press.

The model was derived from the results of studies on the pharmacological effects of the enantiomers of epinephrine. It was profied as follows: *a)* three groups in the molecule, the amino group, the aliphatic hydroxy group, and the electron-rich aromatic ring, interact with three complementary sites on the chiral biological receptor of the drug; *b)* given the three-dimensional geometry of the contact between the chiral drug and the chiral receptor, while all three groups of (–)-(*R*)-epinephrine simultaneously fit three complementary sites on the receptor, for (+)-(*S*)-epinephrine only two of the interacting groups of this enantiomer could simultaneously bind to the receptor. This model based on differential binding explained the different biological effects of the enantiomers. In 1935, Bergmann et al. postulated three points of contact for enantioselective enzymatic reactions,¹³⁰ but did not cite the work of Easson and Stedman. In 1948, Ogston also referred to the *three-point-interaction model*, in the course of a study on prochirality in enzymatic reactions.¹³¹ He proposed the three-point-interaction model to explain the ability of one of the enzymes, in the tricarboxylic-acid cycle in intermediary metabolism, to recognize two identical CH₂COOH groups of amino malonic

acid, an achiral (prochiral) molecule. Today these groups are defined as *enantiotopic*,³⁶⁻³⁸ a term that is referred to two groups located in equivalent positions that are related by a symmetry plane (or center or alternating axis of symmetry), but not by a simple symmetry axis. Replacement of one of the two enantiotopic groups by a new group generates a chiral molecule. Although the three-point-interaction model was originally proposed to describe a specific biological behavior related to epinephrine enantiomers, later it was used as a general model suitable to explain biological enantioselectivity of chiral drugs (Figure 8).

Given that this model is based on geometric considerations, not inherently bound to a biological context, it has been also used in chromatography to explain enantiomer separations and related enantioselective recognition mechanisms using chiral stationary phases (CSPs) or other CSs.^{54,132,133} On the basis of the three-point binding theory of Ogston, Pirkle adapted the model to chromatographic enantioselective recognition defining the *three-point rule*: “Chiral recognition requires a minimum of three simultaneous interactions between the CSP and at least one of the enantiomers, with at least one of these interactions being stereochemically dependent.”¹³³ The three-point rule does not require all three interactions to be attractive because, in many cases, repulsive steric interactions may occur in combination with attractive interactions.

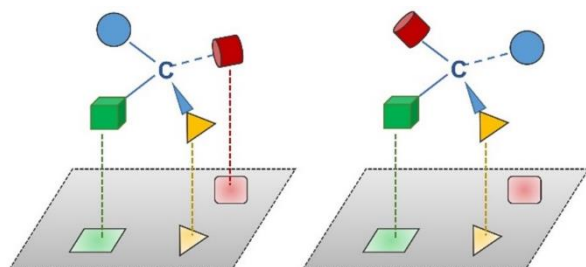


Figure 8. General scheme of the three-point-interaction model.

Over time, some re-interpretations of the Easson-Stedman model or the introduction of other models has been considered necessary. Sokolov and Zefirov proposed a two-point binding, they named *rocking tetrahedron model*.¹³⁴ Advancing from a static to a dynamic understanding of the enantioselective recognition, the conformational adjustment of the substrate and enzyme was considered a key step in enzymatic conversion.¹³⁵ A model based on conformationally driven enantioselective recognition mechanism was also proposed in enantioseparation science.^{54,136}

Reliability and limitations of the Easson-Stedman model have been discussed,^{133,136-138} and in some models more than three points of interaction involved in enantioselective recognition were also considered.¹³⁹⁻¹⁴³ Some authors have discussed the fundamental reliability of the three-point-attachment model,^{140,144,145} but such views have not gained a great consensus in the literature. Diastereoisomerism being the fundamental prerequisite for enantioselective recognition, so far, the most

models proposed to explain enantioselectivity remain based on the three-point contact concept.^{54,133,146}

Historically, the main consequence of the recognition of biological enantioselectivity and its importance was a growing interest towards the possibility to access pure enantiomers of chiral compounds through either asymmetric synthesis or enantioseparation techniques.

The origins of asymmetric synthesis can be found in the studies of Pasteur, Le Bel, van't Hoff, and Fischer because they likely had understood that assistance of a chirality inductor is necessary to control the formation of enantiomerically enriched or pure chiral compounds.¹⁴⁷ In 1904, McKenzie realized the first successful diastereoselective asymmetric synthesis. He obtained enantiomerically enriched atrolactic acid by adding the MeMgBr Grignard reagent, which had been discovered in those years, on menthyl benzoylformate.¹⁴⁸ In early 20th century, the possibility to prepare enantiomerically enriched or pure chiral compounds from prochiral substrates by using enzymes or molds as catalysts was intensively explored. For instance, Rosenthaler in 1908 used emulsin to catalyze the HCN addition on benzaldehyde, obtaining the cyanohydrine with 9% *ee*.¹⁴⁹ In 1913, Bredig and Fiske performed the first non-enzymatic enantioselective reaction on a prochiral substrate.¹⁵⁰ In this study, mandelonitrile was obtained from benzaldehyde and HCN with about 8% *ee*, by using quinine or quinidine as chiral catalysts.

The first unsuccessful attempt to resolve enantiomers based on their selective adsorption from the liquid phase onto chiral material was reported in 1904 by Willstätter in the course of his investigation to understand if coloring of wool is a chemical or physical process.¹⁵¹ Other attempts of enantiomer separation through the use of chiral nonracemic adsorbents date back to the 1920s, including the observation of induced optical rotation in racemic dye solutions used to dye wool.^{152,153} In general, these early attempts were carried out by using natural chiral polymeric adsorbents such as wool and cellulose or other polysaccharides. In 1939, Henderson and Rule reported the first example of partial separation of enantiomers by using the disaccharide lactose as chiral adsorbent,¹⁵⁴ and later Prelog and Wieland used the same lactose to separate Tröger's base enantiomers.¹⁵⁵ In 1951, cellulose was used as CS for enantioseparation in paper chromatography by Kotake and co-authors.¹⁵⁶ Although it was shown that native polysaccharides can discriminate enantiomers by liquid chromatography,¹⁵⁷ more useful CSs for liquid-phase enantioseparation were obtained through modification of the native polysaccharides in the 1970s.^{50,51,158} Supercritical fluid chromatography (SFC) was proposed for the first time in the 1960s, when Klesper et al. realized the first chromatographic separation of etioporphyrines using chlorofluoromethanes in supercritical state.¹⁵⁹ This study opened the possibility of using CO₂, as a nontoxic, chemically inert, nonflammable, environmentally safe, and relatively cheap medium for chromatographic separation. Meanwhile, in

1966 Gil-Av and co-authors had reported the first separation of enantiomers in gas-chromatography.¹⁶⁰ The first separation of enantiomers by employing voltage for propulsion of the analyte through the separation capillary was reported by Zare et al. in 1985,¹⁶¹ but the potential of the techniques was recognized only in the 1990s, and some pioneering papers in this field were published in the late 1980s.¹⁶²⁻¹⁶⁷ Also in the 1990s the first examples of capillary electrochromatography application for enantiomer separation were reported.^{168,169} These first studies paved the way to a growing interest towards chromatographic and electromigration techniques as the privileged tools to resolve racemic mixtures of chiral compounds and make pure enantiomers available for various applications.

While these discoveries and advancements profiled the bright future of molecular chirality domain, in the 1950s chirality imbalance was also discovered in nuclear processes,^{170,171} observing a violation of the parity suggested by all basic laws of physics, which are invariant under mirror reflection. The concepts of *parity conservation* and *parity violation* cannot be considered as intuitive, as noted by Bouchiat,¹⁷² because the effects of parity violation do not belong to our everyday experience. The first studies indicating that parity conservation may not be universal appeared in the period 1950s-1970s. In particular, the theory of electroweak force was formulated in the 1960s, predicting that the electron interacts with the nucleons (protons and neutrons) with a force that depends on its helicity.^{173,174} Different forces act on left- and right-helical electrons and, as a consequence, chirality imbalance also concerns atoms, making them optically active. Very small optical activity of atoms has been measured and found to be of the order of 10^{-7} radians as predicted by the electroweak theory.¹⁷² The physical consequence of this theory at chemical level is that the ground-state energy of a pair of enantiomers must be different.⁶ So far, this difference has been calculated using the electroweak theory and it was found to be of the order of 10^{-14} J/mol, thus too small to be detected by current experimental methods.^{175,176} Currently, parity violation and its possible correlation with the origin of biomolecular homochirality continue to be matter of research and discussion, in particular in physics and physical chemistry.¹⁷⁷⁻¹⁷⁹

As stressed by Prelog,¹⁸⁰ “*chemistry takes a unique position among the natural sciences for it deals not only with material from natural sources but creates the major part of its objects by synthesis*”. The huge potential of chemistry in the domain of molecular chirality have been witnessed for decades by the growing interest towards chiral non-natural small-molecules and macromolecules which have been designed and prepared to produce asymmetric induction by taking inspiration from the natural world but, at the same time, going beyond the nature’s chiral pool. Inspired by enzymes that catalyze reactions with high enantioselectivity in living systems, over time chemists have designed and prepared very efficient chiral ligands for asymmetric synthesis such as 1,1’-bi-2-

naphthol (BINOL), 2,2'-bis(diphenylphosphino)-1,1'-binaphthalene (BINAP), salen, bisoxazoline, and $\alpha,\alpha,\alpha,\alpha$ -tetraaryl-1,3-dioxolane-4,5-dimethanol (TADDOL)¹⁸¹ as well as CSs for enantioseparations.^{54,56} The importance of the stereospecific polymerization of non-natural monomers was demonstrated by Natta in the 1960s showing that in most cases the stereoregularity of linear polymers determines crystallinity.¹⁸² Later, design, preparation and application of homochiral metal organic frameworks (MOFs)¹⁸³ demonstrated the potential of these synthetic polymers by building 1D, 2D, and 3D macromolecular structures with new types of network topologies such as grids, pillared layers, channels, nanotubes, and cages, and a widespread selection of micro- and mesopore sizes and surface areas. In particular, it has been demonstrated that organometallic building units can serve to transform single fragments into extended homochiral polymeric porous networks characterized by conformational chirality, such as helicity (Figure 9),¹⁸⁴ in a manner, mimicking biopolymers (proteins, polysaccharides), which are characterized by a definite helical sense associated with the chirality of their building blocks (amino acids or sugars).¹⁸⁵

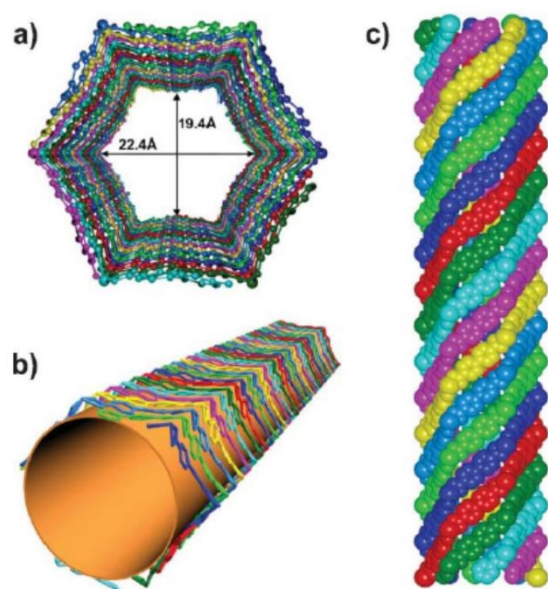


Figure 9. $[(\text{CH}_3)_2\text{NH}_2][\text{Cd}(4,4'\text{-biphenyldicarboxylate})_{1.5}] \cdot 2\text{DMA}$ (*N,N'*-dimethylacetamide): a) parallel association of eight helices into a chiral nanotube with a 19.4 Å by 22.4 Å free aperture, b) perspective view of a chiral nanotube, c) a space-filling representation of octuple helices, highlighting the extralong pitch. Reproduced with permission from ref. 184. Copyright 2007 Royal Society of Chemistry.

2.2 The language of molecular chirality and stereochemistry

The terms *chiral* and *chirality* were coined by W. H. Thompson (Lord Kelvin) in the period 1884-1904.^{186,187} However, the historical roots of the language of chirality date back to the late 1820s. In 1827, Möbius pointed out that the volume of a tetrahedron, the simplest three-dimensional object, and of its mirror image have different signs, which are not dependent on the position of the tetrahedron

but change by reflection, as the volume is expressed as a determinant involving the Cartesian coordinates of its labelled vertices.^{180,188}

In the 1830s, Berzelius coined the terms *isomer* and *isomerism* to indicate compounds having the same elemental composition but different properties.¹⁸⁹ In the course of the studies of Pasteur on tartaric acid, the combination of natural (+)-tartaric acid and its (-)-isomer was known as racemic acid (or paratartaric acid) which had been isolated from fermenting grape juice (*racemic* derives from *racemus*, Latin for a cluster of grapes).¹⁹⁰ During the second half of the 19th century words such as *chemical structure*, *configuration*, *stereochemistry* were introduced by physicists and chemists.^{191,192} Terms based on the prefix *enantio-* such as enantiomer, enantiomorph, and enantioselective were introduced in 1856 by the crystallographer Naumann.^{36-38,193} In 1874, van't Hoff defined the asymmetry at the carbon atom,¹¹⁵ twenty years before the introduction of the term chirality by Lord Kelvin,¹⁸⁶ who said about the term chiral: “*I call any geometrical figure, or group of points, chiral, and say that it has chirality, if its image in a plane mirror, ideally realized, cannot be brought to coincide with itself*”. In the beginning, the term was almost ignored and, later, re-discovered by Whyte in 1957, and extended to field others than chemistry.¹⁹⁴ In the 1960s, chiral and chirality were re-introduced into the stereochemical literature by Mislow^{195,196} and Cahn, Ingold and Prelog,¹⁹⁷ who defined a model as chiral when it has no element of symmetry (plane, center, alternating axis) except at most an axis of rotation. Analogously, in 1975 Prelog assigned to the term chiral the meaning: “*An object is chiral if it cannot be brought into congruence with its mirror image by translation and rotation*”.¹⁸⁰ Accordingly, the IUPAC recommendations for basic terminology for stereochemistry define chirality itself as follows with reference to symmetry: “*The geometric property of a rigid object (or spatial arrangement of points or atoms) of being nonsuperimposable on its mirror image; such an object has no symmetry elements of the second kind (a mirror plane, $\sigma = S_1$; a centre of inversion, $i = S_2$; a rotation-reflexion axis, S_{2n})*”.¹⁹⁸ In 1996, Avnir and co-authors proposed a new definition of chirality in the terms that “*Chirality is the inability to make a structure coincide with a statistical realization of its mirror image; the probe-dependent measure of this inability is the chirality content of the structure*”.¹⁹⁹ The authors justified this definition arguing that the classical definitions of chirality are quite suitable for small molecules, whereas more general concepts must be introduced for large random objects derived by growth and disintegration phenomena such as polymerizations, coagulations, electrodepositions, dissolution, etc. In particular, the definition was considered as applicable to the separation of enantiomers on a chiral support in the following terms: “*each of the specific particles of the chiral chromatographic material, such as chirally derivatized silica, is different in detail from the other. It is a large collection of small chiral objects, randomly structured, yet with a characteristic chirality value, determined by a minimal unit, the derivatizing unit. The*

*chromatographic interactions of the analyte with a given particle are not unique, but are determined by the distribution of orientations of the chiral ligands and by the diffusion, in and out, of the analyte, which, again, is dictated by the chirality of the surface”.*¹⁹⁹

Some authors stressed that a certain level of confusion and ambiguity has arisen in the use of the term chiral.^{38,199-206} Apart semantic discussions on the need of a precise use of the language of molecular chirality, an important aspect is that with the development of asymmetric synthesis, chiral and chirality have been often associated with reactions and processes. In this regard, in their textbook on organic stereochemistry, Eliel and Wilen discourage the use of chirality or chiral for the separation or transformation of stereoisomers, recommending the use of these terms should be restricted to molecules and models.¹⁰⁴ Indeed, chirality is a geometrical property and as such, it should only be applied to molecules or objects such as chiral substrate, chiral catalyst, or chiral stationary phase. Eliel and Wilen emphasized the geometrical character of chirality when they discuss the topic of stereoisomer differentiation (both enantiomer and diastereomer differentiation), stressing the incorrect use of the terms chiral differentiation/discrimination and/or chiral recognition: “*We prefer the term stereoisomer discrimination to the more widely used expression chiral discrimination (or chiral recognition) to emphasize its nature. There is nothing chiral about the discrimination per se; and while it is exhibited by chiral substances, it is caused by diastereomer, not enantiomer differences*”.²⁰⁷ Despite that, terms such as chiral recognition, chiral separation, and chiral chromatography continue to be widely used in the scientific literature.

Kelvin also introduced the terms *homochiral* and *heterochiral*, when in his lectures he defined chirality as a relational term and two relations, homochiral and heterochiral, are possible.^{186,187,208} In this perspective, the stereochemical use of homochiral refers to the same sense of chirality between similar molecules. Homochiral has also been used in a different sense to indicate a sample with all molecules of the bulk having the same sense of chirality, as a synonym for enantiopure. This usage is rather discouraged in the IUPAC recommendations for stereochemical terminology.¹⁹⁸ The controversy on the meaning of the term homochiral has been discussed by Gal,²⁰⁹ who proposed the term *unichiral* to define the macroscopic enantiomeric homogeneity. However, in some fields the term homochiral continues to be used in its macroscopic meaning. For instance, nowadays a MOF is called homochiral when all crystals of the bulk sample are of the same chirality.^{183,185}

Some historians of molecular chirality have discussed about the evolution of the term dissymmetry to asymmetry and their relationship with the term chirality. As mentioned above, Pasteur never used the terms chiral and chirality, whereas in all his lectures and commentaries he always used the terms “*dissymétrie*” (dissymmetry) and “*dissymétrique*” (dissymmetric) to describe the phenomenon of handedness in chemistry and crystallography.^{27,91} It is likely that he had in mind the

concept of chirality, nevertheless in his first reports the use of the word dissymmetry was related to the disruption or reduction of symmetry observed in crystallographic analysis of hemihedral crystals, without any connotation of handedness.⁹² On the other hand, in later studies,^{210,211} Pasteur used “dissymétrie moléculaire” (molecular dissymmetry) referring to molecular handedness and using dissymmetry as synonymous of chirality, either in the molecular and in the crystallographic contexts.⁹¹

In stereochemistry, asymmetry is defined as the absence of all symmetry elements other than the identity E or C_1 , an asymmetric object belonging to the symmetry point group C_1 .³⁶ Asymmetry and chirality are not synonymous. Indeed, an asymmetric object is necessarily chiral, but a molecule (or object) may be chiral but not asymmetric, since the presence of a simple axis of symmetry does not prevent the existence of chirality. For instance, the molecules of (+)- and (-)-tartaric acid are chiral but not asymmetric, since they have a C_2 axis of symmetry. In this regard, Gal considered¹⁰⁰ that Pasteur, likely, was aware of the difference between dissymmetry and asymmetry as he chose to use the French term “dissymétrie”. Given that, Gal ascribes the disuse of the term dissymmetry, in the sense of what we now call chirality, to the translations of Pasteur’s lecture *Recherches sur la dissymétrie moléculaire des produits organiques naturels*²¹² into English²¹³ and German,²¹⁴ where the words “asymmetry” and “asymmetrie” were used for “dissymétrie”. For clarity, it is worth noting that such considerations may appear rather speculative because, actually, Pasteur never explained the reasons for using dissymétrie (dissymmetry) over the French term asymétrie (asymmetry). So far, the terms dissymmetry and dissymmetric have been used with different meanings in the scientific literature. Indeed, in some cases, dissymmetric has been re-defined as chiral but not asymmetric, or to express concepts other than chirality, such as the absence of symmetry, reduction of symmetry, or even divergence or dissimilarity.²¹⁵ A limited use of the term as a synonym of chirality has been made in the stereochemical context.²¹⁶ The term is defined as “obsolescent synonym for chirality” in the “Basic Terminology of Stereochemistry (IUPAC Recommendations 1996).¹⁹⁸

In the 1960s-1980s, seminal papers have been published by Cahn, Hamson, Hirschmann, Ingold, Mislow, Prelog, and Siegel, which defined the meaning of the essential words of molecular chirality and related transformations such as *element of chirality*, *chirotopic*, *pseudo-asymmetry*, *stereogenic*, *prochirality*, and *stereotopic* (diastereo- and enantiotopic).^{197,217-221} For rigorous definition of these words, the reader can refer to the comprehensive glossary of Eliel and Wilen’s textbook,³⁶ and the book chapter “Principles, Concepts, and Strategies of Stereoselective Synthesis”
.37

Over time, some other terms have been reported in the literature, in general used to express and define specific tasks related to the domain of molecular chirality. In this regard, the concepts of

holantimer and *stereoisograms* which were proposed by Fujita²²² to re-define the stereoisomeric relationships between stereoisomers of molecules with different chiral elements are worth mentioning. However, so far, the popularity of the concepts has remained rather limited. In addition, some words formed with the suffix *-phore* (Greek term for “bearer of”) have been successfully used in different fields. In 1999, Lipkowitz and co-authors defined the concept of *chiraphore* as the key fragment that, in a catalytic system, is responsible for stereo-induction.²²³ As an extension of this concept in the context of enantioseparation science, in 2005 Del Rio et al. coined the term *enantiophore* stating that “*an enantiophore can be defined as the basic combination of the common structural features which are shared by a given group of molecules and supposed to be important for the enantioselectivity observed in chiral HPLC (high-performance liquid chromatography)*”.²²⁴ It is interesting to note that the semantic roots of both terms lies in a term, *pharmacophore*, which does not strictly belong to the field of chirality, defined by Ehrlich as “*a molecular framework that carries the essential features responsible for a drug’s biological activity*”.²²⁵ The common feature of all these terms is that they have been coined to provide a conceptual basis for structure-activity relationship assessment in asymmetric synthesis, enantioseparation science and drug discovery, respectively. Indeed, all these words aim to define *a*) the molecular features required for the interaction (binding + recognition + selection) between two chemical objects, and *b*) the mechanism by which these important features act, not considering those parts of the molecules that do not impact the interaction process.

In the current literature, transformations have been usually designated as asymmetric if they at least preferentially follow one of two possible stereochemical paths. However, the meaning of asymmetric synthesis has undergone significant changes in the course of time in order to suit it to the acquisition of new knowledge and scientist’s awareness of mechanisms and processes regulating asymmetric induction. In 1898, Japp in a lecture on the subject “Stereochemistry and Vitalism” emphasized the role of the living cell in asymmetric induction: “*Only the living organism with its asymmetric tissue, or the asymmetric products of living organisms, or the living organism with its concept of asymmetry can produce this result. Only asymmetry can beget asymmetry*”.²²⁶ In 1904, Marckwald in a paper entitled *Über asymmetrische Synthese* gave the following definition of asymmetric synthesis: “*Asymmetric syntheses are those reactions which produce optically active substances from symmetrically constituted compounds with the intermediate use of optically active materials but with the exclusion of all analytical processes*”.²²⁷ This definition was modified in 1971 by Morrison and Mosher giving a broader interpretation to the term asymmetric synthesis: “*An asymmetric synthesis is a reaction in which a chiral unit in an ensemble of substrate molecules (the substrate molecules must have either enantiotopic or diastereotopic groups or faces) is converted by*

a reactant into a chiral unit in such a manner that the stereoisomeric products are produced in unequal amounts.”²²⁸ While the terms asymmetric synthesis and asymmetric induction refer to the effects of the induced perturbation exerted by a chiral agent upon the relative stability of the enantiomers (thermodynamic control) or upon the enantiomeric activated complexes (kinetic control),³⁵ more recently the effect of a chiral physical natural force on a synthesis which would be symmetric *per se*, obtaining enantiomer imbalance, has been referred to as *absolute asymmetric synthesis*.^{32,35} This term has also been used referring to spontaneous mirror-symmetry breaking processes, occurring when a racemate becomes unstable with respect to the corresponding enantiomeric imbalanced mixtures.³¹ This kind of nomenclature has also referred to crystals and conglomerate formation²²⁹ and nonlinear stereochemical effects in asymmetric reactions.²³⁰

Words such as *racemization*, *enantiomerization*, and *diastereomerization* belong to the domain of *dynamic stereochemistry* which describes processes related to the interconversion of configurational and conformational stereoisomers.²³¹ The term *dynamic (conformational) chirality* was proposed by Fuji and Kawabata,²³² which defines the case when the chirality (stereochemistry) changes without breaking and formation of chemical bonds, and is time- and temperature dependent, while *static chirality* defines the case when enantiomer conversion requires the breaking of a bond followed by the formation of new bond. It is worth mentioning that the stereodynamic behavior of some chiral compounds has greatly contributed to the development of artificial machines and molecular motors with a huge impact in chemistry, engineering, physics and molecular biology.²³³

The terms *parity violation* and *parity conservation* are more frequently used in physics than in chemistry. These terms are related to the fact that chirality imbalance (parity violation) was also found at nuclear and atomic level. As mentioned above, these observations seem to contradict the parity conservation regulated by the physics laws which are invariant under translations in space and time, and rotations in space.⁶ Gardner stressed the key issue by stressing the so-called Ozma problem: *How can two intelligent civilizations agree on the description of an asymmetric object as left- or right handed without a prior understanding of such terms?*²³⁴ In this regard, Cintas noted that they cannot unless we are able to introduce the concept of handedness as universal and constant, such as parity violation, together with a detectable parameter of its manifestation,²⁰ these questions being still open and matter of theoretical and experimental research.^{10,13,177} Remaining in these frames, it has to be mentioned that in the late 1980s Barron introduced the concepts of *true* and *false chirality*²³⁵ with the aim to extend the notion of chirality to the sub-molecular world as well as to fields that can be represented by scalar or vectorial magnitudes explaining chirality of systems in motion: “*True chirality is exhibited by systems that exist in two distinct enantiomeric states that are interconverted by space inversion (parity P), but not by motion reversal (time reversal T)* (time-invariant

enantiomorphism) combined with any proper spatial rotation” and “False chirality is exhibited by systems that exist in two distinct enantiomeric states that are interconverted by time reversal as well as space inversion combined with a proper spatial rotation”. On this basis, chiral polarization at thermodynamic equilibrium, which induces the change of the free energy degeneracy between enantiomers, can only be promoted by true chiral forces such as specific combinations of magnetic and electric fields.³⁵ In the last three decades, some experiments confirmed Barron’s considerations.³⁵ However, the results in this field tend to be always evaluated with caution by the scientific community. This is especially true after the publication of an unexpected absolute asymmetric synthesis, induced by a static magnetic field alone applied to the synthesis of chiral aryl ethanols from prochiral ketones, as reported in 1994.²³⁶ In the same year, the scientific community clearly demonstrated the inconsistency of these results revealing a scientific fraud.²³⁷⁻²⁴¹ Despite the actual attractiveness and potential of absolute asymmetric synthesis and spontaneous asymmetric processes, in the field of classical enantioselective asymmetric induction discussions about true and false chirality did not involve many scientists, and the concept has been rather overlooked in both practice and theory of this domain, apart from the criticism initiated by Mislow to this dual definition of chirality.²⁰²

On the other hand, while it is commonly recognized that spatial effects determine recognition and discrimination of chirality, recent studies have suggested that charge redistribution in chiral molecules may occur with an enantiospecific preference in electron spin orientation.²⁴² In fact, it was shown that when electrons move through chiral molecules, this motion is spin dependent, with the preferred spin orientation determined by the handedness of the molecule and the direction of motion. This effect is known as chirality-induced spin selectivity (Figure 10).²⁴²⁻²⁴⁵

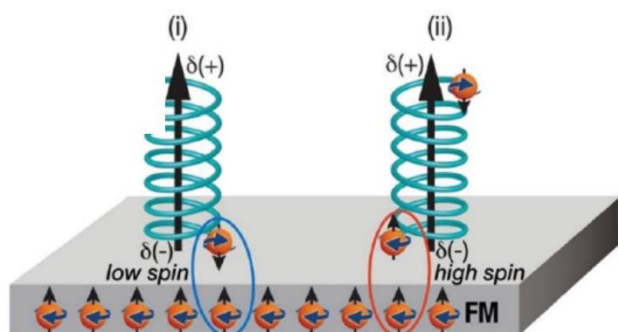


Figure 10. The diagram illustrates the concept that charge polarization is accompanied by spin polarization for chiral molecules. For a given enantiomer the interaction between the magnetized surface and the molecule follows either a low-spin (i) or a high-spin (ii) potential, depending on the direction of magnetization of the substrate (FM, ferromagnetic). Reproduced with permission from ref. 245. Copyright 2020 American Chemical Society.

In the last few years, the concept has found some pilot applications in enantioseparation science. Indeed, Banerjee-Ghosh and co-authors showed experimentally that the interaction of chiral molecules with a perpendicularly magnetized substrate is enantiospecific. On this basis, one enantiomer adsorbed preferentially when the magnetic dipole is pointing up, whereas the other adsorbed preferentially for the opposite alignment of the magnetization.²⁴² Later, Waldeck and co-authors used electrochemical quartz crystal micro-balance methods to demonstrate the enantiospecific interaction between a magnetized surface and a chiral amino acid.²⁴⁶ This study showed that the enantiospecific adsorption of cysteine on a ferromagnetic surface arises from the kinetics of adsorption and not from a thermodynamic stabilization. Very recently, Tassinari and co-authors crystallized pure conglomerates of several molecules from racemic solution through a resolution based on the spin-dependent charge reorganization effect.²⁴⁷ In fact, by using two surfaces with opposite magnetization, it was possible to simultaneously crystallize on each surface a different enantiomer. The electron's spin dependence of the electron transmission through chiral molecules has been also exploring in chiral light-driven molecular motors.²⁴⁸

2.3 Chiral elements and stereochemical descriptors

The knowledge of the absolute configuration of a chiral molecule is a key factor to understand the relationships between the spatial array of the atoms and properties and functions of the molecule. Single crystal X-ray diffraction (XRD) analysis is the most direct and powerful method for absolute configuration assignment under conditions of anomalous dispersion (the Bijvoet method).²⁴⁹⁻²⁵¹ If single crystals of good quality are not available for a given chiral compound, absolute configuration may be determined through other techniques such as Mosher analysis via NMR spectroscopy, and comparison of experimental and theoretical optical rotatory dispersion, Raman optical activity, and electronic and vibrational circular dichroism (ECD and VCD, respectively) spectra.²⁵²

As highlighted by Prelog,¹⁸⁰ one problem in dealing with the multiplicity of stereoisomers and chiral structures is that of communication, namely, how to transfer the information about their absolute configuration. Models that describe the complete molecular topography and conventions to define these models are essential for any discussion concerning the sense of molecular handedness. To define human laterality, the position of the heart is arbitrarily defined as left.²⁰ At the molecular level, chemists describe the configuration referring to a reference conventionally accepted (for instance, clockwise or anticlockwise) that differentiates two enantiomorphous objects. Fischer contributed to stereochemistry with his system of drawing known as the Fischer projection.²⁵³ It deals with a two-dimensional projection in which vertical drawn bonds are considered to be behind the plane, whereas horizontal bonds lies above that plane (Figure 11).

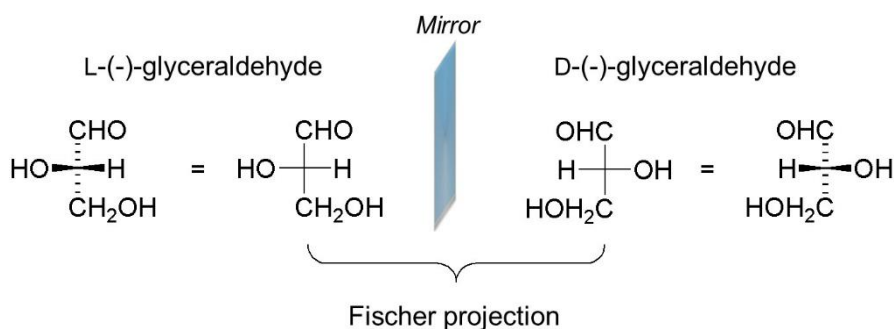


Figure 11. Fischer projection of glyceraldehyde enantiomers.

Until the 1960s, the configurations of chiral centers were denoted by the descriptors D and L by referring to the Fischer planar projection. In this case, the stereochemistry of a compound is related to that of the dextrorotatory or levorotatory enantiomers of glyceraldehyde, as a template chiral molecule, indicating the two configurations as D and L.³⁷ Currently, these descriptors are rather obsolete and used only for carbohydrates and α -amino acids. Otherwise, the Cahn – Ingold – Prelog (CIP) system is the most established system of rules for the assignment of descriptors (*R*, *S*, *P*, *M*) for stereoisomers of chiral compounds.^{197,220,254} Given a tetrahedral atom **Xabcd**, once the priority of the groups **a**, **b**, **c**, **d** is established on the basis of the sequence rules,²⁵⁵ the descriptors *R* or *S* are assigned. Given a priority **a** > **b** > **c** > **d**, to apply the CIP chirality rule, the model **Xabcd** has to be viewed from the side opposite to that occupied by the ligand **d** with the lowest priority (Figure 12). The other three ligands present a tripodal array pointing toward the viewer. If the sense of direction of the ligands **a** → **b** → **c** is clockwise or counterclockwise, the configurational descriptor is *R* (from Latin *rectus*) or *S* (from Latin *sinister*), respectively.

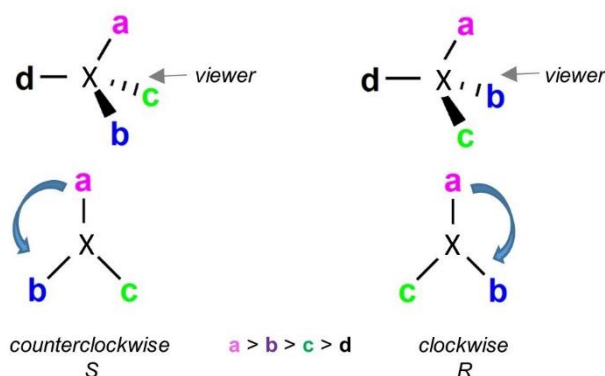


Figure 12. CIP chirality rule.

Chiral elements others than the chiral center may originate chirality in a molecule. *Axial chirality* originates from the nonplanar arrangement of four groups around an axis called “chiral axis”. For instance, this situation occurs in substituted allenes (**1**) and biaryl compounds (**2-5**) (Figure 13).

Stereoisomers such as some biaryl structures, resulting from restricted rotation around single bonds, where the rotational barrier is high enough to allow for their isolation, are called *atropisomers*. They are chiral for *atropisomerism*. This term (from the Greek, *a* = not and *tropos* =

turn) was introduced by Kuhn in 1933.²⁵⁶ However, optical activity due to axial chirality had been first described by Christie and Kenner in 1922.²⁵⁷

Necessary preconditions for axial chirality in biaryl molecules are, in general, a rotationally stable axis, and the presence of different substituents on both sides of the axis, namely $A \neq B$ and $A' \neq B'$ (**2**).²⁵⁸ If $A=A'$ and $B=B'$, the chiral molecule has C_2 axis as element of symmetry (**3**). Biaryl compounds with four identical substituents may be chiral as these groups are bridged-connected, as it can be observed in the D_2 -symmetric biaryl **4** described by Mislow et al. in 1964.²⁵⁹ Axial chirality may also result from the presence of different *meta* substituents (H and I) as found in the 4,4'-bipyridine **5**.²⁶⁰ It is worth mentioning that biaryl stereoisomers can be classified into configurational and conformational isomers depending on their chemical stability. While interconversion of configurational isomers, in general, requires bond breaking, conformational axial isomers usually isomerize without bond breaking. An energy barrier to racemization or diastereomerization high enough is associated with configurational isomerism.²³¹

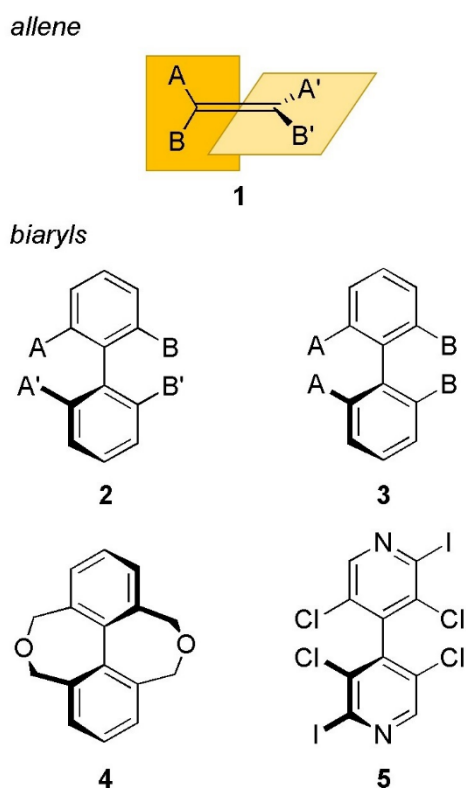


Figure 13. Axially chiral compounds.

The absolute axial configuration can be indicated by using the stereochemical descriptors *P* and *M*. For biphenyls, the analysis of a Newman projection along the biaryl axis can be used to exemplify the assignment of the descriptors (Figure 14).²⁵⁸ After assignment of priority to the *ortho* substituents according to the CIP rules ($A > B$), we have to advance from A to A', namely from the substituent of highest priority at the proximal ring to the highest-ranking one at the distal ring, through the shortest

path. If the turn is counterclockwise, the absolute configuration is *M* (minus), whereas it is *P* (plus) if the turn is clockwise.

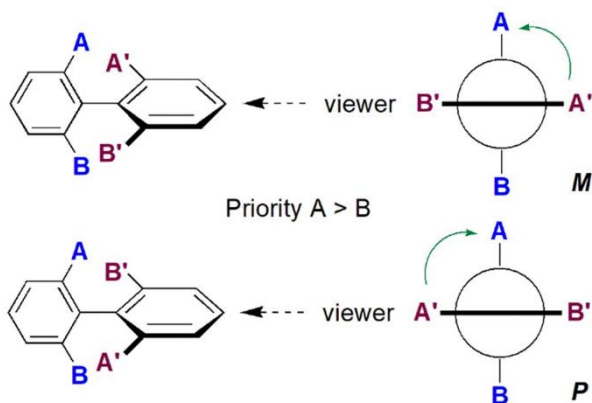


Figure 14. Method for absolute configuration notation of axial chiral biphenyls.

The same descriptors *P* and *M* may be used to notate the helicity, namely chirality of helical or propeller-shaped molecules. A helix is described as right-handed (*P*), if the sense of the twist is clockwise advancing along the axis of the helix, whereas it is left-handed (*M*), if the sense of the twist is counterclockwise (Figure 15). Chirality related to the structural helicity of tris(bidentate) and other octahedral metal complexes is usually denoted by using the descriptors Λ (left-handed) and Δ (right-handed).

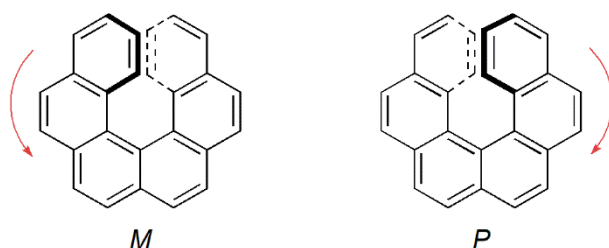


Figure 15. (*M*)- and (*P*)-enantiomers of hexahelicene.

Planar chirality resulted from the arrangement of out-of-plane groups with respect to a reference plane called “chiral plane”. For instance, this is the case of chiral ferrocenes (Figure 16). One nomenclature rule to define the absolute configurations of these planar chiral transition-metal complexes was proposed by Schlögl in 1964.²⁶¹⁻²⁶³

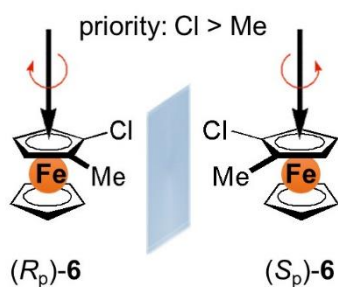


Figure 16. Method for absolute configuration notation of planar chiral ferrocenes.

For a transition-metal complex to be planar chiral, at least one atom is necessary to be located out of the chiral plane to discriminate the two enantiotopic faces of the plane. Among the atoms being out of the chiral plane and binding directly to the chiral plane, the one with the highest priority based on the CIP priority rules is assigned as a ‘pilot atom’.²⁶⁴ As shown in Figure 16, the central iron atom is the pilot atom in 1-chloro-2-methylferrocene (**6**), the chlorine and methyl substituents having the highest and the second-highest priority, respectively. On this basis, if the relative orientation from the first-priority substituent to the other is clockwise, from the view point opposite to the pilot atom with respect to the chiral plane, the molecule is assigned as an (*R*)-enantiomer. Analogously, if the priority order between the two substituents is counterclockwise, the molecule is an (*S*)-enantiomer. The descriptors (*R_p*) and (*S_p*) indicate that assigned absolute configuration is referred to planar chirality.

The rules for absolute configuration notation are a matter which is in constant transformation in order to adapt the concept to compounds not containing classical chiral elements, but rather non-conventional chiral motifs prepared by synthesis (Figure 17).^{203,265-269}

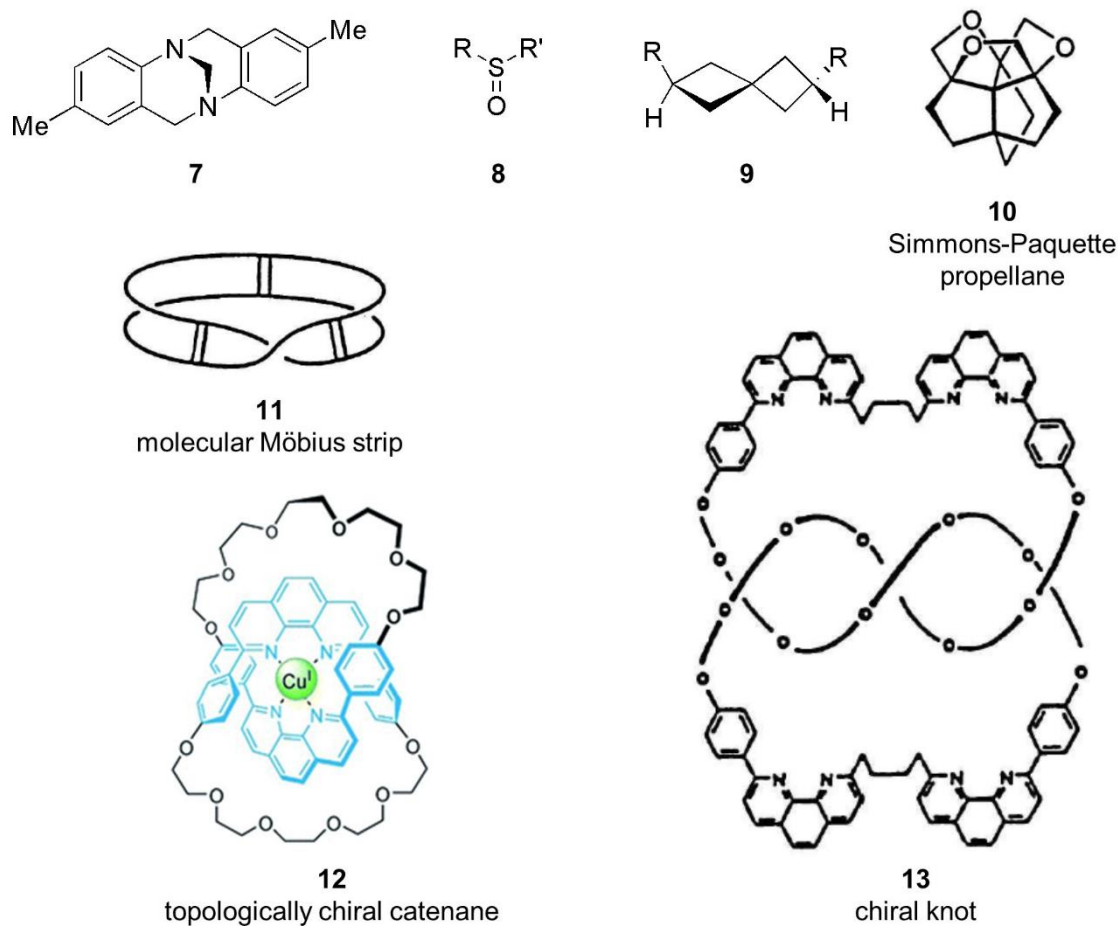


Figure 17. Examples of chiral molecular structures. Adapted with permission from refs. 265 (Copyright 1981 Elsevier), 267 (Copyright 1982 American Chemical Society), 268 (Copyright 2010 Royal Society of Chemistry) and 269 (Copyright 1989 John Wiley and Sons).

In general, the application of the CIP rule to complex structures is possible but, sometimes, it may appear rather difficult.²⁷⁰ The chirality of a molecular system can also be analyzed in terms of Euclidian geometry, using metric elements such as distances and angles.²⁷¹ This may be particularly useful in case of topologically chiral compounds such as derivatives **10-13**. Going beyond the classical CIP system, a notation based on the Cartesian system proved to be more adaptable to structures which do not contain classical chiral elements (chiral center, axis, and plane). In this regard, recently Baldrige and Siegel assigned a “Cartesian” configuration to the enantiomers of substituted indenocorannulenes (Figure 18),²⁷¹ where chirality arose from the concave-convex bowl-shape of the π -conjugated molecule due to the so-called bowl-to-bowl inversion.²⁷² In this case, defining the absolute molecular geometry with regard to the conventional cartesian frame does not require the existence of any configurational elements typical of the CIP system. On this basis, the symbols ⚡ and ⚡ were used to denote the enantiomers. Indeed, as the convex-facing indenocorannulene skeleton is oriented with its mirror plane vertical, and the benzene ring at 6 o'clock (**14**), in derivatives **15** and **16** the substituents to the left or to the right have been represented by the first (⚡) and the second (⚡) Chinese *pinyin* symbols, respectively. These symbols identify the two enantiomeric forms which were enantioseparated and isolated by HPLC on chiral stationary phase.²⁷¹

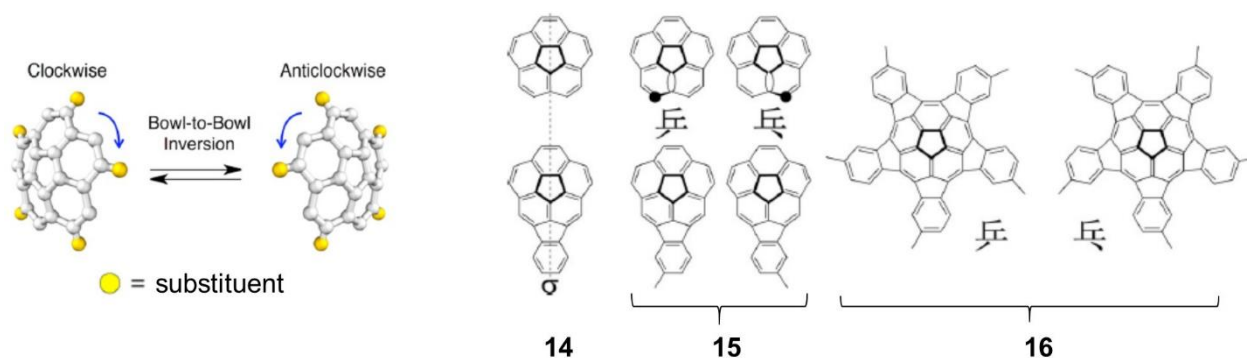


Figure 18. Configurational labels and absolute configuration notation for substituted indenocorannulene. Adapted with permission from refs. 271 (Copyright 2018 John Wiley and Sons) and 272 (Copyright 2014 American Chemical Society).

3. Noncovalent interactions: history, features, and trends

The importance of noncovalent interactions in nature as well as in chemistry, physics and life sciences have been fully recognized. The structures of biomacromolecules such as deoxyribonucleic acid (DNA) and proteins, solvation phenomena, and molecular recognition are determined by noncovalent interactions, which play a pivotal role in supramolecular chemistry, the “*chemistry beyond the molecule*”.²⁹ Noncovalent interactions acting in the condensed phase are very important

because most processes occur in solution, life itself most likely originated in liquid water phase. It is worth noting that covalent bonds, having large binding energies, can only rarely be broken under biological conditions, this feature being incompatible with the biochemical dynamics of living cells. Otherwise, even if a single noncovalent interaction can be easily broken, the combination of several noncovalent bonds acting cooperatively can ensure stable but flexible chemical and biochemical systems. At biological level, the concept was clearly expressed by Watson in 1965: “...interactions in biological media must be sufficiently strong to ensure preferential bonding of a given functional group of the molecule with a functional group of a second molecule. Simultaneously, however, these interactions should not be too strong in order to avoid the formation of crystalline species within the cell”.^{66,273}

In modern chemistry, the interest in noncovalent interactions have been witnessed by the exponential growth of articles, containing the term “noncovalent interactions”, published in chemical sciences in the last few decades.

This trend was predicted in 2009 by Schneider: “With courageous simplification, one might assert that the chemistry of the last century was largely the chemistry of covalent bonding, whereas that of the present century is more likely to be the chemistry of noncovalent binding.”.²⁷⁴ Anticipating this conceptual transition from covalent to noncovalent bonding, in 1995 Desiraju used Corey’s definition of synthon (...structural units within molecules which can be formed and/or assembled by known or conceivable synthetic operations)²⁷⁵ with almost the same connotation but in a supramolecular sense, stating that “supramolecular synthons are structural units within supermolecules which can be formed and/or assembled by known or conceivable synthetic operations involving intermolecular interactions”,²⁷⁶ and defining crystal engineering as the new organic synthesis. In this perspective, in supramolecular synthesis, supramolecular synthons assume the same role that molecular synthons have in molecular synthesis, a concept which can be also applied to molecular recognition and noncovalent interaction chemistry in solution. Actually, there is a tight relationship between noncovalent interactions and crystal engineering. On one hand, XRD analysis of crystal structures extracted from the Cambridge Structural Database (CSD)^{277,278} and the Protein Data Bank (PDB)²⁷⁹ remains the most important tool to define geometric parameters for a large series of intermolecular interactions.²⁸⁰⁻²⁸⁴ On the other hand, crystal engineering aims to the synthesis of targeted solid-state structures having desired properties through the understanding and a fine control of intermolecular interactions in the crystal packing.^{65,285}

Scientists working in the domain of molecular chirality commonly use the terms *nonenantioselective* and *enantioselective* noncovalent interactions to indicate the forces underlying (nonenantioselective) binding and enantioselective recognition, respectively.⁵⁴ However, the chemo-

physical description of noncovalent interactions as such is independent of their potential enantioselective function and of the chirality of the molecular environment where the enantioselection occurs. Otherwise, chemo-physical properties of binding sites and noncovalent interactions impact the enantioselective function of noncovalent interactions themselves when they act collectively in a chiral environment, provided that a single noncovalent interaction as such is not enantioselective.

The following subsections are aimed at discussing the subject of noncovalent interactivity, but in a way that can help a non-expert reader find his way through the huge number of articles published in this field. For this purpose, features and properties of noncovalent interactions have been overviewed, with particular emphasis on issues and open questions concerning their characterization, understanding and computational treatment.

3.1 From chemical bond to chemical bonding: a unifying view

The term “noncovalent interactions” was used for the first time in 1964, in the title of the article “Noncovalent Interactions between Amino Acid Side Chains and a Coenzyme Model”.²⁸⁶ In 1977 Kollman defined “*noncovalent interactions as those in which: (1) electrons stay paired in reactants and products and (2) there is no change in the type of chemical bonding in reactants and products*”,⁶⁰ highlighting the different nature of noncovalent interactions compared to covalent bonds. Actually, a covalent bond between two atoms is in general shorter than 2 Å, and consists of a pair of electrons which are shared by these atoms through the overlap of partially occupied orbitals. Noncovalent interactions show longer intersystem distances usually ranging from 2 to 4 Å, and sometimes more than that. The covalently bound molecules have typical binding energies of about 100 kcal/mol (418.4 kJ/mol), whereas total stabilization energy of a noncovalent molecular cluster ranges usually from 1 and 20 kcal/mol (4.2-83.7 kJ/mol).

The term “vdW interaction” has also been used as a general designation for weak noncovalent interactions.^{66,287} For instance, Müller-Dethlefs and Hobza described the difference between covalent and vdW interactions as follows: “*Atoms and molecules can interact together leading to the formation of either a new molecule (reactive channel) or a molecular cluster (nonreactive channel). The former is clearly again a covalent interaction; the latter one in which a covalent bond is neither formed nor broken is termed a noncovalent or van der Waals (vdW) interaction.*”⁶⁶ However, as noted by the same authors, nowadays the use of the term “noncovalent interaction” is recommended because, in the case of empirical potentials, the term vdW interaction is frequently adopted with meaning of the sum of attractive London dispersive forces and exchange-repulsion terms.^{66,287} Accordingly, Desiraju also used the term “vdW interaction” to describe interactions between dipoles and/or induced dipoles, which have a r^{-6} energy/distance dependence, referring the term “electrostatic” to interactions that have an r^{-1} to r^{-3} dependence, including dipole-dipole interactions.²⁸¹

On the other hand, the concept of chemical bond itself and its suitability to define covalent and noncovalent bond have been questioned over time.²⁸⁸ In 2007, Gillespie and Robinson stated “*a bond is the word that chemists use to explain the idea that two atoms are held strongly by a constraining force, but of course a bond has no physical reality*”.²⁸⁹ In 2009, Bader expressed his view that a chemical bond is “*neither measurable nor susceptible to theoretical definition*”.²⁹⁰ In the same year, Jacobsen also argued that “*it has become clear that the chemical bond per se does not exist. Each bond possesses its very own specific character*”.²⁹¹ Grimme et al. also stated that “*a precise and unambiguous definition of when a chemical bond exists between atoms is difficult*”.²⁹² The authors noted that the existence of a chemical bond must be related to something observable, namely chemical bonding must have an effect on measurable properties of the system, and any definition of bonding that has no real consequences is meaningless. Very recently, Murray and Politzer discussed the subtle difference between chemical bond and bonding arguing that, if chemical bond *per se* has no physical reality, the detailed nature of the bonding can vary significantly in progressing through the continuum of forms that chemical bonding can have.²⁸⁸ In this perspective, the notion of chemical bond is too restrictive and unsuitable to account for the physical description underlying all possible interactions between atoms and molecules that determine the properties of matter, the authors stressing the idea that the definition of bonding rather than of bond is more adequate for the purpose.

Thus, even if the main differences between covalent and noncovalent bonding are classically defined as reported above, the definition of the boundaries between the two concepts has been matter of discussion for decades. IUPAC provided a general description of chemical bond, stating “*there is a chemical bond between two atoms or groups of atoms in the case that the forces acting between them are such as to lead to the formation of an aggregate with sufficient stability to make it convenient for the chemist to consider it as an independent ‘molecular species’*”,²⁹³ a definition which can be also extended to the term noncovalent interaction given the word “bond” as synonym of “interaction”.⁷²

Given that, theoretical scientists still debate on the question: *Should covalent and noncovalent bond be viewed as separate types of bonding?*²⁸⁸ In 1972 Slater had already suggested that there is no very essential difference between the noncovalent and covalent binding.²⁹⁴ Accordingly, recently Hobza noted that “*from a physical perspective, there is no sharp border between covalent and noncovalent interactions, and thus, there is no physical reason to separate them into different groups*”.⁶⁸ In 1998, Bader defined the concept of “bond path,” as “*a line of maximum density that denotes that the atoms it links are bonded to one another*”.^{290,295} In this view, as noted by the author, a bond path is not a bond, but rather, this definition of bonding goes beyond all categories of atomic interactions, providing a unified physical understanding of atomic interactions. The roots of the bond path concept lie in the first milestones of quantum chemistry.²⁹⁶ In the 1920s, presenting his

relationship $H\Psi = E\Psi$ between the Hamiltonian operator H for a system of nuclei and electrons, the energy E of the system, and the state function Ψ ,²⁹⁷ Schrödinger concluded that Ψ is not a function in real space and should not be used directly to interpret physical observations.²⁹⁸ Rather, according to Schrödinger, is the “density of electricity,” which is what is currently defined as the electronic density $\rho(\mathbf{r})$, that has physical significance. Later, the concept of a “bridge of density” between bonded atoms was described by London in 1928, following the Schrödinger’s definition of the electron density.^{296,299} Recently, Rahm and Hoffmann explored chemical bonding and, correlating a chemical interaction descriptor with bond energy in known bonding domains, concluded that “*there are no sharp boundaries between these domains*”.³⁰⁰

In summary, on one hand it is true that complexity reduction may be necessary to direct scientists toward a deep understanding of the essence of phenomena, and the unifying physical view of chemical bonding which express itself in a continuum of forms goes in this direction. On the other hand, in practice, distinguishing the two concepts of covalent and noncovalent bonds and trying to classify different types of observable bonding are definitely helpful to communicate about the nature of the mutual perturbation of two (or more) molecular entities.

In the literature, the term bond continues to be commonly used to indicate the (measurable) effect of the mutual perturbation between two chemical entities, and in this review article we have also taken this choice. We could say that the term “bonding” defines the physical conditions of an interacting system that may produce those measurable properties of the system that we can approximatively name (covalent or noncovalent) “bond”. However, it has to be clear that the questions of the physical meaning of the term bonding, the physical meaninglessness of the term bond, and the distinction between covalent and noncovalent bonding still remain matter of scientific discussion.

3.2 Classification of noncovalent interactions: limitations and current proposals

The spectrum of noncovalent interactions ranges from the strong Coulombic attraction between ions of opposite charge to weak forces arising between nonpolar species such as noble gas atoms.⁶¹ Even a single interaction type such as HB, in crystals, may have a great chemical variety, showing energies between 0.25 and 40 kcal/mol (1.05-167 kJ/mol).³⁰¹ However, noncovalent interactions of moderate strength, ranging from few to about 20 kcal/mol (83.7 kJ/mol), have been shown to be of particular use to modulate efficiently binding and molecular recognition phenomena in most cases. In this frame, strong and weak HB, dipole-dipole, π - π , π -cation, and π -anion interactions, XB, ChB, σ -hole bonds, hydrophobic forces, triel, tetrel, regium, and spondium bonds, are only some of the terms used to define the features of the mutual perturbation occurring between two interacting

molecular species, and it is likely that, in the next future, advancements in comprehension and quantification of noncovalent forces will make this scenario even more crowded.

Classifying noncovalent interactions on the basis of the acquired knowledge may be possible with some limitations. Noncovalent interactions originate from interaction between permanent multipoles, between a permanent multipole and an induced multipole, or between an instantaneous time variable multipole and an induced multipole.⁶⁶ On the basis of perturbation theory, the total stabilization energy of noncovalent interactions can be partitioned into various energy terms, the *electrostatic*, *induction (polarization)*, *charge-transfer*, and *dispersive* which are all attractive. Actually, the electrostatic term may be also repulsive due to the overlap of occupied orbitals which forbids two interacting molecules from approaching too closely. The interaction type depends on the relative importance of these energy terms, structure of the interacting partners and medium. Even if one particular energy term is dominant in rather rare cases, nevertheless the electrostatic interaction may play a dominant role.^{66,302-304} Thus, using the strength of noncovalent interactions as a criterion, a first question for whatever classification arises from the fact that the strength of a single noncovalent force may be different depending on the molecular context where the contact occurs (Table 1).⁶³ Indeed, the same type of interaction may contribute to the overall contact between interacting species differently, in different contexts, because any subtle change of the interacting molecular structures and their environment will have multiple effects on a single noncovalent interaction. On the other hand, multiple interactions occurring within a complex, between protein and ligand, chiral auxiliary, catalyst, or selector and selectand, host and guest are usually the result of a compromise of attractive and repulsive interactions, which may be really challenging to deconvolute.

In this regard, some questions have to be considered. In thermodynamic terms, a noncovalent binding occurs if the binding free energy change (ΔG), which consists of an enthalpic (ΔH) and an entropic term ($-T\Delta S$), is negative. An increase in strength of the noncovalent interaction corresponds to an increasing negative contribution to ΔH , and a more favorable binding process. This enthalpy gain is accompanied by a restriction in the relative motion of the interacting partners which corresponds to a commonly negative contribution to ΔS , thus unfavorable to binding.^{305,306} This opposing interplay between enthalpy and entropy is known as *enthalpy-entropy compensation*, and compensation effects have been frequently observed in processes controlled by noncovalent interactions.³⁰⁶⁻³⁰⁸ In this case, noncovalent interactions are treated as additive, and therefore, average binding energies can be derived for common interactions. However, the approach based on noncovalent interaction additivity is not applicable when noncovalent interactions behave in a nonadditive fashion³⁰⁹⁻³¹² and, consequently, the knowledge of the binding free energy associated with the three-dimensional structure of a complex does not necessarily provide a complete description

of the energetic contributions of individual interactions. Indeed, noncovalent interactions may either mutually reinforce (*positive cooperation*) or mutually weaken (*negative cooperation*).^{274,313-317} When two noncovalent interactions act with positive cooperation, this means that the sum of the two interactions is larger than the simple addition of the individual interactions. Another source of nonadditivity may be *multivalency* or *chelate effect*.^{274,315} In this case, additive interactions involving a multitude of binding sites can lead to binding strengths approaching those of covalent bonds. For instance, the binding of two molecules, both having multiple recognition sites, may occur with affinity greater than the sum of the corresponding monovalent interactions.

Table 1. Typical Binding Free Energies for Major Noncovalent Interactions. Reproduced with permission from ref. 63. Copyright 2016 American Chemical Society

Interaction type	System	$-\Delta G$ [kJ/mol]
Salt bridges and ion pairs	inorganic salts in H ₂ O	5 to 6
	organic ions in H ₂ O	5 to 8
	ionic groups at protein surface	0 to 7
	ionic groups buried in protein core	12 to 20
Hydrogen bonds, <i>neutral</i>	PhO-H \cdots amide in CCl ₄	11
	PhO-H \cdots amide in CDCl ₃	6 to 8
	amide \cdots amide in CDCl ₃	5 to 8
	amide \cdots amide in protein core	2 to 10
	C-H \cdots indole in CDCl ₃	4
Hydrogen bonds, <i>with cation</i>	⁺ N-H \cdots O-CH ₂ (18-crown-6) in H ₂ O	3
	⁺ N-H \cdots O-CH ₂ (18-crown-6) in MeOH	8
Hydrogen bonds, <i>with anion</i>	ureas \cdots Cl ⁻ in DMSO	9
	ureas \cdots COO ⁻ in DMSO	20
Halogen bonds	C ₆ F ₅ I \cdots Cl ⁻ > Br ⁻ > I ⁻ in acetone	7 to 9
	C ₈ F ₁₇ I \cdots Cl ⁻ > Br ⁻ > I ⁻ in acetone	14 to 19
	Ph-Cl \cdots O=C-NR ₂ in protein pocket	6
	Ph-I \cdots O=C-NR ₂ in protein pocket	10
Dispersive and stacking	porphyrin \cdots pyridine in H ₂ O	7
	porphyrin \cdots quinoline in H ₂ O	17
	H ₂ O \cdots Kr in gas phase	2
Cation $\cdots\pi$	indole \cdots pyridinium in H ₂ O	2
	phenyl \cdots alkylammonium in H ₂ O	1 to 3
Anion $\cdots\pi$	RC ₆ F ₅ \cdots Cl ⁻ in acetone	7
	3,5(NO ₂)C ₆ H ₄ \cdots Cl ⁻ in C ₆ H ₆	3 to 4
	3,5(NO ₂)C ₆ H ₄ \cdots Cl ⁻ in MeCN	2 to 3
Hydrophobic	host-guest complexes in water	~0 to 60

All these effects are important in chemistry, biology, and material sciences, regulating not only the structure of biomacromolecules such as DNA, and the stability of protein-ligand complexes, but also secondary structure and function of synthetic macromolecules such as polysaccharide carbamate-based selectors for enantioseparation,^{59,318} metal organic frameworks,^{183,319} and self-assembly

processes.^{314,315} As noted by Stoddart and Turnbull, interaction mechanisms based on multivalency and cooperativity of noncovalent interactions could have an important meaning in evolutionary terms, as a consequence of the relative ease of multiplying the number of existing interactions to increase binding affinities, rather than addressing the more challenging task of evolving stronger interactions.³¹⁵

Another issue concerns the extension of the features of noncovalent forces from the gas phase, where the interacting partners are isolated without any surroundings, to solid state and solvated environments, where the effects of crystal packing and solvation, respectively, impact deeply noncovalent interactions. Moreover, while complexes in the solid state give a static view of interactions, complexes in solution may be characterized by multiple structures due to the conformational freedom of the interacting partners. Thus, in solvated environment, the thermodynamic result of a system, which is underlain by a set of noncovalent interactions, also depends on solvation processes and possible conformational changes.

Despite these considerations, as already reported in various articles,^{53,54,59,320} a general and approximate ranking of the most observed noncovalent interactions can be attempted accounting for their relative strength and directionality (Tables 2).

Table 2. General Ranking of Noncovalent Interactions

Interaction	Strength	Direction	Distance dependence	Angular dependence
Coulombic	Very strong	Attractive or repulsive	1/r long range	Non-directional
Ion-dipole	Strong	Attractive	1/r ² long range	Directional
Hydrogen bond	From weak to strong	Attractive	1/r ³ Intermediate range	Directional
Hydrophobic	From weak to strong	Attractive	Intermediate range	Non-directional
Dipole-dipole	Intermediate	Attractive	1/r ³ Intermediate range	Directional
π - π interaction	Intermediate	Attractive	Intermediate range	Directional
Steric contact	From weak to strong	Repulsive	Short range	Non-directional
vdW induction ^a	Weak	Attractive	1/r ⁶ Short range	Non-directional
London dispersive ^b	Weak	Attractive	1/r ⁶ Short range	Non-directional

^a permanent dipole-induced dipole; ^b induced dipole-instantaneous dipole

The term of London dispersive forces defines an electron correlation effect (quantum mechanical many-body interaction), representing the attractive part of vdW interactions, with a short-range energy/distance dependence (equation (1)) compared to long/intermediate range electrostatic forces (equation (2)).

$$E_{\text{vdW}} = \sum_{i,j>i} (A_{ij}/r_{ij}^{12} - B_{ij}/r_{ij}^6) \quad (1)$$

$$E_{\text{es}} = \sum_{i,j>i} (q_i q_j)/(4\pi\epsilon_0 r_{ij}) \quad (2)$$

In equations (1) and (2), q_i and q_j represent electric charge of atoms i and j , respectively, ϵ_0 is the dielectric constant, r_{ij} is the interatomic distance computed from the Cartesian coordinates, and the parameters A_{ij} and B_{ij} are repulsive and attractive terms dependent on outer shell electrons and

atom polarizabilities, respectively. Dispersive interactions are usually considered the weakest interactions occurring in supramolecular systems.^{321,322} This is true for the strength of a typical single interaction which is about of 0.5 kcal/mol or less for molecules composed of light elements ($Z < 40$). Recently, Machado, de Oliveira et al. showed by calculations that the interaction energy between methanol (MeOH) and a rare gas atom ranges from 0.07 kcal/mol to 0.44 kcal/mol, being composed largely of dispersive energy, and rising in value as the size of the particular rare gas atom.³²³ Despite the weakness of a single dispersive interaction, these forces are extremely important in condensed matter and biochemical systems. The main reason for this evidence is that dispersive interactions are always attractive and approximatively additive.³²¹ Thus, in medium-sized molecular systems their sum may surpass a single covalent and ionic interaction in terms of energy. For instance, Grimme considered two interacting point charges at a typical distance of 5 Å, as a reference system, with an electrostatic interaction energy (E_{es}) about of 60 kcal/mol (Figure 19).³²¹

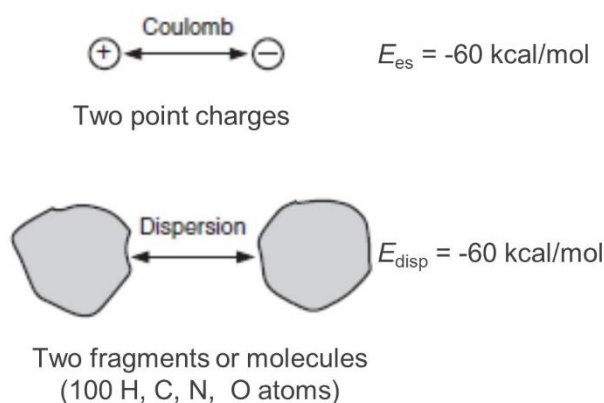


Figure 19. Comparison of electrostatic versus dispersive interactions in two systems that yield the same interaction energy ($E_{es} \cong E_{disp}$). Reproduced with permission from ref. 321. Copyright 2014 John Wiley and Sons.

This was compared to a medium-size molecule or aggregate composed of about 200 H, C, N, O atoms, consisting of two interacting fragments with 100 atoms each. An E_{disp} about of -60 kcal/mol was also estimated for this second system as the interaction in the first electrostatic case.

In protein-ligand complexes, geometrical parameters of noncovalent contacts have been derived from crystallographic structures extracted from CSD and PDB databases (Table 3).³⁰⁵ On this basis, the most important noncovalent interaction types observed in biochemistry are HB, π - π stacking, X-H $\cdots\pi$, cation \cdots anion, cation $\cdots\pi$, and dispersive interactions. More recently, analysis of crystallographic structures from the PDB has also focused on XBs^{324,325} and ChBs^{326,327} bonds and their huge potential in drug design.

The limitations inherent in any possible classification of noncovalent interactions emerge when one considers the nature of the HB, which is the best known and studied noncovalent interaction due

to the pivotal role exerted in many chemical and biochemical processes. Adopting the notation used in the IUPAC recommendations,^{69,328} a typical HB may be depicted as X–H···Y–Z, where X–H represents the HB donor, and typical X,Y = F, O, N. However, during the time the terms HB has undergone a huge extension of its original meaning, and now it describes a wide range of different proton and acceptor species,⁶¹ including a wide diversity of systems from the strong HB in HF₂⁻ to the weak CH··· π .⁷² Indeed, the first idea of lone pairs as unique nucleophilic HB acceptors has been abandoned, recognizing that the acceptor Y–Z may be not only a lone pair of Y, but also other electron-rich regions.

Table 3. Summary of the Typical Protein-Ligand Interaction Distances of Selected Noncovalent Interactions Extracted from CSD and PDB. Reproduced with permission from ref. 305. Copyright 2010 American Chemical Society

Interaction type	Typical distance range [Å]		
Hydrogen bonds	X = O	X = N	
Carbonyl/sulfonyl O···H-X	2.7-3.0	2.8-3.1	
Heteroaromatic N···H-X	2.7-3.0	2.8-3.2	
Carboxylic acid O···H-X	2.6-2.8	2.7-3.0	
Halogen bonds	Y = Cl	Y = Br	Y = I
Carbonyl O···Y	3.0-3.4	3.0-3.5	2.9-3.5
Multipolar interactions			
F···Carbonyl C	3.0-3.7		
Interaction with aliphatic C			
F···C	3.3-3.9		
Cl···C	3.6-4.3		
Aliphatic C···C	3.7-4.4		
Sulfonyl O···C	3.3-3.9		
Divalent S···C	3.8-4.2		
Interactions with aryl C			
	in plane	above plane	
Aromatic C···divalent S	3.7-4.2		
Aromatic C···F	3.3-3.7		
Aromatic C···Cl	3.6-4.1	3.5-4.0	
Aromatic C···Br	3.7-4.2	3.5-4.1	
Aromatic C···(CH ₂)	3.8-4.4	3.6-4.2	
Aromatic C···(CH ₃ O)		3.4-4.0	
Aromatic C···(CN ⁺)		3.4-4.0	
Aromatic C···amide N		3.4-3.8	
	parallel displaced	edge to face	
Aromatic C···aromatic C	3.4-3.6	3.6-3.8	

On this basis, all other halogens (Cl, Br, I),^{329,330} chalcogens,^{331,332} and pnictogen^{333,334} atoms have been shown to form HB as proton acceptors, along with π -systems of alkenes or aromatics,³³⁵⁻³³⁷ these latter with a r^{-4} energy/distance dependence.²⁸¹ In addition, metal atoms can behave as proton acceptors,^{338,339} and even the σ -bonds of molecules such as H₂ can take this function.^{340,341} The energy values determined by experimental and theoretical techniques are rather variable from 1-5 kcal/mol to values higher than 20 kcal/mol for weak and strong HBs, respectively.²⁷⁴ As it occurs for other interactions, the forces characterizing the nature of a HB are electrostatic, charge-transfer between the donor and acceptor leading to partial covalent bond formation between H and Y (with energy range of 20-40 kcal/mol), and dispersive. However, if an interaction is primarily due to dispersive

forces which are not directional, then it should not be characterized as a HB which, on the contrary, is highly directional. In this perspective, neither $\text{Ar}\cdots\text{CH}_4$ nor $\text{CH}_4\cdots\text{CH}_4$ are considered HB systems. Otherwise, the extent of charge-transfer was shown to correlate with HB strength. The covalent character of charge-transfer-based contacts is due to the fact that charge-transfer implies an electron flow from the donor to the acceptor. According to the type of orbital donating or accepting the electrons, these species are classified as nonbonding orbital, σ , and π , and vacant orbitals, σ^* , and π^* , respectively. The strongest charge-transfer complexes are formed between nonbonding and vacant orbitals, whereas π - π^* interactions are the weakest.⁶⁶ In Figure 20, some variations of HBs observed in the solid states as described by Desiraju are represented.²⁸¹

As the atoms X and H are covalently bonded and the X–H bond is polarized, the H \cdots Y bond strength increases as the electronegativity of X. Thus, the electrostatic component, mainly dipole-charge and dipole-dipole contributions,⁶⁶ plays a significant role in the directionality of HB. In terms of geometrical parameters, the X–H \cdots Y angle tends toward 180° and should preferably be above 110°, given that the closer the angle is to 180°, the stronger is the HB and the shorter is the H \cdots Y distance. As reported,²⁸¹ the change between O–H \cdots O contact on one hand, and C–H \cdots O contact on the other is due to the gradual decrease of the electrostatic character and increase of the dispersive character of the interaction. This trend was confirmed by Steiner and Desiraju in a study of the angular preferences of the HB contacts observed in the CSD (Figure 21).³⁴² However, weak interactions such as C–H \cdots O may have energetic consequences. In this regard, Dixon et al. calculated a lower limit of -2.1 kcal/mol stabilization per bond for C $^\alpha$ –H \cdots O bond in protein.³⁴³

Given all these features, in 2011 IUPAC defined that *the HB is an attractive interaction between a hydrogen atom from a molecule or a molecular fragment X–H in which X is more electronegative than H, and an atom or a group of atoms in the same or a different molecule, in which there is evidence of bond formation.*⁶⁹

The question of the evidence of bond formation is not trivial. First, given that the distances between H and Y range typically from 2.8 to 3.2 Å, using the extent of this distance with respect to the sum of the r_{vdW} as an absolute criterion to evidence a HB is rather inadequate (see subsection 3.4.1). The evaluations based on this criterion may provide trends and clues but cannot be considered conclusive. The X–H \cdots Y–Z HB may be evidenced by means of NMR spectroscopy, showing a pronounced proton deshielding for H in X \cdots H HB, spin–spin couplings between X and Y, and nuclear Overhauser enhancements. Moreover, a suitable criterion is also represented by the fact that the length of the X–H bond usually increases on HB formation, leading to a red shift in the infrared X–H stretching frequency. Indeed, the greater the lengthening of the X–H bond in X–H \cdots Y, the stronger

is the $H \cdots Y$ bond. There are, however, certain HBs in which the $X-H$ bond length decreases, and a blue shift in the $X-H$ stretching frequency has been observed.

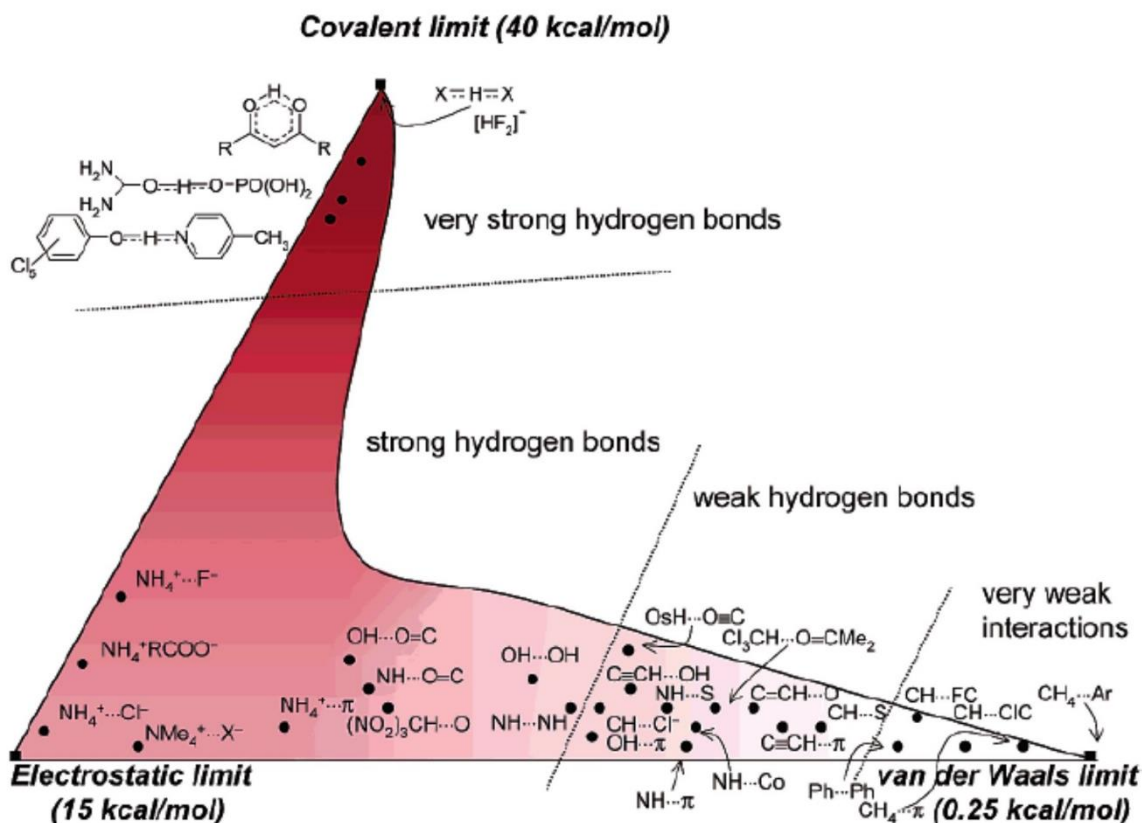


Figure 20. The multiple nature of HB is highlighted by three extreme situations of widely differing energies, this figure serving as a rough guide to the balance of electrostatics, vdW nature, and covalency in any $X-H \cdots Y-Z$ interaction. Reproduced with permission from ref. 281. Copyright 2002 American Chemical Society.

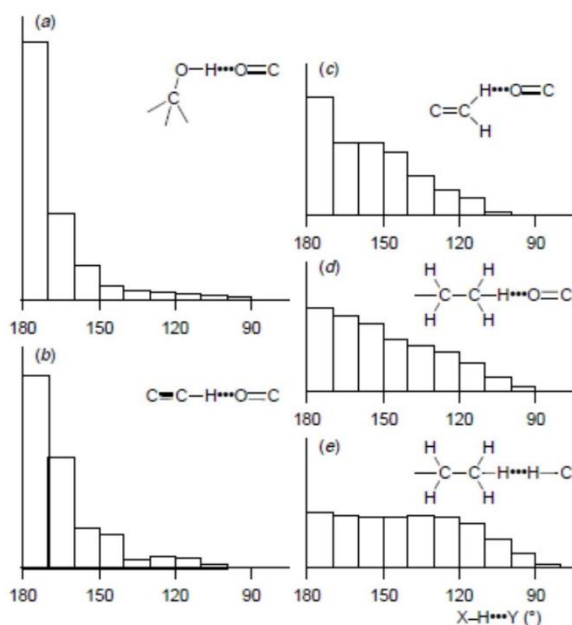


Figure 21. Histograms with angular frequencies of X–H···O contacts for different donor types, and of C–H···H–C vdW contacts: (a) hydroxy, (b) ethynyl, (c) vinyl and (d) ethyl donors and (e) vdW contacts. Reproduced with permission from ref. 342. Copyright 1998 Royal Society of Chemistry.

This improper (*blue-shifting*) HBs are less numerous than classical HBs. The C–H··· π improper HB was theoretically predicted and later confirmed experimentally by Hobza et al.,³⁴⁴⁻³⁴⁶ observing a contraction of the C–H bond length and a blue-shift of the stretch frequency. The class of improper HBs also includes the C–H···O and C–H···X⁻ (X = halogen) interactions. Natural bond orbital (NBO) analysis demonstrated that the improper HB in the latter complexes derives from a geometrical adjustment of the electron acceptor after charge-transfer from an electron donor.³⁴⁶ Indeed, while in a classical HB charge-transfer occurs from the electron donor toward the H atom, as the closest part of the X···H bond, for improper HB the charge-transfer is directed to the remote part of the electron acceptor.

It is worth mentioning that for a long time it was believed that HB impact is much stronger than π - π stacking, playing a key role in determining biomolecular structure. However, theoretical studies and experimental observations demonstrated that both motifs can occur in biological complexes, contributing to the stabilization of the complex in a comparable manner.^{347,348} In this regard, very recently Wetmore et al. analyzed noncovalent interactions between the nucleobases or ribose and amino acids containing π -clouds in (ribonucleic acid) RNA–protein complexes, finding that more than 80% of structures searched in the PDB contained at least one RNA–protein-interaction, with π -contacts making up 59% of the identified interactions.³⁴⁹ Interestingly, strong aromatic-aromatic interactions were also found in the crystal structure of the complex of the C-terminal domain of the severe acute respiratory syndrome coronavirus 2 (SARS-CoV-2) spike (S) protein with the human angiotensin-converting enzyme 2, complex involved in virus entry.³⁵⁰

π - π interactions are attractive and represent a subcategory of a wider class of interactions involving π -clouds centered on aromatic rings.³⁵¹ Along with the interactions summarized in Figure 22, π -hole interactions involving electron-poor aromatic ring, such as lone pair- π and anion- π interactions can be included.³⁵¹⁻³⁵³ For π - π interactions, theoretical calculations showed that the global minimum of the benzene dimer corresponds to the T-shaped structure, with each ring located in perpendicular planes.⁶⁶ Both T-shaped and parallel-displaced structures were observed in protein-ligand crystal structures.³⁰⁵

In the most recent literature,^{72-74,354,355} it has been proposed that noncovalent interactions can be named by identifying an element or moiety functioning as the electrophile and by referring to the corresponding Group of the Periodic Table. The terminology emerging from the application of this criterion was used in the recent IUPAC definition of HB,^{69,328} XB⁷⁰ and ChB,⁷¹ and is summarized in

Figure 23. As a matter of fact, this classification is founded on the conceptual similarity of $X-H \cdots Y-Z$ HB and other $X-L_A \cdots Y-Z$ interactions, where the H, as an electrophilic species, has been changed to the atom L_A behaving as Lewis acid (Figure 23). The ability of bound atoms to serve as electrophiles (L_A) is based on the anisotropic charge distribution which surrounds them. Indeed, while electronegativity assigns an overall negative partial charge to atoms such as halogens (Group 17) or chalcogens (Group 16), there is a reduced electron charge density on the elongation of the $R-L_A$ bond, generating a region of positive electrostatic potential (V) on an anti-bonding σ^* orbital, the so-called σ -hole (see next subsection).³⁵⁶⁻³⁵⁸

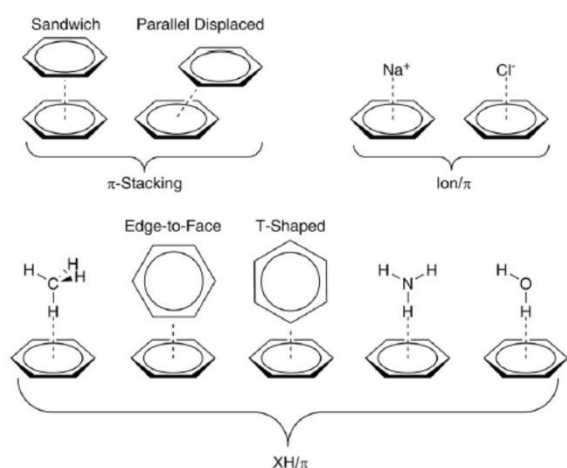


Figure 22. Models of noncovalent interactions involving aromatic rings. Reproduced with permission from ref. 351. Copyright 2014 American Chemical Society.

ALKALI METAL BOND		ALKALI EARTH METAL BOND		COINAGE (REGIUM) BOND (CiB)		SPONDIUM BOND (SpB)		ICOSAGEN (TRIEL) BOND (TriB)		TETREL BOND (TiB)		PNICTOGEN BOND (PniB)		CHALCOGEN BOND (ChB)		HALOGEN BOND (HaB, XB)		AEROGEN (Noble gas) BOND (NgB)	
Group 1	Group 2	Group 10	Group 11	Group 12	Group 13	Group 14	Group 15	Group 16	Group 17	Group 18	IUPAC recommended								
H																			
Li	Be				B	C	N	O	F	He									
Na	Mg				Al	Si	P	S	Cl	Ar									
K	Ca	Ni	Cu	Zn	Ga	Ge	As	Se	Br	Kr									
Rb	Sr	Pd	Ag	Cd	In	Sn	Sb	Te	I	Xe									
Cs	Ba	Pt	Au	Hg	Tl	Pb	Bi	Po	At	Rn									
Fr	Ra	Ds	Rg	Cn	Nh	Fl	Mc	Lv	Ts	Og									

Figure 23. Classification of donor-acceptor interactions by using the name of the group of the periodic table of the elements that acts as the electrophile (Lewis acid, L_A) based on IUPAC recommendations for HB, XB, and ChB, and on the most recent literature for the other noncovalent interactions.

Considering that electrophilicity and other properties impacting the interactions given by an atom, such as Lewis acidity and basicity, and polarizability, show specific trends, by linking the name of attractive interactions to the Group of the element at the electrophilic site, interactions are organized with a scheme where periodicities is easily identified.^{72,355} On the basis of this unified view of noncovalent interactions, the specific feature as a Lewis acid which is associated with atomic and molecular regions, where there is a situation of electron deficiency, explains the interaction behavior of electropositive species such as cations and metals, σ - and π -hole regions.^{67,355}

Despite its novelty, this classification refers to the interpretation of acid and base behavior published by Lewis in 1923.³⁵⁹ Very recently, noncovalent interaction types have been comprehensively reviewed by Alkorta, Elguero and Frontera.³⁵⁵

3.3 A historical overview: from van der Waals description to current theory

The idea that atoms had different features, and that some were equipped with hooks or spikes in order to be combined in different ways, generating different types of matter, dates back to the Greek atomistic philosophy.^{360,361}

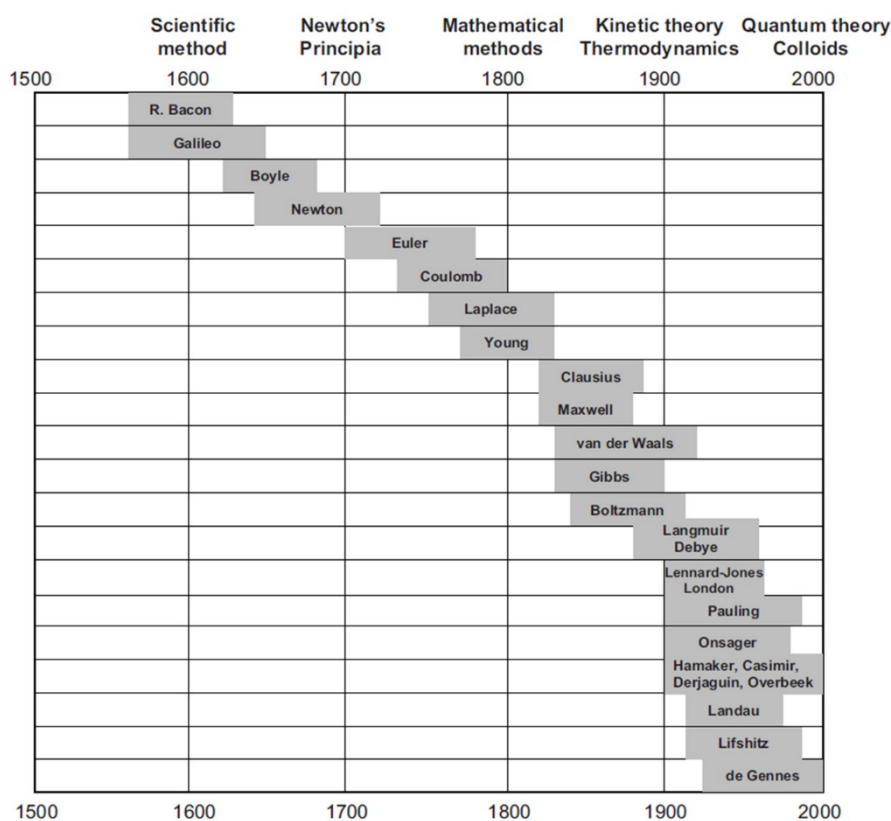


Figure 24. Scientists who made major contributions to the understanding of noncovalent interactions. Reproduced with permission from ref. 361. Copyright 2011 Elsevier.

Over time the interest toward possible forces regulating the properties of matter has constantly characterized the development of human culture and science (the reader can find a comprehensive overview in refs. 360 and 361), and since the introduction of the modern “scientific method” in the 17th century, several scientists contributed, directly or indirectly, to our understanding of noncovalent interactions (Figure 24).³⁶¹

But, in particular, it was in the 1870s that van der Waals’s studies provided a huge contribution to the understanding of molecular cohesion and intermolecular forces.³⁶² With the aim to describe the real behavior of gases, van der Waals introduced the concepts of attractive pressure and molecular volume to formulate the well-known equation of state. Thus, he demonstrated that molecules exist, that they have a molecular size and are able to exert molecular attraction and repulsion.

3.3.1 Dispersive forces

In his pioneering studies, van der Waals recognized the role of dispersive forces in the formation of condensed matter,³²² but the first recognition of attractive interactions of gases is due to the studies of Clausius on molecular motion in 1857. Indeed, he observed that “[...] *ein Molekül von einem*

einzelnen anderen Molekül mit viel geringerer Kraft angezogen wird, als von der ganzen Menge von Molekülen...” (two molecules are attracted much less by one another compared to when they are surrounded by many other molecules).^{322,363} In the 1930s, London related dispersive forces to spectroscopic properties, in particular polarizability of the interacting species. He described a dispersive force as “[eine] kurzperiodische gegenseitige Störung der inneren Elektronenbewegung der Moleküle, welcher Beitrag bei den einfachsten nichtpolaren und auch noch bei schwach polaren Molekülen den Hauptbestandteil der Molekularattraktion darstellt” (an interaction characterized by a short-period mutual perturbation of the inner electron motion of molecules whose magnitude is the major attractive contribution in the simplest nonpolar and also weakly polar molecules).^{322,364,365} In 1956, Pitzer and Catalano pointed out that the differences between the isomerization energies of branched and linear alkanes are due to intramolecular dispersive forces.³⁶⁶ In 1960, Bartell observed that “*intramolecular van der Waals forces may be even more important than effects of hybridization and conjugation or hyperconjugation in governing bond angles, bond distances, energies of isomerization and hydrogenation, and bending vibrations of molecules*”.³⁶⁷ In the early 2000s, Autumn et al. provided the first direct experimental evidence for dry adhesion of gecko setae by vdW dispersive forces. The authors showed that vdW mechanism implies that the remarkable adhesive properties of gecko setae are merely a result of the size and shape of the tips, and are not strongly affected by surface chemistry, rejecting the use of mechanisms relying on high surface polarity, including capillary adhesion.^{368,369}

In terms of theory, dispersive energy is a many-body electron correlation effect, which appears already for two-electron systems.³⁷⁰ As explaining by Grimme, single excitation of the electron from a ground-state level to an excited state changes the electronic distribution, and if one considers the corresponding de-excitation, this process can be seen as “charge fluctuation”. In a time-independent stationary state description, these fluctuations merely represent possibilities. They are realized when a second electron comes into play, representing electronic correlations. The amplitudes of the resulting double-excitations, in other words coupled single excitations, represent the basic quantity in all wave function theories (WFTs) to compute the dispersive energy. Grimme, again, stressed that a dispersive force is transmitted by electromagnetic radiation and not by electron exchange as in covalent bonding, thus screening effects in very dense materials might appear. Because electronic transition densities, and not charge densities, are the basic quantity for the dispersive bonding mechanism, conventional (charge-density-based) methods of Kohn–Sham density functional theory (DFT)³⁷¹ have shown fundamental problems to describe properly dispersive forces. Some adaptation of DFT methods are required for describing properly dispersive forces.³⁷⁰ For clarity, it has to be mentioned that, in the 1930s, Feynman, in his paper on the electrostatic explanation of chemical

bonding, argued that vdW attractive forces are not the result of “the interactions between oscillating dipoles” but arise from the accumulation of electron density between the nuclei.³⁷² In particular, considering Xe···Xe attraction, Feynman explained that the electronic charge of each xenon atom is slightly polarized toward the other, and that it is “*the attraction of each nucleus for the distorted charge distribution of its own electrons that gives the attractive $1/r^7$ force*”. Later, Feynman’s view has been confirmed by other studies.³⁷³⁻³⁷⁵ However, dispersive interactions remains widely attributed to fluctuating dipoles.

3.3.2 Hydrophobic effect

Along with dispersive interactions between nonpolar and weakly polar entities, in the 1930s scientists also tackled the question of the low affinity of nonpolar groups for water, and of the consequent observed spontaneous tendency of nonpolar groups in water to adhere each other in order to minimize their contact with water molecules,³⁷⁶ as expression of what later will be named “hydrophobic bond”. In the 1930s, Butler postulated an entropic origin for the effect because of its strong temperature dependence.³⁷⁷ Later, Frank and Evans provided the first proposal for a theory of the hydrophobic effect, namely that around the molecule of the nonpolar solute, an *iceberg* is formed, namely a kind of cage, an ordered structure consisting of molecules of water.³⁷⁸ In this view, the explanation of hydrophobic forces is based on the fact that a smaller number of water molecules solvates two lipophilic species confined in a large cavity, compared to those required when the species are confined in two smaller separate cavities.³⁷⁹ In 1959, the term “hydrophobic bond” was introduced by Kauzmann to describe the tendency toward adhesion between the nonpolar groups of proteins in aqueous solution.³⁸⁰ Starting from the 1960s, the nature of the interaction itself was discussed by several authors.^{376,379-381} One of the most critical aspects of the hydrophobic effect is the pivotal role of water as privileged medium, which as a matter of fact is the driving force of hydrophobic interactions. From the structural point of view, the origins of hydrophobic effect have been ascribed to many factors such as the tetrahedral geometry of the water molecule, its HB abilities, formation of networks, and its small size.³⁸²⁻³⁸⁷ Very recently Zielkiewicz and co-authors studied the structural properties of solvation water of three hydrophobic molecules as models, methane and two fullerenes (C₆₀ and C₈₀) by using computer simulations.³⁸⁸ The authors, by analyzing both the local ordering of the molecules of water in the solvation layers and the structure of HB networks, showed that ordered aggregates consisting of water molecules are formed in the solvation layer of hydrophobic molecules. The existence of the ordered aggregates around the hydrophobic solutes appears to be in accordance with the concept of “icebergs” proposed by Frank and Evans.^{378,388}

In the last few decades, the origins of the hydrophobic effects were explored in several studies involving the cavities of receptors such as cyclodextrins (CDs), cucurbituril, calixarenes, pillararenes,

and molecular clips and tweezer and related complexes.³⁷⁹ On the basis of the Frank-Evans model, hydrophobicity is driven by the entropy gain associated to the relocation of the ordered water solvating the solute before complexation to the bulk medium. As a consequence, in general positive enthalpy and entropy changes are considered as a confirmation of the hydrophobic effect.³⁸⁹ In another model developed in early 1990s, the enthalpy gain is considered to be associated to the formation of more cohesive water-water interactions between the liberated water molecules.³⁹⁰ On the other hand, the formation of some complexes involving concave hosts such as CDs, cucurbituril, and cyclophane, have been found to be “enthalpy driven”, with both negative ΔH° and ΔS° . In a more recent model, the so-called “high energy water” was invoked to explain enthalpically driven hydrophobic contact in host-guest complexes (Figure 25).^{379,391}

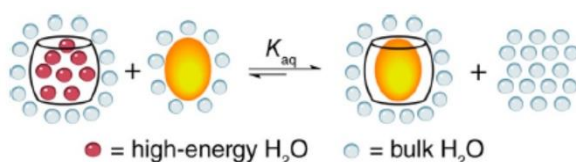


Figure 25. Release of high energy water molecules upon host-guest complex formation under hydrophobic conditions. Reproduced with permission from ref. 391. Copyright 2012 American Chemical Society.

The phenomenon of the high energy water originates from the condition of the water molecules which fill an uncomplexed cavity in aqueous solution and in the absence of a guest molecule. Being confined within the cavity, these water molecules may not fully participate in the HB network as in bulk medium and, consequently, they are energetically frustrated.³⁹² However, as a nonpolar guest enters inside the cavity, the high energy water molecules move to the bulk. This process makes the cavity-guest complexation an enthalpically-driven process due to the energy gain generated by the liberation of water to the bulk.^{379,393} Actually, in the beginning, the term “high-energy water” was not used, and other terms such as “enthalpy-rich water”³⁹⁴ and “activated water”³⁹⁵ were introduced to describe this phenomenon as explanation of the hydrophobic effect. In the first years, this idea attracted some criticism related to the problem that high-energy water hypothesis appeared to neglect the role of the interacting species and the energetics of the entire system.³⁹⁶ However, later the high-energy water hypothesis was confirmed experimentally, through isothermal titration calorimetry (ITC), and computationally, through molecular dynamics (MD) simulations as the main driving force explaining the high affinity binding of neutral guest molecules with cucurbit[n]urils.³⁷⁹ Very recently, the MD simulation was applied to the study of native CDs in water, also demonstrating the impact of the high-energy water in CD complex formation.³⁹⁷

3.3.3 From hydrogen bond to σ - and π -hole interactions

In 1923, the Lewis theory provided a model to rationalize the features of noncovalent interactions as the result of the complementary association between an electron-donor (the Lewis base) and an electron acceptor (the Lewis acid), such as any species with a reactive vacant orbital or available lowest unoccupied molecular orbital.^{355,359} The first mention of the term “hydrogen bond” in the published literature also dates back to the 1920s with the study of Latimer and Rodebush.³⁹⁸ Later, in 1939 the term “hydrogen bond” was also reported in “The Nature of the Chemical Bond” published by Pauling, who had concluded that HB has to be electrostatic as it cannot be chemical (covalent).³⁹⁹ In previous studies, different definitions had been used to describe HB. For example, Werner had mentioned *Nebenvalenz* (German for secondary or weak valence),⁴⁰⁰ and Moore and Winmill had used the term “weak union”.⁴⁰¹ In 1936, Huggins used the term *hydrogen bridge* as HB,⁴⁰² a definition which was retrieved later by Desiraju.²⁸¹

As described in the previous subsection, several type of HBs have been observed over time, depending on the HB acceptor type and of the covalent character of the HB. Murray and Politzer proposed the electrostatic potential, $V(\mathbf{r})$, and the σ -hole as unifying concepts for all different types of HB interactions.^{67,403} Electrostatic potential analysis provided an interesting perspective to gain new information on noncovalent interaction features and functions through the evaluation of the electron charge density distribution on molecular regions involved in noncovalent contacts. Given a molecule, the $V(\mathbf{r})$ at each point \mathbf{r} in the surrounding space, is generated by each nucleus in a system (first positive term) and by the system’s electron distribution (second negative term), accordingly with equation (3):

$$V(\mathbf{r}) = \sum_A \frac{Z_A}{R_A - \mathbf{r}} - \int \frac{\rho(\mathbf{r}')d\mathbf{r}'}{|\mathbf{r}' - \mathbf{r}|} \quad (3)$$

where Z_A is the charge on nucleus A located at R_A , and $\rho(\mathbf{r})$ is the electron density function.^{304,404,405} Thus, the sign of $V(\mathbf{r})$ may be positive or negative as result of positive and negative contribution derived from nuclei and electrons, respectively. $V(\mathbf{r})$ is a real physical property which can be determined experimentally and theoretically.⁴⁰⁴ In addition, $V(\mathbf{r})$ may provide information on specific regions of the molecules, such as lone pairs and π -clouds. The concept is that when two molecules approach each other, the tendency will be that the regions of positive $V(\mathbf{r})$ on a molecule is attracted to those of negative $V(\mathbf{r})$ on another molecule and, as noted by Politzer and Murray, the molecules will “recognize” that this will lead to favorable interactions.⁴⁰⁵ The $V(\mathbf{r})$ analysis of the interacting parts in their isolated state can be advantageously used to predict and explain noncovalent interaction strength and direction by mapping $V(\mathbf{r})$ on molecular electron density isosurfaces (V_s).^{304,405} On this basis, one can envisage the HB behavior of specific binding sites by evaluating the $V(\mathbf{r})$ values associated with the electron charge density distribution. Referring to some clear examples reported

by Murray and Politzer,⁴⁰³ in Figure 26 computed V_S of seven hydrogen-containing molecules are depicted. Each hydrogen in surfaces of (a) NH_3 , (b) H_2O , (c) HF , (d) HCF_3 , (e) HCN , and (f) C_2H_2 has a fairly hemispherical region of positive V_S (red regions) located on the outer side of the surface, opposite to its bond. The most positive value, $V_{S,\text{max}}$, is located approximately along the elongation of the bond. This positive region originates from the fact that the single electron of the hydrogen atom is involved in the bond, leaving a low electron density and, consequently, positive potential on the opposite side.

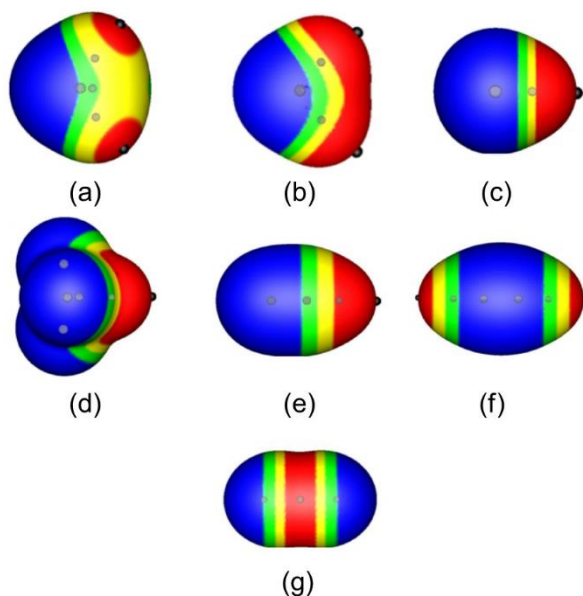


Figure 26. Computed electrostatic potentials on molecular surfaces of (a) NH_3 , (b) H_2O , (c) HF , (d) HCF_3 , (e) HCN , (f) C_2H_2 , and (g) BeH_2 . In molecules (a)-(e), the hydrogens are at the right; in (f) and (g), the hydrogens are at the left and right ends of the molecules. Gray circles show positions of atoms. Black hemispheres indicate most positive potentials ($V_{S,\text{max}}$). They are approximately on the extensions of the bonds to the hydrogens. Color ranges (in kcal/mol): red, more positive than 20; yellow, between 20 and 10; green, between 10 and 0; blue, negative. Adapted with permission from ref. 403. Copyright 2020 Springer.

Otherwise, the hydrogens in BeH_2 (g) have a hydridic character, being bonded to an electropositive atom and gaining electron density from it and, thus, have hemispherical regions of negative electrostatic potential (blue regions) on their outer sides.⁴⁰³

The anisotropy of the electron charge distribution is a characteristic of bound atoms. Indeed, whereas an isolated free atom has a spherically symmetrical electron density, if bound, the electron density of the same atom loses its spherical symmetry, and it becomes higher in some regions, and lower in others.^{357,358,405} It was in 1992 that Brinck, Murray and Politzer observed these regions of electronic charge density depletion in bound halogens by calculations, and called them “ σ -holes”.⁴⁰⁶ Later, Clark et al. showed that Cl, Br and I atoms bound to electron-withdrawing groups closely

approximate the $s^2p_x^2p_y^2p_z^1$ configuration, where the z-axis is directed along the electron-withdrawing group–X bond, and the three unbonded pairs of electrons generate a belt of negative V around the central part of X, orthogonal to the covalent bond, leaving the outer lobe of the p_z orbital depleted of electron charge density, this situation defining the σ -hole as a region of electron charge density depletion.⁴⁰⁷ Evidence of the anisotropy is that in bound atoms the radii are greater perpendicular to the bond than along its extension. This phenomenon has been described in 1990 by Ikuta as “polar flattening”.⁴⁰⁸ The (red) regions of lower electronic density observed for the hydrogens reported in Figure 26 also are “ σ -holes”.

As we mentioned in the previous subsection, atoms of other groups, in particular Groups 14–17, have also been found to have lower electronic densities opposite to their bonds, on the elongation of the bonds themselves, the number of the σ -hole depending on the valence of the atoms (Figure 27). Through the positive V , associated with the lower electronic density of a σ -hole, these regions can interact favorably with a negative site. This kind of interactions are commonly called “ σ -hole interactions”, HB can be considered as belonging to this class of interactions.

Among σ -hole interactions, in the last decades, the association of R–X \cdots Y (X = halogen, Y = negative site) type, which is called XB, has been widely studied, attracting interest due to its directionality, with typical geometrical parameters, angles and distance (typical values for I \cdots O contacts: $2.8 \text{ \AA} \leq d_{I\cdots O} \leq 3.4 \text{ \AA}$). For a typical R–I \cdots O=C interaction, reference value for R–I \cdots O and I \cdots O=C angles are 180° and 120° , respectively. Indeed, whereas the positive regions on bonded hydrogens tend to be almost hemispherical, because of hydrogen having only one electron, those on halogens are more narrowly focused. Thus, HBs are often less linear than XBs.⁴⁰⁹

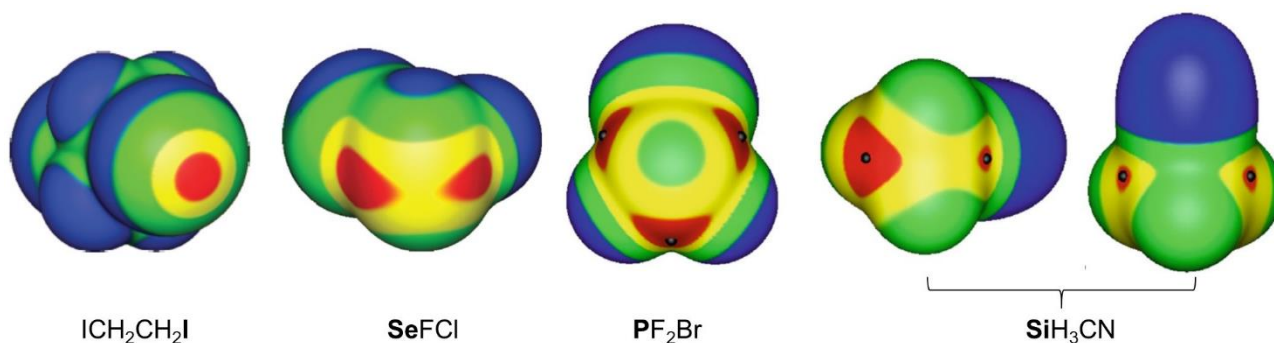


Figure 27. Molecular surface electrostatic potential of ICF₂CF₂I, SeFCl, PF₂Br, and SiH₃CN. Color legend: red, positive V ; blue, negative V ; yellow/green, intermediate V values. Adapted with permission from refs. 67 (Copyright 2015 Springer) and 357 (Copyright 2013 Royal Society of Chemistry).

Actually, the history of XB dates back to the 19th century. Indeed, a XB association was observed for the first time in the iodine-ammonia complex (I₂ \cdots NH₃) obtained by Colin in 1814 through the reaction of iodine and gaseous ammonia.⁴¹⁰ Later the same complex was reported by

Guthrie upon reaction between iodine and liquid ammonia.⁴¹¹ The first use of the term “halogen bond” can be traced back to the study of Zingaro and Hedges in 1961,⁴¹² the authors describing the complexes formed between halogens and phosphine oxides or phosphine sulphides. In 1968, Bent published a review on the chemistry of donor-acceptor adducts, where he treated about “Organic Molecules with Oxygen Atoms as Electron Donors and Halogen Atoms as Acceptors” and “Molecules with Halogen Atoms as Electron Donors and/or Acceptors”. In this paper, the author highlighted the distinctive geometric features of the interactions, evidencing that the distances between the electron donor atom and the halogen atom were shorter than the sum of their respective vdW radii.⁴¹³ Later, in his Nobel lecture, Hassel considered that “*Particular importance may be attributed to complexes in which direct bonding exists between one atom belonging to the donor molecule and another atom belonging to the acceptor molecule. Complexes of this kind are above all those formed by donor molecules containing atoms possessing "lone pair electrons" and halogen or halide molecules*”.⁴¹⁴ Even if a number of studies were performed in the period 1970s-1980s, nevertheless for a long time these data did not provide a reliable and convincing picture of the XB.^{415,416} On the contrary, in the late 20th century, the introduction of basic concepts such as charge anisotropy of bound atoms and σ -hole, theoretical analysis and experiments shed light on the great potential of XB. In 2013 the IUPAC issued the “Definition of the halogen bond (IUPAC recommendations 2013)” stating that “*a halogen bond occurs when there is evidence of a net attractive interaction between an electrophilic region associated with a halogen atom in a molecular entity and a nucleophilic region in another, or the same, molecular entity*”.⁷¹

The strength of the XB depends on the properties of donor, acceptor and medium,⁴¹⁷ which increases following the order $F < Cl < Br < I$. Given this trend, bromine and iodine being considered as more powerful XB donors.³⁵⁷ In general, molecules with properties as nucleophiles can act as acceptors towards both XB and HB donors. As a consequence, XBs may be destabilized by solvents possessing HB donor functionalities such as alcohols because of XB-HB competition.⁴¹⁸

Halogens can behave as Lewis bases, or as XB donors with properties of Lewis acids able to interact with an acceptor through the σ -hole (Figure 28). This amphoteric behavior is just explained by the anisotropy featuring the charge distribution on halogens and generating both electrophilic and nucleophilic regions of halogen surface. It is worth mentioning that in Figure 28, a different color code is reported compared to Figures 26 and 27. Thus, in this case, and in other figures reported in the review, we refer the reader to the figure captions for color legend explanation. Considering that a Lewis base can function as HB and XB acceptor, in the last few years the interplay between HB and XB has been intensively investigated in self-assembly processes,⁴¹⁹ crystal engineering,^{420,421}

molecular recognition,⁴²² preorganization strategies,^{423,424} theoretical studies,^{425,426} and medicinal chemistry.⁴²⁷

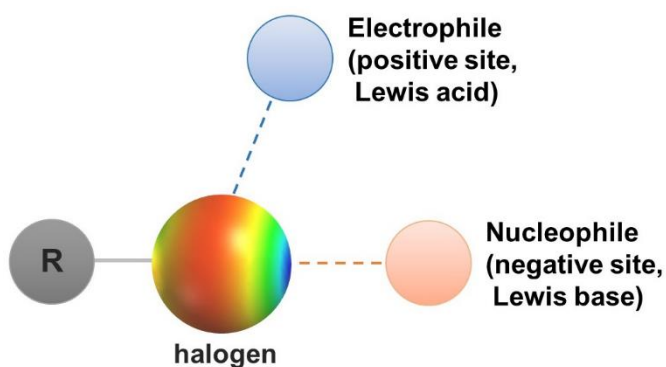


Figure 28. Interaction directionality of halogens with nucleophiles (XB) and electrophiles (HB).

It is worth mentioning that in 1963 Sakurai et al. noted that $R-X \cdots X-R$ contacts ($X =$ halogen atom) occur preferentially according to two different geometries,⁴²⁸ which, in 1989, Desiraju and Parthasarathy classified as type I (symmetrical interactions where $\theta_1 = \theta_2$) and type II (bent interactions where $\theta_1 \approx 180^\circ$ and $\theta_2 \approx 90^\circ$) (Figure 29).⁴²⁹

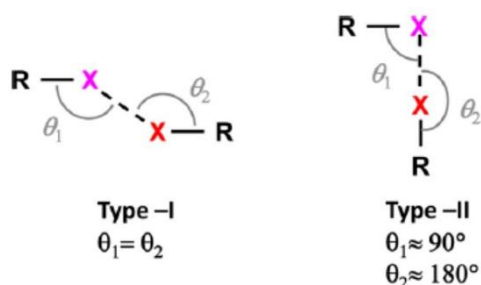


Figure 29. Structural scheme for type I (left) and type II (right) halogen \cdots halogen short contacts. $X =$ halogen atom, and $R = C, N, O,$ halogen atom. Type II contacts are XBs. Reproduced with permission from ref. 415. Copyright 2016 American Chemical Society.

ChBs and pnictogen bonds (PnB) have one common feature with the XBs, namely their σ -holes are easily accessible by electron donors, and the respective bonds are thus important as structure-making factors as well as for fine tuning of mechanisms and processes. The name ChB was introduced in 2009 by Ji and co-authors.⁴³⁰ The history of ChB has been recently reviewed by Werz et al.,⁴³¹ the authors reporting that traces of ChBs in the literature date back to the 1960s. ChBs and PnBs involve atoms of groups 16 (S, Se, Te) and 15 (P, As, Sb), respectively, their strength increasing following the order $S < Se < Te$ and $P < As < Sb$. These noncovalent interactions possess many similarities with XB, but with a different interaction pattern. Indeed, while in bound halogens one σ -hole can be observed, up to two and three σ -holes can be identified in Ch and Pn atoms, respectively, due to their valence (Figure 27). Otherwise, the σ -holes of tetrels (Group 14) are located in the middle of three

sp^3 -hybridized bonds, which makes their accessibility rather low. For this reason, XBs,⁴¹⁵ ChBs,^{432,433} and PnBs⁴³⁴ have been finding applications in chemistry, biology, and material sciences, while so far exploration of tetrel bonds has been limited to theoretical and crystallographic studies.⁴³⁵⁻⁴³⁷

The notation π -hole, conceptually analogous to that of σ -hole, was introduced by Politzer et al.⁴⁰⁹ to describe regions of positive potential involving p-orbitals that are perpendicular to a portion of a molecular framework such as an aromatic ring, bearing strong electron-withdrawing substituents (for instance hexafluorobenzene) (Figure 30).^{351,352,438}

Anion/lone-pair $\cdots\pi$ interactions have attracted much attention and discussion about their physical nature. Frontera et al. treated anion $\cdots\pi$ interactions focusing on the concept of π -acidity or π -electron deficiency.^{352,439} Given the permanent quadrupole associated with an aromatic ring, comprising the positively charged nucleus and a pair of negative charges located at the same distance above and below the molecular plane, benzene presents a scenario, in terms of permanent quadrupole, which is similar in magnitude, but of opposite sign compared to hexafluorobenzene (Figure 31).⁴³⁹

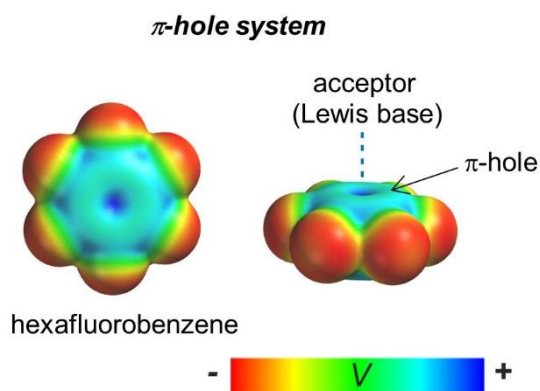


Figure 30. General description of π -hole and related noncovalent bonding.

This difference may offer a key to interpret the difference between cation $\cdots\pi$ interactions,⁴⁴⁰ simple electrostatics facilitating a natural attraction of cations to the benzene cloud, and anion $\cdots\pi$ interactions which are favored with aromatic rings showing opposite quadrupole sign such as hexafluorobenzene.^{439,441}



Figure 31. Representation of the quadrupole moments of benzene and hexafluorobenzene. Adapted with permission from ref. 439. Copyright 2002 John Wiley and Sons.

In the early 2000s, Kim et al. provided gas-phase *ab initio* interaction energies for some π -stacking interactions,⁴⁴² also studying the effect of substituted benzenes.⁴⁴³ Although total interaction energies of anion $\cdots\pi$ and cation $\cdots\pi$ interactions are similar, they found that, in contrast to cation $\cdots\pi$

interactions, anion $\cdots\pi$ forces present a relevant contribution from dispersive energies. Anions also have an important influence on the nature and magnitude of the anion $\cdots\pi$ interactions, and interactions involving halide anions are dominated by electrostatic and induction energies. Wheeler et al. evidenced that the ability of a phenyl ring with electron-withdrawing substituents to bind an anion is mainly due to favorable interactions of the anion with the substituents, this effect overwhelming the unfavorable interactions of the anion with the ring.³⁵¹ More recently, Matile et al. reported that both anion $\cdots\pi$ and cation $\cdots\pi$ interactions can occur on the same aromatic surface, this kind of interactions being referred to as ion pair $\cdots\pi$ interactions.⁴⁴⁴

Among noncovalent interactions involving aromatic rings,⁴⁴⁵ π - π stacking interactions have received the most attention in recent years.^{446,447} Popular models for this kind of interactions are those of Hunter-Sanders⁴⁴⁸⁻⁴⁵⁰ and Wheeler-Houk^{351,451,452} (Figure 32). In these two competing models, a nonlocal effect occurs in which tuning of the π density by the substituent on the phenyl rings alters the interaction (Hunter-Sanders model), or the direct interaction of the added substituent, and changed polarity of the phenyl-substituent, alter the interaction (Wheeler-Houk model), in terms of local effect.

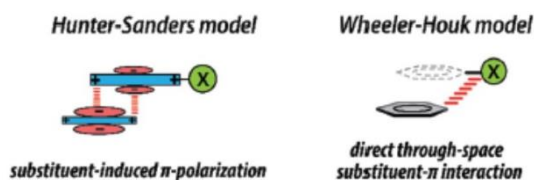


Figure 32. Schematic representations of two mechanistic hypotheses for aromatic substituent effects: Hunter-Sanders (left) and Wheeler-Houk models (right). Adapted with permission from ref. 453. Copyright 2019 Royal Society of Chemistry.

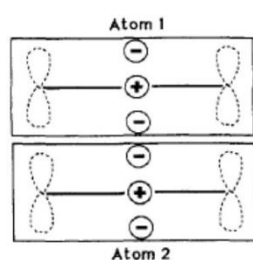
Treating the π - π interaction as an interaction between permanent quadrupoles (Figure 33), the original Hunter-Sanders model considered the substituent-induced changes in the aryl π -electron distribution as a more important factor than the overall molecular properties.⁴⁴⁸ On this basis, Hunter and Sanders presented a set of rules that could be used to rationalize and predict strength and geometries of stacking interactions involving various aromatic systems. Later, Hunter and co-authors, proposed a view where the quadrupoles of the original model were replaced with the “ π -electron system”.⁴⁴⁹ In this electrostatic model, the substituents act as modulators of the strength of π -stacking interactions through their impact on the π -electron density of the aromatic ring.⁴⁵⁰ Cozzi and Siegel also proposed the polar/ π model in terms of molecular quadrupole moments.^{454,455}

Later, Wheeler and Houk showed that substituent effects in the benzene sandwich dimer were retained even if the substituted benzene was replaced with a hydrogen atom, suggesting that the changes in the aryl π -electron density are not so critical in determining the outcome of the stacking

interaction.^{351,451,452} Recently Wheeler et al., on the basis of *ab initio* computational data, developed simple predictive models of the strength of stacking interactions between heterocycles commonly found in biologically active molecules and the amino acid side chains of phenylalanine, tyrosine, and tryptophan.⁴⁵⁶

In 2014, Sherrill and Parrish, by calculating the energy contribution to the π -stacking interactions, showed that both Hunter and Wheeler models may explain the changes in interaction energy, but that the Wheeler–Houk picture is usually dominant.⁴⁵⁷ Recently, substituent– π interactions associated with aromatic stacking interactions were experimentally measured by Li, Shimizu et al.,⁴⁵³ and also determined by Cabaleiro-Lago, Rodríguez-Otero et al. through calculations.⁴⁵⁸ The authors confirmed that in monosubstituted benzene dimers the changes on electrostatics, as the substituent changes, is mainly controlled by the direct interaction of the substituent and the other phenyl ring. Otherwise, the contribution from the interacting rings is smaller.

Face-to-face model



T-shaped model

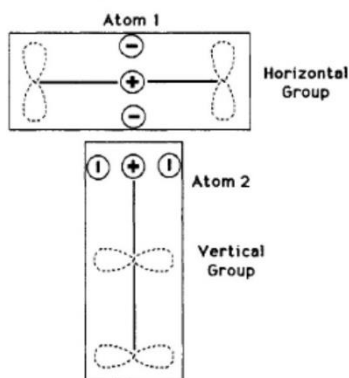


Figure 33. Schemes of the face-to-face and T-shaped π -stacked geometries. Adapted with permission from ref. 448. Copyright 1990 American Chemical Society.

Actually, it was also evidenced that a combination of both effects generates the overall result, and the two contributions become similar in magnitude if the substituent is located further away. Indeed, at closer distances, the interaction of the substituent and the other ring also dominates compared to changes associated with the substituted ring. Otherwise, as the substituent is located further away, its contribution really decreases and the contribution from the ring becomes more

relevant.⁴⁵⁸ Accordingly, very recently Zarić et al. showed by high-level *ab initio* calculations that the most stable stacking for benzene-cyclohexane is 17% stronger than that for benzene-benzene.⁴⁵⁹ However, as these systems are displaced horizontally the benzene-benzene attraction retains its strength. At a displacement of 5.0 Å, the benzene-benzene attraction still maintains ~70% of its maximum strength, while benzene-cyclohexane attraction decreases to ~40% of its maximum strength. These results indicate that aromatic rings can recognize each other at relatively large distances.

In 2008, Grimme calculated interaction energies for a series of complexes accounting for contribution of dispersive forces to the overall energy, recommending that the term “ π - π stacking” should be used as a geometrical descriptor of the interaction mode in unsaturated molecules, and to understand π - π interactions as a special type of electron correlation (dispersive force) effect that can only act in large unsaturated systems when they are spatially close, which is only possible in the stacked orientation.⁴⁶⁰ On the other hand, it is now well recognized that both sandwich and parallel displaced π - π configurations are bound primarily by dispersive interactions.

3.4 Molecular modelling and experiments: a synergistic and necessary interplay

The existence of noncovalent interactions enables the formation of stable intermolecular complexes, intermediates and transition states (TSs) controlling processes and their mechanisms. On the other hand, supramolecular assemblies represent the main tool to identify and analyze noncovalent interactions which express themselves in complex formation.

The knowledge of noncovalent interactions has been acquiring for decades through a synergistic interplay between theory and experiments. On one hand, calculation of interactions energies and complex structures has to be addressed to understand the fundamental nature of noncovalent forces and explain experimental trends. On the other hand, model calculations are based on a number of assumptions and approximations. Some concepts such as orbitals, correlation, bond orders, chemical bonds do not really exist and are not physically measurable, even if they play an important function in bonding understanding, arising from approximations made in order to describe the system mathematically. As stated by Politzer et al. “*It is important to understand, however, that models are simply models; one should not be tempted to think of them as reality*”.³⁰² Thus, the experimental data serve to check the accuracy of the calculations, for verifying assumptions, approximations, and parameters of the calculation methods.

In the last few decades, descriptions of noncovalent interactions at computational level have seen huge advancement but some shortcomings still remain. First, the most advanced theoretical methods shed light on the chemo-physical description of single noncovalent interactions, providing a huge contribution to the understanding of their nature, but in practice these methods are accessible

for small- and medium-size supramolecular systems exclusively. In general, high-level treatment of real-life systems needs to partially neglect boundary conditions and/or to build simplified models as approximate representations of the reality. Thus, as a matter of fact, the computational treatment of most real-life applications with explicit consideration of solvent effects still need further improvements. This is a key question because some interactions such as HB, dispersive, and polar forces are strongly dependent on the medium. For instance, hydrophobic interactions are solvent-driven forces. In particular, it is worth stressing that currently available experimental and theoretical tools are not yet sufficient for understanding, and for really adequate description, of fine mechanisms of enantioselective recognition processes which are characterized by very low values of free energy differences between two competitive pathways ranging from 0.1 to few kcal/mol.

As noted recently by Hobza, the ongoing improvement in both software and hardware used to address issues in chemistry and other natural sciences have been decreasing the level at which one needs to understand a theory to run computations. Thus, this positively allows chemists with limited programming and computational science abilities to compute and model experimental molecular systems. On the other hand, *“it reduces the barrier for doing computational science, often negatively affecting the quality and/or impact of the output”*.⁶⁸ We say that this consideration is definitely true. However, it is equally true that theoretical scientists still have been discussing about several issues concerning the nature and treatment of noncovalent interactions.^{461,462} Even if different points of view of the same horizon have allowed this field to grow over time, the multitude of theoretical techniques, methods and approaches available nowadays makes computational approaching to noncovalent interactivity rather challenging for non-theoretical chemists. This aspect has been clearly highlighted by Politzer and Murray recently, in their review discussing the main approaches to describe chemical bonding: *“Sometimes, it seems that they have in common only the conviction of each set of respective advocates that their approach is absolutely correct and others are absolutely wrong”*.²⁸⁸

Thus, as noted by Hehre *“the chemist is confronted with “too many choices” to make, and “too few guidelines” on which to base these choices”*.⁴⁶³ This lack of guidelines and benchmark protocols, in particular for large systems in non-gaseous environment, results in the fact that experimental scientists often use trial and error strategies to find the proper computational method to treat an experimental molecular system, by simply picking the model that best fits with experimental data but without any consideration about the actual reasons of this agreement. In other cases, the computational approach is tailored to the features of the specific experimental system, in terms of interacting partner structures and medium composition and polarity, with the consequence that several results are strongly method- and case-dependent. In practice, all choices are the result of a fine equilibrium between two pivotal factors: a) the urgency to obtain theoretical results as reliable as

possible to describe molecular reality, and b) approximations, which in general are imposed by computational time and performances, and by the complexity of the modelled molecular system.

These terms of discussions reveal that the community of scientists working in the field of noncovalent interactions is divided in theoretical and experimental scientists which tend to remain apart from each other behind their respective needs and convictions. A subtle controversy which has been recently summarized by Clark *“I think that it is the theoreticians’ responsibility to get their act together and stop arguing about how many angels can dance on the head of a pin. We really cannot expect experimentalists to appreciate, for instance, that many of their favourite concepts are models of theoreticians, who should know better, continue to indulge in fake controversies about the exact nature of weak interactions”*.⁴⁶¹ To solve this question and improve quality and reliability of applications of theoretical and computational methods to real-life chemistry, in the next future will be necessary to develop a new and common level of knowledge where experimental and theoretical approaches integrate each other more deeply.

Given this scenario, a comprehensive compilation of theoretical and experimental studies on noncovalent interactions published so far has not been attempted herein. In this regard, we refer the reader to excellent reviews and books which have summarized and highlighted the advancements in this field at both experimental^{163,64,274} and theoretical^{61,66,68,287,302,304,348,464-466} level.^{72,305,317,322,325,355,467-472} Rather the sections below intend to guide the reader across theoretical and experimental approaches currently available to explore noncovalent interactions, in particular addressing subtle issues, advantages and limitations.

3.4.1 Van der Waals radius

The atom of each element is characterized by an atomic size, considering different sizes for the atom as ion, as bound in a molecule, and as connected through noncovalent interactions. In most cases, these sizes have been derived from experimental interatomic distances, and correspond to ionic, covalent, and vdW radius (r_{vdW}), respectively.⁴⁷³ In particular, the assignment of the r_{vdW} to a bound atom in a molecule originates from the need to assign a size to the atom in its non-bonded directions. Indeed, a commonly used criterion to assess the occurrence of a close contact, which may indicate the presence of an attractive noncovalent interaction, is an interatomic distance shorter than the sum of the r_{vdW} of the interacting atoms. The more these two atoms have penetrated their vdW spheres, the stronger the interaction is considered to be. By comparing the sum of the r_{vdW} and the observed interatomic distance of the interacting atoms, the penetration degree of the vdW spheres is usually evaluated as percentual reduction of the sum of r_{vdW} of the interacting atoms.^{474,475} For instance, given an interaction between oxygen and iodine atoms, having r_{vdW} of 1.52 and 1.98 Å,⁴⁷⁶ respectively, a distance of 3.33 Å between the two interacting atoms corresponds to a 95% percentage of the sum of

their r_{vdW} (3.5 Å), with a percentual reduction of -4.8%, calculated on the basis of the equations (4) and (5):

$$d\% = 100 \times \{(d_{O...I}) / [r_{vdW} (O) + r_{vdW} (I)]\} \quad (4)$$

$$\text{penetration degree (\%)} = 100 \times \{(d_{O...I}) / [r_{vdW} (O) + r_{vdW} (I)] - 1\} \quad (5)$$

The use of r_{vdW} assigned to atoms is widespread in structural chemistry and crystallography. In the last three decades, the criterion based on the r_{vdW} to identify noncovalent interactions has been matter of discussion because its application requires caution and flexibility as stressed by some authors.^{473,477,478} Indeed, some questions have been addressed over time, and as a result nowadays r_{vdW} derived from various sources are available for hydrogen and atoms of Groups 13-17⁴⁷⁷ (Table 4) as well as for transition metals and uranium elements.⁴⁷³

A first set of values were proposed by Pauling.^{399,479} The most used r_{vdW} in literature are those of Bondi which dates back to 1964, and are based on a combination of crystalline, gas phase, and liquid properties.⁴⁷⁶ It is interesting to note that at the end of his paper Bondi stated “*It cannot be overemphasized that the van der Waals radii of this paper have been selected for the calculation of volumes. They may not always be suitable for the calculation of contact distances in crystals*” acknowledging the shortcomings of his system.

Table 4. van der Waals radii from various source for hydrogen and atoms in groups III-VII. Values are given in angstrom (Å)

Atom	Pauling ³⁹⁹	Bondi ⁴⁷⁶	Badenhoop/ Weinhold ⁴⁸¹	Rowland/ Taylor ⁴⁸⁰	Batsanov ⁴⁸²	Alvarez ⁴⁷³	Chernyshov/ Pidko ⁴⁸³
H	1.2	1.20	1.42	1.10	--	1.20	1.21/1.29
B	--	--	1.78	--	1.8	1.91	--
C	--	1.70	1.62	1.77	1.7	1.77	1.87/1.91
N	1.5	1.55	1.63	1.64	1.6	1.66	1.76
O	1.40	1.52	1.46	1.58	1.55	1.50	1.65/1.74
F	1.35	1.47	1.27	1.46	1.5	1.46	1.55
Al	--	--	2.30	--	2.1	2.25	--
Si	--	2.10	2.21	--	2.1	--	--
P	1.9	1.80	2.44	--	1.95	1.90	--
S	1.85	1.80	2.16	1.81	1.8	1.89	1.95
Cl	1.80	1.75	1.89	1.76	1.8	1.82	1.91
Ga	--	--	--	--	2.1	2.32	--
Ge	--	--	--	--	2.1	2.29	--
As	2.0	1.85	--	--	2.05	1.88	--
Se	2.00	1.90	--	--	1.90	1.82	2.04
Br	1.95	1.85	--	1.87	1.90	1.86	2.00
In	--	--	--	--	2.20	2.43	--
Sn	--	--	--	--	2.25	2.42	--
Sb	2.20	--	--	--	2.20	--	--
Te	2.20	2.06	--	--	2.1	1.99	--
I	2.15	1.98	--	2.03	2.1	2.04	2.17

First, as noted by Alvarez,⁴⁷³ the Bondi's radii are available for only 38 elements, and these radii show no clear periodic trends and, in some cases, they are close to the respective covalent radii.

On the other hand, later Rowland and Taylor, deduced r_{vdW} , which were found to be consistent with those proposed by Bondi, through a statistical analysis of the intermolecular contacts extracted from XRD crystal structures.⁴⁸⁰ In 1997, Badenhoop and Weinhold computed a set of effective *ab initio* r_{vdW} for free and covalently bonded atoms and ions of H-Ar ($Z = 1-18$) determined using a helium atom probe.⁴⁸¹ They examined the degree of anisotropy, dependence on charge state, and the *ab initio* steric force (gradient of steric energy at vdW contact) as a measure of “hardness” of the atomic vdW spheres. Comparison with empirical r_{vdW} available at that time showed reasonable agreement, with some exceptions, attributed by the authors, to a wider range of variability and anisotropy for the computed values compared to any fixed constant radius derived experimentally as intermediate value. In 2001, Batsanov reported data for 68 elements, including some transition metals.⁴⁸²

More recently, Alvarez proposed a method to derive representative r_{vdW} of as many elements as possible from the structures reported in the CSD. Given the element E, with an unknown r_{vdW} , and the reference element X, with a known vdW radius, r_X , the method was based on the extraction of the r_{vdW} for E from the distances of the interatomic contacts $\text{E}\cdots\text{X}$.⁴⁷³ For this purpose, the method considers the distribution of interatomic E–X (bonding) and $\text{E}\cdots\text{X}$ (non-bonding) distances (Figure 34), where R_E and R_X are the covalent radii, g_1 and g_2 indicate the lower and the upper limits of the vdW gap (the longest bonded and shortest non-bonded distances, respectively), r_E and r_X are the r_{vdW} , 2.35σ is the width of the vdW peak at half height of the distribution curve, z indicates the borderline between the vdW peak and the region of random distribution of atom pairs, and d_{max} corresponds to the maximum of the distribution function.

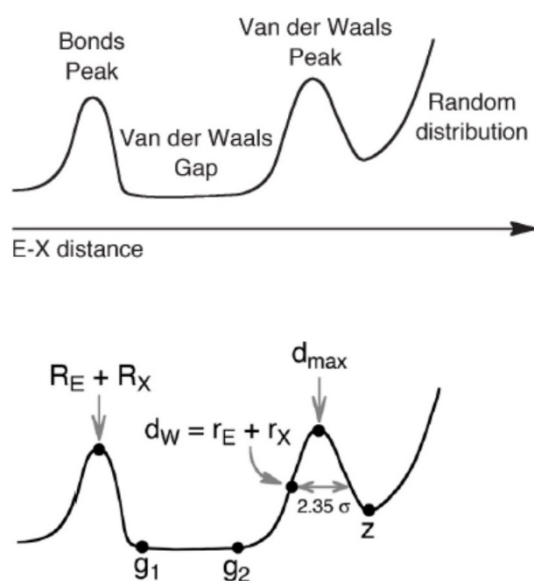


Figure 34. Distribution function of the generic interatomic distances E–X (bonding) and $\text{E}\cdots\text{X}$ (non-bonding) extracted from CSD. Adapted with permission from ref. 473. Copyright 2013 Royal Society of Chemistry.

Given that, the region of the short distances corresponding to the chemical bonds, the vdW gap between covalent and noncovalent bond regions, where practically no structures were found, and the region of noncovalent interactions could be identified in the graph. On this basis, the analysis of millions of interatomic non-bonded distances allowed for proposing the set of r_{vdW} reported in Table 3. It is worth mentioning that the profile of the distribution function may deviate from that depicted in Figure 34, depending on the specific system $E \cdots X$ under evaluation.

Very recently, considering that about 2% (> 4000) of organic molecular crystals in the CSD do not contain intermolecular contacts shorter than the sum of Bondi's radii, Chernyshov, Pidko et al. described an approach for the analysis of noncovalent interactions in the CSD, and determination of r_{vdW} using the line-of-sight concept.⁴⁸³ It considers a pair of atoms as interacting only when they "see" each other because no other atom in the structure intrudes between them, or shields them from one other. Through this approach, 224 001 CSD entries were processed, 40 000 000 intermolecular line-of-sight contacts were extracted and statistically analyzed, obtaining a set of r_{vdW} accounting for atomic specificity, anisotropy, and steric effects of intermolecular interactions. For instance, for H in the system $C-H \cdots X$, $X \neq H$, a value of 1.21 Å was determined, whereas 1.29 Å for the HB system $C-H \cdots H-C$. Depending on the atom type, for C_{sp2} , C_{sp3} , O_{sp3} , and O_{sp2} , radii of 1.87, 1.91, 1.74, and 1.65 Å were derived.

Thus, the question of choosing the proper set of r_{vdW} to determine if an interatomic contact is really a noncovalent interaction is not a trivial task. For instance, Politzer et al. reported, for the $N \cdots S$ contact in the complex $H_3N \cdots S(CH_3)OCH_3$, an interaction distance of 3.888 Å.³⁵⁷ Referring to Table 4, the sum of Bondi's nitrogen and sulfur r_{vdW} is 3.35 Å, whereas the sum of the Alvarez's values is 3.55 Å. Thus, in this case both systems predict that there is no interaction, despite a relatively significant interaction energy of -6.1 kcal/mol. Otherwise, for the complex $H_3N \cdots P(CH_3)_2OCH_3$, the same authors computed an interaction energy of -2.9 kcal/mol and a $N \cdots P$ distance of 3.488 Å.³⁵⁷ In this case, the sum of the Bondi r_{vdW} is again 3.35 Å, indicating no interaction. On the contrary, the values of Alvarez give a sum of 3.56 Å, indicating an interaction. On the other hand, as stated by Dance,⁴⁷⁸ "*crystal packing analysis should not be limited to distances smaller than the vdW radii sum, and [...] the majority of vdW contacts are beyond that distance*". This consideration emerges from the fact that r_{vdW} are obtained from intermediate values of observed interatomic distances. On this basis, a number of noncovalent interactions that have separations greater than the vdW sum would be overlooked through the assumption that a noncovalent interaction must have an interatomic separation less than the sum of the respective vdW radii.^{473,478}

The concluding remark of this discussion is that an interatomic separation less than the sum of the vdW radii is a sufficient but not a necessary criterion to demonstrate the existence of an

interaction. For example, in the solid state two atoms may be forced close together without an attractive interaction by crystal packing forces, thus in this case it would be incorrect to refer to a noncovalent bond.⁴⁸⁴ Analogously, if the distance is higher than the sum of r_{vdW} , there may or may not be an interaction.⁴⁷⁷ In this case, other criteria should be considered to identify correctly noncovalent interactions such as other geometrical parameters and complex energy. Moreover, if the matter requires attention for interactions studied at the solid state, even more attention is necessary in solution where the molecules constituting the medium may assist, interfere and modulate noncovalent interactions between the interacting partners.

In addition, it has to be considered that the concept itself of the r_{vdW} is based on some approximations. First, assigning a single non-bonded radius to an atom, which is part of a molecule, assumes that the non-bonded portion of that atom is spherically symmetrical. However, several studies demonstrated that a covalently bonded atom tends to be anisotropic, with a smaller radius in the direction opposite to the bond than in directions perpendicular to it.^{405,408,477,485} The second approximation concerns the fact that, given an atom, as a matter of fact the same r_{vdW} is used in different molecular contexts.⁴⁷⁷

3.4.2 Methods, functionals and basis sets

Molecular structures and energetics can be calculated by means of *quantum mechanics* (QM) and *molecular mechanics* (MM).⁴⁶³

QM methods derive from the time-independent Schrödinger equation. Molecules are treated in terms of interactions among nuclei and electrons, and molecular geometry as minimum energy arrangements of nuclei. The solution of the equation is in terms of motions of electrons, but it can be solved exactly only for a one-electron system (hydrogen atom and molecular hydrogen ion) and, consequently, its solution for many-electron systems requires the use of approximations. The nature of these approximations determines the features of QM methods. The term “*ab initio*” is used with meaning of “from first principles”, implying that few approximations are made, and that the adopted methods are pure from a theoretical point of view. The Born-Oppenheimer approximation simplifies the Schrödinger equation for molecular systems, assuming that the nuclei are fixed. Actually, motion of nuclei is “slow” compared to the speed of electrons. Thus, in quantum chemistry, the Schrödinger equation is solved as a function of the electronic variables, keeping “fixed” the values of the nuclear coordinates.

The *Hartree-Fock* (HF) *approximation* replaces the “correct” description of electron motions by a picture in which the electrons behave essentially as independent particles. In practice, it is assumed that the electron is moving within an average field created by all the other electrons. In general, the HF approximation provides the bases for a number of models. In *semiempirical*

models,^{465,486,487} additional approximations as well as empirical parameters are introduced to greatly simplify the calculations. In these models, the problem is simplified by considering valence electrons only, whereas electrons associated with the core are neglected. AM1 (Austin Model 1) and PM3 (Parametric Method 3) are popular semiempirical schemes. The main applications of semiempirical methods falls in the description of chemical bonding, thus several articles in this field focused on heats of formation, structures, and other properties of small molecules.⁴⁶⁵ On the other hand, if *ab initio* QM methods are too expensive and conventional classical force fields are not adequate for certain applications, semiempirical methods may represent the best balanced choice, in particular in condensed phase, while. Nevertheless, these methods present some deficiency to describe noncovalent interactions, in particular dispersive forces, due to the lack of electron correlation. Hobza et al. investigated the performance of PM7 and various variants of PM6 methods for different types of noncovalent interactions, noting that these methods provide significant improvement when compared to other semiempirical models. However, relatively large errors of PM7 for the interaction energy calculations of dispersive force-bound complexes and water clusters, together with large deviations of water cluster optimization, were found to be a limiting factor in the description of noncovalent interactions.⁴⁸⁶

The HF approximation is also the basis for the so-called Hartree-Fock molecular orbital methods. In this case, a type of atomic orbital (AO) basis set is used to construct molecular orbitals (MOs), via the “linear combination of atomic orbitals” (LCAO). The set of MOs leading to the lowest energy are obtained by a process referred to as a “self-consistent-field” (SCF) procedure, in which electron correlation is described in a mean-field way. Energy minimization (geometry optimization) is a process which allows for predicting structural and electronic features of molecules through the following steps: *a*) on the basis of the Born-Oppenheimer approximation, electrons move around fixed nuclei () until they reach a SCF, where the attractive and repulsive forces of all electrons with themselves and the stationary nuclei are in a steady state;⁴⁸⁸ *b*) then, through an iterative process, the nuclei move until the energy of the entire system remains stable. The term *ab initio* is commonly used to describe HF models, but it is also applied more generally to all models arising from “non-empirical” approaches to solve the Schrödinger equation.

Nevertheless, this type of approximation does not provide an adequate description of the impact of the motion of one electron on the motions of the other electrons (electron correlation). Indeed, the view of the electrons as independent particles leads to overestimation of the electron-electron repulsion energy and total energy. Introducing electron correlation produces a lessening of the electron-electron repulsion energy and a lowering of the total energy. In this perspective, two different approaches can improve the HF models. One approach is based on the DFT, with the introduction of

an explicit term to account for the way in which electron motions affect each other. Density functional models are based on the electron density, $\rho(\mathbf{r})$.⁴⁸⁹⁻⁴⁹² These methods offer the advantage of not being significantly costlier than HF methods. Both HF and DFT methods can be applied to molecular systems of moderate size (50-100 atoms). So-called “pure” DFT methods include Becke-Perdew (BP), and popular Becke-Lee-Yang-Parr (BLYP) methods. For description of dispersive forces, DFT methods present some deficiency which may be corrected including focused dispersive force-correction schemes.⁴⁹³ As a second approach, *WF-based electron correlation methods*⁴⁶⁴ concentrate on the design of corrections to the WF beyond the mean-field HF description, in order to describe with higher flexibility the electron motions. Configuration interaction (CI), Møller-Plesset (MP)⁴⁹⁴ and coupled cluster singles and doubles (CCSD) models belong to this class of methods which are significantly costlier than HF models. The second-order MP model (MP2) is widely employed. Higher-order MP models (MP3, MP4, etc.) have been formulated, but in practice are limited to very small systems. The CCSD(T) is considered the “gold standard” quantum chemical method providing accurate results, which has been used as benchmark to evaluate the accuracy of lower computational methods.⁴⁹⁵

A *basis set* is the set of functions combined linearly to model molecular orbitals. Basis functions represent the atomic orbitals of the atoms and are introduced in quantum chemical calculations because the equations defining the molecular orbitals are otherwise very difficult to solve. These orbitals can be roughly classified as minimal (for orbitals 1s, 2s, and 2p), Slater-type orbitals (STO), and Gaussian-type orbitals. In practice, basis sets for use in HF, density functional, MP and CI calculations make use of Gaussian-type functions. Commonly used “*all electron*” *basis sets* are STO-3G, 3-21G, 6-31G, 6-311G, and with the exception of STO-3G and 3-21G, additional polarization functions and/or with diffuse functions can be added to any of these basis sets. In the STO-3G all basis functions are either spherical, or come in sets which describe a sphere. This means that atoms with spherical molecular environments will be better described than atoms with aspherical molecular environments. Moreover, basis functions are atom centered, and this feature restricts their flexibility to describe electron distributions between nuclei. It is worth mentioning that polarization functions are absent in the minimal STO-3G and split-valence 3-21G basis sets and, consequently, these basis sets are not adequate for use with correlated models.

Split-valence basis sets represent core atomic orbitals by one set of functions and valence atomic orbitals by two sets of functions. A basic terminology in this field can be summarized as follows: *a*) 3-21G and 6-31G are the simplest split-valence basis sets; *b*) in the 3-21G basis set, each core atomic orbital is expanded in terms of three primitive Gaussian functions for inner core electrons, two Gaussian functions for small valence orbitals and one Gaussian for extended valence orbitals; *c*)

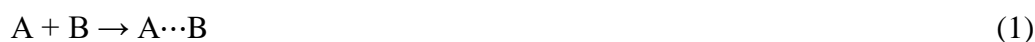
the 6-31G basis sets are constructed with core orbitals described in terms of six Gaussians and valence orbitals split into three and one Gaussian components; *d*) the introduction of the *polarization functions* (6-31G* and 6-311G**, or 6-31G(d) and 6-311G(d,p)) allows for the displacement of the electron distributions away from the nuclear positions. In this case, d-type functions on main-group elements (where the valence orbitals are of s and p type), and p-type functions on hydrogen (where the valence orbital is of s type) are added; *e*) *diffuse s- and p-type functions* on heavy (non-hydrogen) atoms, designated by “+” as in 6-311+G**, may be added to the basis sets. Diffuse functions may be also added to hydrogens, in this case designated by “++” as in 6-311++G**.

MM is a nonquantum mechanical method to model structures, energies, and some properties of molecules. While the exact-theory based on the Schrödinger equation considers a model consisted of nuclei and electrons, MM considers molecules as a combination of atoms held together by the elastic forces.⁴⁸⁸ These forces are defined in terms of internal coordinates such as bond lengths, bond angles, and torsion angles and related potential energy functions. In MM, the potential energy surface of a molecule is determined by using an empirical force field which adjust atom positions on the basis of known structural data. Geometry optimization is obtained by minimizing internal energy, namely by moving the particles toward their equilibrium positions. Thus, the MM energy of a molecule derives from contributions arising from distortions from ideal bond distances, bond angles, and torsion angles, together with contributions due to vdW and Coulombic noncovalent interactions. For instance, for the noncovalent component, the typical force field includes Coulombic terms between point charges or higher order multipoles, Lennard-Jones terms for vdW interactions, and sometimes polarizable dipoles, fluctuating charges, or charge-transfer terms. Classical force fields are very important for condensed-phase simulations due to their computational, and their accuracy for determination of population of various conformations can be rather high for well-designed systems. However, as noted by Christensen at al.,⁴⁶⁵ the parametrization of a force field may be a laborious process that requires extensive tests and refinement of parameters that are not easily decoupled. In this regard, it is worth mentioning that, in more recent years, *ab initio* force fields have been developed and applied, in which parameters are computed rather than fitted.⁴⁹⁶

3.4.3 Computational energetic measures

The knowledge of the energetic contribution to binding from noncovalent interactions is of fundamental interest for several reasons. First, it sheds light on chemical, biochemical and biological binding mechanisms underlying supramolecular binding. Information on noncovalent interaction contribution to the overall binding energy is a pivotal aspect for rational design and optimization of supramolecular complexes of practical interest as well as of synthetic, catalytic, and separation processes involving supramolecular complex formation.

With the aim to calculate the energetics of noncovalent interactions, one can consider the interacting system as a single molecule calculating *binding* and/or *interaction energy*.⁶¹ The strength of a covalent bond represents the energy required to dissociate this bond, thus the dissociation of a noncovalent bond into its constituent monomers can be taken as the bond strength. This quantity is usually defined as the energy of the association reaction (1), ΔE , which is the difference in purely electronic energies of products and reactants and is commonly indicated as the binding energy (E_b),



The interaction energy (E_{int}) is similar to E_b , but in this case the energies of the A and B constituents are not taken in their isolated optimized geometries, but rather in the geometries they adopt within the optimized $A \cdots B$ complex. As a matter of fact, E_{int} results as a measure of the actual interaction occurring within this complex, after the conformational adjustment of the monomer geometries. E_{int} differs from E_b by the energy required to conformationally adjust each optimized monomer within the complex (E_{conf}). In general, the geometries of A and B in the complex are not very dissimilar to the geometries as isolated monomers, thus E_{conf} is small, and $E_{\text{int}} \cong E_b$.

An approach to analyze intermolecular interactions is *energy decomposition* which provides information on energy components such as electrostatics, dispersion, polarization or induction, charge-transfer, exchange, Pauli repulsion, and orbital overlap. This approach may be advantageous to describe noncovalent complexes and classify them according to their nature. As explained recently by Scheiner, taking the XB in the complex $F_3CBr \cdots NH_3$ as prototype system (Figure 34),⁶¹ different energy contributions emerge as the intermolecular distance (R), between interacting Br and N, changes. In Figure 35, the $(\mu-\mu)$ dipole-dipole interaction is illustrated as the red curve, the electrostatic interaction energy as the black curve, dispersion and overall energy as the green and blue curves, respectively. The $(\mu-\mu)$ interaction undergoes only a gradual increase in the absolute value as the two monomers approach one another, remaining below 0.5 kcal/mol even for an intermolecular distance as short as 4 Å. Even if it is comparable to the $\mu-\mu$ interaction for very long distances, the electrostatic term quickly diverges and becomes much more negative, even for intermolecular distances as long as 8 Å. As the two interacting atoms approach one another at distances shorter than 8 Å, the shorter-range components of the interaction, such as induction and dispersion, begin to emerge. Therefore, the full quantum mechanical interaction energy is more negative than the electrostatic for smaller R . Showing a stronger sensitivity to R than the electrostatic component, both induction and dispersion become prominent contribution as R continues to decrease.

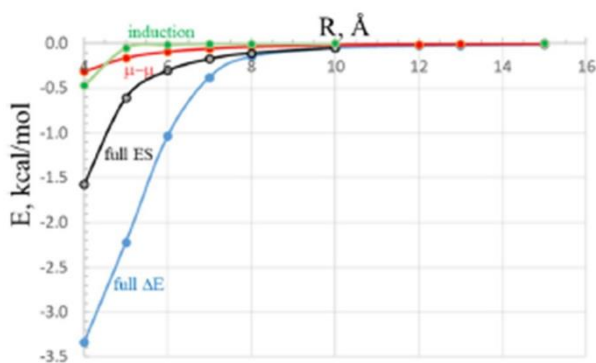


Figure 35. Behavior of various energetic properties of the $F_3CBr \cdots NH_3$ system in terms of intermolecular $R_{Br \cdots N}$ distance. Reproduced with permission from ref. 61. Copyright 2020 AIP Publishing.

It has to be noted that the results of the decomposition procedures are method-dependent. Indeed, in the course of time, a number of schemes have been developed to describe the physical reality of intermolecular binding.^{68,438,497} In this regard, Hobza stressed that, when investigating the nature of molecular binding, it is strongly encouraged to refer to a particular decomposition scheme, express all definitions necessary to understand all energy terms, and keep in mind that it can be difficult, if not impossible, to compare results among various schemes.⁶⁸ Another flaw emerges from the fact that some energy components are real and physically measurable, while others are simply constructs derived from a mathematical model.³⁰² Moreover, many components are not independent of each other, so that different decomposition schemes can increase the role of a component at the cost of another.³⁰²

Among available partition schemes, the method based on symmetry-adapted perturbation theory (SAPT)⁴⁹⁸⁻⁵⁰⁰ was introduced in the 1990s, and it has become the most widely used energy decomposition scheme. It computes the interaction energy directly as a sum of physically distinct electrostatic, exchange repulsion, induction, and dispersive contributions, which allows for better insight into the nature of intermolecular noncovalent interaction. The SAPT E_{int} ^{65,501} is given as

$$\begin{aligned}
 E_{int} &= E_{elst}^{(1)} + E_{exch}^{(1)} + E_{ind}^{(2)} + E_{exch-ind}^{(2)} + E_{disp}^{(2)} + E_{exch-disp}^{(2)} = \\
 &= E_{elst} + E_{exch} + E_{ind} + E_{disp}
 \end{aligned}
 \tag{6}$$

where $E_{elst}^{(1)}$ refers to the first-order electrostatic (polarization) energy, $E_{exch}^{(1)}$ is for the first-order valence repulsion energy due to the Pauli exclusion principle, $E_{ind}^{(2)}$ is the second-order induction energy, $E_{exch-ind}^{(2)}$ refers to the second-order induction-induced exchange energy, $E_{disp}^{(2)}$ represents the second-order dispersion energy, and $E_{exch-disp}^{(2)}$ is the second-order dispersion-induced exchange energy. However, this method also has the disadvantage of being extremely difficult to perform with many or large atoms, often providing inaccurate results in these cases.^{66,502} Moreover, Misquitta and Stone evidenced that the perturbation expressions for exchange-repulsion and charge-

transfer, which are opposite in sign, contain terms that make their energies too large in magnitude.⁵⁰³ This makes a separate estimation of these two quantities meaningless. The authors recommend that any SAPT analysis that reports large and opposing exchange-repulsion and charge-transfer energies should be treated with caution.

NBO analysis provides an alternative and useful approach to understand the nature of binding, in a donor-acceptor perspective.^{469,504,505} As exemplified by Scheiner,⁴⁶⁹ NBO analysis of a dimeric complex provides a series of second-order perturbation energies that correspond to the energetic consequence of the transfer of charge from one orbital of a first molecule, to another orbital of a second molecule. For instance, in the case of a HB-based complex A–H··D, the energy corresponds to the transfer of charge from the lone pair of the HB acceptor D to the σ^* antibonding orbital of AH. It is just this increment of density in the σ^* antibonding orbital of AH which is the source of the observed red-shifting of the A–H covalent bond in the HB complex. It has to be noted that NBO cannot distinguish adequately between polarization and charge-transfer energies.^{469,302,504}

Politzer, Murray and Clark proposed a unifying view, alternative to the concept of energy decomposition, arguing that the only nature of any interatomic interaction is electrostatics, which includes other contributions such as covalency, London dispersive forces, and polarization.³⁰² In particular, the author stressed that polarization is an observable quantity, whereas charge-transfer between donor and acceptor is not. Indeed, according to Born–Oppenheimer approximation, molecules are groups of fixed positive nuclei within clouds of indistinguishable electrons, and no atoms or bonds can be identified under these conditions, so that electrons cannot be assigned to particular atoms or molecules, whereas the model of charge-transfer implies the definition of some arbitrary way which defines borders between atoms. The theoretical bases of the electrostatic view lie in the Coulomb's law which, in its original formulation "*Il résulte [...] que l'action repulsive que les deux balles électrisées de la même nature d'électricité exercent l'une sur l'autre, suit la raison inverse du carré des distances*",^{304,506} defines the inverse distance dependence of the interaction energy between two charged bodies. This dependence is the basis of energy calculations in quantum chemistry, the potential energy part of a molecular Hamiltonian in $H\Psi = E\Psi$ containing only the Coulombic term, in terms of the reciprocal distance $1/R_{ij}$ between the particles i and j . Later proposed, the Hellmann-Feynman theorem considers a set of fixed nuclei with electrons moving among them according to the principles of wave mechanics, and states that the force component acting on a nuclear coordinate is the force which would be calculated by pure classical electrostatics acting on this nuclear coordinate, resulting from the electronic charge cloud and all other nuclei.^{294,372,375,507} Thus, if the electronic density of a molecule is known, bonding interactions can be determined using purely classical electrostatics.

The view of the noncovalent interactions in terms of electrostatics also represents the basis of the use of V in analyzing bonding which was pioneered by Scrocco and Tomasi.⁵⁰⁸ In 1975, Kollman applied molecular V to HB.⁵⁰⁹ For series of HBs with the same acceptor, ΔE_{int} was found more negative as the $V_{S,\text{max}}$ of the HB donor becomes more positive.⁴⁰³ In the 1990s, Politzer et al. showed that $V_{S,\text{max}}$ on donor hydrogens and the most negative potentials ($V_{S,\text{min}}$) on acceptor sites correlate well with experimentally determined measures of HB donating tendencies (α) and HB accepting tendencies (β), respectively,⁵¹⁰⁻⁵¹² α and β correlating with the HB equilibrium constants K ⁵¹³ as

$$\log K \sim \alpha\beta \quad (7)$$

Similar results were obtained in 2004 by Hunter who suggested that equation 7 is equivalent to express the free energy of the HB in terms of the product of $V_{S,\text{min}}$ and $V_{S,\text{max}}$, concluding that “*there is good experimental evidence for the dominant role of electrostatics in intermolecular interactions*”.⁵¹⁴ Later, Politzer and Murray re-formulated the equation using ΔE_{int} instead of the change in free energy,

$$\Delta E_{\text{int}} = c_1|(V_{S,\text{max}})(V_{S,\text{min}})| + c_2 \quad (8)$$

and tested equation (8) with a series of HBs, obtaining the results shown in Figure 36 with $R^2 = 0.931$.⁴⁰³ Recently, the same authors tested, with encouraging results, a modified equation accounting for polarization effects.⁵¹⁵ Indeed, the electrostatic contribution is often modelled using the unperturbed molecules in their equilibrium states, unaffected by the interactions. This may be incomplete because it ignores polarization of the charge distribution of a molecule by the electric field of the other, polarization being an intrinsic and inseparable part of an electrostatic interaction. This inductive effect changes to some extent V of the molecules, and magnitude and location of $V_{S,\text{min}}$ and $V_{S,\text{max}}$. On the other hand, a pure electrostatic treatment is often sufficient at least on a qualitative level or if the electrostatic component of the weak noncovalent interaction dominates. In particular, regions with high (with nucleophile character) and low (with electrophile character) electron density can be identified by $V_{S,\text{min}}$ and $V_{S,\text{max}}$ values, respectively. V analysis may be very useful to study interaction phenomena occurring in the solid state,⁵¹⁶⁻⁵¹⁸ and in solution at biological,^{427,519} synthetic,⁴³⁵ and analytical level.⁵²⁰⁻⁵²²

Given the concepts of phamacophore,²²⁵ chiraphore,²²³ and enantiophore,²²⁴ calculating V_S provides relevant information on the three-dimensional shape of the *-phore* system, on the geometry of the interacting sites, and on the directionality of the noncovalent interactions potentially involved in an enantiodifferentiation mechanism.⁵⁹ As representative examples, in Figure 37 calculated V_S of DFT energy-minimized structures of **7** and *trans*-stilbene oxide (**17**) are reported, where regions of high electron charge density functioning as HB acceptors are colored in red. Even if V_S is not a chiral

descriptor, it may be useful to describe those interactions which, acting in the neighboring chiral environment, govern enantioselective processes.

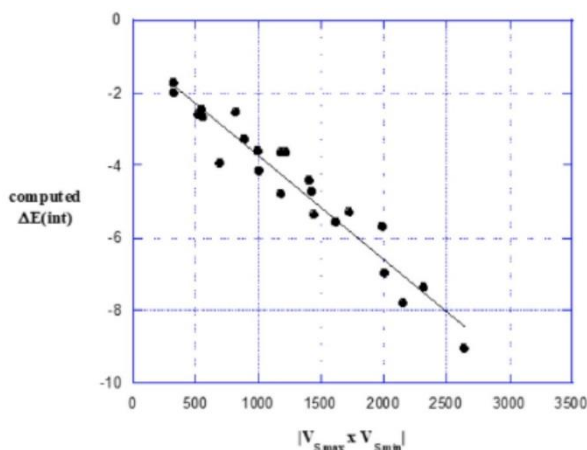


Figure 36. Relationship between computed ΔE_{int} (kcal/mol) and absolute value of product $(V_{S,\text{max}})(V_{S,\text{min}})$ (kcal/mol) for HB complexes. Adapted with permission from ref. 403. Copyright 2020 Springer.

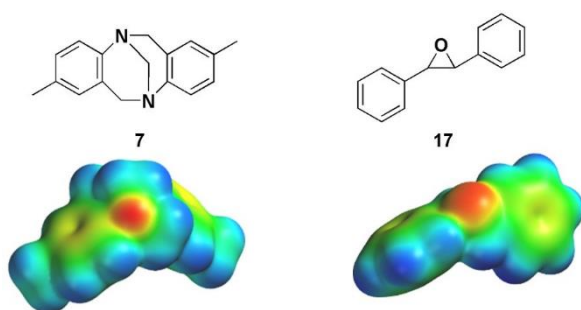


Figure 37. V_S calculated for compound **7** and **17** employing the DFT method, with the B3LYP functional, and the 6-31G** as basis set. Colors toward red depict negative potential, while colors toward blue depict positive potential and colors in between (orange, yellow, green) depict intermediate values of potential.

Concerning the calculation of V and related surfaces, the following aspects have to be highlighted:

1) recently, Murray et al. computed $V_{S,\text{min}}$ and $V_{S,\text{max}}$ values for a series of molecules, some of which contained atoms from the second and third rows of Groups 14, 16 and 17, by using three different methods, HF and the density functionals B3LYP and M06-2X, and numerous basis sets of various sizes.⁵²³ The results of this study suggested that the use of any of the three methods, along with the 6-31G* basis set should produce $V_{S,\text{min}}$ and $V_{S,\text{max}}$ values that are as consistently reliable as those of larger basis sets. The authors stressed that, in terms of the $V_{S,\text{min}}$ and $V_{S,\text{max}}$ calculation, there is no need to use a basis set larger than 6-31G*. Even, if using the 6-31G* basis set is not possible, for instance due to the size of the system, the 3-21G* may be a good alternative. It is worth mentioning

that this evaluation does not apply for calculation of interaction energies which requires proper computational methods/basis sets, accounting for polarization;

2) when V is used to analyze noncovalent interactions, it is computed on the “surfaces” of the molecules, taking the 0.001 au (atomic unit) contour, as suggested by Bader.⁵²⁴ The 0.001 au surfaces are typically beyond the vdW radii of the atoms in the molecules, thus the electrostatic potentials on these surfaces are representative of what an approaching molecule “sees”.⁴⁰⁵ However, in certain cases the 0.001 au isosurface may not be adequate for computation of $V_{S,max}$ on electrophilic regions located on less polarizable atoms such as sulfur, or fluorine.⁵²⁵ In these cases, the 0.002 au isodensity surface has been preferred over the 0.001 au one;⁵²⁵⁻⁵²⁷

3) conformational features of a molecule,⁵²⁷⁻⁵³⁰ as well as the presence of both σ - and π -hole on the same molecule,^{527,531} may impact magnitude and location of $V_{S,min}$ and $V_{S,max}$ values and, consequently, the interaction capability of a binding site, in particular in multi-binding site systems. For instance, in a molecule, electron-rich regions can saturate (stabilize) neighboring positive regions through their negative V ;

4) recently, the reconstruction of calculated $V_{S,max}$ values from atomic or atomic group contributions was performed by Gatti, Peluso, and Mamane,⁵²⁷ by extending the Bader–Gatti source function (SF) for the electron density to V .⁵³²⁻⁵³⁴ In this study, factors affecting σ - and π -holes were decomposed in separate contributions from meaningful moieties of the molecule that can either contribute to or oppose the observed $V_{S,max}$ values, even if these moieties are far from the holes. This type of computational analysis provided unprecedented insights into the factors leading to $V_{S,max}$ value changes and trends.

The *quantum theory of atoms in molecules* (QTAIM) was introduced by Bader. This technique defines the character of the bonding on the basis of the topology of the electron density ρ and its Laplacian $\nabla^2\rho$.⁵³⁵ The QTAIM analysis introduced the concept of “basins” that surround each atom and separate it from the others; the total density within this basin can then lead to the assignment of AIM atomic charges. Between atoms, bond paths are viewed as noncovalent bonding in the context of intermolecular interactions. Along each path, the “bond critical point” is located more or less in the middle between the two atoms. The numerical value of the density ρ and Laplacian $\nabla^2\rho$ at the bond critical point have been shown in many cases to correlate with other measures of the strength of the bond such as distance or energetics. However, this technique has moved some criticism,²⁹² and particularly in the case of weak noncovalent bonds, the characterization of a bonding through QTAIM was shown to be not consistent with other types of analysis.^{536,537}

Currenty, a hot topic concerns the definition of nature of noncovalent interactions given by the relative contributions of electrostatic, dispersion, charge-transfer and polarization components. .

Recently, with the aim of developing a unifying view on this point, Clark proposed that noncovalent interactions can be theoretically analyzed by considering three levels of interaction:³⁰³ i) a first level considering the classical $\delta^+ - \delta^-$ electrostatic interactions (*permanent electrostatic interactions*) that can be explored through the $V_S(\mathbf{r})$ of an isolated molecule, ii) the second level improves the previous type of analysis by introducing the mutual polarization of the interacting molecules (*induced electrostatic interactions*), and iii) the third level includes *dispersion*, which can only be evaluated theoretically because it is not a real and measurable quantity.

3.4.4 Computational treatment of large systems

One of the most important application of computational chemistry concerns large systems where noncovalent interactions occur within biomolecular and host-guest complexes, clusters formed by large molecular ensembles, and at surfaces. Large systems encompass real-life systems where solvation effects play a role in the interaction process. In all these cases, when a microscopic (atomistic) model has to be built as a virtual representation of the real event to predict or to explain the experimental outcomes at molecular level, this task continues to be challenging. In the last few years, it has been frequently stressed that a huge enhancement of computational tools, hardware and software allows molecular modelling to become an essential tool for understanding noncovalent interactions. Even if this wise saying is undeniably true for small systems, the shortcomings arising when large molecular systems have to computationally treated, weakening its strength. In term of QM calculations, it is common practice to consider systems exceeding 100 atoms large and especially challenging (Figure 38).⁵³⁸ As a result, in the last few decades integrating experimental observations and theoretical predictions allowed to improve understanding of noncovalent interactions, but producing significant advancements within the limits of tens-of-atoms systems. For the application of high-level theoretical methods to large system, the question has to be viewed as a many-body problem. Thus, in this cases the main difficulty in predicting noncovalent interactions emerges from the prohibitive expense of computing the correlation energy of electrons.^{66,538,539} Moreover, in general these methods require approximations to be applied to large systems, and this factor increases the uncertainty of the calculations.

As noted by Al-Hamdani and Tkatchenko,⁵³⁸ there is a tendency to exploit the information collected for the small molecular systems to advance atomistic level understanding of more complex systems, such as proteins and other macromolecules. In part, this trend is due to the availability of experimental information regarding small molecular systems and the greater challenges of studying large and extensive systems under vacuum conditions. Nevertheless, some questions have to be addressed:

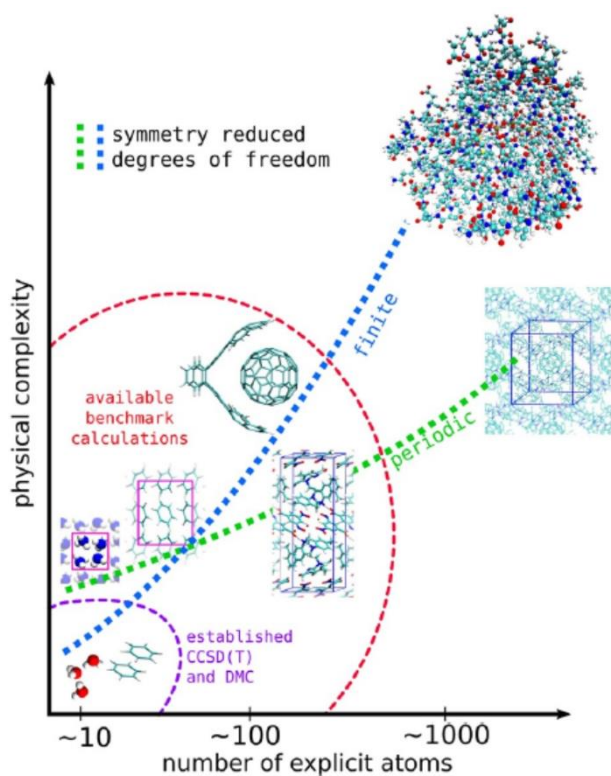


Figure 38. Conceptual overview of the system size and physical complexity of molecular systems. The green and blue dashed lines indicate the computational challenge corresponding to computing periodic and finite molecular systems, respectively. The region enclosed in red dashed line indicates the extent of systems that diffusion Monte Carlo (MC), localized CCSD(T), and wavefunction based methods in general are being applied to. The smallest systems are well established by now using CCSD(T) and diffusion MC methods. Reproduced with permission from ref. 538. Copyright 2019 AIP Publishing.

1) experimental reference information in large systems are based on multiple variables. As a consequence, experimental evidences that are not expected may be obtained on the basis of predictions related to the understanding of small molecules exclusively.⁵³⁸ This is one of the reasons that have limited the prediction ability of calculations applied to large systems;

2) it has to be considered that noncovalently bound molecular complexes can have many accessible meta-stable energy minima in the range of few kJ/mol. For these systems, very accurate predictions or precise measurements have to be made at experimental level;

3) computed interaction energies, in general, are not directly comparable to experimental measurements. Moreover, association constants derived from experimental studies incorporate solvent effects;

4) computational advancements in treating large systems, such as proteins and macromolecules, has been made possible by the evolution of dozens of computational tools, including open-source and commercial packages. Krylov et al. evidenced that if it is true that multiple code bases ensure a robust

software ecosystem in constant growth, this also leads to the lack of algorithmic interoperability between codes resulting in a series of non-confrontable and not homogeneous results.⁵⁴⁰ The consequence may be that often the choice of computational protocols is determined by the methodological availability in specific software packages rather than by the best theoretical considerations.

Given that, aiming at getting a better comprehension of both affinity and binding between interacting partners, theoretical techniques such as MM, molecular docking,⁵⁴¹ Monte Carlo (MC)⁴⁸⁸ and MD simulations^{542,543} are more practicable for large system in the range 500-thousands of atoms.⁵⁴⁴ It is worth mentioning that most software packages and related codes have been developed for biochemical applications in water, specifically tailored for the features of biological interacting partners (protein, enzymes, receptors). This implies that the application of these techniques to non-biological contexts, in particular in organic medium, may be challenging due to the need to adapt available methods and force fields to a different use compared to that they were designed for.

MM methods are widely applied in the case of large molecular systems for which the QM approach is, in general, computationally time-consuming. Considering a large system consisting of two interacting partners, the calculation has to provide results which are representative of the considered experimental system, thus the main issues are where to locate one molecule with respect to the other molecule,^{54,57} and how many complexes must be computed. Molecular docking and MD provide solutions to address these questions by sampling possible reciprocal orientations of the interacting partners and define their initial and equilibrium mutual positioning. In particular, molecular docking is generally used to simulate the interaction between the interacting molecules in order to predict both energy and geometry of the binding. A docking process consists of two general steps, namely conformational search through various algorithms, and scoring or ranking of the docked conformations (mutual orientations of interacting molecules). The most used software package to perform molecular docking is AutoDock,⁵⁴⁵ which employs Lamarckian Genetic Algorithm to identify binding conformations^{57,541} by using geometrical variables which are interaction distance, the mutual orientation between the interacting molecules, and the torsional degrees of freedom of the flexible molecules. MD is a simulation that shows how molecules move and interact over time.^{542-544,546} This approach is based on classical mechanical equations of motion related to the system under investigation consisting of interacting particles. Nowadays, several programs are available for MD simulations including Assisted Model Building with Energy Refinement (AMBER)⁵⁴⁷ and Chemistry at HARvard Macromolecular Mechanics (CHARMM),⁵⁴⁸ among others. The MD protocol consists roughly of six phases: initial assignment, system minimization, heating, cooling, equilibration, and dynamics production.⁵⁷ In MD simulations solvent can be parametrized by treating it explicitly or

implicitly.⁵⁴⁹ Explicit-solvent methods introduce solvent molecules in the virtual system by computing interactions involving solvent atoms, whereas implicit-solvent methods approximate the discrete solvent as a continuum. Moreover, in docking as well as in MD, the proper dielectric constant value can be used to define the screening effect of solvent on noncovalent interactions, with values ranging from 1 (vacuum) to 80 (water).⁵⁷

It is true that classical MD and QM MD approaches represent the major resources available today for modelling the dynamic behavior of large systems with a high number of rotatable bonds. As we mentioned above, the results of this type of simulations is force-field- and software-dependent. So far, just general guidelines on approaches and procedures have been published in this regard, while in most cases tailored computational methods are developed on a case-by-case basis using procedures and force fields adapted to the specific features of the experimental systems.

It is worth mentioning that conventional MM force fields fail to describe the XB and other σ -hole interactions because they do not account for the anisotropic distribution of the electron density. On this basis, several MM approaches to describe σ -hole in halogens^{68,550-556} and chalcogens⁵⁵⁷ were proposed in the last few years and applied successfully to biological⁵⁵⁸ and supramolecular systems.^{559,560} All these methods are based on the concept of modelling the σ -hole as a massless point charge called positive extra point (PEP) by Ibrahim,^{550,551} and later explicit σ -hole (ESH) by Hobza and co-authors.^{554,555} This approach was successfully implemented in the AMBER force fields package, and XBs were also parametrized in CHARMM⁵⁶¹ and GROMOS⁵⁶² force fields. Recently, Costa et al. performed a focused study for the optimization of the geometrical parametrization of the PEP.^{563,564}

In most cases, large supramolecular aggregates are very difficult to characterize at QM level. Despite that, several efforts have been reported in the last few years to improve reliability and accuracy of calculations applied to large systems. Less expensive semiempirical approaches, in particular PM3, and more recent PM6 and PM7,⁴⁸⁶ have shown a good level of reliability in modelling large systems, such as CDs and related complexes, as well as two levels hybrid methods.⁵⁶⁵ These methods are based on the partition of a large system in a QM region and a MM, or a lower level QM region.^{566,567} Recently Grimme et al. also proposed a DFT based composite electronic structure approach to efficiently compute structures and interaction energies in large chemical systems.⁵⁶⁸

In a different perspective, a number of databases have been proposed for understanding noncovalent interactions typically occurring in larger systems such as biomolecules based on high-level calculations performed with small models as benchmark data. In order to have a broader set that is more representative of interactions occurring in biomolecules, Hobza et al. assembled the large S66 dataset, consisting of 66 noncovalent pairs, generated from 14 monomers in various combinations.⁵⁶⁹

The selection of monomers was based on their frequency as motifs or functional groups in the most commonly found biomolecules. The smaller molecules considered in the dataset are generally carriers of the functional group of interest such as MeOH and methylamine, while the larger molecules are actual biomolecular building blocks, such as uracil, N-methylacetamide as a peptide bond model. Then, the same group extended the S66 set, creating the S66x8 dataset.⁵⁷⁰ More recently, Martin et al. reported a revision of the benchmark interaction energies of the S66x8 dataset by using the explicitly correlated MP2 and coupled cluster methods.⁵⁷¹ Performing calculations on the S66x8 dataset, Peccati et al. tested the possibility of computing high-level accurate interaction energies of small non-covalent complexes starting from a DFT energy corrected for dispersive forces, and using descriptors derived from the promolecular density, showing that these local descriptors can reduce to one third the mean absolute error of DFT results at a virtually negligible computational cost.⁵⁷² Working in the frame of the NonCovalent Interaction index (NCI) which enables identification of attractive and repulsive noncovalent interactions from promolecular densities, very recently Peccati, Contreras-García et al. developed a new version of the NCIPLOT code, NCIPLOT4, which allows quantifying the properties of the NCI regions in a fast manner. The tool was applied to access local information in supramolecular chemistry and biosystems at the static and dynamic levels.⁵⁷³⁻⁵⁷⁵

3.4.5 Accuracy of calculations and uncertainty quantification

The term “scientific reproducibility” of experimental results and observations, and theories means that the reliability of these data does not depend on who produces them but rather the same findings should be obtained by anyone performing similar procedures.⁵⁷⁶ Coveney and co-authors observed that for computer modelling three factors assess the reliability of calculations to be compared with existing experimental measurements and to make predictions for which no experimental data are available: a) *validation*, namely the confirmation that the results are in agreement with experiment, b) *verification* that the software does what it is supposed to do, and does not contain any errors arising from an incorrect implementation or incorrect numerical methods, and c) *uncertainty quantification* to identify the source of errors within the model, for instance systematic errors due to parameter estimation.⁵⁷⁶

In classical MD simulations, the lack of reproducibility depends primarily on the intrinsically chaotic nature of the technique. Errors occurring in MD simulations were recently discussed by Coveney et al..⁵⁷⁷ There are two sources of errors in this type of simulations emerging from random and systematic sources. Random variation, also called system noise, aleatoric or stochastic error, is caused by the intrinsically chaotic nature of classical MD and produces apparently random deviations from what is considered the ‘true’ value. Systematic errors are due to factors like the imperfect design, parameterization, boundary conditions, conduct and/or analysis of a study, which result in an

estimation of a property deviating consistently from its true value. In particular, systematic errors are introduced by inaccuracies inherent to the system investigated and within the measurement method performed. They may come from assumptions and approximations made when a theory is applied, a model is built, or a process is modelled by the simulation of a real-life problem. Indeed, there are many choices to be made, such as which degrees of freedom are to be modelled explicitly, what components are to be excluded, the kind of interactions between the components, and what boundary conditions are to be used.⁵⁷⁷ For instance, given the extreme sensitivity of MD to initial conditions, two independent MD simulations will sample the microscopic states with different probabilities even if the initial conditions are very close.⁵⁷⁸ In this case, the difference produced in two simulations introduces a variation in results that can often be larger than the quantity of interest, making the results practically useless. In a recent study, the impact of box size on simulations of protein dynamics in water was also stressed by El Hage et al..⁵⁷⁹ Extensive studies, recently reviewed by Coveney,⁵⁷⁷ confirmed that the most effective and reliable computational route to reproducible binding free energies of ligands to proteins using MD simulation can be achieved using ensemble methods that employ a set of independent MD simulations, referred to as ‘replicas’, both in statistical mechanics and within the uncertainty quantification domain, to obtain the required average quantities. Calculating macroscopic properties in this manner from classical MD provides the means to report reproducible results including errors intrinsic to the method. In this way, the errors are under the direct control of the person performing the calculations through the choice of number of replicas and duration of the MD simulation time.^{577,578}

Otherwise, QM methods have no error, unlike experimental values.³⁵⁵ In this case, the question concerns the assessment of the accuracy of a method compared to what is considered the benchmark approach. As noted by Řezáč,⁴⁹⁵ the validation of the accuracy of approximate computational methods and the development of those that rely on empirical parameters depend on external reference data. In the field of noncovalent interactions, accurate experimental data for isolated noncovalent complexes are scarce, and the comparison between computed interaction energy and experimentally observed variables is not unambiguous. Thus, it is common practice to rely on accurate calculations as the benchmark. CCSD(T) is considered the “gold standard” of CC approximations due to its outstanding accuracy to computational costs ratio.^{68,580,581} However, a routine application of CCSD(T), on systems above ~10 non-hydrogen atoms, is currently prohibitively expensive. Since these calculations are very expensive, the common practice is to reuse previously published results, referring to existing dataset. At present, the most widely used data sets, such as S66,^{569,570} offer very accurate interaction energies for dozens of systems.

Very recently, the Non-Covalent Interactions Atlas project (www.nciatlas.org) was started off by Řezáč to cover a wide range of noncovalent interactions with a new generation of benchmark data sets. The inspiring concept behind this project is that building a large universal database covering every noncovalent interaction is impossible, in particular due to the computational demands of a similar operation. A more rational approach has been envisaged in constructing individual data sets covering specific areas of the chemical space. On this basis, so far, the performances of WF, DFT and semiempirical methods have been determined with respect to gold standard methods, mapping HB,^{495,582} and repulsive contacts.⁵⁸³

As mentioned above, QM methods have been benchmarked and optimized on relatively small systems, this fact being due mainly to the difficulty of conducting accurate QM calculations for larger systems.⁴⁶⁵ As stressed by Řezáč and Hobza,^{581,584} the coverage of larger systems is sparse and the accuracy of the benchmark data available for them is questionable. This is still an open issue, even if it has high importance in many real-life applications.

3.4.6 Experimental techniques and strategies for exploring of noncovalent forces

Noncovalent interactions involved in a supramolecular complex can be studied experimentally by evaluating the binding affinity (thermodynamics) of the interacting species and the structure of the supramolecular complex. As stressed by Israelachvili,⁵⁸⁵ in principle any measurement of a physical or chemical property is a measurement of intermolecular forces. For instance, a common property as the boiling point of a substance provides information on the strength of intermolecular binding energies. On this basis, Israelachvili proposed a classification of the experiments to measure indirectly (*a-c*) or directly (*h-i*) intermolecular forces according to the type of information they provide.⁵⁸⁵ While indirect measurements do not furnish any information on the nature and range of the force laws, the most experiments for direct measurements of noncovalent forces employ macroscopic bodies or extended surfaces suspended from springs, where distances can be measured to 0.1 nm, provided that the forces are large and measurable enough and entropic (thermal) effects are negligible:

a) thermodynamic data on gases, liquids, and solids, such as pressure-volume-temperature data, boiling points, latent heats of vaporization, or lattice energies, provide information on the short-range attractive potentials between molecules. Adsorption isotherms provide information on the interactions of molecules with surfaces;

b) physical data on gases, liquids, and solids derived from molecular beam scattering experiments, viscosity, diffusion, compressibility, NMR spectroscopy, XRD, light and neutron scattering, and optical microscopy of liquids and solids provide information on the short-range interactions of molecules and colloidal particles, especially their repulsive forces, and their involvement in the structure of condensed phases;

c) thermodynamic data on liquid mixtures and multicomponent systems like phase diagrams, solubility, partitioning, miscibility, osmotic pressure makes information on short-range solute-solvent and solute-solute interactions available;

d) particle detachment and peeling experiments provide information on attractive short-range forces like particle adhesion forces, and on the adhesion energies of solid surfaces in contact. These experiments are important in specific fields such as powder technology, xerography, ceramic processing, and the making of adhesive films;

e) the full force law of an interaction can be derived by measuring the force between two macroscopic surfaces as a function of surface separation;

f) surface studies such as surface tension and contact angle measurements give information on liquid-liquid and solid-liquid adhesion energies;

g) various optical techniques like reflected intensity, total internal reflection spectroscopy, or ellipsometry have been used to measure film thickness within 0.1 nm, these experiments providing information on the long-range repulsive forces stabilizing thick wetting films;

h) equilibrium or mean interparticle separations and motions in liquids can be measured using NMR spectroscopy, light scattering, X-ray scattering and neutron scattering;

i) information on the interplay of repulsive and attractive forces in systems consisting of many particles that often involve many-body additive interactions can be provided by coagulation studies on colloidal dispersions, where salt type or concentration, pH, or temperature of the suspending liquid medium is changed until the dispersion becomes “unstable” and the particles coalesce through precipitation, coagulation, or flocculation.

In terms of experimental techniques used to confirm computed data, or usually associated to theoretical studies in an integrated way, XRD, spectroscopic techniques, and calorimetric techniques are more frequently applied. As mentioned in the previous subsections, a deeper understanding of noncovalent interactions, their nature, and their roles has emerged in particular from chemical crystallography and crystal engineering.⁶⁵ While individual intermolecular energies are not accessible in crystallography, accurate information about contact geometry as well as the effects of crystal packing forces on the final structure can be extracted from crystal data. However, geometries of complexes formed in condensed phase may be perturbed by crystal packing forces and solvent molecules, in the solid state and solution, respectively. Microwave (MW) rotational spectroscopy allows for determining the geometry of a given complex in the gas phase.^{354,586} The gas phase provides an experimental environment which is suitable for comparison with calculations, and MW structures, if available, are useful to check validity and accuracy of geometries derived from quantum calculations. The concept behind this technique is that the positions of each molecule relative to the

other allow some presumptions about the nature of the interaction, and the intermolecular distance is typically related to the strength of the noncovalent bond holding them together. Of course, the outcome of such analysis depends on the ability to form such a complex in a population high enough to be studied.⁴⁷¹ Vibrational spectra may also provide essential information about the nature of the intermolecular normal modes, whose frequencies can be connected to bond strength.⁵⁸⁷ NMR spectroscopy and NMR titration methods lead to thermodynamic quantities, allowing to distinguish between enthalpic and entropic contributions to free energy of association, in particular studying the binding of different pair of interacting species in the same solution and minimizing possible errors.^{588,589} Recently, surface plasmon resonance has been used to measure not only affinities but also kinetics of complex formation.⁵⁹⁰ Chemical force microscopy also allows direct measurement of noncovalent forces.⁵⁹¹ ITC, including high throughput calorimetry is of particular interest because it gives direct access to ΔG , ΔH , and $T\Delta S$ as reliable alternative to van't Hoff method.⁵⁹²⁻⁵⁹⁴

Investigating kinetics and dynamics of structural and conformational changes at specific stages during the evolution from one state to another is of great interest to gain information on processes at molecular level. In this regard, multidimensional ultrafast spectroscopy, which uses sequences of ultrashort light pulses with femto- (fs, 10^{-15} s) to attosecond (as, 10^{-18} s) durations, have disclosed several structural, energetic, and dynamical information on molecular and biological systems and nanomaterial.⁵⁹⁵ These techniques are capable of overcoming the limitations of our senses in the investigation of natural phenomena going beyond visual perception which can resolve processes taking places over time scales longer than 50×10^{-3} s.⁵⁹⁶ Indeed, in order to observe in real time faster dynamic processes and produce “molecular motion pictures”,⁵⁹⁷ the principle is to use short illumination times in order to “freeze” the motion of the object under study, allowing taking snapshots of its different evolution phases.⁵⁹⁵ A clear example of the possibility to apply these techniques for exploring noncovalent interactions is provided by Hamm and co-authors, who used transient 2D infrared (IR) spectroscopy to study in real time the weakening of an intramolecular HB, and the concomitant opening of the chain in a short peptide (Figure 39).⁵⁹⁸ This technique combines the ability to sense local contacts and a picosecond (ps, 10^{-12} s) time-resolution. The authors recognized four oscillators in the short peptide, and described the temporal evolution of the amplitude of the cross-peaks in terms of the time-dependent changes of length for a particular HB, observing the dynamics of the HB by MD simulations.⁵⁹⁸ In Figure 39, the peaks on the diagonal line are generated by vibrations of the chemical groups in red and blue in the structures. The cross-peaks in green originate by the coupling of these vibrations due to the presence of the HB. As the molecule unfolds, the length of the HB increases and the vibrational coupling decreases, so that the cross-peaks become less intense. The cross-peaks disappear when the HB is broken.

Recently, Yang and co-authors measured the ultrafast structural response to the excitation of the OH stretching vibration in liquid water with femtosecond temporal and atomic spatial resolution using liquid ultrafast electron scattering.⁵⁹⁹ In this study, integration of ultrafast spectroscopy and MD simulations disclosed the intermolecular character of the water vibration preceding the relaxation of the OH stretch.

Ultrafast spectroscopy also found applications in real-time probing of chirality. Nevertheless, this kind of applications still may be rather challenging due to the inherent weakness of chiral light–matter interactions which rely on magnetic-dipole, electric-quadrupole, and higher-order interactions, and the chiral signal may be hindered by different optical artefacts.⁶⁰⁰ On the other hand, in the last few years femtosecond-resolved measurements have been successfully applied to the study of primary electronic dynamics in light-induced chiral response of small molecules.^{601,602}

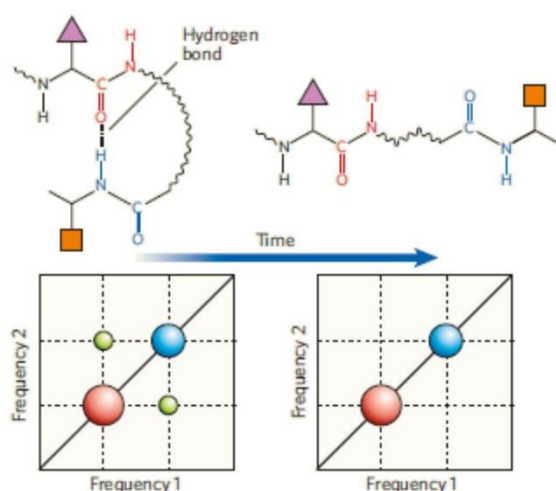


Figure 39. Scheme of HB dynamics detection by transient 2D infrared spectroscopy. Adapted with permission from ref. 597. Copyright 2006 Nature Publishing.

The strategies used to extract noncovalent interaction energy values from the study of supramolecular complexes can be classified in two main groups, namely statistical analysis- and structure-based approaches.⁶² In the last few years, the topic has been treated in some seminal papers.^{63,64,274,322,379,603,604} Thus, this topic will be briefly outlined in the following lines. Statistical analysis techniques such as principal component analysis and discriminant analysis can be used to extract descriptors from experimental data.⁶⁰⁵ Quantitative structure–property relationships or structure-activity relationships can also be used. In the last decade, these approaches have included large-scale structure-activity relationships analysis,⁶⁰⁶ also supported by neural network techniques.⁶⁰⁷ A third approach based on statistical analysis concerns the use of training sets of binding affinities for a given interacting species with many counterparts, then obtaining descriptors that determine the complex stability through a multiparameter equation. Biedermann and Schneider observed that the limits of this approach are that, in general, it requires to consider a large population,

and the descriptors may not be orthogonal (independent of each other) and may be not of significant physical meaning.⁶³ For instance, Xu et al. performed a multiple linear regression analysis of 218 different β -CD complexes led, with a training set of 160 compounds, to acceptable correlations when a minimum of seven descriptors was used, but the assessment of the physical significance of some descriptors may be not trivial.⁶⁰⁸ In the structure-based approach, the structures of the interacting partners, number and type of noncovalent interactions, or medium type and polarity are systematically varied and the resulting change of properties measured, in general in terms of binding free energy, and its enthalpic and entropic contributions.⁶³ Binding energies can be evaluated considering a large variety of small molecules, assembling many data points from a large variety of interacting partners by systematic comparison of a given partner with many others. The best known and comprehensive binding energy factors are those for HB by Abraham.^{513,514} Thousands of binding constants between small molecules have been measured and are currently available, in most cases by using organic solvents such as carbon tetrachloride and chloroform under spectroscopic conditions.⁵¹⁴ However, several interaction types may underlie supramolecular assemblies simultaneously. In this case, even if additivity of free energies can be violated through positive or negative cooperativity and solvent effects, more often it can be assumed that single free energy contributions $\Delta\Delta G$ of interactions of type 1, 2, ... are additive, thus the total binding energy ΔG_b being given by equation 9

$$\Delta G_b = n \cdot \Delta G_1 + m \cdot \Delta G_2 + \dots \quad (9)$$

where n and m designate the number of a single interaction type occurring within the complex⁶³

In 1995, Schreiber and Fersht developed a procedure, known as “double mutant cycle” (DMC), to deconvolute an experimentally determined binding energy into a sum of contributions from different noncovalent interactions,⁶⁰⁹ with the advantage of eliminating the undesirable contribution of the secondary interactions.⁶³ Through this procedure, accurate binding increments, $\Delta\Delta G$, $\Delta\Delta H$ and $\Delta\Delta S$, for the $X \cdots Y$ interaction can be obtained, as depicted in Figure 40. In the seminal paper of Schreiber and Fersht,⁶⁰⁹ differences in the thermodynamic binding parameters were measured between the native protein containing the main $X \cdots Y$ interaction and three protein mutants: the mutated X' , a mutated Y' , and both mutated X' and Y' moieties. The related Born–Haber cycle is summarized in the following equations 10 for the DMC:

$$\Delta G = \Delta G_{XY \rightarrow X'Y} - \Delta G_{XY' \rightarrow X'Y'} = \Delta G_{XY \rightarrow XY'} - \Delta G_{X'Y \rightarrow X'Y'} \quad (10)$$

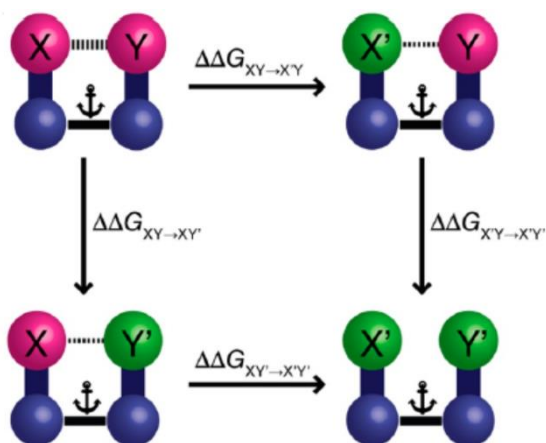


Figure 40. Schematic representation of a DMC for quantifying the strength of the noncovalent interaction between X and Y according to eq. 10. Adapted with permission from refs. 63. Copyright 2016 American Chemical Society.

Later, DMC approaches were reviewed by Cockroft and Hunter in 2006⁶¹⁰ and, very recently, by Horovitz et al..⁶¹¹ While the system lacking symmetry or underlain by multiple interactions can be analyzed by the thermodynamic DMC approach, systems with high degrees of symmetry can be approached through the molecular torsion balances.⁶¹² Folding molecules such as rotamers, topoisomers, atropoisomers, and tautomers are privileged platforms for the study of noncovalent interactions because, in these molecules, the relative stabilities of the conformational states may be driven by intramolecular and solvent interactions that are present in one conformation, but missing in the other (Figure 41). Molecular torsion balances are designed to constrain two pilot groups in an intramolecular arrangement by a suitable molecular scaffold, where the two groups may interact, attractively (folded state) or repulsively (unfolded state). On this basis, rotational barriers (ΔG^\ddagger) and differences in the free energies of ground-state conformers (ΔG_{fold}) are used to assess the thermodynamics of noncovalent interactions. The free binding energy associated to the pilot interaction in the folded state can be quantitatively experimentally determined from the ratio of folded and unfolded states, more frequently by NMR spectroscopy.^{63,612-615} SAPT analysis was also applied to torsion balance systems.⁶¹⁶ In the last few years, this intramolecular approach has been used in a number of applications, in particular contributing to quantify noncovalent interactions involving π -clouds.^{63,612-616}

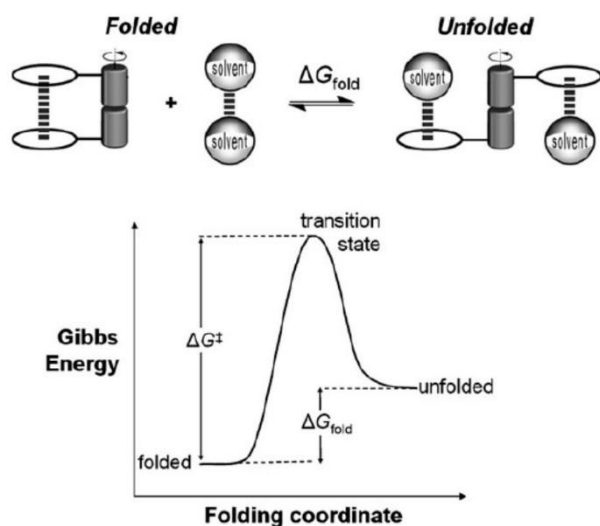


Figure 41. Simplified folding equilibrium for a molecular torsion balance including the solvent and the corresponding energy profile showing the energy barrier to rotation, ΔG^\ddagger , and the free energy of folding, ΔG_{fold} . In this example, folding involves the formation of an intramolecular interaction accompanied by desolvation of the interacting functional groups. Reproduced with permission from ref. 612. Copyright 2010 Royal Society of Chemistry.

It is worth mentioning that the accordance between experimental and theoretical data remains somehow still uncertain in particular for noncovalent interactions like salt bridges, hydrophobic forces, and dispersive interactions.⁶⁴ In these cases, the selection of the proper theoretical method requires the use of large sets of test cases as benchmarks, also on the basis of small host–guest complexes. As reported by Mobley and Gilson, free energy calculations seem to predict free energies within root mean square errors in the 4 to 9 kJ/mol range.⁶¹⁷ A recent case reported by Nau, Grimme, Gilson and co-authors describe well the issues related with the calculation of binding energies and their accordance with experimental data. In the frame of a study on hydrophobic effect and dispersion interactions as driving forces in complex formation, the authors evaluated complexes of hydrocarbons in a cucurbit[7]uril.⁶¹⁸ In this study, before carrying out the experimental data, the complexation energies were calculated in order to test the computational accuracy of the method. For this purpose, three dispersion-corrected DFT methods, and two force field explicit-solvent MD methods were used. On this basis, good correlations between calculated and experimental free binding energies was obtained, but in some cases the theoretical results underestimated the affinities determined experimentally (Table 5). As a matter of fact, one method which provided better results for a particular complex often showed less agreement with another complex, given similar experimental affinity in both cases.^{64,619}

Table 5. Selected binding free energies of hydrocarbons in cucurbit[7]uril (ΔG , kcal/mol).⁶¹⁹ Experimental values ΔG_{exp} and calculated values; calculated values showing the best agreement with the experimental values are reported in bold

Hydrocarbon	ΔG_{exp}	QM1	QM2	QM3	MD1	MD2
Propane	-5.15	-2.14	-4.78	-5.92	-8.34	-8.60
<i>n</i> -Butane	-7.14	-3.74	-7.00	-7.97	-12.18	-12.60
<i>n</i> -Pentane	-7.75	-5.11	-8.14	-8.14	-14.12	-14.42
<i>n</i> -Hexane	-8.43	-5.98	-6.48	-6.98	-15.81	-15.68
<i>n</i> -Heptane	-8.94	-6.85	-4.94	-5.21	-12.44	-12.54
Propene	-4.19	-0.72	-3.10	-3.45	-4.92	-6.16
Cyclohexane	-8.43	-9.98	-13.25	-13.41	-17.32	-18.03
Benzene	-5.77	-7.64	-7.93	-9.53	-9.75	-13.77

4. Trends in enantioselective recognition in natural and man-made systems

The fundamental meaning of chirality lies in the relational and directional sense of the word.²⁰⁸ Given chirality at asymmetric carbon as an example, it means that an achiral molecule **AACD** interacts equally with the two enantiomers of a chiral molecule **abcd** (Figure 42, left) because its interaction capability is not stereoselective, and it is independent of the direction (orientation) of the four groups **a-d** on the enantiomers which, therefore, are indistinguishable in these isotropic conditions. On the contrary, the chiral enantiopure molecule **ABCD** can recognize the two enantiomers of the chiral molecule **abcd** through stereoselective, anisotropic interactions (Figure 42, right).

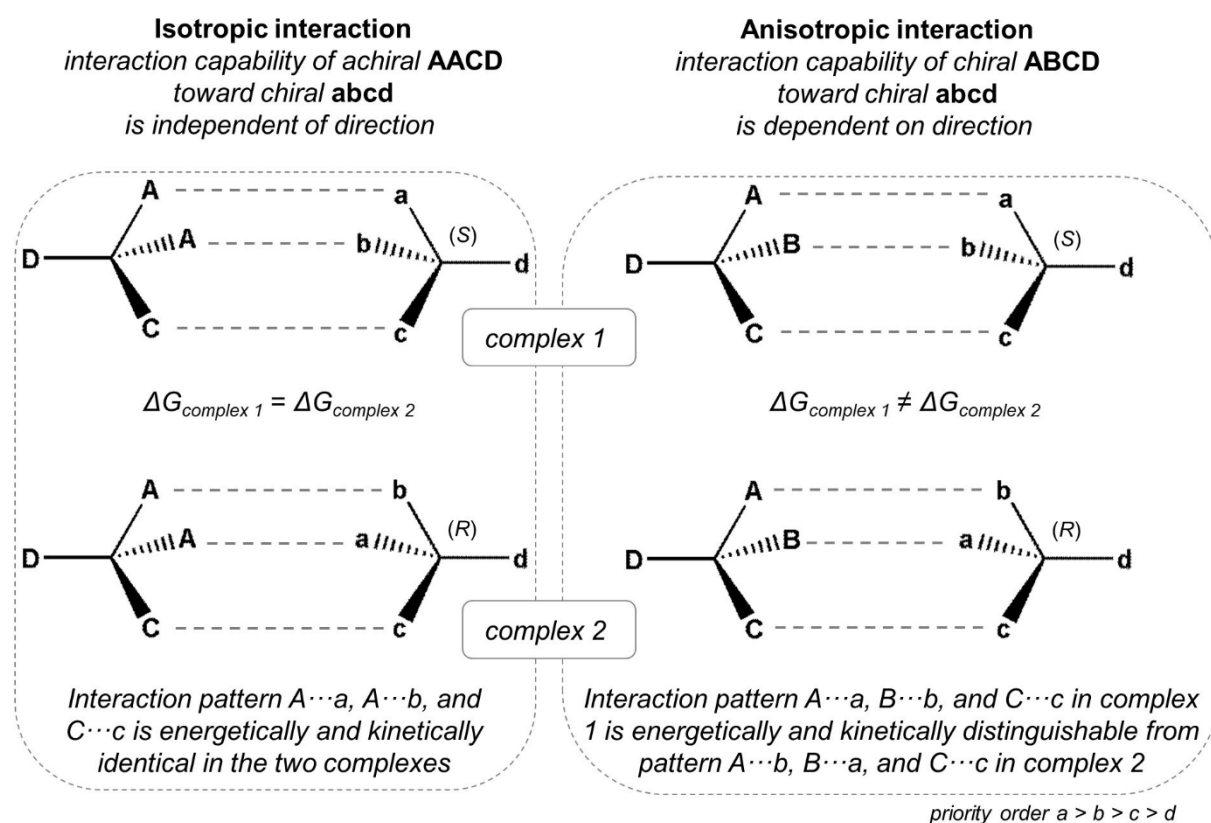


Figure 42. Chirality, non-enantioselective (left) and enantioselective (right) relationships.

These anisotropic differences produce two energetically and kinetically distinguishable diastereomeric relationships, and this is the basic requirement for enantioselection. Thus, chirality expresses itself through interactive processes involving chiral molecules, the importance of the

concept of “*interaction*” for enantioselectivity being inherent just in the meaning of chirality as a relational property.

As stated by Hirschmann and Hanson, chirality “*is an all-pervasive property, as it affects all parts of a chiral structure*”,⁶²⁰ and enantioselective noncovalent interactions have a relevant role in modulating molecular contacts, and in transferring the chiral information from a chiral molecule toward another chiral or prochiral species located in the neighboring space. The enantioselective function of noncovalent interactions depends on three-dimensional structures (size and shape) and electronic features of the interacting chiral partners, including polarity of the medium, and on the chemo-physical properties of the diastereomeric complexes.

Actually, in most cases enantioselective recognition is based on a synergistic interplay between steric and electronic effects. The lock-and-key model,⁸⁶ which remains the most popular model for molecular recognition, is based on the geometric complementarity between receptor and substrate. However, over time it has been revised with the introduction of the induced fit as a principle regulating the mutual interaction between two interacting species, thus going beyond the original Fischer’s formulation.⁶⁰⁴ The flexibility of substrate-binding sites in protein and enzymes has been demonstrated by several studies, noncovalent interactions enhancing the mutual conformational adjustment of substrate and receptor, and also enhanced by the induced fit.⁶²¹ Ward and Maréshal reported combined docking and saturation kinetic studies which allowed for the formulation of an enantiodifferentiation mechanism based on the “induced lock-and-key” hypothesis.⁶²² In this study, an artificial imine reductase resulted upon incorporation of a biotinylated Ir-cofactor within homotetrameric streptavidin. The host protein was found to dictate the configuration of the biotinylated Ir-cofactor which, in turn, determines the enantioselectivity of the artificial imine reductase for the production of salsolidine with high enantiopurity. An induced lock-and-key mechanism was also demonstrated for the bowl-to-bowl inversion of the non-planar corannulene by complexation with a tetracationic cyclophane.⁶²³ Through the stereoelectronic reorganization of the host in the host–guest complex from a strained to an energetically favorable conformation, only the planar TS of corannulene was stabilized into the host cavity, not its curve ground state, with a rate increase of inversion by a factor of 10. The binding affinity between the cyclophane and corannulene was shown to arise from multiple sources, including charge-transfer interactions, surface-area binding phenomena, vdW force and solvophobic effects.

The role of noncovalent interactions in stereoselective processes was rather overlooked at the dawn of asymmetric synthesis. For instance, in the decades 1950s-1970s, the stereoselectivity of reactions involving chiral small-molecules as substrates, auxiliaries, and catalysts was explained typically by the steric destabilization of all pathways with the exception of one which appeared to be

dominant.⁶²⁴ In the 1950s, the Cram rule, which has been used to correlate the stereochemical course of a large number of 1,2-asymmetric addition reactions of nucleophilic reagents to aldehydes and ketones, states that in noncatalytic (kinetically controlled) reactions of type (**18**→**19**), the diastereomer which predominates would be formed by the approach of the entering group (R" of the reagent R"Z) from the less hindered side of the double bond when the rotational conformation of the C-C bond is such that the double bond is flanked by the two least hindered bulky group (**20**) (R_S and R_M, given R_S = small group, R_M = medium group, and R_L = large group) attached to the asymmetric center (Figure 43a).^{625,626} This concept shows the disadvantage that, in some cases, it is difficult to predict the steric requirements to functional and ancillary groups in TSs. Then, going beyond a pure "steric strain model" by considering the electronic features of the molecules, Cornforth et al. introduced a "dipolar model" (**21**) to explain those examples in which a highly polarizable group, such as halogen, is attached to the chiral centre.⁶²⁷ This model was featured by a *trans* coplanar arrangement of the adjacent dipoles (Figure 43b). Later, other models were introduced by Karabatsos⁶²⁸ and Felkin⁶²⁹ accounting for the polarity of atoms and sites involving in the process. In particular, a key point of Felkin's model (**22**) was that polar effects stabilize those TSs in which the separation between R" and the electronegative groups (R_L, R_M, R_S) is greatest and destabilize others (Figure 43c).

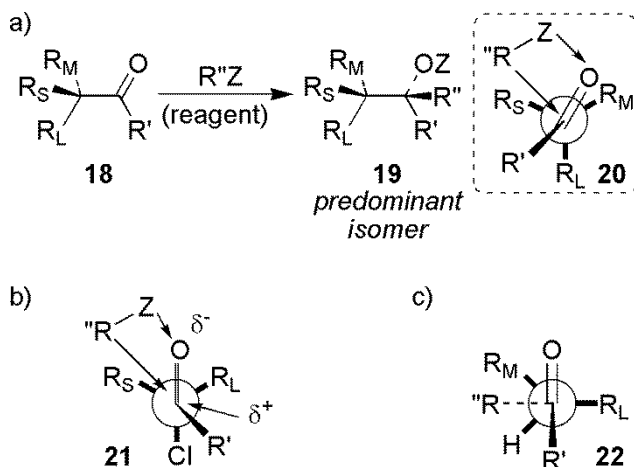


Figure 43. Steric strain-based (**20**) and dipolar models (**21,22**) of 1,2-asymmetric addition of nucleophiles to carbonyl compounds.

Over time, a series of descriptors and equations to determine steric parameters were developed such as Tolman cone angle for phosphine ligands, the author stating in his article that "the steric effects are much more important than electronic effects in determining the exchange equilibria among phosphorus ligands and Ni(0)..".⁶³⁰ The main incongruence of the steric arguments is that the reactivity of a system is expected to be reduced as the steric hindrance increases, whereas the selectivity should increase with increasing steric demand.³²² Allen et al. re-evaluated computationally

Tolman's cone angles which were considered to derive from a classic understanding of molecular structures related to MM approaches.⁶³¹ Indeed, MM minimization is based on the “*steric strain*” as a key optimization parameter, overestimating the role of steric effects, not necessarily providing a balanced picture of the effects of sterically demanding substituents and ligand electronic features. On the other hand, in many reactions, such as those catalyzed by transition-metals, reactivity often was shown to increase with steric bulk. In this regard, in 2012, reviewing bulky palladium *N*-heterocyclic carbene complexes used for cross-coupling reactions, Organ et al. noted that “*increased steric bulk on the ligand that buries the metal deep within its fold has been linked to heightened reactivity in cross-coupling procedures*”.⁶³² On the other hand, in a different reaction domain, Čorić and List carried out an enantioselective spiroacetalization reaction using a “*spatially confined*” Brønsted acid that is supposed to leave a small space for the substrate, therefore achieving high enantioselectivity.⁶³³ These evidences suggested that steric effects were unsuitable to fully explain trends and outcomes of enantioselection processes. In the same year, commenting the spiroacetalization reaction of Čorić and List, and highlighting the pivotal role of noncovalent interactions, Burns and Jacobsen stated that “*The problem with this seemingly straightforward strategy is that a very specific spatial relationship between the reacting site and the chiral catalyst is required to obtain high stereoselectivity. Electrostatic attraction alone is not sufficient to impose the required level of order, because it is direction-independent. This problem could be overcome by incorporating other features into the catalyst, to allow it to orient the charged substrate through attractive, non-covalent interactions — a principle that is well established in enzymatic catalysis, and which has also been established in small-molecule catalysis*”.⁶³⁴ Confirming this view, Knowles and Jacobsen have also remarked that the question of whether selectivity is achieved primarily through stabilizing interactions or destabilizing steric effects represents a fundamental difference in the way macromolecular (enzymes) and small molecule catalysts are assumed to operate.⁶³⁵ Indeed, attractive noncovalent interactions are responsible for many of the rate accelerations and stereoselectivities which are characteristic of enzymatic catalysis, where cooperative noncovalent interactions with specific active site residues can stabilize the electrostatic character of a bound transition structure, thus lowering the kinetic barriers to reactions.⁶³⁵⁻⁶³⁷ Otherwise, as mentioned above, for nonenzymatic asymmetric reactions small chiral molecules used as catalysts are generally proposed to follow a fundamentally different principle for achieving enantioselectivity, invoking steric interactions as a rationalization for energetic differentiation of the pathways leading to two opposite enantiomers. In this conceptual framework, only the TSs that avoid these steric constraints are kinetically viable. The reason envisaged by Knowles and Jacobsen for this conception is that steric destabilization is most effective as a defining element of stereocontrol in strongly bound and conformationally restricted complexes, where any

structural reordering away from equilibrium provides a substantial energetic penalty. On the contrary, noncovalent interactions are generally weaker and less distance-dependent compared to steric constraints. Thus, in a complex where a catalyst would interact with its substrate through a single noncovalent interaction, many geometrical orientations of the substrate relative to the catalyst may be very similar in energy. In this case significant structural reorganizations would occur without substantial destabilization of the binding interaction. Such a lack of conformational priority represents the obvious challenge to achieving high enantioselectivity. This may be overcome, in principle, through implementation of multiple noncovalent attractive interactions operating in concert, because this could afford the conformational constraint required for high stereoiduction. This cooperative model of binding has defined an important requirement of both biological and synthetic receptors, also profiling future trends in catalyst design for the years ahead. The interplay between steric constraints and noncovalent interactions was recently illustrated in a study reported by Houk and Wheeler, describing mechanistic differences between chiral phosphoric acid-catalyzed intramolecular and intermolecular oxetane ring openings.⁶³⁸ Whereas OH \cdots O HBs between catalyst and reagents control TS selectivity in the intermolecular process, the intramolecular reaction requires a significant substrate distortion for both the electrophile and nucleophile to engage in OH \cdots O HBs with the Brønsted acidic and basic sites of the catalyst. Thus, in the latter case, the steric constraints induced the occurrence of a bifunctional mechanism based on a OH \cdots O HB, with the nucleophile mildly activated by a OH \cdots π interaction with an aromatic group of the catalyst.

In the 1980s, the role of noncovalent interactivity had been also recognized in enantioseparation science, Pirkle stating in his article “Consideration of chiral recognition relevant to the liquid chromatographic separation of enantiomers”: “*In order to discuss enantioselective complexation, we should first establish what is meant by “interaction” between two molecules. Two molecules might be said to “interact” when they begin to perturb each other’s electronic orbital energies (i.e., their orbitals begin to overlap appreciably). All intermolecular forces originate from such perturbations, and it would perhaps be more correct to discuss intermolecular interactions in such terms. However, the usual terms “hydrogen bonding”, “dipole stacking”, and “steric interactions” all describe specific types of perturbations...*”.¹³³

Enantioselective recognition is ubiquitous and this term covers a wide range of applications and issues related to availability and use of enantiopure or enantioenriched compounds (Figure 44). Given the homochirality of biomacromolecules such as proteins, enzymes, polysaccharides, enantioselective recognition plays a pivotal role in determining the fate of chiral compounds in nature. Enantiopure or enantioenriched compounds can be accessed from the natural chiral pool, through enantioseparation of racemic mixtures, stereoselective (enantio- and diastereoselective) synthesis, and absolute

asymmetric synthesis. Over time, chemists have used a number of chiral enantiopure or enantioenriched molecules isolated from natural sources as starting materials. Examples of chiral synthons which are achievable from nature are amino acids, carbohydrates, hydroxy acids, terpenes, alkaloids. Chiral pool-based synthetic methods have some advantages such as *a)* relatively low cost, *b)* high enantiomeric purity of final chiral products, and *c)* the fact that stereogenic center(s) featuring the chiral natural starting material can control the stereoselective generation of new chiral centers.^{37,639}

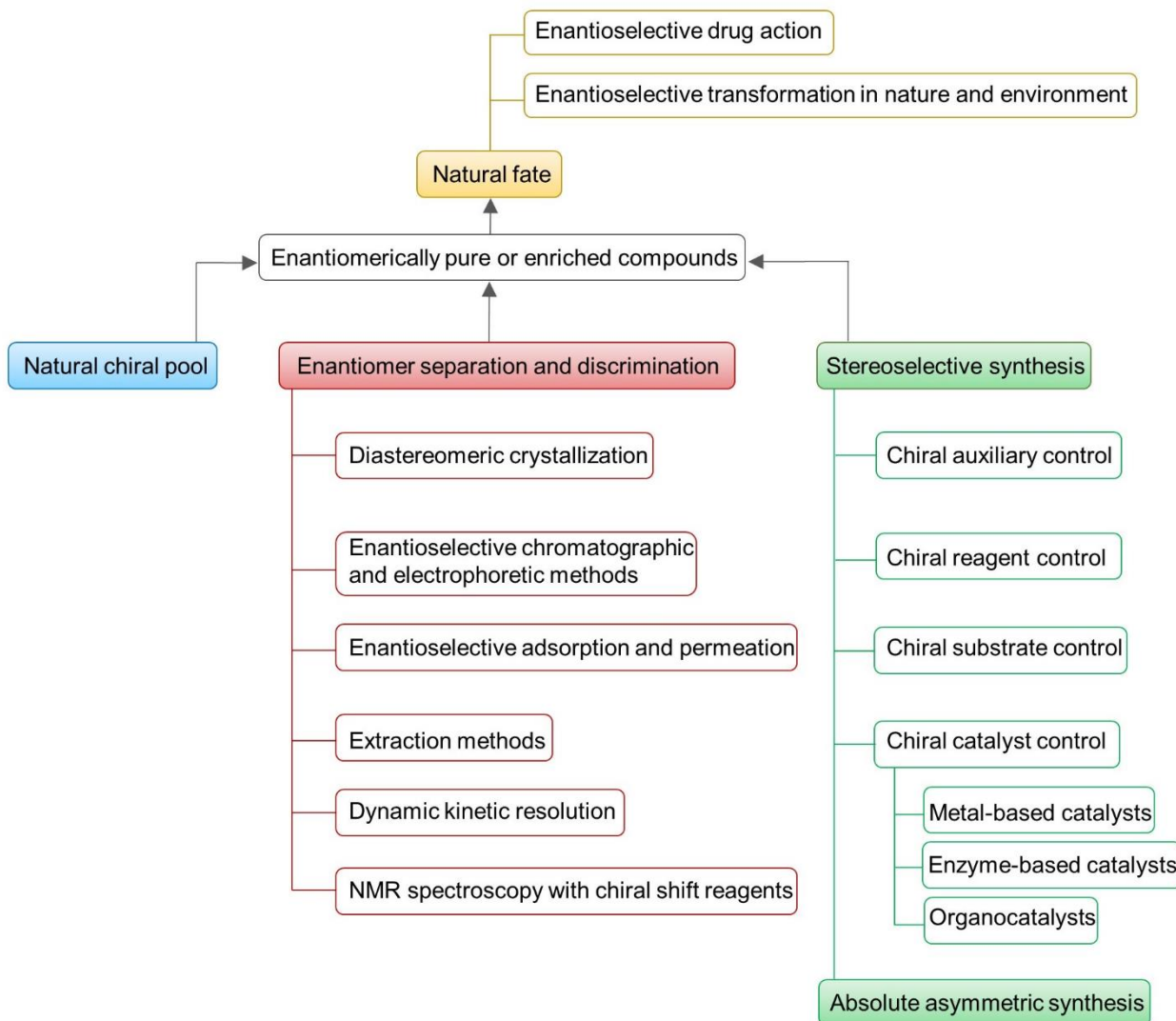


Figure 44. Routes to access enantiomerically pure or enriched compounds and their natural fate.

However, not all enantiopure substrates can be obtained from nature. Moreover, commonly nature makes only one of the enantiomers of a chiral precursor available, this aspect limiting the synthetic versatility of the chiral pool approach. Thus, alternatively several methods are available for analytical and/or preparative chiral resolution of racemates which are based on physical, chemical or biological techniques: diastereomeric crystallization, liquid and gas chromatographic methods,

electromigration methods, chemo- and biocatalytic kinetic resolution, extraction methods, and approaches based on enantioselective adsorption and permeation.⁴² Enantiomers can be also identified and characterized (but not physically separated) by performing NMR spectroscopic experiments with chiral shift reagents.⁶⁴⁰

Stereoselective synthesis concerns the construction of chiral organic molecules from available starting materials by a series of rationally designed stereoselective synthetic transformations.³⁷ It includes the formation of one or more stereogenic centers, starting from prochiral precursors and controlling enantioselectivity by using a chiral auxiliary, a chiral reagent, or a chiral catalyst, whereas the so-called absolute asymmetric synthesis involves a total spontaneous resolution in the terms explained below.

In general, synthetic and analytical systems use enantioselective noncovalent interactions for differentiating enantiomers with lower efficiency compared to biological systems. Thus, understanding the molecular bases of chirality and its consequences in man-made systems, and managing the production of chiral compounds through rational design remain urgent needs for science. In this perspective, in the last few decades, classification, comprehension and quantification of noncovalent interactions have provided new approaches for performing and rationalizing enantioselective recognition processes. In principle, all noncovalent interactions may act enantioselectively contributing to enantioselective recognition processes, not only classical HB, π - π stacking, and dipole-dipole, but even, considered to be nondirectional, steric, dispersive and hydrophobic contacts, these latter being of substantial relevance in aqueous and hydro-organic eluents.^{78,320,641} Recently, Mata et al. explored the impact of dispersive forces in chiral recognition during the formation of homochiral/heterochiral dimers of small diols, showing that dispersive forces are crucial for the manifestation of chiral recognition.⁶⁴² For this purpose, dispersion contributions were “turned on and off” for both DFT and WFT methods by using properly dispersion-correction in order to see how both the energy and structure of the systems were affected by dispersive forces. On the other hand, in most cases directionality has proven to be an important requirement for enantioselection. In this perspective, HB, π - π and dipole-dipole interactions are privileged tools for enantioselective recognition. Directionality being a property of σ -hole bonds, very recently the application of XBs, ChBs and PnBs have paved the way to new recognition modes in both synthetic^{415,432,433,643} and analytical^{644,645} enantioselective recognition processes,⁴³⁵ even if this field is still in its infancy.

Despite the fact that it is common to associate recognition processes to intermolecular interactivity, the next subsection focuses on intramolecular interactions that may have an important role in enantioselective processes, particularly in macromolecular chemistry. Then, enantioselective processes applied in several chemical and biochemical domains are discussed, evidencing rational

noncovalent interaction-based approaches to enantioselection, and focusing on the most recent studies to highlight trends and perspectives in this field. The topic of enantioselective recognition in chromatographic and electrodriven separations is not included in this section 4, which is discussed extensively in the next dedicated section 5. It is worth noting that, even if enantioselective processes are classified herein on the basis of the field of application, some concepts and mechanisms go across different fields, providing a unifying view of enantioselective recognition.

4.1 Intramolecular noncovalent interactions in enantioselective recognition

Most molecule functions, from catalysis to assembly of macromolecular complexes, involve exposed and accessible molecular surfaces that contain binding sites, in turn involved in intermolecular interactions with other molecules, including solvent molecules in liquid-phase. Thus, as a molecule interacts with another chemical species, the overall energetics of complex formation represents the balance of all potential competing noncovalent interactions at both molecular surfaces. Consequently, the interaction ability of a molecule is dependent on its shape, as sum of geometry and electronic distribution, and its conformational properties, in terms of flexibility, rigidity, and steric constraints influencing dynamics of rotatable bonds. In this perspective, intramolecular interactions occurring within each interacting species may impact deeply the intermolecular interactivity of the system. The importance of intramolecular interactions in biological system is well recognized, in terms of stabilization effects of three-dimensional structures of biomacromolecules as well as stabilization/destabilization of ligand-binding complexes.⁶⁴⁶ On the other hand, over time intramolecular interactions have been also exploited as an important tool in man-made systems, for predetermining three-dimensional structures of higher order macromolecules, for improving catalyst efficiency, and for fine tuning of intermolecular interactivity.

The importance of intramolecular interactions in determining features and functions of the well-known polysaccharide-based selectors, widely used for liquid-phase enantioselective separation, illustrates well the concept. In the 1980s, the enantioselective recognition ability of native polysaccharide was successfully improved by converting the three free hydroxyls bearing by each glucosyl rings of the native backbone into three aryl carbamate functionalities (pendant groups) (Figure 45a) having a triple functions (in Figure 45, amylose *tris*(3,5-dimethylphenylcarbamate) (ADMPC) is depicted as a representative structure): *a*) to introduce additional interaction sites (N-H, C=O, Ar), amplifying the intermolecular interaction capability of the native polymer (Figure 45b); *b*) to generate an extension of the polymer in a direction perpendicular to the backbone axis (Figure 45c), producing the transmission of the chiral information from the molecular to the conformational level and originating chiral grooves and ravines (Figure 45d) able to host enantiomers for enantioselective recognition; *c*) to favor formation of intramolecular HBs able to sustain the high-ordered structure of the polysaccharide

derivative (Figure 45e). In 1985, Vogt and Zugenmaier described through X-ray analysis a left-handed threefold 3/2 helix as the conformation featuring a cellulose *tris*(phenylcarbamate) (CTPC) fibre.⁶⁴⁷ In this structure, an intramolecular distance of 2.724 Å was observed between the N-H proton and the C=O carbonyl oxygen, disclosing the presence of HB-based contacts within the polymer. Later, the first computed model of CTPC confirmed a structure related to a left-handed threefold 3/2 helix in accordance with the crystallographic structure.⁶⁴⁸ Again, this model showed intramolecular HBs between the N-H protons and the carbonyl oxygens of the carbamate moieties, with a distance of 2.634 Å. High-ordered structures, sustained by intramolecular HBs, were also determined experimentally and theoretically for cellulose *tris*(3,5-dimethylphenylcarbamate) (CDMPC)⁶⁴⁹ and ADMPC⁶⁵⁰ (Figure 46). For ADMPC, a left-handed 4/3 helical structure was determined as the most probable through spectroscopic and theoretical studies.⁶⁵⁰

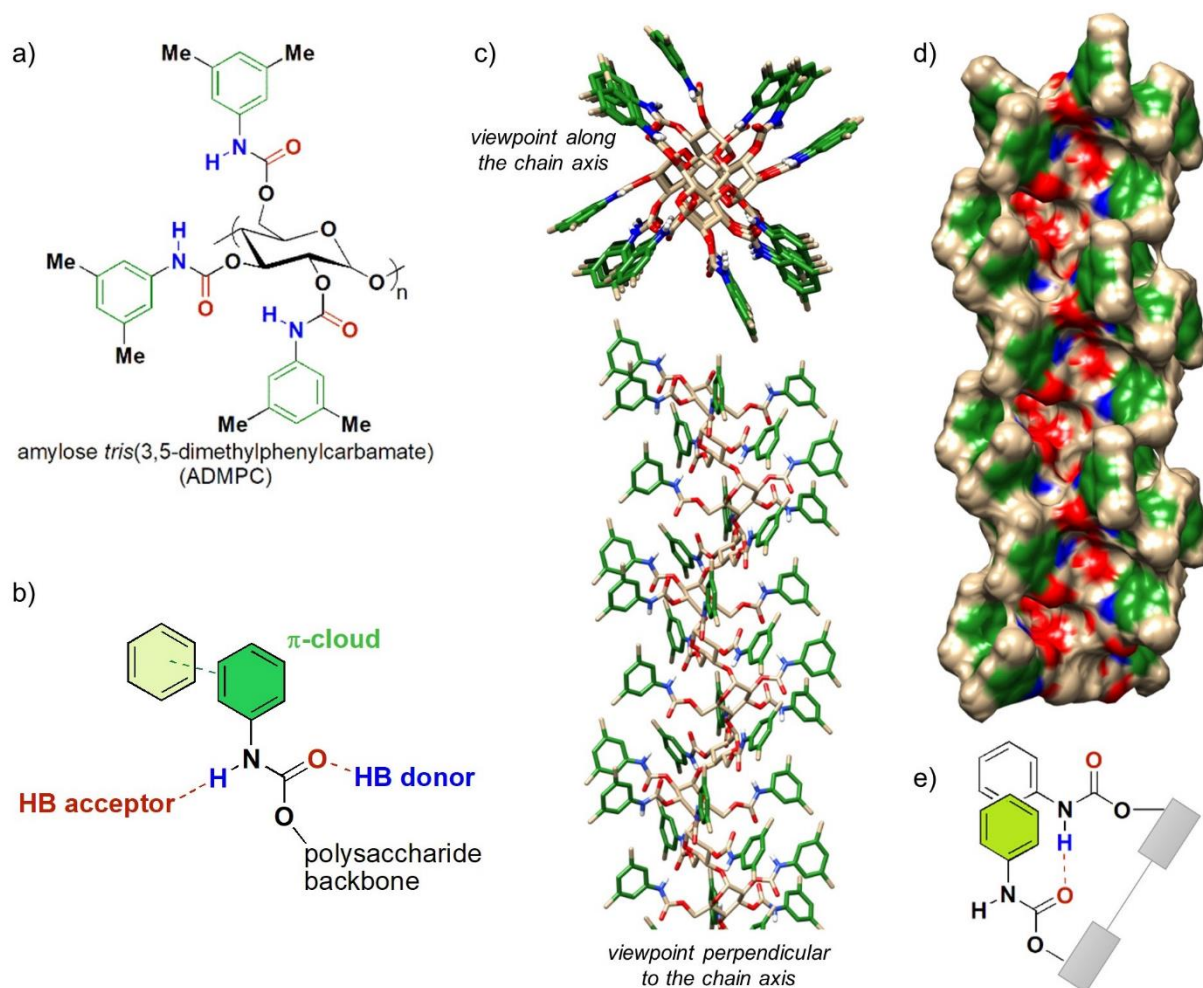


Figure 45. a) Bidimensional drawing of ADMPC; b) scheme of main intermolecular interactions between analytes and carbamate moiety of polysaccharide-based selectors; c) tridimensional drawing of a 12-mer ADMPC oligomer, viewpoint along the chain axis and perpendicular to the chain axis; d) electron density surface of ADMPC; e) drawing of intramolecular HB. Color legend: aryl group (green), N-H (blue), C = O (red).

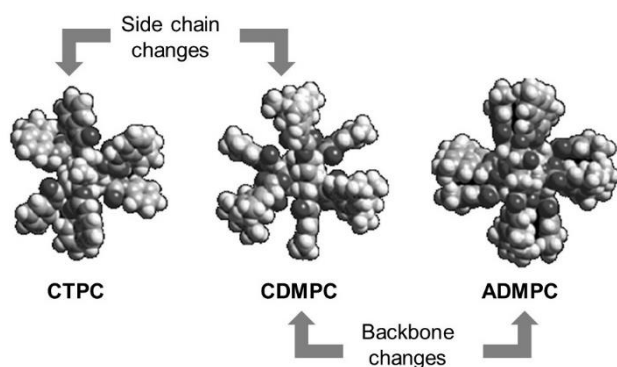


Figure 46. Optimized structures of CTPC, CDMPC, ADMPC. Viewpoint is along the chiral axis. Adapted with permission from refs. 649 (Copyright 1999 The Chemical Society of Japan) and 650 (Copyright 2002 American Chemical Society).

Shape and size of the chiral cavities available in the groove of the polymers for hosting the enantiomeric guests are determined by the strength and the geometry of the intramolecular HBs which, in turn, are affected by the structural changes applied to backbone and pendant groups of the polysaccharide. For instance, the different arrangements of the phenyl rings in the CDMPC and CTPC cellulose-based selectors (Figure 46) can be ascribed just to the above mentioned consideration. In terms of backbone, moving from cellulose to amylose, the glycoside torsion angle changes with a clear effect on the structural features of the polymers. Indeed, for CDMPC, larger distances between adjacent chains, slightly bigger cavities, and weaker intermolecular HBs were observed compared to ADMPC.⁶⁵¹ Intramolecular CH_3 - π contacts were also evidenced for the more compact ADMPC.^{652,653} Another evidence of the intramolecular HB contribution to increase the stability of the high-ordered polysaccharide structures can be found in the lower stability of cellulose benzoates compared to the phenylcarbamate derivatives.⁶⁵⁴ As a result, the chiral recognition properties of cellulose benzoates are more influenced by the conditions used for the preparation of the packing material. The impact of structural changes applied within the polysaccharide carbamate derivatives on the intramolecular HBs were also investigated by comparing CDMPC, cellulose *tris*(3,5-dichlorophenylcarbamate) (CDCPC), and cellulose *tris*(3-chloro-5-methylphenylcarbamate) (CCMPC) (Figure 47a) with ^1H NMR and Fourier transform (FT)-IR analyses.^{318,655-657} In this study, the two diverse bands at different wavelengths around 3500 cm^{-1} of the IR spectra (Figure 47b), which are associated with free and hydrogen-bonded N-H stretching, respectively, were examined. As shown in Figure 47b, by using the two bands as pilot signals, clear information could be gained by IR analysis on the ratio of the two types of HB involvement of the N-H hydrogen within the polysaccharide structure. On this basis, electron-donating substituents on the phenyl ring (CDMPC) were shown to favor intramolecular HBs, whereas the presence of electron-withdrawing chlorines (CDCPC) on the phenyl ring was detrimental for intramolecular contacts. The ^1H NMR spectra of the CDCPC, CCMPC, and

CDMPC confirmed the observed trend. In this case, using the signal of the N-H proton at the 6-position of the glucosyl rings as reference, its chemical shift was found dependent on the substituents on the aryl rings. As a consequence, the chemical shifts of the N-H resonances shift downfield as the acidity of N-H increases (Figure 47c).

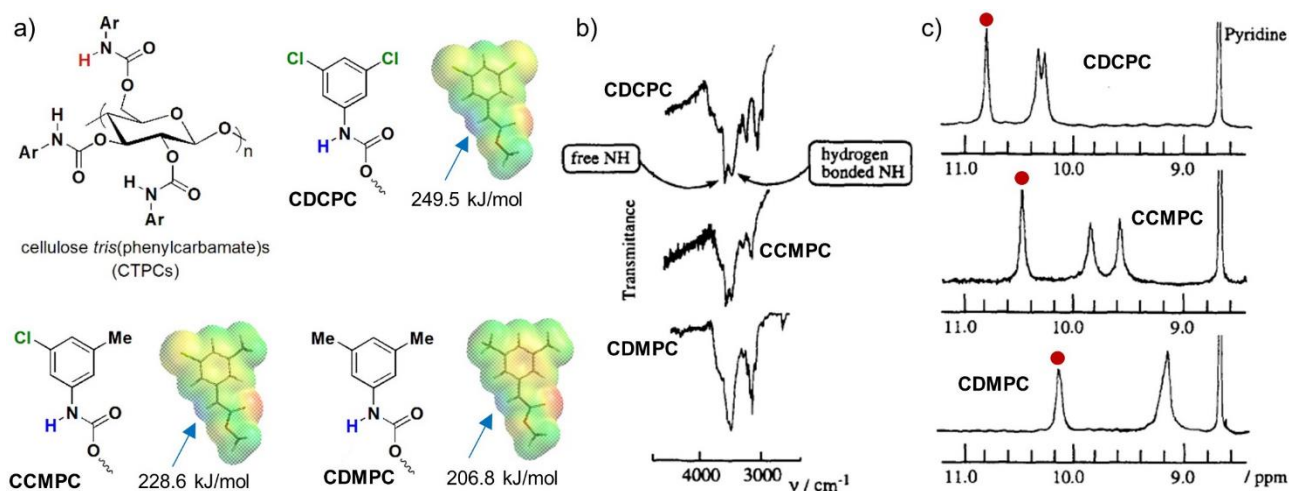


Figure 47. a) Structure of CTPCs and calculated $V_{S,max}$ on N-H, colors toward red depict negative potential, while colors toward blue depict positive potential and colors in between (orange, yellow, green) depict intermediate values of potential; b) IR spectra of CDCPC, CCMPC, and CDMPC; c) ^1H NMR spectra of CDCPC, CCMPC, and CDMPC, NH proton at the 6-position is indicated with the red point. Adapted with permission from ref. 657. Copyright 1997 Elsevier.

Recently, the $V_{S,max}$ and $V_{S,min}$ associated with the electropositive regions centered on N-H hydrogens and the electronegative regions centered on C=O carbonyl oxygens, respectively (Figure 47a), were calculated at DFT level,⁴⁷⁵ observing $V_{S,max}$ values increased as the electron-withdrawing properties of the substituents on the aryl rings, in accordance with the spectroscopic characterization.

The effect of solvent on the high-ordered structure of polysaccharide derivatives has been investigated in experimental and theoretical studies.^{653,658-661} While the adsorption of *n*-hexane did not affect polymer structure, on the contrary the adsorption of polar solvents changed the polymer structure. This effect was due to the action of the alcohol hydroxyl groups which make strong HBs with the C=O and N-H groups of the polymer, competing with intramolecular HBs and intermolecular HBs with guests. Temperature was also found to impact HB networks, high-ordered structure-type, and the enantiorecognition mechanism of polysaccharide derivatives.⁶⁶²⁻⁶⁶⁷

Intramolecular interactions also impact structure and recognition capability of CDs. In native CDs, the round structure is sustained by intramolecular HBs which are formed between the 3-OH and the 2-OH hydroxyl groups of adjacent glucose units (Figure 48). By comparing the crystal structures of α -, β -, and γ -CDs, the length of these HBs. was found to increase following the order γ -CD (2.81 Å) < β -CD (2.86 Å) < α -CD (3.00 Å).⁶⁶⁸

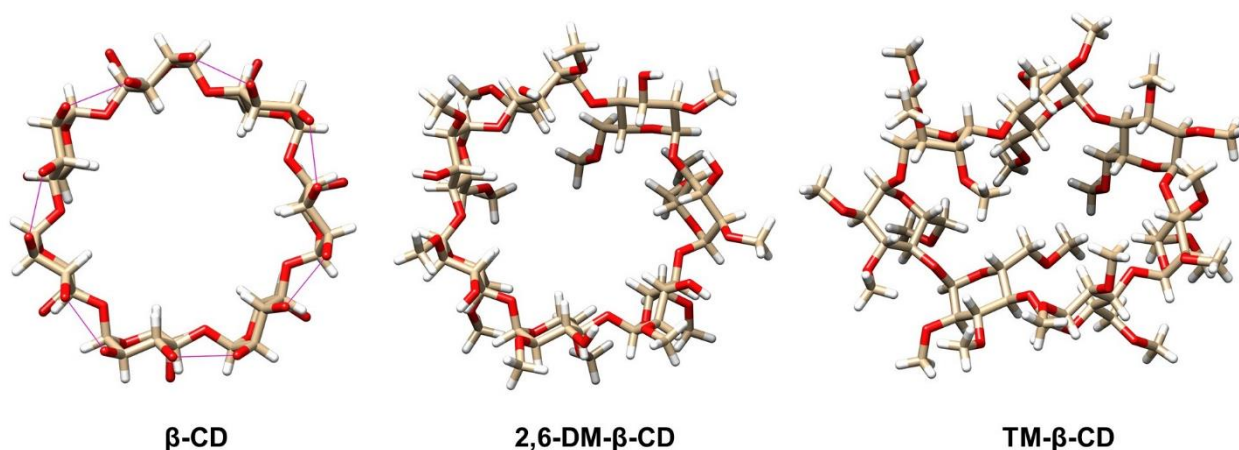


Figure 48. X-ray structures of β -CD (HBs as pink lines), 2,6-DM- β -CD, an TM- β -CD (structures released from the CSD entries AGAZOX,⁶⁶⁹ DEZMIE10,⁶⁷⁰ and HEZWAK10⁶⁷¹). In particular, in β -CD, a dynamical HBs flip-flop between the 2- and 3-hydroxyl groups of the macrocycle contributes to make it more rigid, also reducing its solubility.⁶⁷²⁻⁶⁷⁴ Substitution of CD hydroxyls may impact intramolecular HBs and, consequently, structure and recognition mode of the CD itself. Thus, if the substitution does not affect the formation of the intramolecular HBs, the CD maintains its round shape. This occurs in β -CD and heptakis(2,6-di-O-methyl)- β -CD (2,6-DM- β -CD). On the contrary, when the introduced substituents weakens or impedes intramolecular HBs, the macrocycle becomes more flexible, losing its roundness in part or completely. A typical example of this second situation occurs in the permethylated heptakis(2,3,6-tri-O-methyl)- β -CD (TM- β -CD) (Figure 48).⁶⁷⁵ Indeed, X-ray analysis provided a distorted elliptic-shaped structure for the permethylated macrocycle ring.^{671,672} In this case, due to the methylation of the 3-hydroxyl groups, the distance between the potentially interacting hydroxyl groups located on adjacent residue tends to increase due to the enhanced steric hindrance.

In some cases, intramolecular interactions within the selectand may affect their conformational properties and, in turn, their enantioselectivity. This type of feature was observed in 2-(benzylsulfinyl)benzamide (BSBA) by theoretical studies, which was identified as the origin of the large enantioselectivity ($\alpha > 100$) of BSBA on CDCPC.^{522,676-678} Indeed, by correlating calculated properties with experimental chromatographic parameters a stereoselective intramolecular HB within the analyte were shown to exhibit a pivotal role in enantiodifferentiation, limiting conformational freedom of a single enantiomer and weakening its ability to exert intermolecular HBs with the CS, thus defining different enantiophore systems for each eluted enantiomer (Figure 49).⁵²²

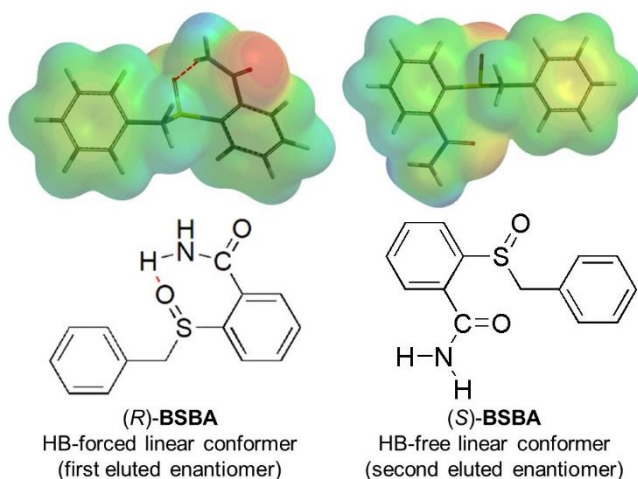


Figure 49. V surfaces of HB-forced linear conformer (first eluted enantiomer) and HB-free linear conformer (second eluted enantiomer) of BSBA.

It is worth mentioning that the impact of intramolecular noncovalent interactions within the analyte was observed for the first time by Carotti et al. in the enantioseparation of carnosine enantiomers on the Teicoplanin A2-2-based chiral stationary phase.⁶⁷⁹ Through MD simulations, (*S*)-carnosine was found to establish intramolecular contacts between its ionized functional groups, that limit its conformational freedom and weaken the association with the CSP, whereas (*R*)-carnosine presents higher conformational freedom and ability to form intermolecular contacts with the CSP. Recently, intramolecular interactions within both analyte and selector have been also observed by MD simulations for the enantioseparation of chiral tetrahydroindazole derivatives on the brush-type Whelk-O1 as chiral column.⁶⁸⁰ These intramolecular interactions determine conformation constraints within the structures that impact interaction modes of both analyte and selector.

Intramolecular interactions may play a significant role in controlling the conformation of catalysts that bear rotatable bonds near the catalytically active center. Very recently, well-defined and uniform asymmetric environments around the catalytically active Rh(II) centers was obtained by Furuta and co-authors by using intramolecular ChB interactions between sulfur and oxygen atoms in ligand **23** (Figure 50).⁶⁸¹

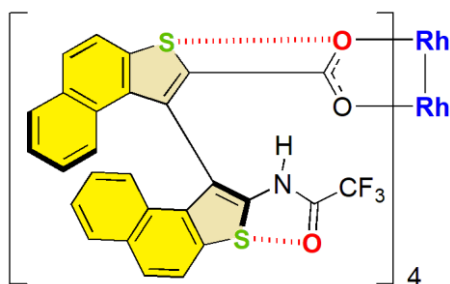


Figure 50. Structure of the Rh(II)-catalyst **23**.

A single-crystal XRD analysis indicated that the Rh centers in **23** are embedded in uniform and defined chiral environments that might arise from the presence of intramolecular ChBs which frozen the catalyst in a paddle wheel-shaped structure. As a result, catalyst **23** demonstrated outstanding catalytic performance in diastereo- and enantioselective intramolecular C–H insertion reactions.

4.2 Biological enantioselective recognition

4.2.1 Enantioselective drug action

A large portion of therapeutic agents is constituted by chiral molecules. Given that many natural molecules are chiral, many of the compounds used as active ingredients in natural therapies over time have been chiral, sometimes occurring in single-enantiomer form. Indeed, for thousands of years, natural mixtures obtained from plant, animal, or mineral sources have been used against human diseases, even if this type of approach based on customs and traditions is, often, without rational and scientific bases. Moreover, the toxicity of many of the products should not be underestimated. However, despite these problems, actually some of the natural preparations have proved to be effective against some symptoms and diseases.⁶⁸²

The enantioselectivity in drug action was scientifically evaluated in the beginning of the 20th century. Starting from this period, many natural products were extracted from their natural source and purified, and their chemical structure characterized. Moreover, many synthetic therapeutic agents were available by designed procedures. On these bases, both enantiomeric forms of many chiral drugs were available for studying their pharmacological activity and biological fate. For instance, as already mentioned in Section 2, in 1920 (-)-hyoscyamine was found to be pharmacologically more potent than its (+)-enantiomer.¹²⁸ Examples of enantioselective toxicity were found for the 3,4-dihydroxyphenylalanine. In the 1960s, initial clinical trials of this treatment for Parkinson's disease used the racemic mixture, but it quickly became clear that unacceptable toxicity was present in the D-enantiomer, and the drug was developed in the single enantiomer L-form.⁶⁸³ The β -adrenergic antagonist activity of propranolol and other β -blockers was related to the (-)-(*S*)-enantiomer.⁶⁸⁴ Thus, biomacromolecules recognize and differentiate enantiomers on the basis of their different dissociation constants from the binding sites. As a consequence, different behaviors and pharmacological responses are observable.^{685,686}

On this basis, in the 1990s, regulatory authorities and the pharmaceutical industry began to act on the recognition that, in many cases, the two enantiomers in a racemic mixture are two biologically distinct substances. Four main factors contributed to produce this renewed attitude toward the role of chirality in new-drug development: *a*) the tragic consequences of the thalidomide administration in the 1960s;⁴⁴ *b*) the considerable advances in stereoselective synthesis during the last decades of the 20th century, which paved the way for a number of single-enantiomer drugs, drug

metabolites, and molecules with highly complex stereochemistry; *c*) the development of powerful methods for enantioselective analysis, in particular enantioselective chromatography. The availability of these methods have allowed for improving procedures for the determination of the enantiomer composition or enantiomeric purity and for studying enantioselective pharmacokinetics and metabolism of chiral compounds, in particular to what concerns low levels of contamination of the eutomer (more active enantiomer) with the distomer (the less active enantiomer). Moreover, analytical methodologies have also allowed the study of enantioselectivity in the pharmacokinetics and metabolism of chiral substances; *d*) improvements of computational techniques, such as molecular docking and MD, and strategies such as virtual screening, and pharmacophore-driven design which continues to have a pivotal role in rational drug design and comprehension of protein-ligand binding mechanism.⁶⁸⁷⁻⁶⁹⁰ The definition of the term “chiral switch” was introduced by Agranat and Caner in 1999,⁶⁹¹ and ten years later refined⁶⁹² in reference to the development of a single enantiomer from a chiral drug that has been developed previously as a racemate, or as a mixture of diastereoisomers.⁶⁹³ In the 1990s, ibuprofen was the first chiral drug of the non-steroidal anti-inflammatory drugs to be switched to the single-enantiomer version.⁶⁹⁴ The reason for such a switch originated from the evidence that the (*S*)-enantiomer was over 100-fold more potent as an inhibitor of cyclooxygenase 1 enzyme than (*R*)-ibuprofen. Nowadays, more than 50% of the pharmaceuticals available in the market are chiral and administrated as pure enantiomers or as racemate.^{686,693} In 2020, almost 60% of the pharmaceuticals approved by the Food and Drugs Administration were chiral.⁶⁹⁵

Stereoselectivity/enantioselectivity of a chiral drug may be observed in all pharmacokinetic processes, absorption, distribution, metabolism, excretion events, and toxicity, in particular in the metabolism of xenobiotics.^{685,686,696} The impact of chirality of β_2 -agonists on their pharmacological and pharmacokinetic activity has been widely studied over time, and recently the topic has been reviewed by Horáková and co-authors.⁶⁹⁷ β_2 -Agonists are a class of drugs that are mainly used in asthma and obstructive pulmonary diseases. These compounds contain one or more stereogenic centers in their structure, and their enantiomers exhibit different pharmacological properties. In terms of bronchodilatory activity, (*R*)-enantiomers showed higher activity. The mechanism of action of the individual enantiomers has been explained through a stronger binding of the more efficient isomer to the β_2 -receptor sites under defined stereochemical conditions. By considering adrenalin as an example,⁶⁹⁸ the key binding sites are mainly linked to three functional groups, such as the amino group, the hydroxyl group of the side chain, and the substituted aromatic nucleus. In Figure 51, a schematic structural model of the β -adrenoreceptor is shown, highlighting the agonist and antagonist binding regions.

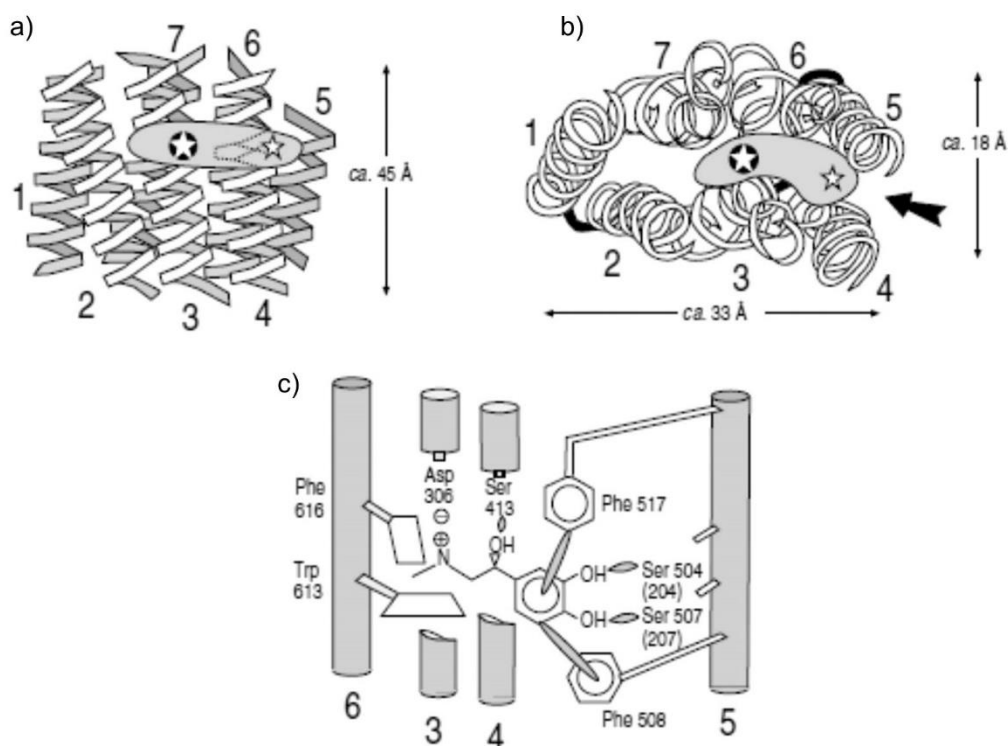


Figure 51. Diagram of the β -adrenoreceptor and its binding domain for agonist (\star) and antagonist (\odot). Helices are numbered, and the approximate dimension of the receptor is marked in Å: a) (side-view) cut-away view of the seven-transmembrane α -helices of the β -adrenoreceptor seen from the plane of the membrane lipid bilayer; b) (top view) the same beta-adrenoreceptor viewed from the extracellular space; c) expanded detail of the ligand-binding site for agonists formed by helices 3, 4, 5, and 6, during binding of adrenaline. Reproduced with permission from ref. 698. Copyright 1994 ERS European Respiratory Society.

The β -adrenoreceptor agonist binds to a hydrophobic pocket or active site located approximately 30–40% into the depth of the receptor. This accommodation corresponds to the position of the several amino acid residues that are critical in the binding of adrenaline. In particular, in terms of relevant noncovalent interactions, aspartate 306 in helix 3 forms a salt bridge with the amine of adrenaline, serine 204 and 205 in helix 5 interact with the two hydroxyl groups of an aromatic ring, phenylalanine 517 and 508 interact with the aromatic nucleus of adrenaline through vdW forces. In terms of enantioselectivity, the hydroxyl group on the stereogenic carbon in the side chain is relevant, forming HBs with serine 413 on helix 4.

In the last few years, molecular interactions between fenoterol stereoisomers (**24**) (Figure 52) and derivatives and the β_2 -adrenergic receptor binding sites were studied by docking and MD simulations.^{699,700} Docking studies indicated that the hydroxyl group at the first chiral center of the ligand creates HB with Asp113 or/and Asn312 in the case of (*R'*)-enantiomer mainly. MD simulations confirmed the existence of the stereoselective effects in ligand–receptor binding, different

stereoisomers exhibiting diverse conformational behaviors and distances between ligand–receptor atom–atom pairs. The marketed product is the racemic mixture of the (*R,R'*) and (*S,S'*)-fenoterol which was selected after initial development studies, demonstrating that this racemic mixture was more active than the (*R,S'*) and (*S,R'*)-fenoterol racemate.⁷⁰⁰

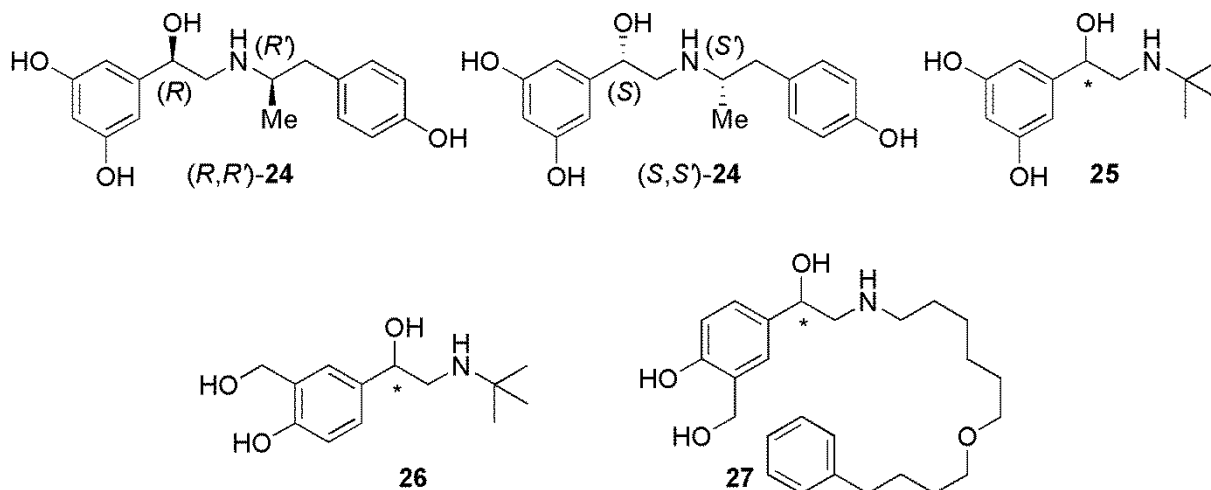


Figure 52. Structures of (*R,R'*) and (*S,S'*)-fenoterol stereoisomers (**24**), terbutaline (**25**), salbutamol (**26**), and salmeterol (**27**).

A series of studies explored the enantioselective pharmacokinetics of β_2 -agonists. In human studies, Borgström et al. reported that the bioavailability calculated from the plasma values was 7.5% for the (*R*)-(+)-terbutaline (*R*-**25**) and 14.8% for the (*S*)-(–)-terbutaline (*S*-**25**).⁷⁰¹ These differences indicated differences in absorption for both enantiomers of terbutaline and their first-pass metabolism. For salbutamol (**26**), Jacobson and co-authors observed enantioselectivity in plasma in experiments on horse model, whereas enantioselectivity was not observed in pulmonary lining fluid and the central lungs.⁷⁰² Recently, the same group observed an enantioselective distribution of salmeterol (**27**) in the central part of the lungs, with the (*R*)-enantiomer exhibiting about 30% higher distribution than (*S*)-enantiomer, an observation which is of importance in anti-doping assessments.⁷⁰³

Noncovalent interactions have been played a pivotal role in rational design of drugs. However, studies focusing on enantioselective noncovalent interactions in this field are rather rare. The most known XB-based interaction at biological level is that between thyroxine (T_4) and transthyretin (TTR), a tetrameric protein which transports the thyroid hormone in blood and cerebrospinal fluid (Figure 53a).⁷⁰⁴

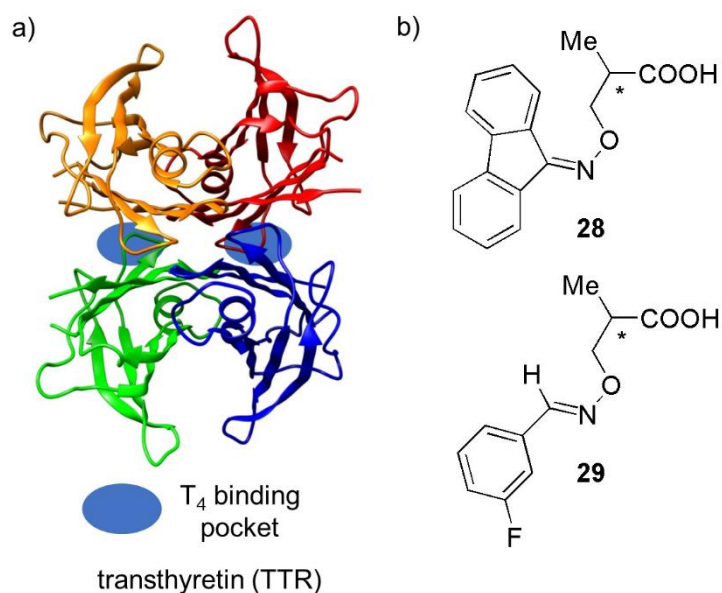


Figure 53. a) Tetrameric structure of TTR; b) structures of compounds **28** and **29**.

Mutations within the TTR structure may originate destabilization of the tetramer and its dissociation into amyloidogenic monomers, which misfold and self-aggregate into insoluble amyloid fibrils. TTR amyloidogenesis is involved as a relevant cause in amyloid diseases (TTR amyloidosis). In the last decades, a huge number of small molecules have been studied as potential inhibitors of the TTR dissociation. In general, this kind of molecules have been rationally designed in order to be accommodated in the halogen binding pockets (HBPs) of the protein and exert their function of stabilizing TTR and reducing fibril formation. In this context, XB may play a pivotal role as noncovalent interaction given that its formation was observed in the crystallographic structures of complexes between TTR and some of the halogenated ligands reported so far. Indeed, halogen substituents of TTR ligands and Ala109, Ser117, and Thr119 carbonyls of the protein, acting as XB acceptors, were found at close distances ranging from 2.8 to 3.5 Å.^{705,706} So far, few studies considered chiral inhibitors and their stereochemical properties. In 2009 Sacchetti et al. explored the inhibition activity of a series of β -aminoxypropionic acids, among them the enantiomeric pairs **28** and **29** bearing a single aromatic moiety, fluorenyl and aryl, respectively, linked through a flexible oxime tether to a carboxylic acid (Figure 53b).⁷⁰⁷ Through molecular docking analysis, only compound (*S*)-**28** revealed an effective interaction with the HBP3 with an activity of inhibition of fibril formation of 69%. The corresponding (*R*)-enantiomer inserted the methyl substituent into HBP3, directing the carboxylic group away from the key Ser117 or Ser117' residue, without any productive interaction, corresponding to a complete inactivity as inhibitor of fibril formation. Otherwise, the pair **29** showed lower enantioselective behavior with inhibition of fibril formation of 27% and 23% for the (*S*) and the (*R*) enantiomers, respectively.

Very recently, 4,4'-bipyridyl derivatives were evaluated as potential TTR stabilizers.⁷⁰⁸ In this frame, the 3,3',5,5'-tetrachloro-2-iodo-4,4'-bipyridyl substructure emerged as a promising chiral scaffold, and several (*M*)/(*P*) enantiomeric pairs containing a 2'-substituent were thus tested as inhibitor of the acid-mediated TTR fibrillogenesis process. For almost all compounds, low or moderate differences were observed between the enantiomer pairs, with the exception of the (*M*)-3,3',5,5'-tetrachloro-2'-(4-hydroxyphenyl)-2-iodo-4,4'-bipyridine (**30**) (Figure 54a). This enantiomer proved to significantly reduce fibril formation of wild type-TTR (16%), showing slightly better inhibition activity against fibril formation compared to the (*P*)-enantiomer.

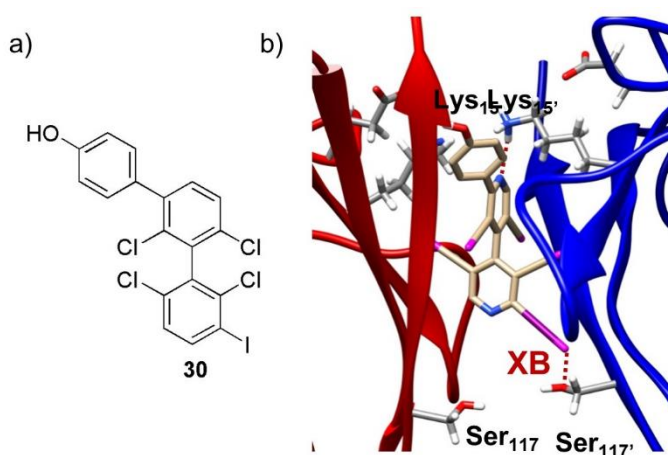


Figure 54. a) Structure of **30**; b) docking modes into the T₄ binding pocket for (*M*)-**30**.

Both experimental and docking results contributed to evidence the importance of HB sites located in the distinctive 2'-substituent and the capability of 2-iodine as XB donor which enhances ligand-protein binding only in the case of (*M*)-enantiomer (Figure 54b).

While the concept that different enantiomers may have different biological activity is well known, very recently Donald and co-authors observed that a single mutation (F98Y) in the methicillin-resistant *Staphylococcus aureus* flips the enantio-preference for cofactor binding and induces stereospecificity for binding of propargyl-linked antifolates as antimicrobial drug.⁷⁰⁹ In this study, the bacterial enzyme target was found to evade inhibitor binding stereoselectively (*chiral evasion*).

Despite the growing production of single-enantiomer drugs, a considerable number of drugs are still used as racemate, in general due to issues related to costly and challenging procedures for their production in enantiomerically pure form.⁷¹⁰ Therefore, exploiting new ways for appropriately using such chiral pharmaceuticals in racemic form may provide alternatives for circumventing problems related to their production in enantiomerically pure form. The concept of “enantioselective release” was put forward in 1993 by Duddu and co-authors.⁷¹¹ Enantioselective release combines two originally separating aspects in a single system, namely chiral separation and controlled release of

the eutomer from a racemate, while retarding the other isomer.⁷¹² Such processes may maximize the efficacy while minimizing the dosage and frequency of administration of chiral pharmaceuticals. Achievements in enantioselective release, which have been made so far, can be classified into two main groups: *a)* the “enantioselective interaction” strategy, where stereoselective interactions occur between chiral compounds and chiral matrices such as hydrogel, nanoparticles, self-assembled materials; *b)* the so-called “key-to-lock” strategy, recognizing sites inside molecular-imprinting polymers. The chiral compounds of interest are not limited to chiral drugs, but also include other biologically active chiral compounds such as amino acids.⁷¹³

An important aspect of the enantioselective drug recognition concerns the enantioselective recognition of biological drug transporters.⁷¹⁴ Indeed, if enantioselectivity has been demonstrated in pharmacological action, in pharmacokinetics, and in the binding mode of drugs, the enantioselective recognition of drug transporters toward drugs, and the inhibitory effects of drugs on drug transporters themselves have been found to be equally important.

4.2.2 Enantioselective transformations in nature

Enantioselective processes occurring in nature attract interest for *a)* human health and utilization and *b)* assessing the impact of chiral compounds in terms of pollution of aquatic and soil environments.

Proteinogenic amino acids, other than glycine, have chiral centers at the α carbon, with D- or L-configurations. In all domains of life, organisms exclusively use *l*-amino acids in ribosomal protein synthesis, metabolic pathways for amino acids being mostly enantioselective for *l*-enantiomers in order to maintain the predominance of these enantiomers. Otherwise, bacteria release D-amino acids as essential components of the peptides that cross-link sugar backbones in peptidoglycans in bacterial cell walls, and as signaling molecules in their ecosystems.⁷¹⁵ Free D-amino acids derived from bacteria are also involved in antibacterial responses in mammals. Indeed, symbiotic bacteria convert L-amino acids to D-amino acids in the intestines of mammalian hosts, whereas mammals maintain L-enantiomer dominance by expressing two flavin adenine dinucleotide-dependent oxidoreductases that degrade D-amino acids, and D-amino acid oxidases. Given this scenario, recently Sasabe and co-authors tested the *in vivo* effect of amino acids L→D conversion by symbiotic bacteria on development of mammalian immunity.⁷¹⁶ The results of this study revealed an unexpected roles of D-amino acid catabolism in the adaptive immune system of the small intestine, with D-amino acids functioning as bacterial signatures to promote mammalian immune responses to bacteria, and providing a new perspective on host-microbe symbiosis *via* amino acid chirality. It is worth mentioning that advanced analytical techniques have demonstrated that several D-amino acids are present in mammals, including humans, against the common opinion that L-amino acids are natural

and D-amino acid enantiomers are unnatural. On this basis, D-amino acids have also attracted interest as novel biomarkers in the prognosis of human diseases and novel bioactive substances.⁷¹⁷

Many important functions are carried out by the inner bacterial cell membrane such as respiration processes, transport, and biosynthesis of lipids. Factor disturbing structure and functionality of this membrane may cause metabolic dysfunction and cell death. Thus, the membrane disruption is considered to be one of the mechanisms of the antibacterial activity. Polyphenols such as catechins have been shown a strong antibacterial activity, being able to disrupt the bacterial membrane by binding to the lipid bilayer and by inactivating or inhibiting the synthesis of intracellular and extracellular enzymes.⁷¹⁸ Tsuchiya studied the catechin impact on membrane fluidity by measuring fluorescence polarization of liposomal membranes prepared with phospholipids and cholesterol, observing a dependence on the stereochemical properties of the polyphenols. Indeed, (–)-epicatechin, (+)-epicatechin, (–)-catechin and (+)-catechin were found to reduce membrane fluidity in increasing order of intensity. Such difference between enantiomers being increased by adding cholesterol to membrane lipids, the enantioselective impact of catechin stereoisomers could be induced by a combined effect of hydrophobicity and the chirality of membrane lipid components.⁷¹⁹

Chirality also plays an important role in flavor chemistry.⁷²⁰ Enantioselective analysis has become the main tool in the assessment of flavors, and increasing information are also available on structure-odor relationships of chiral flavor compounds and the influence of their configurations on odor thresholds and properties.⁷²¹ The first example of odor difference between enantiomers was reported by Ohloff and co-authors, who described sensory differences between the enantiomers of citronellol⁷²² and linalool.⁷²³ In the period 1990s-2000s, among the sulfur-containing aroma compounds present in foods, polyfunctional thiols attracted interest owing to their pronounced odor qualities and their low odor thresholds.⁷²¹ 3-(Methylthio)hexanol, and *cis*- and *trans*-2-methyl-4-propyl-1,3-oxathianes had been identified in yellow passion fruits in 1976.⁷²⁴ In the 1990s, 3-mercaptohexanol and the respective esters of 3-mercaptohexanol and 3-(methylthio)hexanol were reported for the first time in these fruits.⁷²⁵ The naturally occurring enantiomeric distributions of 3-mercaptohexanol shows a rather broad range, in some cases only a slight preponderance of the (*S*)-enantiomer.⁷²⁶ Otherwise, 3-(methylthio)hexanol and 3-mercaptohexyl acetate showed a predominance of the (*S*)-enantiomer. In terms of activity, odor thresholds of the 3-mercaptohexanol enantiomers were quite similar, whereas those of 3-mercaptohexyl acetate enantiomers differed. In the late 1990s, these sulfur-containing flavors was detected in Sauvignon blanc wines.^{727,728} Analogously to passion fruits, the alcohol showed only a minor preponderance of the (*S*)-enantiomer, whereas the enantiomeric purity of the acetate was significantly higher. In 1971, Teranishi's group reported differences in the odor properties of the carvone (**31**) enantiomers. Humans significantly

distinguish between the spearmint-like (*R*)-(-)-carvone (*R*-**31**) and caraway-like (*S*)-(+)-carvone (*S*-**31**) enantiomers.⁷²⁹ Recently, through a multidisciplinary approach, Krause, Krautwurst et al. revealed 11 amino acid positions characterizing the enantioselective binding pocket necessary for the carvone function in human odorant receptor OR1A1 (Figure 55).⁷³⁰ The odorant-interacting amino acid positions were identified within certain transmembrane helices (TMHs). In detail, five amino acid positions interact directly with the carvones, either by forming an HB (Asn109), in a **sterical** way (Gly108; Ile205), or by means of a hydrophobic interaction (Tyr251; Tyr267). Otherwise, six amino acid positions interact indirectly, either by spatial or hydrophobic contacts.

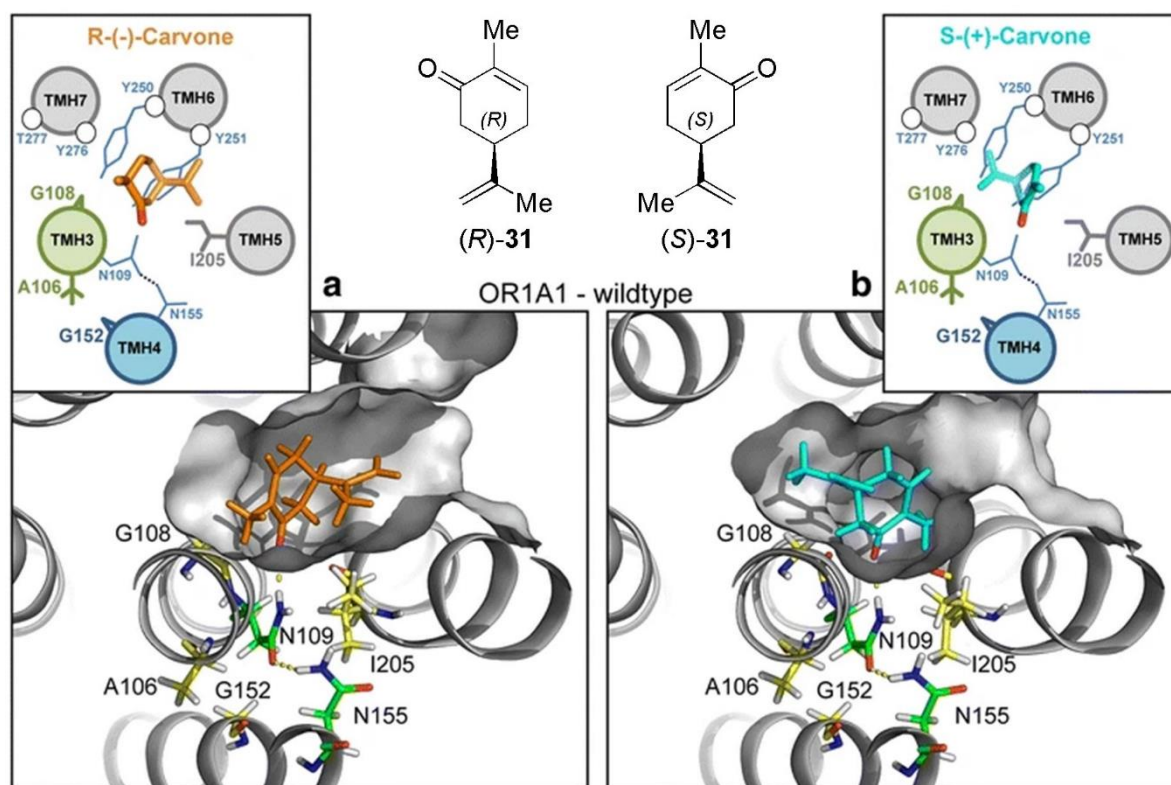


Figure 55. Molecular docking of carvone enantiomers (*R*-**31** and *S*-**31**) in the binding pockets of OR1A1. Adapted with permission from ref. 730. Copyright 2017 Springer.

In the last decades, the interest toward chiral drugs have been covering not only their pharmacological action, but a major concern also originates from the evidence that chiral pharmaceuticals are emerging environmental contaminants. Indeed, they have been showing to have persistent and toxic properties in the environment, exhibiting enantioselective behavior in terms of environmental occurrence, fate, and toxicity.⁷³¹ For instance, Kasprzyk-Hordern and co-authors showed that the (*S*)-enantiomer of amphetamine degraded faster in rivers and activated sludge.⁷³² As a chiral compound, residue of ibuprofen enantiomers is present in rivers, lakes, and sewage treatment plants, and exhibits enantioselective bio-behavior and bio-effects on the environment. An investigation into the enantioselective biodegradation of ibuprofen demonstrated that *S*-enantiomer

is preferably degraded, whereas the (*R*)-enantiomer may cause adverse effects to biota.^{733,734} Very recently, Wang and co-authors reported the effects of the co-presence of triclocarban (TCC), (3,4,4-trichlorocarbanilide), as a contaminant in sediment, on the enantioselective degradation of ibuprofen enantiomers.⁷³⁵ TCC is a broad-spectrum antiseptic, which has been used for decades in commercial products including detergents, cosmetics, and other personal care products for the prevention of microbial infections. Meanwhile, TCC may be harmful to aquatic organisms, and exposure to low concentration of TCC resulted in immune dysfunction and various adverse effects in wildlife and humans. Given that, the study of Wang indicated that ibuprofen and TCC significantly stimulated the activity of catalase and urease at low concentration treatment, and displayed inhibition effects at high concentration treatment. Moreover, different levels of TCC can lead to different half-lives of ibuprofen, and enantioselective degradation leading to *S*-enantiomer persistence.

Another urgent environmental issue concerns the usage of chiral agrochemicals, and the consequent need to understand the risk assessment to non-target organisms and human beings, liver microsomes being responsible for metabolisms of agrochemicals *in vivo*. In most cases, studies in this field are based on biological assays on environmental matrices, and chiral liquid chromatography/tandem mass spectrometry for identification and quantification of the enantioselective fate of the chiral contaminant.⁷³⁶ Most recent studies confirmed that chiral fungicides,^{737,738} herbicides,⁷³⁹ and pesticides⁷⁴⁰⁻⁷⁴² undergo stereoselective degradation in food, soil, and aqueous environment, the extent of the enantioselective processes being dependent on the features of the bulk matrix, and environmental conditions. In particular, stereoselectivity fate of chiral agrochemicals has been found to be more likely under aerobic conditions compared to sterile and anaerobic conditions, this evidence implies that the process is biologically driven.⁷³⁶ Stereospecific degradation in soils may also be affected by organic carbon content, and soil pH and texture.⁷⁴³ Very recently Tan et al. carried out focused studies on the potential effects of microplastics on the enantioselective degradation and distributions in water, sediment, and water–sediment microcosms of the three herbicides imazamox, imazapic, and imazethapyr.⁷⁴⁴ On this basis, it was found that microplastics could significantly increase herbicide persistence in water and sediment. While stereoselective degradation was not substantially found for the three herbicides, in the case of imazapic enantioselective degradation in water containing microplastics was observed.

In a mechanistic perspective, most studies concern the molecular causes of enantioselective concentration of chiral agrochemicals and their metabolites in tissue. Hamdy and Brock assessed the molecular causes of this phenomenon at protein binding level and *via* hepatic metabolism.⁷⁴⁵ Accordingly, Zhang et al. reported different affinities between enantiomers of chiral triazole fungicides and metabolic and cytochrome P450 enzymes (CYPs), and molecular interactions between

the enantiomers and CYPs were studied by molecular docking.⁷⁴⁶ In another study, Zhuang et al. focused on the free-energy-perturbation calculations, and in MD simulations unfavorable vdW interactions between the *cis*-metconazole isomers and the CYP3A4 binding pocket were observed and suggested as an explanation of the different binding affinities of the enantiomers.⁷⁴⁷ In particular, through molecular docking, the *cis*-(*R,S*)-metconazole was found to adopt an extended structure in the binding region of the enzyme, with its Cl atom exposed to the solvent, whereas *cis*-(*S,R*)-metconazole lies within the hydrophobic region of the active pocket. By molecular docking, Zhang et al. envisaged the enantioselective receptor binding affinities and binding modes with estrogen, and thyroid hormone receptors, as likely explanations for the greater hormonal effects of *S*-prothioconazole compared to (*R*)-prothioconazole.⁷⁴⁸ Racemic prothioconazole showed 3.4- and 2.4-fold higher estrogenic activities than (*R*)- and (*S*)-enantiomers, respectively, showing potential synergistic effects of the enantiomers in mixture. This study also reported that the metabolites of the *S*-prothioconazole-desthio, forming two HBs with His412 and Trp418 of thyroid hormone receptor, showed better binding than the other enantiomers. In the case of the estrogen hormone receptor, *S*-prothioconazole-desthio was the only enantiomer to form three HBs with Arg394, Glu353, and Lys449, while the *R*-enantiomer formed one HB bond with estrogen hormone. Fonseca et al. reported stereospecific differences in the metabolism of myclobutanil stereoisomers also in human liver, where the human CYP450 enzymes only metabolize the (*S*)-(+)-myclobutanil, whereas the (*R*)-(–)-enantiomer remains longer in the human body with potentially higher toxic effect.⁷⁴⁹

4.3 Enantioselective recognition in classical asymmetric synthesis

4.3.1 Enzyme-based enantioselective processes

Enzyme are nature's catalyst that are able to accelerate reactions up to 10^6 times with high selectivity.⁷⁵⁰ The potential of enzymes as enantioselective catalysts was recognized at the dawn of chirality history, but starting from the late 1990s,^{751,752} and more in the last decade, this field has evolved significantly. If in the beginning mainly lipases and esterases were used for the synthesis of chiral compounds, nowadays a wider range of both wild-type and mutant enzymes are available, and improvements in industrial applications and biochemical engineering have allowed to limit the impact of traditional issues such as cost and stability of enzyme-based catalysts.⁷⁵³ In the last few years, reaction classes such as reductive aminations, C-H functionalization and C-C bond formation have attracted interest, as well as advancements in this field have been enlarging the portfolio of available enzymes and related applications including cyclopropanation, N-H insertion, and S-H insertion. Indeed, the progress in sequencing technology has made available an increasing number of sequence data, these genes encoding for novel and unexplored enzymes useful for biocatalysis.⁷⁵⁰ Advanced XRD and computational techniques mainly contributed to providing information on shape and size

of catalytically active binding sites, function of specific residues populating the binding pockets, and noncovalent interactions controlling enantioselection.

A first important action allowing significant improvements in this field is directed evolution.⁷⁵⁴⁻⁷⁵⁶ This strategy is based on the concept that, as nature's enzymes are the product of evolution, scientists can control the evolution of enzymes in the laboratory, making them able to catalyze specific non-natural reactions (Figure 56). For instance, by engineering CYPs Arnold's group has identified a highly active and enantioselective catalyst for cyclopropanation of electron-deficient olefins, observing that cyclopropanation activity is mainly determined by the electronic properties of the P450 proximal ligand, which consequently can be used to tune the activity of the mutated enzymes.⁷⁵⁷ By engineering CYPs through T268A and C400S mutations, the same group also reported the first highly active enzyme catalysts for C-H amination, the T268A mutation enhancing the stereoselectivity of C-H amination through steric effects.⁷⁵⁸

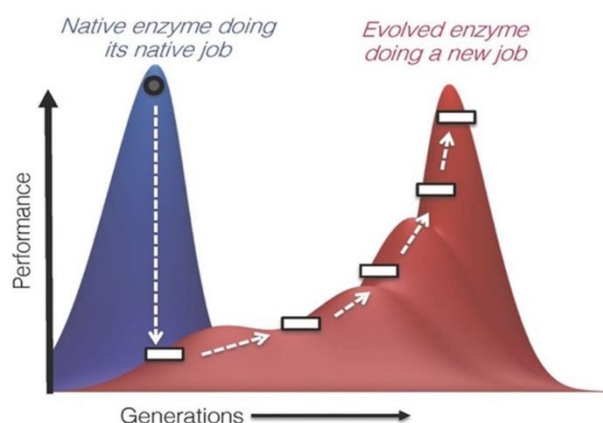


Figure 56. Directed evolution through cycles of mutation and screening can discover changes in sequence that improve performances of mutate enzymes towards new reactions. Reproduced with permission from ref. 755. Copyright 2019 John Wiley and Sons.

Using the Turner system for the deracemization of primary amines catalyzed by monoamine oxidase mutants as a model experimental platform,⁷⁵⁹ recently Reetz et al. described a new directed evolution approach to improve the activity of the enzyme, and to modulate stereoselectivity of the chiral products by applying mutagenesis strategies simultaneously on residues lining the binding pocket of the enzyme (five sites A-B-C-F-H) and of the entrance tunnel (three sites D-E-G) (Figure 57).⁷⁶⁰ Reversal of enantioselectivity compared to the results of Turner was obtained in some cases, and MD simulations indicated that the modified catalytic profile is due to the altered shape of the binding pocket and to the enhanced hydrophobicity of the entrance tunnel.

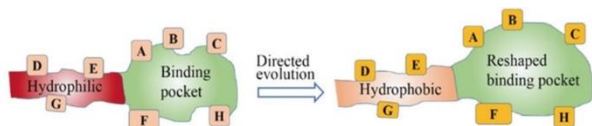


Figure 57. Schematic representation of simultaneous entrance tunnel and binding pocket tuning for activity and enantioselectivity by directed evolution of monoamine oxidase mutants, starting from the Turner system of chiral 1,2,3,4-tetrahydroquinoline synthesis. Adapted with permission from ref. 756. Copyright 2020 John Wiley and Sons.

Based on a close interaction between chemistry, biology and engineering, “*chemomimetic*” strategies that draw from synthetic chemistry mechanisms and non-biological reagents, or strategies, have been guiding the development of novel biocatalysts. As noted by Arnold, “*Synthetic chemists have been drawing inspiration from biology for decades, and now is the time for protein engineers to use inspiration from synthetic chemistry to generate new enzymes that will improve on and replace synthetic catalysts and reaction pathways*”.⁷⁵⁴

In the frame of this concept, the synthetic potential of cofactor-dependent enzymes has been explored to create new catalysts,⁷⁶¹ a given cofactor being often able to catalyze a multitude of chemically diverse transformations, with the protein structure acting as a guide toward one out of many possible pathways. Fasan’s group demonstrated that myoglobin (Mb), a heme-containing protein that naturally bears an axial histidine ligand, also performs cyclopropanation efficiently *via* carbene transfer (Figure 58a) when a second, distal histidine is replaced with a smaller side chain.⁷⁶² Whereas under reducing anaerobic conditions wild-type Mb (Figure 58b) catalyzes the cyclopropanation of styrene with ethyl diazoacetate with good diastereoselectivity for the *trans* isomer, but minimal enantioselectivity (6% *ee*), the introduction of mutations at H64 and V68, both located at the distal face of the heme, creates a highly diastereo- and enantioselective (> 99.9% *ee* and *de*) catalyst, which was shown to be capable of 46000 turnovers at high substrate concentration. The mutations control the accessibility of the heme center to the reactants, and expand the size of the distal cavity above the nitrogen atom N2 of the heme group (Figure 58c). In geometry A, the carbene ester group is above heme N2 and the styrene phenyl group extends toward the solvent, this picture being consistent with the experimentally observed *trans* and 1*S*,2*S* selectivity of the catalyst for ethyl 2-phenylcyclopropanecarboxylate (**32**) formation, and appearing sterically feasible. Otherwise, geometry B imposes a steric contact between the styrene ring and Phe43. On this basis, the V68A mutation could favor A by better accommodating the carbene ester group in proximity of N2, thereby explaining the dramatic effect of this mutation toward improving 1*S*,2*S* enantioselectivity (6→99.9% *ee*). Recently, re-designing the active site of Mb, the same group developed a sustainable biocatalytic system for the enantioselective synthesis of cyclopropyl- δ -lactones, which are versatile substructures in bioactive molecules as well as starting materials for the preparation of trisubstituted cyclopropanes.⁷⁶³ Moreover, metalloenzymes have been shown to be ideal platforms for achieving catalyst-controlled selective C–H bond functionalization as their reactivities can be tuned by protein

engineering and/or re-designing their cofactor environment. On this basis, engineered heme and non-heme iron dependent enzymes have emerged as promising scaffolds for executing C–H functionalization with high chemo-, regio-, and stereocontrol as well as tunable selectivity.⁷⁶⁴

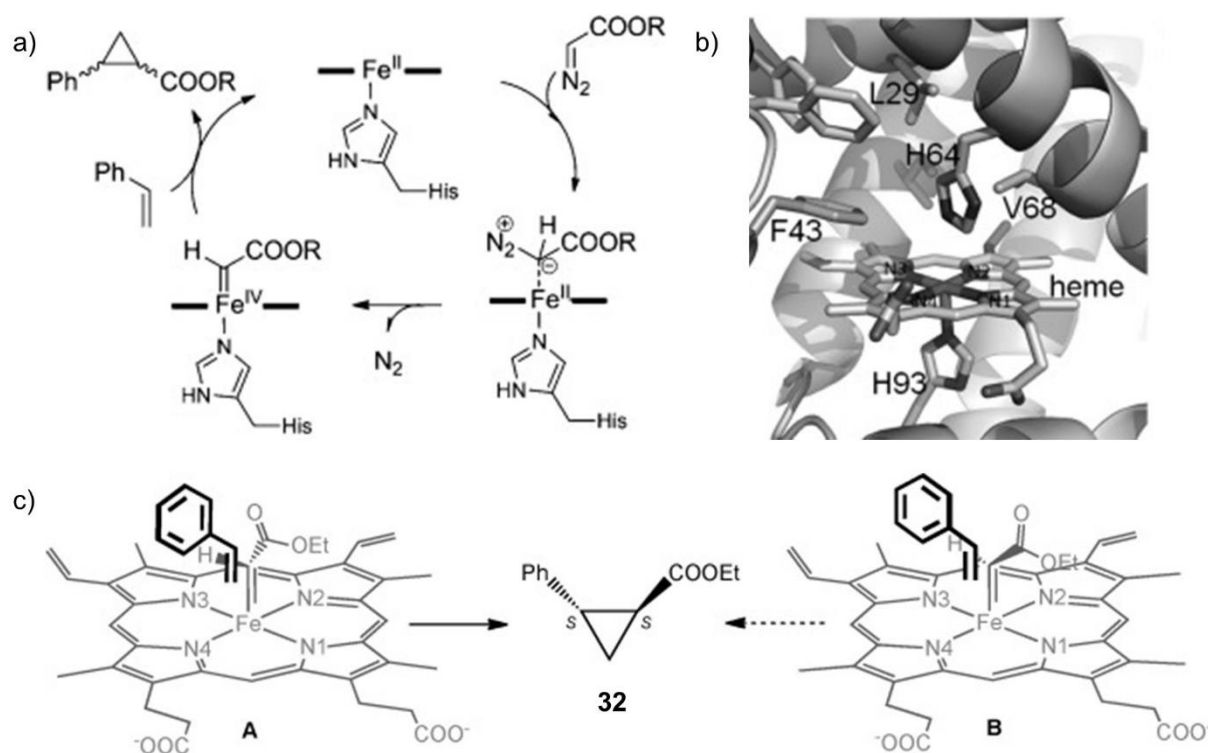


Figure 58. a) Proposed mechanism for myoglobin-catalyzed styrene cyclopropanation with diazo esters; b) active site of sperm whale Mb (pdb 1A6K), the residues targeted for mutagenesis are Phe43, His64, and Val68; c) proposed geometries for styrene approach to the heme-carbene complex leading to the (1*S*,2*S*)-ethyl 2-phenylcyclopropanecarboxylate (**32**) stereoisomer, with the orientation of the heme rings being the same as in figure a). Adapted with permission from ref. 762. Copyright 2015 John Wiley and Sons.

A second factor underlying the implementation of enzymes is the increasing number of computational methodologies and tools which have been developed to assist the design of smaller and smarter enzyme mutant libraries by disclosing reaction mechanisms and factors governing specificity and selectivity.⁷⁶⁵⁻⁷⁶⁷ In particular, *de novo* design of biocatalysts binding small ligands with good affinity may be a challenging problem, requiring precise calculation of rather weak protein–ligand interactions.^{765,768}

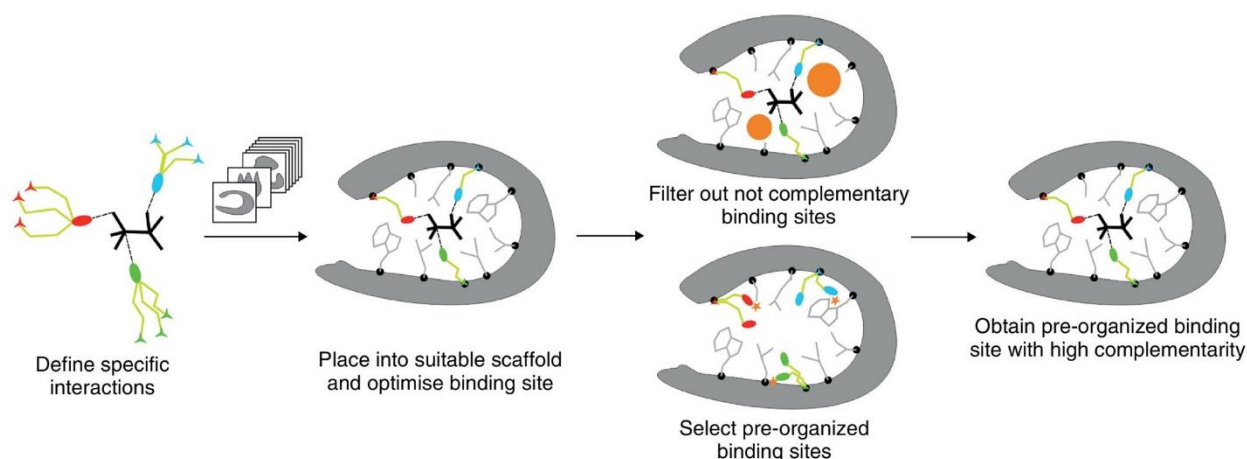


Figure 59. Workflow for *de novo* design of ligand binding protein. Reproduced with permission from ref. 765. Copyright 2014 Elsevier.

As summarized in Figure 59, the workflow for *de novo* design of biocatalysts binding small ligands is based on *a*) a specific, energetically favorable HB and vdW interactions with the ligand, *b*) high overall shape complementarity to the ligand and *c*) structural pre-organization in the unbound protein state to minimize entropy loss upon ligand binding. Recently, Janssen and Wu re-designed computationally a highly selective aspartase for regio- and enantioselective hydroamination of different acrylates (> 99% *ee*).⁷⁶⁹ With the aim of engineering an effective catalyst for the enantioselective β -hydroamination of α,β -unsaturated carboxylic acids, the authors evaluated aspartase from *Bacillus* sp. YM55-1 (AspB), which catalyzes the reversible deamination of aspartate to yield fumarate and ammonia. The authors first investigated the reaction mechanism and the interaction network (Figure 60) of the starting AspB by X-ray crystallography, site-directed mutagenesis and QM calculations, then defining a model to predict enzyme variants carrying sets of compatible mutations for the optimization of the interactions between the new substrate (acrylates) and enzyme.

The most useful approaches used in the field of enantioselective enzyme-based catalysis are molecular docking, MD, hybrid QM/MM and the quantum chemical cluster approach. Molecular docking and MD have been widely exploited to qualitatively rationalize the observed enantiopreferences of the enzyme and in directing enzyme engineering rationally. The main limitation is that these methods are based on the assumption, which is not always justified, that the factors controlling the enantioselectivity in the selectivity-determining step of the reactions are the same as in the ground-state enzyme-substrate complex.⁷⁶⁷

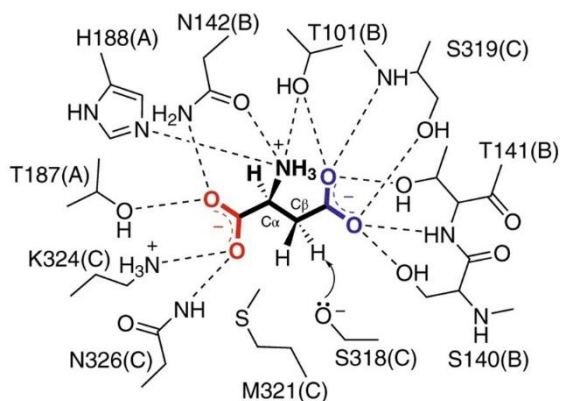


Figure 60. Schematic representation of the interactions between aspartate and AspB, based on PDB 3R6V. Reproduced with permission from ref. 769. Copyright 2018 Nature Publishing.

First proposed lock and key models were based on *a*) the binding of a substrate molecule to the active site on the enzyme resulting in activation of the substrate (reactive conformation),⁸⁶ and later *b*) on the hypothesis that the “*key does not fit the lock perfectly but with a certain strain on it*”, namely a ground-state destabilization occurs.⁷⁷⁰ Later the concept evolved toward the transition-state theory, which considers the preferential binding based on enzyme-substrate complementarity in the TS as the source of catalysis.⁷⁷¹ Another aspect concerns the fact that reproducing selectivity requires higher accuracy in the calculations of relative TS energies. With this aim, QM/MM calculations have been used successfully to study enzyme enantioselectivity, higher accuracy in part emerging from the cancellation of systematic errors between similar TS structures. In the cluster approach, QM methods, in general DFT, are used to treat the part of interest of the enzyme, approximating the rest as a homogeneous medium. In this case, the model has to be large enough to represent properly the environment of the active site. Recently, using a model of ca. 270 atoms, Himo et al. performed a computational analysis to model the enantioselectivity of the acyl transferase from *Mycobacterium smegmatis* in enzyme-catalyzed transesterification reactions when 1-isopropyl propargyl alcohol (**33**) and 2-hydroxy propanenitrile (**34**) were chosen as the acyl acceptor.⁷⁷² Indeed, the enzyme exhibited opposite enantioselectivities for these substrates, despite their structural similarity, acyl transferase from *Mycobacterium smegmatis* favoring the (*S*)-enantiomer of **33** and the (*R*)-enantiomer for **34**. As shown in Figure 61a, the barriers for the (*S*)-**33** and (*R*)-**33** were calculated to be + 12.1 and + 17.1 kcal/mol, respectively. Otherwise, for the hydroxy propanenitrile **34**, the barrier for the (*R*)-enantiomer was lower by 1.1 kcal/mol (Figure 61b).

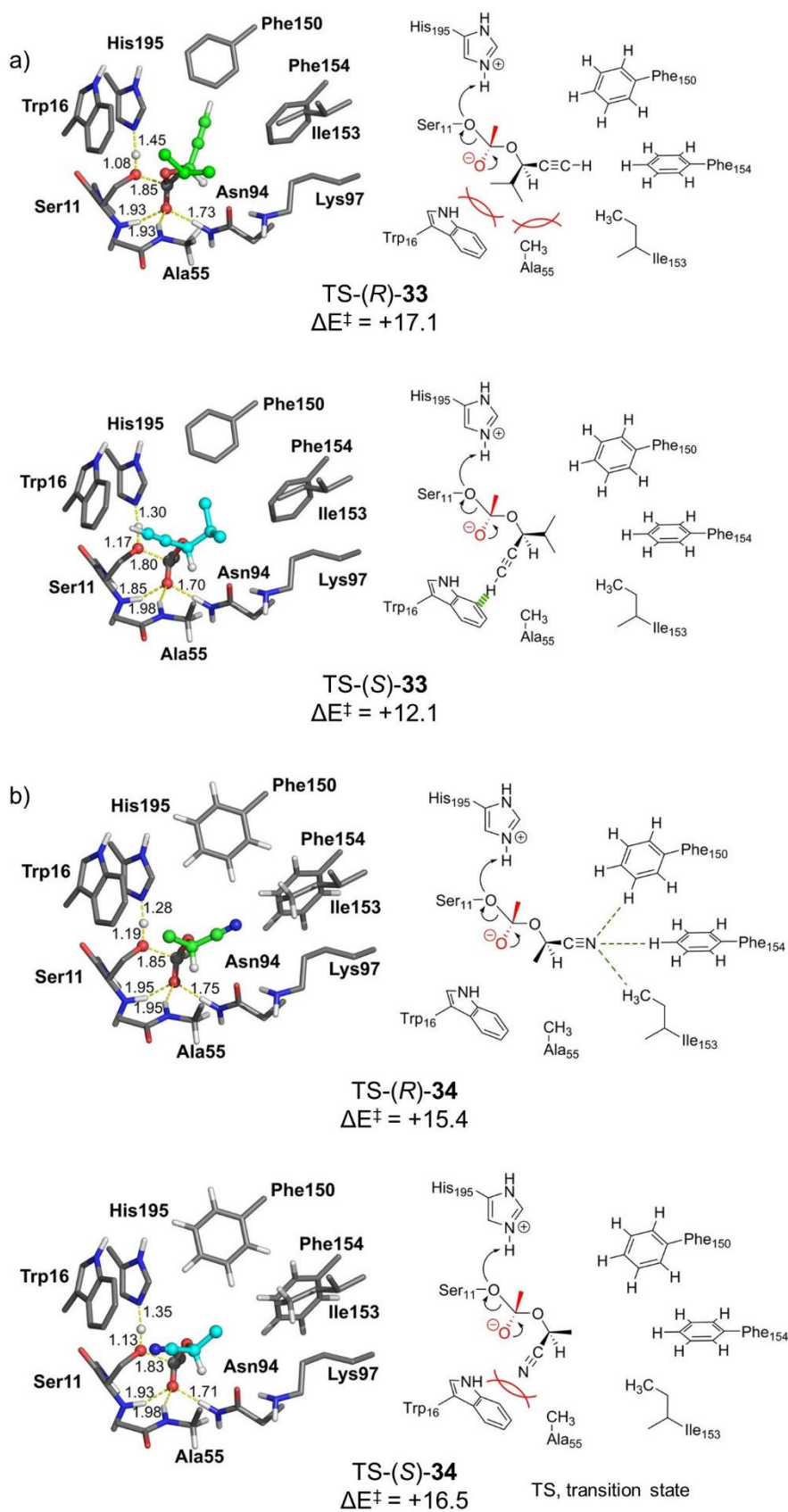


Figure 61. Optimized structures of the rate-limiting TSs for the reactions of the enantiomers of **33** (a) and **34** (b). Relative energies are given in kcal mol⁻¹. Adapted with permission from ref. 772. Copyright 2019 John Wiley and Sons.

The analysis of the optimized geometries of the rate-determining TS could reveal the noncovalent interactions contributing to the opposite enantioselection of the two substrates, the orientations of the substituents of the chiral carbons being the key to understand the selectivity in both cases. In the (*R*)-**33** TS (Figure 61a), the bulky propyl substituent points toward the Trp16 and Ala55 residues, causing a steric repulsion, while for (*S*)-**33** TS, the acetylenic group points in that direction, giving rise to a favorable C–H $\cdots\pi$ interaction between the acetylenic group and Trp16. In the case of **34** (Figure 61b), the nitrile substituent in (*R*)-**34** TS points toward the area of Phe154, Phe150, and Ile153, forming favorable electrostatic interactions to the C–H groups of these residues. In (*S*)-**34** TS, the nitrile group points toward Trp16, causing steric repulsion. Thus, beyond the most frequent HB, also π -clouds were found to be factors governing the enantiopreferences of enzymes.

Among enzymes, lipases can resolve many chiral compounds of commercial interest. However, for some substrates, it has been challenging to find lipases with the necessary chemo-, regio- and enantioselectivities. In this field, X-ray crystallography and computational simulation methods like molecular docking have allowed a detailed analysis of complementarity between the active site and various substrates, evidencing structural flexibility, HBs and electrostatic interactions as the molecular bases to explain lipase enantioselectivity.⁷⁷³ In particular, these studies have shown that the active site of lipases is cleft-shaped. Recently, Krieger and co-authors have reviewed studies on engineering of bacterial and fungal lipases for increasing enantioselectivity of kinetic resolutions. The authors evidenced the question as to how the features of the catalytic cleft of lipases influence enantioselectivity, using this analysis to identify key regions for introducing mutations through protein engineering.⁷⁷⁴ Thus, the regions of the catalytic cleft were re-classified as: *a*) the acyl-binding pocket, *b*) the hydrophobic cavity, *c*) the hydrophilic cavity and *d*) the oxyanion hole. Given this classification, for reactions involving carboxylic acids, the key regions impacting enantioselectivity have been found to be located in the acyl-binding pocket, the hydrophobic cavity and the oxyanion hole. For reactions involving chiral alcohols, the key regions are located in the hydrophilic cavity, the hydrophobic cavity and the oxyanion hole.

XB has been reported in small degree in the field of enantioselective enzyme-based catalysis, likely due to the fact that this noncovalent interaction was introduced to the biological community just in 2004, with the first survey of their occurrence in the structures of biological molecules.⁷⁷⁵ However, some pioneering studies on the XB-based catalytic activity of enzymes have been published, which are expected to pave the way to enantioselective applications of the concept in the next future. The role of XB in the nitrilase-catalyzed synthesis of *ortho*-, *meta*-, and *para*-chlorophenylacetic acid was explored by Wei, Zhang and co-authors, observing that different distributions of XB induce conformational modifications of substrate binding, affecting substrate

selectivity.⁷⁷⁶ Therefore, by modulating the halogen interaction, the substrate selectivity of the enzyme changes, with the consequence that XB could be also used as a versatile tool in enantioselective enzymatic catalysis. Starting from the evidence that (*R*)-chloromandelate is less active as substrate for D-mandelate dehydrogenase, Yu et al. engineered XB into the enzyme–substrate complex by site mutation in order to improve the catalysis activity toward chloromandelate.⁷⁷⁷ To investigate the impact of XB on enzyme activity, mutants were designed by introducing XB acceptor sites in the enzyme through site mutagenesis, thus engineering potential XB into the complex formed by D-mandelate dehydrogenase and chlorinated inactive substrate. Based on the directionality of the XB, the residues located within 6 Å of the chlorine atom, in the elongation of C–Cl bond in the substrate, were taken as the mutation hot-spots. On this basis, alanine at site 89 was designated as the mutation site, and five amino acids which have the potential to form XB with the substrate, including histidine, serine, cysteine, aspartic acid, and asparagine were considered to replace the 89A. All five mutants were tested by MD simulations, and the substrate binding and XB formation were examined. Only the histidine substitution with two nitrogen atoms was found to form a XB with the chlorine of the substrate ($d_{C\cdots N} = 4.5 \text{ \AA}$, $C\text{--}Cl\cdots N$ angle = 161.7°). As a result, the catalytic activity of the resulting mutant A89H toward *o*-chloromandelate resulted to be improved by 5 times. More recently, Ho and co-authors observed that introducing the unnatural amino acid *m*-chlorotyrosine (^mClY), in place of the tyrosine at position 18 (Y18) of T4 lysozyme, increases both the thermal stability and the enzymatic activity at elevated temperatures.⁷⁷⁸ The chlorine of ^mClY was shown to form XB to the carbonyl oxygen of the peptide bond at glycine 28 (G28) close to the active site. Indeed, QM calculations showed that an intramolecular HB from the adjacent hydroxyl substituent of the tyrosyl side chain, resulting in a distinctive synergistic HB-enhanced XB interaction, could enhance the XB potential of chlorine by polarization.

Finally, Xu and co-authors have recently reviewed enzymatic noncovalent synthesis (ENS) which refers to processes where enzymatic reactions control intermolecular noncovalent interactions for spatial organization of higher-order molecular assemblies that exhibit emergent properties and functions.⁸⁵ While in the enzymatic covalent synthesis the enzyme catalyzes the formation of covalent bonds to generate individual molecules, ENS covers the domains of functions, morphologies, and locations of molecular ensembles in cellular environments. The molecular building blocks used for exploring ENS are mainly peptides, but other building blocks, such as small organic molecules or drug candidates may be useful as substrates for ENS.

4.3.2 Enantioselective metal-based catalysis and organocatalysis

Recent studies reported in the last few years support the concept that the stereoselectivity of most catalytic reactions is based on the balance of both favorable and unfavorable noncovalent

interactions in the stereocontrolling TS.^{779,780} Thus, the versatility of enantioselective catalysis promoted by small molecules and ligands lies on the possibility to tune noncovalent interactions, which may be involved in the enantioselective processes, through insertion of specific groups or frameworks which are stereoelectronically able to carry out specific interactive functions. While in enzymatic catalysis noncovalent interactivity remains mainly driven by HBs, in metal/ligand-based catalysis and organocatalysis other interactions may impact reactivity and enantioselection. The development of DFT methods able of identifying dispersion-driven^{370,460,493} and other weak noncovalent interactions has allowed for quantifying their role in enantioselective processes with good accuracy. In particular, the dispersion-corrected B97-D and the ω -B97X-D functionals, paired with a triple- ζ basis set, have provided reliable relative free energies for many asymmetric reactions.⁷⁷⁹ Recently, Sunoj et al. proposed a computational-assisted method to quantify the total noncovalent interactions in stereocontrolling TSs of three asymmetric catalytic reactions involving chiral phosphoric acids.^{781,782} The authors found that catalysts equipped with large aromatic groups provide cumulative noncovalent interactions (C–H $\cdots\pi$, N–H $\cdots\pi$ and $\pi\cdots\pi$) with a stabilization force of 10 to 15 kcal mol⁻¹, confirming the *multipoint contacts* as a new model for chiral discrimination, and a versatile tool for catalyst design. Based on computational studies, dispersive forces have been shown to contribute significantly to π – π interactions, but this contribution is largely cancelled by exchange repulsion, a subtle boundary separating favorable dispersive interactions from unfavorable steric (repulsive) interactions.⁷⁸² Bistoni and co-authors explored the mechanism and stereocontrolling factors of two catalytic asymmetric Diels–Alder reactions of cinnamate esters with cyclopentadiene through high-level QM calculations.⁷⁸³ These reactions employ binaphthyl-allyl-tetrasulfone and imidodiphosphorimidate as two structurally and electronically different silylated enantiopure Lewis acid organocatalysts. In the first case, computational analysis showed that dispersive interactions overcome the repulsive steric interactions at the more congested face of the dienophile reagent, thus determining the most stable TS structure and process selectivity. Otherwise, in the second case, the selectivity was found to be governed by a delicate balance of dispersion and steric effects. Very recently, through computational analysis of the involved TS structures, attractive dispersive interactions were also found to impact on the outcome of enantioselective ruthenium-catalyzed C–H alkylations induced by a chiral carboxylic acid.⁷⁸⁴

Despite the management of dispersive interactions for catalyst design remains still a challenging exercise for chemists,^{322,779} Raynal and co-authors highlighted the potential of supramolecular catalysis as a discipline based on the fact that the properties of classical metal and organic catalysts can be carefully tailored through reversible interactions such as HB, metal–ligand, electrostatic and hydrophobic interactions. In this perspective, ligand, metal, organocatalyst, substrate, additive, and

metal counterion are reaction partners that can be held together by noncovalent interactions, the resulting catalytic species possessing unique properties compared to analogues lacking the assembling properties. Thus, through noncovalent interactions, several actions can be carried out, such as *i*) the building of bidentate ligand libraries, *ii*) the building of di- or oligonuclear complexes, *iii*) the alteration of the coordination spheres of a metal catalyst, and *iv*) the control of the substrate reactivity. Features of these supramolecular catalytic assemblies are the possibility to modulate easily the catalytic performance by modifying one of their building blocks, having at disposal new catalytic pathways or reactions which are not achievable with classical covalent catalysts.⁷⁸⁵ In enantioselective transition metal catalysis,⁷⁸⁶ while traditional approaches typically rely on repulsive steric interactions between chiral ligands and substrates in order to raise the energy of one of the diastereomeric TSs over the other, recent approaches are based on using noncovalent interactions to control enantioselectivity. In this field, a dual catalytic noncovalent assembly was used by Sunoj et al. in enantioselective Heck–Matsuda arylation.⁷⁸⁷ More recently, the same group explored the mechanistic details of Rh-(*S,S*)-YanPhos (Rh-**35**) (Figure 62) catalyzed asymmetric hydroformylation of α -methylstyrene through a DFT (ω -B97X-D and M06) computational study.⁷⁸⁸ After an exhaustive conformational sampling of the double axially chiral ligand **35**, bearing a *N*-benzyl BINOL-phosphoramidite and a BINAP-bis(3,5-*t*-Bu-aryl)phosphine, C–H $\cdots\pi$, $\pi\cdots\pi$, and lone pair $\cdots\pi$ noncovalent interactions between the *N*-benzyl and the rest of the chiral ligand were found to limit the *N*-benzyl conformers. Analogously, the C–H $\cdots\pi$ and $\pi\cdots\pi$ noncovalent interactions between the chiral catalyst and α -methylstyrene make the *si*-face binding to the Rh-center more preferred over the *re*-face. On this basis, the TS for the hydride addition to the *si*-face was calculated as 1.5 kcal/mol lower than that to the *re*-face, with a predicted *ee* of 85% for the *S* aldehyde (exp. 87%). Zhao and co-authors developed a series of noncovalent interaction-assisted chiral ferrocenyl phosphine ligands, including Wudaphos (**36**) (Figure 62).^{789,790} Due to the assistance of noncovalent interactions, the transition metal-ligand catalyst is capable to catalyze asymmetric hydrogenation and other transformations with remarkable improvement of reactivity and selectivity. By calculations, transition metal-Wudaphos **36** was shown to utilize both HB and ion pairing interactions in asymmetric hydrogenation of α -substituted unsaturated carboxylic acids and phosphonic acids. Mori, Sawamura and co-authors developed an iridium-catalyzed enantioselective transfer hydrogenation of ketones with formic acid by using a prolinol-phosphine as the chiral ligand.⁷⁹¹ In this case, QM calculations revealed that the sp^3 -C–H $\cdots\pi$ interaction between a sp^3 -C–H bond of the prolinol-phosphine ligand and the aryl substituent of the ketone is crucial for the enantioselection, in combination with O–H \cdots O/ sp^3 -C–H \cdots O two-point HB between the chiral ligand and carbonyl group of substrate.

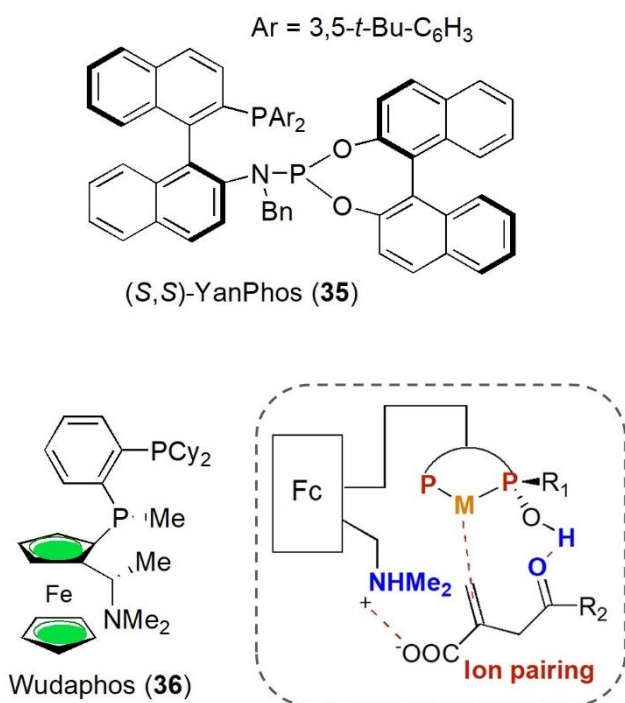


Figure 62. Structures of (*S,S*)-YanPhos (**35**) and Wudaphos (**36**) (Fc = Ferrocenyl).

In principle, computational QM chemistry allows to predict molecular properties by describing the electronic motion, providing valuable pieces of information for understanding reaction mechanisms, predicting structures and energies of the operative TSs, quantifying the impact of noncovalent interactions, and finally designing catalysts. However, in noncovalent catalysis, catalyst and substrate can interact in a number of ways, therefore too many potential transition-state structures make the application of computational direct approaches rather challenging. Alternatively, data-intensive methods for defining and applying predictive mechanistic models for enantioselective reactions have been developed in the last few years.⁷⁹²⁻⁷⁹⁶ In this regard, Milo, Neel et al. reported a data-intensive method for the enantioselective intramolecular dehydrogenative C-N coupling reaction of substrate **37**, catalyzed by chiral phosphoric acid derivatives **38**, in which catalyst-substrate association involves weak, noncovalent interactions (Figure 63).⁷⁹⁷ The authors probed steric and electronic effects of catalyst and substrate substituents by means of systematic physical organic trend analysis based on simple molecular descriptors (such as vibrational frequencies and dipole moments) that characterize the species involved in the reaction. These wealth of data regarding the impact of steric and electronic factors on enantioselectivity were more easily obtained than the computation of all possible TSs for each catalyst-substrate combination. The results confirmed that a perpendicular geometry of the triazole ring of **38** and the aryl ring of **37** could lead to higher enantioselectivities, supporting the hypothesis that the orientation of the triazole ring, coupled with its R group's steric constraints, controls π - π interactions involving the triazole core, optimizing the design of catalyst **39**.^{78,797}

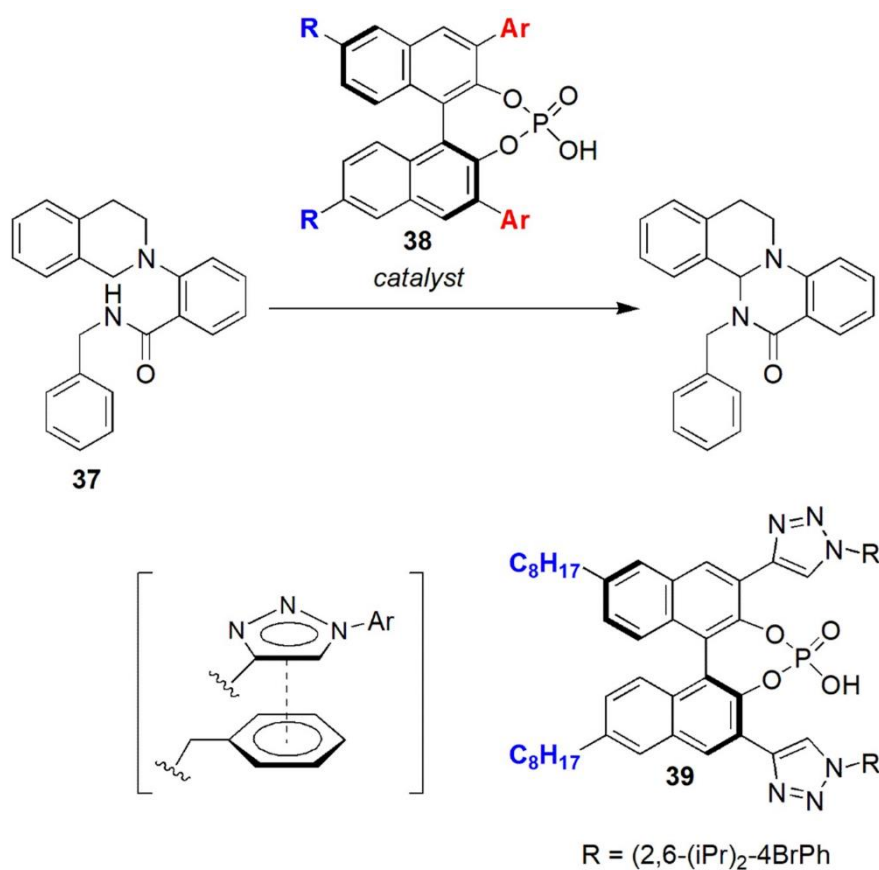


Figure 63. Screening of an initial library of chiral phosphoric acid derivatives **38** yields extensive data sets for the dehydrogenative C-N coupling reaction of substrate **37**, which are then used to define a predictive mathematical model through multivariate regressions, providing new mechanistic insights to design effective catalyst **39**. Abbreviations: *iPr*, isopropyl; Ph, phenyl

Very recently, discussing a workflow to relate computationally derived features of reaction components to enantioselectivity using data science tools, Sigman et al. stressed the advantages of merging traditional physical organic experiments with statistical modeling techniques to derive information enabling both evaluation of multiple mechanistic hypotheses and further catalyst design.⁷⁹⁸ The authors highlight how the mathematical representation of molecules can incorporate many aspects of a transformation, such as molecular features from substrate, product, catalyst, and proposed TSs. Statistical models relating these features to reaction outputs can be used for various tasks, such as performance prediction of untested molecules, and can guide the generation of mechanistic hypotheses that are embedded within complex patterns of reaction responses.

Noncovalent interactions may contribute to modulate the interplay between flexibility and selectivity of catalysts exhibiting a fluxional structure and, consequently, conformational heterogeneity, against the conventional view that highly selective catalysts should be fairly rigid. For instance, in small peptides, directional intramolecular noncovalent interactions, in general HBs, can stabilize a single conformation acting as a catalyst, among other possible structures. In this field,

Jorgensen et al. utilized MD simulations to investigate the role of conformational mobility on the reactivity and selectivity exhibited by a catalytic, β -turn-biased peptide, and of involved noncovalent interactions, in an atroposelective bromination reaction.⁷⁹⁹ Schreiner, Thiele et al. reported a NMR spectroscopic study of the catalyst-substrate interactions of a highly enantioselective oligopeptide catalyst that they used for the kinetic resolution of *trans*-cycloalkane-1,2-diols via monoacylation. In this case, the exceptional selectivity of the kinetic resolution was also rationalized by MD as well as DFT computations, envisaging the key role of dispersive interactions.⁸⁰⁰ Using DFT calculations, Wheeler et al. examined kinetic resolutions of axially chiral biaryls **40**, catalyzed by fluxional chiral 4-dimethylaminopyridines (DMAP), affording **41** and **42** (Figure 64a),⁸⁰¹ a reaction which had been previously reported by Sibi and co-authors.⁸⁰² This kinetic resolution exhibited high degrees of selectivity despite the use of a highly-fluxional chiral catalyst. Computational analyses led to a revision of the understanding of this reaction in which the interplay of numerous noncovalent interactions was shown to control the conformation and flexibility of the active catalyst, the preferred mechanism, and the stereoselectivity. Notably, while the DMAP catalyst itself was confirmed to be highly fluxional, electrostatically driven intramolecular $\pi \cdots \pi^+$ interactions lock the activated catalyst into a single conformation, making this active and acylated form of the catalyst highly rigid (Figure 64b), thus explaining its pronounced stereoselectivity. The authors used SAPT to quantify the noncovalent interactions between the individual components of catalyst forms A and A' (Figure 64a). It was observed that the isobutyrate reagent plays a central role in the mechanism by engaging in key HB networks. Exploring the TSs through conformational search for both atropisomers of alcohol **40** revealed that the *trans* (*re*) orientation (**43**) is strongly favored (Figure 64c), with a distinct relative orientation of the catalyst, alcohol, isobutyrate, and *N*-acyl group. The counterion (modelled as acetate) was shown to engage in a HB with the alcohol and a CH \cdots O interaction with DMAP. Moreover, subtle dispersion-driven interactions with the naphthyl group of the substrate were also found to enhance the stereoselectivity of the kinetic resolution.

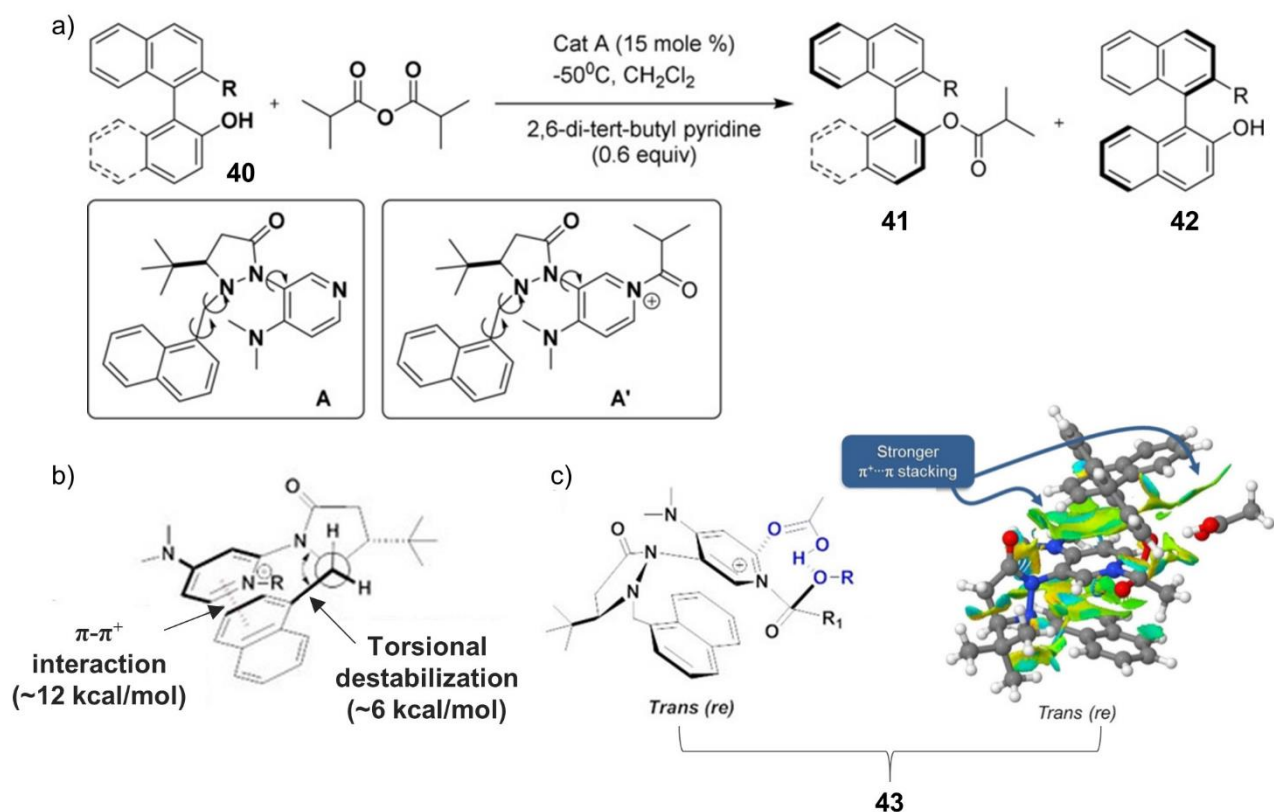


Figure 64. a) DMAP-catalyzed kinetic resolution of chiral biaryls **40**, b) key conformation of catalyst **A** after acylation (**A'**) along with the important intramolecular $\pi \cdots \pi^+$, c) orientations of the N-acyl group and relative positions of alcohol and isobutyrate counter-ion (modelled here as acetate) in a lower-lying *trans (re)* configuration **43**, and related NCI plot showing the greater number of dispersion-driven noncovalent interactions. Adapted with permission from ref. 801. Copyright 2019 John Wiley and Sons.

The interplay between steric effects and noncovalent interactions has been recently exploited by Chang et al., who described the Ir-catalyzed enantioselective access to chiral spiro lactam products **44** via the nitrenoid transfer to aromatic *ipso*-carbons (Figure 65a).⁸⁰³ The authors obtained the precise stereocontrol of the reaction by enhancing the secondary attractive and repulsive noncovalent interactions to eventually enable the aminative spirocyclization reaction with high enantioselectivity. For this purpose, a traceless O-silyl achiral auxiliary was introduced in the arenol-derived dioxazolone substrate, effectively differentiating two prochiral faces of the substrate (Figure 65b). Repulsive interactions between the bulky TBS group and the cyclopentadienyl (Cp) ligand resulted to be more significant in the (*R*)-TS (**45**) (Figure 65c, left). In sharp contrast, this steric repulsion was largely depleted in the (*S*)-TS (**46**) (Figure 65c, right) by arranging the bulky auxiliary downward. Interestingly, in **46**, a C–H $\cdots\pi$ attractive interaction is present between the incoming naphthyl group and methyl moiety of the Cp ligand in the distance range 2.73–2.77 Å. Thus, the computational analysis led the authors to rationalize that the traceless achiral auxiliary endows the catalyst system

with a more intimate asymmetric environment by the enhanced noncovalent attractions as well as the decreased steric repulsions, leading to more precise enantiocontrol over the spirocyclization process.

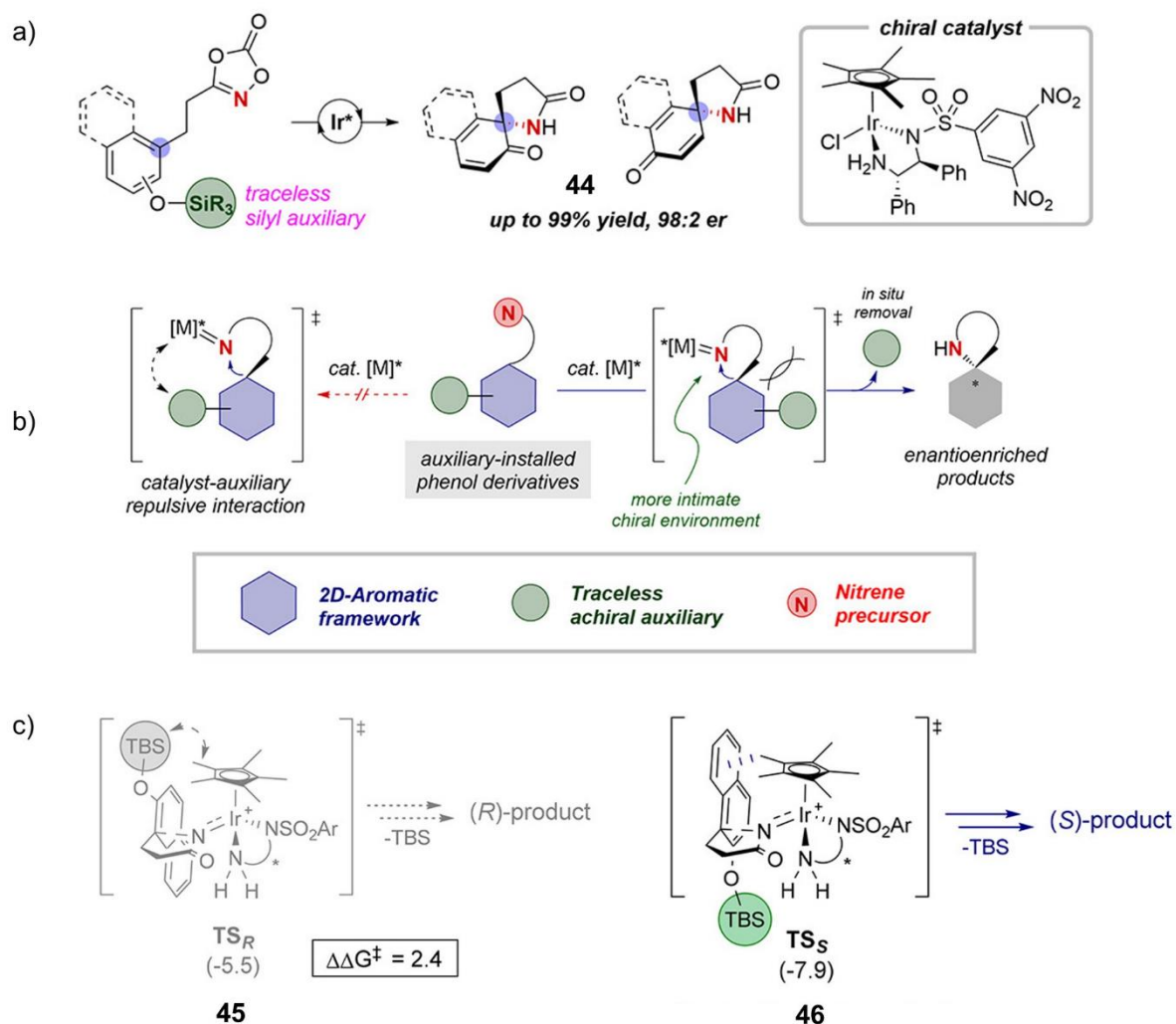


Figure 65. (a) Asymmetric synthesis of spiro lactams achieved by enhanced noncovalent interactions; (b) harnessing metal-nitrenoid and traceless achiral auxiliary; (c) computational structures of (*R*)-(**45**) and (*S*)-TSs (**46**) of enantioselective spirocyclization pathways. Adapted with permission from ref. 803. Copyright 2021 American Chemical Society.

An interplay between noncovalent interactions, again involving C–H··· π interactions was realized in the List's catalytic asymmetric Fischer indole reaction,⁸⁰⁴ which was computationally explored by Wheeler later.⁸⁰⁵ Both π -stacking and C–H··· π interactions of the substrate with the 3,3'-aryl groups of the 1,1'-binaphthyl chiral phosphoric acid catalyst was shown to impact the stability of the stereocontrolling TS. However, these noncovalent interactions oppose each other, with π -stacking interactions stabilizing the TS leading to one enantiomer, and C–H··· π interaction preferentially stabilizing the competing TS. In particular, the C–H··· π interaction dominates and, when combined with HB interactions, was found to lead to preferential formation of the product observed experimentally.

While a huge number of studies have been performed in the field of asymmetric HB-based catalysis,^{806,807} there are very few studies on XB-based asymmetric catalysis.^{642,808,809} The question of XB-based catalysis is that this interaction has a divergent character with respect to the relative position of the chiral backbone bearing the halogen and the substrate as XB acceptor, given XB directionality with a C-X...acceptor angle tending to the reference value of 180°. Thus, with the aim to engineer the interaction in exploitable manner, it is necessary that XB converges toward a chiral confined space which, in principle, may accommodate substrate and reagents involved in the catalytic process. In this perspective, monodentate catalyst have proven be too flexible and not suitable to induce chirality in these reactions.⁸¹⁰ Moreover, given that cationic *N*-heterocyclic substructures are able to activate by polarization potential σ -hole sites and originate strong XBs, the majority of chiral XB donors prepared so far contains this type of motif. The first studies in this field were reported by Tan^{811,812} and Arai⁸¹³⁻⁸¹⁵ but, in these cases, asymmetry was induced with bifunctional systems combining the use of XB and further noncovalent interactions. Thus, in these cases it was difficult to assess the actual role of XB. The first chiral triazolium-based bidentate catalysts were reported by Huber⁸¹⁶ and Kanger,⁸¹⁷⁻⁸¹⁹ but without noticeable asymmetric induction. In a recent study, Huber's group prepared a series of rigid chiral bidentate imidazolium-based XB donors, including the pre-organized **47** (Figure 66).⁸²⁰ By using this imidazolium-based XB donor as an organocatalyst, moderate enantioselectivity (33% *ee*) was observed in a Mukaiyama aldol reaction. This reaction represents the first example in which enantioselectivity has been obtained solely based on XB, with the *syn*-preorganization of the XB donor resulting in improved reactivity and selectivity.⁸²¹

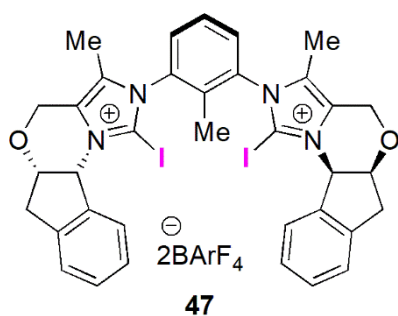


Figure 66. Structure of chiral bidentate imidazolium-based catalyst **47**.

Recently Taylor, García Mancheño et al. described a novel chiral tetrakis-iodo-triazole structure as a neutral XB donor for both chiral anion—recognition and enantioinduction in an asymmetric Reissert-type reaction.⁸²² Interestingly, the catalyst containing an iodine-based bidentate system favored the formation of the (*S*)-product with 30% *ee*, whereas the analogue bearing H in place of I favored the formation of the (*R*)-product with 56% *ee*. Kanger et al. developed a new asymmetric organocatalytic methodology that utilizes a HB-enhanced bifunctional XB catalyst for the activation of vinyl phosphonates in an asymmetric Michael addition of malononitrile to vinyl phosphonates.⁸²³

This approach represents the unprecedented utilization of organophosphorus compounds as substrates in XB catalysis, expanding the field of asymmetric XB catalysis. The authors also performed comparative experiments with catalysts containing different XB donor units and their hydrogen-analogues, confirming the superiority of the iodoperfluoro group as a neutral activating and enantioinducing unit. Very recently, Mamane, Peluso and co-authors designed and prepared a new family of chiral XB donors which were analyzed in the solid state and evaluated in catalysis. These compounds are based on: *i*) iodine as the σ -hole donor atom, *ii*) the triazolium ring to increase the σ -hole depth, and *iii*) a disubstituted ferrocene as the chiral source. Good catalytic activity was observed at room temperature with a iodotriazolium triflates in an aza-Diels-Alder reaction, and the best performance was achieved with a bidendate derivative. Low asymmetric induction (6.4%) was observed in the reaction with an enantiopure bidendate catalyst.⁸²⁴ Exploring the asymmetric pnictogen-bonding catalysis, Tan and co-authors reported an enantioselective transfer hydrogenation of benzoxazines catalyzed by a novel chiral antimony cation/anion pair.⁸²⁵ The catalyst showed remarkable efficiency and enantiocontrol even at 0.05 mol % loading. The authors also investigated the properties of the catalyst and the mechanistic insights by nonlinear effect studies, ¹H NMR, and liquid chromatography (LC)-mass spectrometry (MS).

In conclusion, it has to be noted that despite relevant advancements in comprehension of enantioselective noncovalent interactions acting in catalytic processes, some challenging questions still remain:⁷⁷⁹ *a*) treatments of the entropic component of the free energy. With respect to this topic, Wheeler noted that in some cases relative energies provide more reliable predictions of enantioselectivities than free energy predictions; *b*) the impact of explicit solvent interactions; *c*) treatment of processes where there is no clear stereocontrolling TS, or for reactions in which the relative stability of downstream intermediates controls the stereoselectivity; *d*) deconvolution and identification of multiple interactions acting in multifunctional catalysts, where each interaction may modulate another in the TS, in stabilizing or in destabilizing direction; *e*) at the moment it has to be recognized that designing catalysts that are perfectly complementary to any TS through noncovalent interactions engineering is still challenging.⁷⁸⁰ Despite that, some motifs appear particularly versatile to introduce modularity in catalyst design such as aromatic frameworks which may be readily introduced at multiple catalyst positions and decorated with functional groups featuring different steric and electronic properties. In this frame, organocatalysts such as chiral phosphoric acids, thioureas, and amino acids are attractive structures. It is worth mentioning that aromatic frameworks have also constituted the distinctive motif of catalytic systems able to *in situ* switch their chiral preference. This type of system was described by Feringa et al. integrating catalytic functions on a light-driven molecular motor, in which the stepwise change in configuration during a 360°

unidirectional rotary cycle governs the catalyst performance both with respect to activity and absolute stereocontrol in an asymmetric transformation.⁸²⁶ During one full rotary cycle, catalysts were formed that provide either racemic or preferentially single enantiomers of the chiral product of a conjugate addition reaction, demonstrating how different molecular tasks can be performed in a sequential manner, with the sequence controlled by the directionality of the rotary cycle. More recently, the same group used photoresponsive phosphoramidite ligands based on a chiral biaryl-substituted molecular switch to alter the activity and invert the stereoselectivity of a copper-catalyzed asymmetric conjugate addition,⁸²⁷ noncovalent interactions acting in a chiral space under the dynamic control of the molecular motor in the enantioselective catalytic reaction.

4.4 Enantioselective recognition in separation science: non-chromatographic methods

4.4.1 Enantioselective adsorption and permeation

In the last decades, chiral porous materials have attracted great attention in the field of enantioselective processes. These materials have been exploited for both adsorption and permeation processes owing to their homochirality and permanent pores and cavities. The presence of permanent pores and cavities favors the accessibility of chiral recognition sites during the enantioselective process, enhancing stereoselective interactions between chiral molecules with homochiral pores due to the confinement effect. On the other hand, the advantages of chiral cavities for enantioselective recognition has been successfully exploited in other homochiral materials classically used for enantioselective separations such as CDs, crown ethers, proteins, polysaccharide derivatives, and macrocyclic antibiotics. Nowadays, various homochiral porous materials such as metal-organic frameworks (MOFs), covalent-organic frameworks (COFs), porous organic cages (POCs) and metal-organic cages (MOCs) have been developed. With ultrahigh surface area, versatile chemical functionalities and tunable topology, these materials have proven to be promising for applications in enantioselective adsorption, chiral chromatography, and enantioselective membranes (Figure 67). In most cases, applications of these materials for enantioselective adsorption have been developed for enantioseparations of amino acids.⁸²⁸

An advantage of synthetic materials is the possibility to tune their properties in a modular sense. Recently, Cheng et al. reported preparation and enantioselective adsorption properties of $\text{Fe}_3\text{O}_4@\text{SiO}_2@\text{PNCD}$, chiral magnetic microspheres with core/shell/shell structure, which are composed of a Fe_3O_4 nanoparticle core, an acidic-resistant SiO_2 middle shell, and PNCD as a thermosensitive microgel functional shell which is the key of enantioselectivity of the functional material towards tryptophan enantiomers.⁸²⁹ Indeed, in the PNCD the β -CD molecules act as CSs, whereas the poly(*N*-isopropylacrylamide) (PN) chains serve as mediator for the association constants of β -CD/tryptophan complexes, with higher enantioselectivity toward L-tryptophan compared to the

D-enantiomer. Interestingly, the regenerated material could be conveniently recovered from the amino acid solution by using an external magnetic field for reuse.

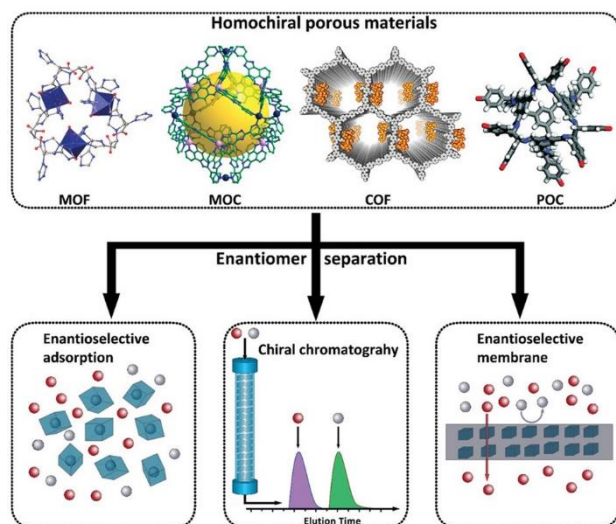


Figure 67. Possible applications of homochiral MOFs, MOCs, COFs, and POCs for enantioselective adsorption, chiral chromatography, and enantioselective membrane. Reproduced with permission from ref. 828. Copyright 2021 John Wiley and Sons.

Recently, Lee and co-authors reported the synthesis of homochiral porous nanosheets performed by the 2D self-assembly of non-chiral macrocycles, with open/closed pore switching.⁸³⁰ In this material, pore chirality is spontaneously induced by a twisted arrangement of dimeric macrocycles, and the 2D porous structure was used as enantiomer sieving membranes, obtaining uptake capacity greater than 96%. Later the same group constructed single-layered chiral sheet structures in aqueous MeOH solution using self-assembly of a rectangular plate-shaped aromatic amphiphile **48** that forms a 2D porous structure and consists of a tetrabranched aromatic segment and an internally grafted oligoether dendron (Figure 68).⁸³¹ The 2D chiral sheets consist of a lateral arrangement of chiral aromatic clusters, generating dual chiral void spaces in a hydrophilic solvent. These nanosheets with chiral void spaces were shown to function as superfast enantiomer separation nanomaterials which absorb rapidly a single enantiomer in a racemic mixture of hydrophobically substituted tartrates with > 99% *ee*. (*S*)-**48** porous sheet showed to uptake exclusively the L-form, with perfect inclusion preference over the D-form (>99% *ee*). NMR spectroscopic experiments confirmed that the chiral guest is entrapped in the void spaces of the sheet through host–guest aromatic (π - π) interactions. Otherwise, the (*R*)-**48** sheet uptakes exclusively the D-form in the racemic tartrate solution, demonstrating that the enantioselective absorption of the sheet in a racemic mixture solution arises from the chirality of the sheet itself.

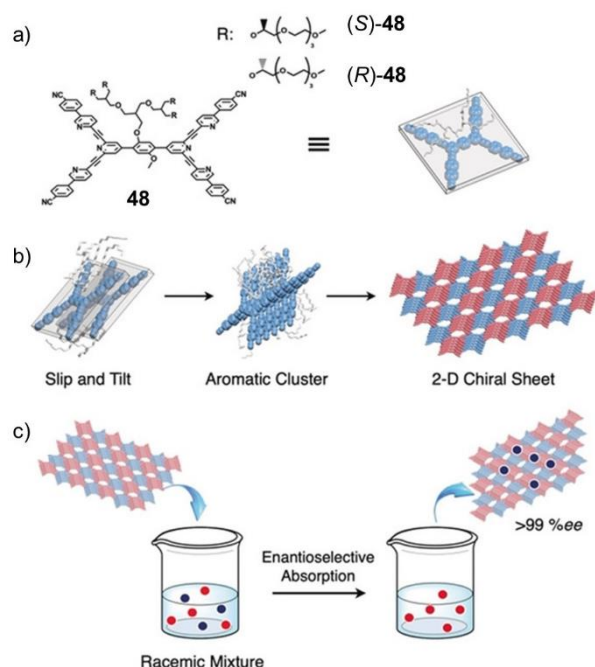


Figure 68. a) Molecular structure of **48**; b) schematic representation of the formation of a single-layered chiral nanosheet structure through lateral assembly of chiral clusters consisting of slipped planar aromatic segments; c) enantioselective absorption of the chiral sheets in a racemic mixture solution. Adapted with permission from ref. 831. Copyright 2020 John Wiley and Sons.

Among porous materials, the growing interest in the application of MOF for enantioselective processes has been witnessed by the numerous reviews published in this field in the last decade.^{183,185,319,828,832-837} The enantioselective adsorption on homochiral porous materials constituted the background to the development of successive chromatographic applications. In 1992, Mallouk and co-workers reported the first enantiomer resolution of chiral organic molecules through intercalation into a microcrystalline layer of a Zr-based phosphate bearing an optically active building block.⁸³⁸ Later, Kim and co-workers reported the first example of enantioselective inclusion of chiral molecules into the well-defined pores of a 2D layered homochiral MOF, able to resolve racemic [Ru-(2,2'-bpy)₃]Cl₃ (bpy = bipyridine) with a 66% *ee*.⁸³⁹ The main disadvantage of this type of structures is that in most cases, the cavities lack flexibility which is needed for mutual conformational adjustments between enantioselectivity inductor and selectand. In this perspective, size and shape complementarity of pores and selectand is a strict requirement for porous materials. In this regard, recently Aubert, Mamane et al. studied the enantioselective adsorption of three chiral compounds, with volumes ranging from 229.0 to 137.3 Å³, on an Ag(I)-based MOF featured by small pores, demonstrating the enantioselective adsorption for the smallest compound (16% *ee*) exclusively, along with a molecular sieve-like behavior toward the two larger racemates.⁸⁴⁰

Permeation mechanisms are of huge interest for transdermal drug delivery systems, and in recent years this field has been received much attention in the pharmaceutical industry for improving

administration of drugs in terms of extended therapeutic actions, decreased side effects, convenient use, and better patient compliance.⁸⁴¹ Stratum corneum, which is composed of ceramides, cholesterol and free fatty acids, is the main barrier against foreign bodies and the penetration of drugs.⁸⁴² On this basis, enantioselective permeation of drugs has been explored with the aims of *a*) understanding the enantioselective mechanisms of permeation, and *b*) developing enhancers favoring the transdermal delivery through the stratum corneum. Permeation behavior determining pharmacological action, (*S*)-propranolol has been found to be 100 times more active as a β -adrenergic blocker than the (*R*)-enantiomer, with the amount of (*S*)-enantiomer permeation being about 4 times higher than that of the (*R*)-enantiomer.⁸⁴³ Yuan et al. studied *in vitro* the influence of the chemophysical properties on skin permeation of enantiomers and racemate of ibuprofen, observing higher permeation for the pure enantiomers compared to *rac*-ibuprofen.⁸⁴⁴ Che et al. also confirmed that difference in skin permeability between (*S*)- and (*R*)-ibuprofen was due to the chiral nature of stratum corneum.⁸⁴⁵ Different transdermal permeation was also observed for (*S*)- and *rac*-ketoprofen.⁸⁴⁶ Very recently, through a multidisciplinary study involving *in vitro* transdermal permeation of the enantiomers through rat skin by diffusion cells, FT-IR, ¹³C NMR, differential scanning calorimetry (DSC) and molecular docking, Fang et al. have found that the amount of percutaneous permeation of (*S*)-flurbiprofen is greater than that of the (*R*)-enantiomer.⁸⁴⁷ FT-IR results confirmed that the different binding strength of the two enantiomers originated from the formation of different HBs between each enantiomer and the ceramides. By molecular docking, the authors verified that steric hindrance weakens the binding between ceramide and (*R*)-enantiomer, whereas (*S*)-flurbiprofen formed stronger HBs.

Enantioselective permeation enhancers can selectively promote the permeation of enantiomers. L-menthol has higher permeation enhancing effects on (*S*)-metoprolol than on (*R*)- and *rac*-metoprolol.⁸⁴⁸ The effects of linalool on the enantioselective skin permeation of naproxen has been also explored,⁸⁴⁹ as well as the enhancement mechanisms of transdermal enantioselective delivery of flurbiprofen by chiral 4-O-acylterpineol.⁸⁵⁰ Very recently, studies focused on the enantioselective permeability of chiral lipid bilayers have been reported.⁸⁵¹ Henriques, Craik et al. showed that the chiral environment of lipid bilayers can modulate the function of membrane-active peptides against the view that peptide–lipid interactions are achiral.⁸⁵² Coherently, Stupp and co-authors reported that supramolecular assemblies of peptide amphiphiles interact with lipid bilayer membranes in a stereospecific manner. Indeed, when negatively charged chiral phospholipid bilayer vesicles were subjected to the assemblies, peptide amphiphiles with L-amino acids show stronger affinity for the liposomes compared to the ones with D-amino acids.⁸⁵³

Lipid membranes exert a very important function at biological level, many processes occurring within compartments surrounded by these membranes which control the access of some substances, but at the same time stop others from entering the compartment. Given this concept, recently Lee and co-authors demonstrated that a pyrene-substituted helical peptide self-assembles into vesicular structures with enantioselective membranes.⁸⁵⁴ Starting from a solution of racemic carboxylic acids, the peptide vesicles were shown to encapsulate only a single enantiomer through enantioselective diffusion across the membranes. Moreover, the interior of the vesicle acted as an enantioselective nanoreactor where the encapsulated enantiomer could be chemically transformed, yielding a highly enantiopure product. Liu et al. designed and prepared a light-stimuli responsive vesicle which was self-assembled by the host–guest complex of α -CD and an *M*-helical quinoline oligoamide foldamer in water.⁸⁵⁵ Due to the presence of the photo-sensitive azobenzene group, this vesicle displayed a dynamic behavior when alternately irradiated by UV and visible light, showing an interesting potential as a nanocarrier for drug delivery. Interestingly, the *M*-helix-based vesicle also exhibited enantioselective release abilities toward *rac*-propranolol.

The phenomenon of enantioselective permeability through membranes has been widely exploited in the field of enantioseparation of chiral compounds as a useful methodology for scale-up enantiomeric separation by using different types of solid^{856,857} and liquid membranes,⁸⁵⁸ providing a complementary choice to the enantioselective liquid-liquid extraction, LC and SFC techniques.⁴² Some of the advantages of membranes in enantioseparation science are low energy consumption, high processing capacity, continuous operability, and variety of polymeric materials available for their preparation.⁸⁵⁸ The liquid membranes have the advantage of rapid mass transfer, but usually their stability is poor. Otherwise, the solid membranes tend to exhibit low consumption, high stability, and easy of automation, with huge industrial application perspectives.⁸⁵⁵ The chiral information in enantioselective membranes can be assessed through chiral molecules such as chitosan, sodium alginate and polyamino acid derivatives, achiral molecules with the assistance of some helical templates, or by modification of proteins, amino acids, metal-compounds surfaces, DNA, polyphenols, enzymes, CD and crown ether derivatives.

Two mechanisms have been proposed for chiral resolution via membrane-based process, which are based on the concepts of facilitated transport and retarded transport.⁸⁵⁹ Enantioselective membranes are classified just on the basis of these mechanisms as ‘diffusion-selective’ and ‘sorption selective’ membranes, functioning with facilitated and retarded transport mechanisms, respectively (Figure 69). In the first case, the principle underlying enantioseparation is the higher binding affinity of one enantiomer toward the chiral active sites in the membrane. In general, with diffusion-selective membrane the highest *ee* value (~100%) can be obtained in the initial period of separation, whereas

the resolution performance tends to decrease over time owing to the phenomenon of non-enantioselective diffusion of the other enantiomer. In the sorption-selective membrane, the enantioselective binding affinity between one enantiomer toward the membrane is generally stronger than in a diffusion-selective membrane. As a consequence, the adsorbed single enantiomer can be held by the membrane, and the other enantiomer dominantly diffuses non-enantioselectively through the membrane.

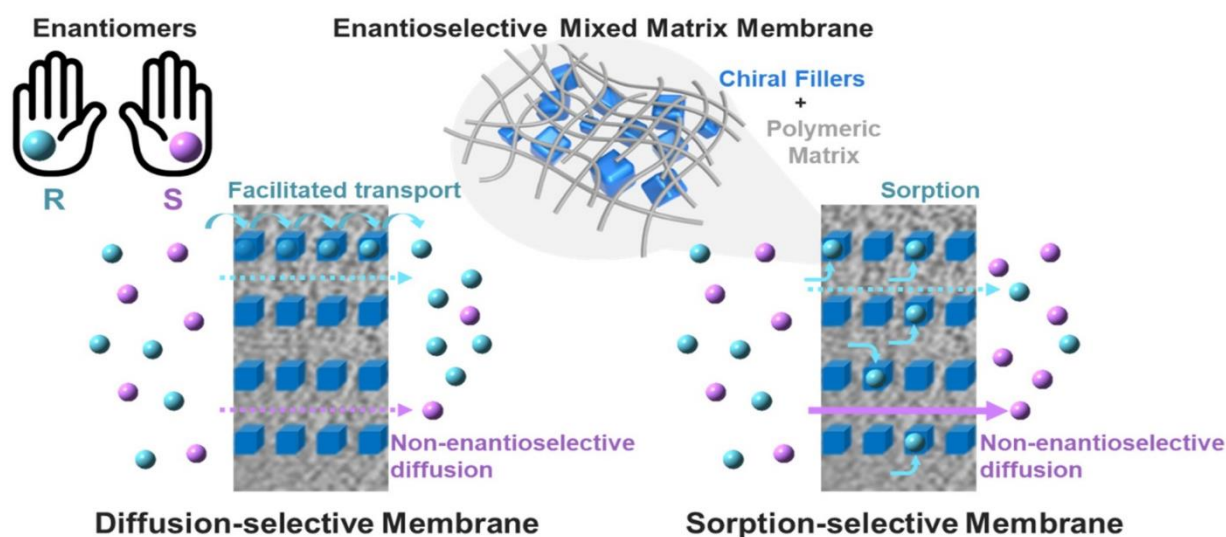


Figure 69. Schematic diagram of principles between a diffusion—selective membrane and sorption—selective membrane. Reproduced with permission from ref. 859. Copyright 2021 MDPI.

Pioneering studies on the enantioenrichments of racemic mixtures via permeation through enantioselective membranes date back to the 1980s.⁸⁶⁰ However, more recently the availability of different types of polymeric structures suitable for construction of enantioselective membranes gave a considerable boost to the field. Yuan and co-authors reported the enantioseparation of mandelic acid on a cellulose solid membrane, and of *p*-hydroxyphenylglycine on solid membranes of sodium alginate and hydroxypropyl- β -CD, obtaining *ee* of 89.1%, 42.6%, and 59.1%, respectively.⁸⁶¹ The authors suggested that a mechanism based on “adsorption – association – diffusion” was able to explain the enantioresolution of the enantioselective membrane, observing that the first adsorbed enantiomer was not the enantiomer that first permeated the membrane. Enantioselective enrichment of racemic oxprenolol, achieved with a solid chiral polymer membrane consisting of CDMPC coated on a Teflon membrane filter, was reported by Okamoto and co-authors in the 1990s.⁸⁶² Very recently, Otsuka et al. reported the preparation of electrospun nanofibers of CDMPC, with a mean diameter of 329 nm, forming a self-standing nonwoven textile with a specific surface area of 5.6 m²/g.⁸⁶³ The textile was sandwiched between commercially available polytetrafluoroethylene membrane filters as a support material to fabricate a CDMPC membrane system for the chiral resolution of *rac*-1-(1-naphthyl)-ethanol. The membrane system was exploited in the vacuum filtration of the racemic

mixture using a solvent mixture of *n*-hexane/propan-2-ol = 9/1 (v/v). As a result, the process enriched the (*S*)-enantiomer in the filtrate due to the enantioselective sorption of the (*R*)-enantiomer, with the enantiomeric excess of the (*S*)-enantiomer in the filtrate increasing up to 32.9 by repeating the vacuum filtration–extraction process for 15 cycles. The sorption capacity of the membrane was regenerated repeatedly *via* extractions of the adsorbed enantiomer after the filtrations.

Polymers of intrinsic microporosity (PIMs) are an important class of materials for preparation of enantioselective membranes.⁸⁶⁴ The first examples of chiral PIMs were reported, in 2015, by Weng et al..⁸⁶⁵ They prepared and characterized the fluorescent polymers (+)-PIM-CN and (+)-PIM-COOH (Figure 70) derived from condensation and polymerization of 5,5',6,6'-tetrahydroxy-3,3,3',3'-tetramethyl-1,1'-spirobisindane (**49**) and 2,3,4,6-tetrafluorophthalonitrile (**50**). Both soluble polymers were introduced directly into semipermeable membranes and evaluated for their ability to enable the selective permeation of several racemates, obtaining products with good enantiomeric excesses. The authors measuring for (+)-PIM-CN the adsorption of the racemate by this material, observing that the adsorption was not selective, whereas the permeation through the membrane was based on a selective diffusion-permeation mechanism.

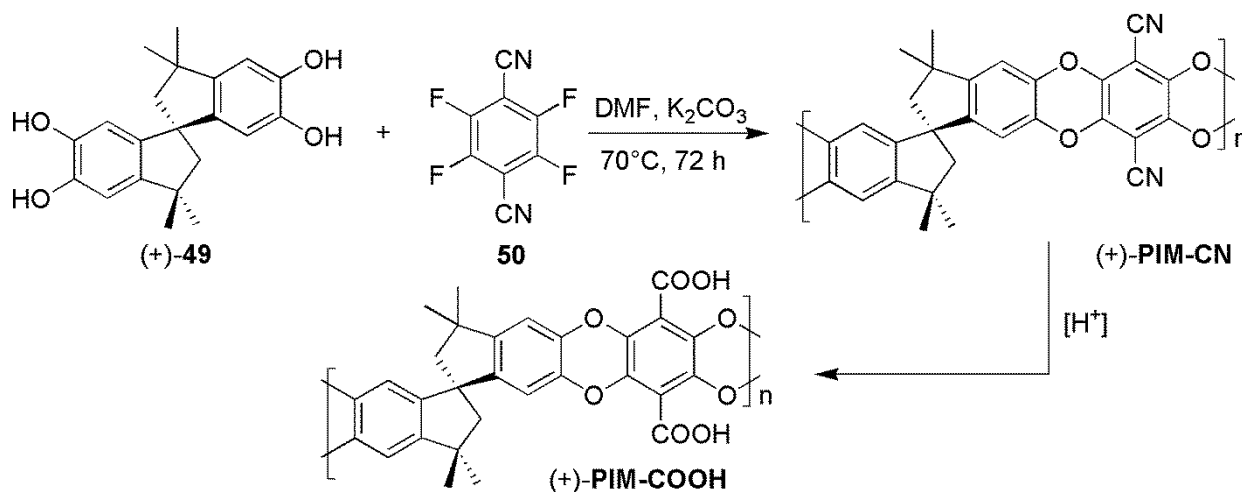


Figure 70. Condensation and polymerization of 5,5',6,6'-tetrahydroxy-3,3,3',3'-tetramethyl-1,1'-spirobisindane (**49**) and 2,3,4,6-tetrafluorophthalonitrile (**50**), and hydrolysis of (+)-PIM-CN to (+)-PIM-COOH.

More recently, Zhang et al. synthesized and enantioseparated the racemic mixture of 2,6-diaminotrypticene obtaining the (*R,R*)- and (*S,S*)-enantiomers, which were used as monomers to synthesize a couple of chiral porous polyimides, *R*- and *S*-FTPI which combine high porosity with intrinsic chirality.⁸⁶⁶ Showing good solubility in organic solvents, FTPIs were cast into porous solid membranes for enantioselective separation. Enantioselective separation experiments were carried out by using three kinds of racemates including 1,1'-binaphthyl-2,2'-diol, 2-naphthyl-1-ethanol and mandelic acid. All the (*S*)-enantiomers displayed better selective permeation than (*R*)-enantiomers in

the presence of *S*-FTPI membrane at 1 h of permeation time, with *ee* values of 85.8%, 11.4%, and 7.7%, respectively. Otherwise, *R*-FTPI exhibited better permeability of (*R*)-enantiomers than (*S*)-enantiomers in the same experimental condition with *ee* values of 96.3%, 11.1% and 7.4%, respectively. This behavior was similar to other examples of homochiral porous materials for selectively separating guest molecules with opposite chirality. Adsorption experiments of racemates by FTPI were carried out in the study, and the results displayed that the adsorption of these chiral guests was not selective, concluding that the enantioselective membrane separation of chiral-FTPI is based on a selective diffusion-permeation mechanism. Zang et al. prepared three kinds of chiral conjugated microporous polymer composite membranes with porous silica as the support layer for enantioselective permeation of amino acids in aqueous solution.⁸⁶⁷

Homochiral MOF-based membranes have been also reported for chiral separations through enantioselective permeation,^{868,869,870} although the production of high-quality homochiral polycrystalline MOF membranes may present serious difficulties to obtain by crystallization chiral MOF layers without defects on porous substrates.⁸⁷¹ Alternatively, mixed matrix membranes (MMMs) have been made available in last few years, which feature potential advantages of both MOFs and polymers..⁸⁵⁹ Recently, Wang, Zhang et al. reported a new type of enantioselective MMM derived from homochiral MIL-53 nanocrystals (MIL, Materials Institute Lavoisier) with polyethersulfone as a polymeric matrix.⁸⁷¹ The homochiral MIL-53 nanocrystals were synthesized through post-synthetic modification, by grafting L-histidine into the frameworks of MIL-53-NH₂. The obtained MIL-53-NH-L-His nanocrystals showed excellent enantioselective adsorption for (*R*)-(+)-1-phenylethanol over the (*S*)-enantiomer (*ee* value up to 100%) (Figure 71), demonstrating a facilitated transport mechanism for chiral resolution using ethanol as solvent. However, the enantioselectivity of the homochiral MOF-based MMMs declined with permeation time.

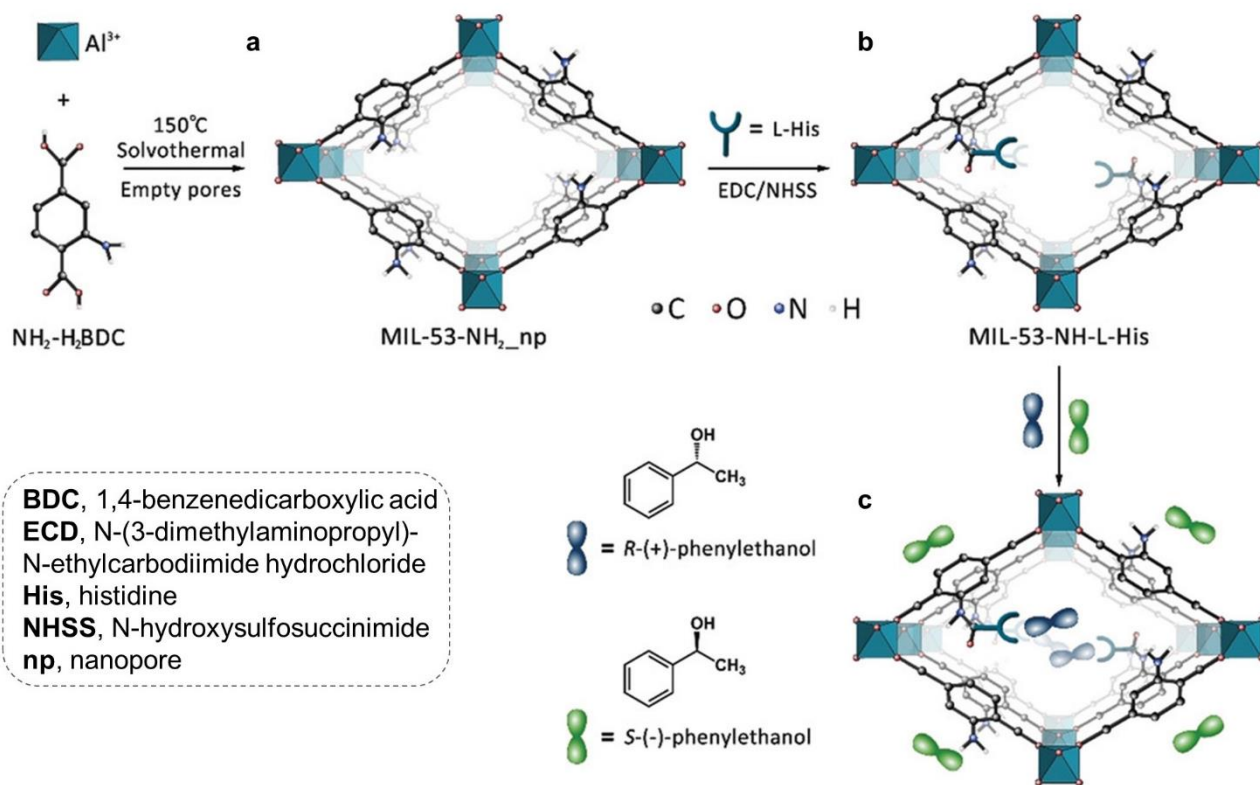


Figure 71. Preparation and function of amino acid-functionalized MOF nanocrystals: a, b) preparation of L-histidine-functionalized MIL-53-NH₂, c) enantioselective adsorption of MIL-53-NH-L-His nanocrystals for *rac*-1-phenylethanol. Adapted with permission from ref. 871. Copyright 2019 John Wiley and Sons.

Later, the same group reported the use of γ -CD-MOF-based MMMs with PES as a matrix for efficient separation of *rac*-1-phenylethanol (100% *ee*).⁸⁷² In particular, in this study it was found that the solvent polarity has a critical effect on the enantioselective performance of CD-MOF/polyethersulfone MMMs. Indeed, when non-polar solvent (*n*-hexane) was used, the membranes retained well their enantioselectivity in the permeation process due to reduced interference of the solvent to intermolecular interactions between the chiral molecules and chiral membrane. Otherwise, when polar solvents such as methanol and ethanol were used, a significant reduction in enantioselectivity was observed with time. In recent studies, Chen, Huang, and co-authors reported preparation and performances of three new chiral membranes prepared by modification of gold nanochannel membranes with L-proline,⁸⁷³ and D-penicillamine and *N*-acetyl-L-cysteine.⁸⁷⁴ L-proline-modified gold nanochannel membrane was applied for the enantioselective permeations of amino acid enantiomers including tyrosine, tryptophan and phenylalanine, experimental results showing higher enantioselectivity for tyrosine and tryptophan. The mechanism of the enantioselection process was explored through DFT calculations (M06-2X/6-31+G(d,p)), and the results indicated that electrostatic interactions and HBs were responsible for the binding of CS and enantiomers, vdW

interactions contributing to large binding energies. The D-penicillamine-modified membrane showed good enantioselectivity toward tyrosine and phenylalanine enantiomers, whereas the *N*-acetyl-L-cysteine-based membrane exhibited good enantioselectivity toward tyrosine and tryptophan enantiomers. DFT calculations indicated for D-penicillamine and *N*-acetyl-L-cysteine the formation of 1:1 and 2:1 selector/enantiomer complexes, respectively. Moreover, the NH_3^+ group of D-penicillamine was observed to play a pivotal role in enhancing interactions between complexes and improving enantioselectivity. Enantioselective permeation of L-tyrosine was also performed by using functionalized single-walled carbon nanotube thin film nanocomposite membrane and D-tryptophan as the chiral probes.⁸⁷⁵

In the last few years, functionalized one-handed helical polyacetylenes have been also used as enantioselective membranes for the enantioseparation of phenylethylamine^{876,877} and mandelic acid.⁸⁷⁸

4.4.2 Crystallization

An approach to obtain products with high enantiomeric purity is to utilize crystallization procedures.^{83,84} Diastereomeric crystallization is commonly applied to separate racemic mixtures of chiral compounds also on industrial scale. Depending on the difference in solubility of a pair of diastereomeric salts derived from a racemate and a chiral enantiopure resolving agent, one of the diastereomeric salts can be purified by repeated re-crystallization, and the subsequent decomposition of the purified diastereomeric salt provides one of the enantiomers of the racemate in a pure form.⁸⁷⁹⁻⁸⁸¹ An advantage of this method is that the enantiopurity may be improved by repeated re-crystallization of the less-soluble diastereomeric salt. The main disadvantage is that the corresponding more-soluble diastereomeric salt may be difficult to purify, and additional operations are required to obtain it. Acting on solvent allows for improving the versatility of the techniques due to solvation effects on the diastereoselective process. Indeed, it has been reported that the dielectric constant of the crystallization solvent may impact the absolute configuration of the preferably deposited diastereomeric salt. Thus, the main advantage of the so-called *dielectrically controlled resolution* is that both enantiomers of a chiral compound can be accessed by using only one enantiomer of the resolving agent. Even other properties of the crystallization solvent may impact the diastereomeric crystallization outcome. In the enantioseparation of *rac*-mandelic acid *via* diastereomeric salt formation with enantiopure (1*R*,2*S*)-2-amino-1,2-diphenylethanol, Kodama, Hirose et al. reported that the configuration of the less-soluble salt was mainly determined by the size and shape of the solvent molecules.⁸⁸² Indeed, crystallization from short-chain alcohols such as MeOH, ethanol, propan-2-ol and *t*-butanol afforded (*S*)-mandelic acid·(1*R*,2*S*)-2-amino-1,2-diphenylethanol salt crystals, while (*R*)-mandelic acid·(1*R*,2*S*)-2-amino-1,2-diphenylethanol salt was obtained from a

solution of longer alcohols such as *n*-propanol, *i*-butanol, *s*-butanol, and *n*-butanol.⁸⁸³ More recently, the solvent-induced chirality switching phenomenon with 2-amino-1,2-diphenylethanol was also observed during the enantioseparation of hydroxyphenylpropionic⁸⁸⁴ and hydroxyphenylbutyric⁸⁸⁵ acids. In particular, X-ray crystallographic analyses of the diastereomeric salts were performed in order to elucidate the mechanism of chiral recognition of 3-hydroxyphenylpropionic acid (**51**). The less-soluble (*S*)-**51**·(*1R,2S*)-2-amino-1,2-diphenylethanol salt crystal was observed to form a columnar HB-network constructed with a 2-fold screw axis. Moreover, two CH··· π interactions were found to play an important role to fix the substituents of (*S*)-**51** and recognize the chirality. In this case, the crystallization process was not solvent-dependent. Otherwise, crystallization from water or MeOH afforded the (*R*)-2-hydroxy-3-phenylpropionic acid ((*R*)-**52**)·(*1R,2S*)-2-amino-1,2-diphenylethanol salt, while aqueous alcohols, propan-2-ol, and 1,4-dioxane preferentially afforded the (*S*)-**52**·(*1R,2S*)-2-amino-1,2-diphenylethanol salt. From ¹H NMR and TGA analyses, it was suggested that the crystallization solvents were incorporated in the deposited salts. These included solvent molecules were envisaged to stabilize each diastereomeric salt changing their relative solubilities. In this regard, the (*R*)-**52**·(*1R,2S*)-2-amino-1,2-diphenylethanol·2H₂O crystal was arranged to form a sheet-like HB-network, together with two water molecules, rather than a columnar HB-network.⁸⁸⁴ Recently Białońska et al. studied the mechanisms of resolution of the *N*-(3-nitrobenzoyl)aspartic acid by formation and fractional crystallization of brucinium diastereomeric salts, finding that the recognition leads to effective or ineffective resolution depending on the nature of the solvent used in the process.⁸⁸⁶ Double salts and solid solution were formed in the unsuccessful resolution, whereas during successful resolution, bis(brucinium)-*N*-(3-nitrobenzoyl)-l-aspartate hydrate MeOH solvate precipitates as the first fraction, owing to more dispersive or more directional interactions occurring as the solvent system changes according to its dielectric constant. On this basis, the racemic resolution and formation of bis(brucinium)-*N*-(3-nitrobenzoyl)-l-aspartate hydrate MeOH solvate was found related to three-point recognition of the anions by brucinium self-assembly. The effects of solvent, temperature and time were explored by Li et al. in the diastereomeric crystallization of bridging chiral *de-tert*-butylcalix[4]arenes by using (*1S*)-(+)-10-camphorsulfonyl chloride as chiral auxiliary.⁸⁸⁷

As shown in Figure 72 diverse outcomes are possible upon crystallization of achiral and chiral molecules.⁸⁸⁸ Upon a crystallization process without the involvement of a chiral resolving agent the racemic mixture may provide *a*) a racemic compound, *b*) a pseudoracemate, namely a racemic solid solution, or *c*) a racemic conglomerate through the formation of an equimolar mechanical mixture of crystals, each formed by homochiral molecule. This latter is the case of the sodium ammonium tartrate crystals which was described by Pasteur in 1848.²⁶ If a racemic mixture forms a conglomerate in

which each single crystal is assembled from a single-handed enantiomer, it is possible to resolve each enantiomer from the racemic mixture by the *preferential crystallization method*. In this frame, the term “spontaneous resolution” (or symmetry breaking) describes the formation of a mixture of crystalline enantiomers through crystallization from a racemic melt or solutions.^{35,889,890} Spontaneous resolution and conglomerate formation in absence of any chirality source are issues related with the homochirality of life and absolute asymmetric synthesis at the solid state.³⁵ As mentioned in section 2, few compounds crystallize as conglomerates, this evidence indicating that heterochiral interactions are often favored and predominant compared to homochiral interactions during crystal formation from racemic sources.

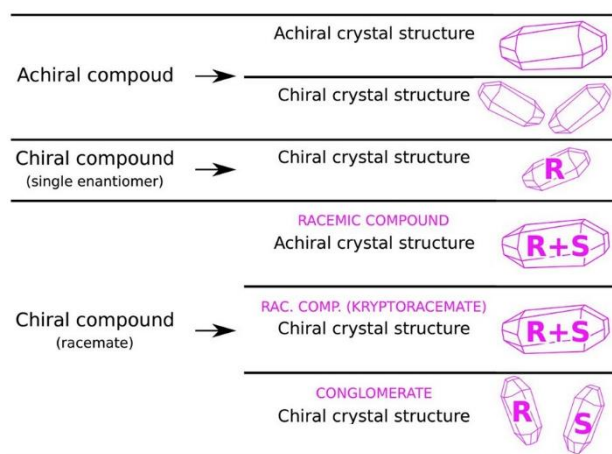


Figure 72. Possible outcomes of crystallization of chiral and achiral molecules. Adapted with permission from ref. 888. Copyright 2020 IUCr.

In 2007, Pérez-García and Amabilino coined the terms *enantiophobic* and *enantiophilic* referring to molecules forming a conglomerate and a racemic compound, respectively.⁸⁹⁰ A number of studies tried to explain the ability or inability of a chiral molecules to give spontaneous resolution by a specific combination of functional groups present in a molecule, its symmetry and conformational properties, and the effect of a co-crystallized achiral molecule.^{889,890} In any case, the formation of certain supramolecular structures and crystal forms appear to be guided by structural and thermodynamic properties of the system under discussion. In some cases, a condition for conglomerate formation may be the growth of homochiral motifs such as chains or helices.⁸⁹¹ However, this feature not always leads to spontaneous resolution.⁸⁹² Recently, Gerasimova et al. reported a doubly enantiophobic behavior during the crystallization of *rac*-1-benzyl-3-chloro-4-[(4-chlorophenyl)sulfanyl]-5-hydroxy-1,5-dihydro-2H-pyrrol-2-one (**53**), observing the formation of two conglomerates with different crystal structures (Figure 73).⁸⁹³ The main supramolecular motifs of the polymorphic modifications was shown to consist of HB chain or helix of different symmetry. Reproducibility and stability of these supramolecular motifs, as well as the observed polymorphic

diversity, were found to be related to the specific conformation (*cisoid* or *transoid*) of the α -hydroxyamide chain synthon, and to the crosslinking of the homochiral chains in the crystals through weak noncovalent interactions. In particular, through XRD analysis, a $\text{Cl}\cdots\pi$ interaction was found to stabilize the *transoid* conformation in the crystal. The conglomerates being thermodynamically stable in certain temperature ranges, in this study a binary phase diagram for the chiral system complicated by an enantiotropic phase transition was reconstructed based on experimental data, which resulted to be characterized by the presence of a thermodynamic stability permutation line between the two racemic conglomerates. Analogous behavior was also reported by the same group for a brominated analogue of **53**.⁸⁹⁴

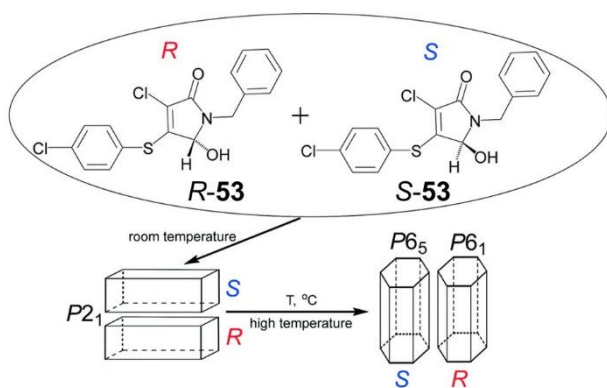


Figure 73. Doubly enantiophobic behavior for compound **53**. Adapted with permission from ref. 893. Copyright 2021 Royal Society of Chemistry.

If preferential crystallization is applied under conditions in which fast racemization proceeds in the mother liquor, it becomes possible to direct the entire system to the desired single-handed enantiomer.⁸⁹⁵ As a racemic mixture of a conglomerate is dynamically crystallized from a supersaturated solution, the molecule repeatedly aggregates and dissolves until the first chiral crystal nucleus is formed. Under these conditions, the crystals grow through molecules of the same enantiomer, whereas the crystallized enantiomer decreases in the mother liquor and, as a consequence, it is restored in solution through racemization in order to maintain the equilibrium state. The total resolution method, which couples crystallization and an asymmetric transformation, is called crystallization-induced enantiomer transformation (CIET), a type of crystallization-induced stereoisomer transformation (CIST).^{896,897} The term CIST accounts for the term stereoisomer transformation which indicates a mutual interconversion between stereoisomers, and the term crystallization-induced which specifies the driving force of the process. This type of process involves interaction of two phases: a solid (crystalline) phase and a second phase, represented by a solution. In recent years, dynamic systems with relatively low racemization rates have been also applied to chiral amplification by attrition-enhanced deracemization or Viedma ripening.³¹ During this process, a racemic population of conglomerate crystals in contact with their saturated solution, where

racemization takes place, completely transforms to a single chirality upon continuous grinding of the crystals achieved by stirring the suspension in the presence of grinding media.⁸⁹⁸ Sakamoto et al. obtained optically active *trans*-3,4-diphenylsuccinimides from the corresponding achiral *cis* isomers in quantitative yields and excellent *ees* by simple crystallization from solution in the presence of a catalytic amount of 1,8-diazabicyclo[5.4.0]undec-7-ene as a basic agent,⁸⁹⁹ achieving an asymmetric transformation from achiral materials by dynamic crystallization involving isomerization, racemization and preferential crystallization.

Given that accessing crystal chirality is not easy, a diastereomeric reaction can be used to access total resolution by introducing optically active substituents into the molecule, or by forming chiral ion pairs (salts), co-crystals, or chiral inclusion compounds (host–guest complexes), followed by diastereoselective crystallization of the less soluble diastereomer, and epimerization of the diastereomer remaining in solution. In this case crystallization-induced diastereomer transformation occurs (CIDT).⁹⁰⁰ Yamashita, Akazome and co-authors prepared chiral 3-oxocycloalkanecarbonitriles by fractional crystallization and CIDT of diastereomeric ketals with (1*R*,2*R*)-1,2-diphenylethane-1,2-diol. By X-ray diffraction analysis, it was demonstrated that the difference in HBs originated the differences of the solubilities between (*R*)- and (*S*)-diastereomers. Moreover, a CIDT producing the (*R*)-diastereomer in good yield (95% yield) and with high diastereoselectivity (97% *de*) was performed through epimerization promoted by potassium *t*-butoxide.⁹⁰¹ More recently, Sakamoto et al. provided the first example of CIDT for thiohydantoins through a complete diastereomer transformation of thiohydantoins by dynamic crystallization with high diastereoselectivity. Interestingly, stereoselective switching of CIDT diastereoselectivity was achieved with suitable solvents.⁹⁰²

The first XB-based enantiorecognition processes was reported in 1999 by Resnati and co-authors, who resolved racemic 1,2-dibromohexafluoropropane by using the Lewis base (–)-sparteine hydrobromide as chiral inductor.⁹⁰³ The resolution occurred as a result of a highly specific inclusion of only the (*S*)-enantiomer of the 1,2-dibromohexafluoropropane in a chiral crystal with a helical arrangement formed by XB between the C-bound Br atoms of the 1,2-dibromohexafluoropropane and the Br[–] ions of sparteine. Later, the same authors enantioseparated racemic perfluorocarbons through a XB-driven recognition mechanism.⁹⁰⁴

The application of ultrasound to stereoselective crystallization processes (sonocrystallization) has been shown to have several beneficial effects on the process in order to determine some properties of the product such as size, shape and polymorphic modification. The exact mechanisms of sonocrystallization and sonofragmentation are still rather unclear, however it is believed that most

effects arise from mechanical effects which includes the generation, growth and implosive collapse of μm -sized cavitation bubbles when ultrasound waves propagate in a liquid medium.^{905,906}

In the last decade, resolution procedures by crystallization have been also reported for chiral metal nanoclusters and nanocrystals (Figure 74).⁹⁰⁷ The interest in the enantioseparation of nanomaterials is related to the evidence that chiral nanocrystals may interact enantioselectively with biomolecules and biological tissues.⁹⁰⁸ For instance, it has been demonstrated that certain cancer cells exhibit a highly selective uptake of chiral CdS quantum dots, with an almost 100% uptake of the D-type quantum dots, and a negligible uptake of the L-type quantum dots.⁹⁰⁹

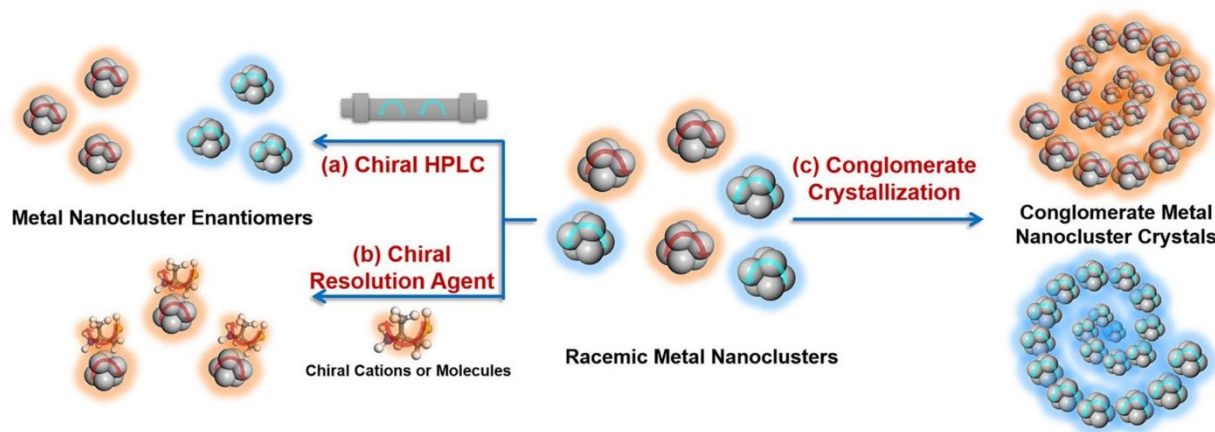


Figure 74. Schematic illustration of chiral resolution strategies for metal nanoclusters. Reproduced with permission from ref. 907. Copyright 2020 American Chemical Society.

Wang and co-authors reported the synthesis of intrinsically chiral silver nanoparticles consisting of a 30-silver-atom core (Ag_{30} nanoclusters), stabilized by eight achiral carboranetrithiolate units and six achiral phosphine ligands, and their crystallization in a dual-solvent system of tetrahydrofuran and acetonitrile (ACN).⁹¹⁰ The X-ray crystallography analysis of single crystals of the racemic nanoclusters ($\text{Ag}_{30}\text{-rac}$) revealed an “outside-in” chirality transfer scheme as the origin of cluster chirality. In the cluster, the interactions of $\text{B-H}\cdots\pi$ and $\text{C-H}\cdots\pi$ between neighbored ligands arrange surface phenyl rings into a spiral pattern, which induces chiral arrangement of carboranetrithiolate units and phosphine ligands at the metal-organic interface. Recrystallization of the racemic Ag_{30} nanoclusters in DMA produces enantiomorphic crystals with a double-helical architecture, which is maintained through diverse noncovalent interactions between clusters ($\text{B-H}\cdots\pi$, $\pi\cdots\pi$, $\text{C-H}\cdots\text{O}$, $\text{H}\cdots\text{H}$), also involving a host-guest binding between DMAc molecules and the enantiopure nanoclusters. The enantioseparation of chiral metal nanoclusters has been also achieved by diastereoselective crystallization by using chiral cations as resolving agents.⁹¹¹ More recently, α -CD has also been used as chiral resolution agent for Au nanoclusters.⁹¹² It is worth mentioning that Bürgi et al. designed a chiral HPLC method by using a polysaccharide-based CSP for the enantioseparation of intrinsically chiral nanoclusters such as $\text{Au}_{38}(\text{SR})_{24}$, $\text{Au}_{40}(\text{SR})_{24}$,

Au₂₈(SR)₂₀, and Au₃₈Cu(SR)₂₄ (SR denotes the thiolate ligand), which are usually produced in the form of racemic mixtures.⁹¹³

Arguing that fast and reliable separation of enantiomers of chiral nanoparticles requires *a*) elimination of all the forces that are independent of the nanoparticle handedness, and *b*) creation of a sufficiently strong force that either pushes different enantiomers in opposite directions or delays the diffusion of one of them with respect to the other, recently Rukhlenko et al. described how to construct such a completely chiral optical force using two counterpropagating circularly polarized plane waves of opposite helicities.⁹¹⁴ The concept of a completely chiral optical force was proposed to potentially advance enantioseparation and enantiopurification techniques for all kinds of chiral nanoparticles that strongly interact with light.

The noncovalent interaction system underlying crystallization may be very complex, involving *a*) intramolecular contacts contributing to conformational stabilization of the crystal, *b*) intermolecular contacts between solvent and chiral compound, and *c*) supramolecular contacts favoring the formation of supramolecular motifs impacting crystallization.⁹¹⁵ The elucidation of the mechanism acting at molecular level is very important for defining crystallization conditions which are critical in the rational design of a resolution process by crystallization. Nevertheless, although the intermolecular interactions can be predicted to some extent, they are still not fully elucidated in this field. Analogously, design and optimization of the crystallization process through understanding of equilibria involved, and knowledge of the phase diagram and metastable limits of a given system⁹¹⁶ still remain rather challenging.

4.5 Enantioselective recognition in chemical sensing

4.5.1 Enantioselective sensing

The term “enantioselective sensing” describes the detection of enantiomer-dependent measurable signals originated from chirality-dependent chemical or physical property. NMR spectroscopy has been widely exploited for recognition and sensing of enantiomers by using chiral shift reagents. In particular, recently this strategy has been used in anion recognition and sensing by XB and ChB. As described in section 3, compounds containing elements of Groups 14–17 as electron-deficient sites are capable of attractive and directional interactions with Lewis bases. If the Lewis base is a chiral and negatively charged species, such interactions can be employed as the basis for the development of anion receptors exploitable for enantioselective chemical sensing.⁹¹⁷ In this field, Beer et al. employed bis(triazolium) receptors derived from BINOL, and contained a bidentate iodinated system, for enantioselective recognition of chiral carboxylates.⁹¹⁸ For example, receptor **54** showed a 1.67-fold selectivity for binding to the L-enantiomer of *N*-*tert*-butoxycarbonyl (Boc)-tryptophan (**55**) over the D-enantiomer in ¹H NMR titration (99:1 CD₃CN/D₂O) (Figure 75). The HB-

based analogue, containing H in place of I atoms, showed lower association constants for carboxylates and reduced levels of enantiodifferentiation. The introduction of ferrocenyl groups in the bis(triazolium) receptor resulted in a new receptor able of enantioselective electrochemical detection of carboxylates. Later, the same group also used tetradentate XB foldamers as anion receptors.⁹¹⁹ Also in this case, the ability of the chiral receptor **56** to discriminate between enantiomeric carboxylates was evaluated using ¹H NMR spectroscopic titrations in 1:1 CDCl₃/acetone, the highest level of enantioselectivity ($K_D/K_L = 1.69$) was obtained for the Boc-protected tryptophan derivative **55**.

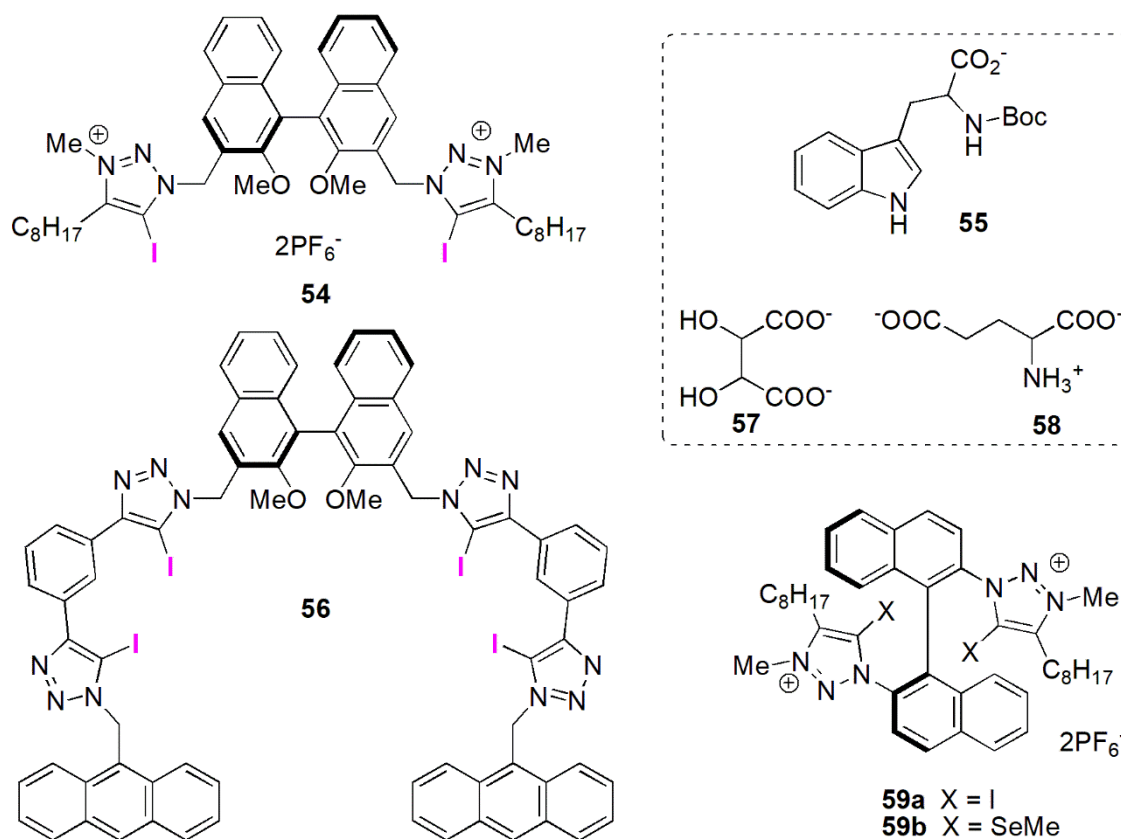


Figure 75. Structures of chiral XB and ChB donors **54**, **56** and **59** as hosts for sensing of chiral anions such as **55**, **57**, and **58**.

A comparative study of the discrimination of enantiomeric dicarboxylates by chiral receptors incorporating ChB and XB donor groups was also conducted by Beer's group.⁹²⁰ The highest enantioselectivities for binding of tartrate **57** and *N*-Boc derivative of glutamate **58** were obtained using XB donor **59a** (Figure 75), whereas the levels of enantioselectivity of the ChB donor **59b** were relatively modest. Recent studies in the field of enantioselective recognition and sensing also achieved enantiodifferentiation with various chiral triazole-based XB donors⁸¹⁷ or through the implementation of the (*S*)-BINOL core in chiral [2]rotaxanes⁹²¹ and in [3]rotaxane⁹²² host systems.

The attractiveness of chiroptical sensing is related to the fact that this approach may allow for eliminating reaction work-up and product isolation, reducing analysis time and waste production. In

this field, it is important to develop sensing strategies and probe design that integrate fast substrate binding capabilities and a distinctive chiral recognition or amplification process in order to obtain a prompt chiroptical sensor response suitable for quantitative enantiomeric excess and yield determination. This approach has especial advantages for in process analysis. Recently, Wolf and co-authors reported the binding of α - and β -hydroxy acids to the Brønsted/Lewis acidic probe **60** through a dual interaction site mechanism. Thenonplanar adduct **61** resulted from the chirality imprinting onto the stereodynamic sensor scaffold, generating an ECD-active response that could be correlated to the absolute configuration, enantiomeric composition and total amount of the target compounds (Figure 76).⁹²³

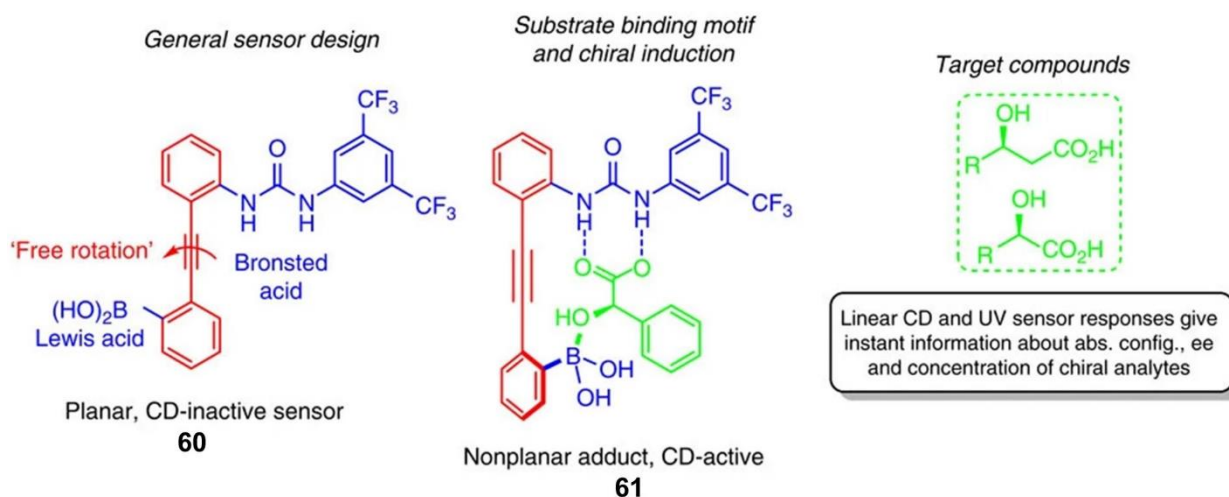


Figure 76. Synergistic substrate binding with complementary Brønsted/Lewis acid sites and chiral amplification. Adapted with permission from ref. 923. Copyright 2016 Nature Publishing.

Probe **60** displays several key features: *a*) the hydroxy acid moiety is anchored at two spatially separated sites through directional HBs between the carboxylate group and the urea unit, and reversible formation of a dative B–O bond of the alcohol group to the boronic acid region; *b*) the central triple bond contributes to maintain a rigid structure of the host at the same time allowing rotational freedom about the elongated axis as a prerequisite for spontaneous chiral amplification; *c*) **60** features a conjugated π -system to shift the chiroptical sensor response to higher wavelengths than the individual phenylboronic acid and diphenylurea moieties. The operating mechanisms and noncovalent interactions involved in the process was confirmed by ultraviolet ECD, NMR spectroscopic and electron-spray ionization (ESI)/MS experiments. The utility of this approach was confirmed in terms of yield, enantiomeric excess and sense of asymmetric induction, by using just 0.5 mg of crude reaction mixtures obtained by asymmetric reductions of an α -keto acid as a benchmark reaction. Recently, Wolf's group developed a bis(urea) oligo(phenylene)ethynylene foldamer based on the same molecular motif of **60** for the enantioselective sensing of carboxylic acids.⁹²⁴

Analogously to enantioselective chromatography and electrophoresis, CSs can be also employed in electrochemical, optical or mass sensitive sensors for enantioselective detection of particular enantiomers, although the sensitivity of electrochemical sensors toward the minor enantiomeric component is still rather low. Chiral electrochemical sensors can be based on *a*) CS incorporated in an electrode membrane,⁹²⁵ *b*) differences in uptake of enantiomers by molecularly imprinted polymers (MIP),^{926,927} and also *c*) chiral doping of electrodeposited conducting polymers.⁹²⁸ Song et al. developed electroactive chiral sensors for chiral amine by synthesizing binaphthol-containing electropolymers which were characterized by cyclic voltammetry, potentiometry, and *in situ* conductivity measurements, showing discrimination ability toward chiral amines.⁹²⁹ The binaphthyl scaffold contains the chiral information and its phenol groups play a role in the charge transporting mechanism. Recently, Nowicka et al. developed a highly effective voltammetric enantiosensor based on a chiral naphthalene bis(sulfonamide) for determination of thalidomide enantiomers, in particular the toxic (*S*)-enantiomer, in blood plasma.⁹³⁰ The recognition process relies on the specific interaction between the (*R*)-receptor, which was shown to be able to exert HBs and π - π interactions, and the (*S*)-enantiomer of thalidomide. The specific interaction, evident in the voltammetry analysis, was confirmed by molecular modelling. As a matter of fact, the 1,1'-binaphthyl scaffold has been widely used in enantioselective sensing due to its peculiar properties in terms of rigidity because of high rotational barrier, and possibility of functionalization at different position of the aromatic rings to form modular structures.⁹³¹ Using a tetra(naphthol) motif, Jiang and co-authors developed enantiopure naphthotubes as biomimetic macrocyclic receptors for enantioselective sensing of neutral chiral molecules in water,⁹³² these hosts containing HB donors in their deep hydrophobic cavities. Enantioselective recognition in water remains challenging in supramolecular chemistry even if it is routine in nature. Later, the same group found that these macrocycles are able to selectively recognize carboxylic acids in water through the combined action of salt bridges and hydrophobic effect.⁹³³ Moreover, it was demonstrated that these receptors can be used in circular dichroism-based optical chirality sensing of chiral carboxylic acids and fluorescent sensing of phenylpyruvic acid which is a biomarker for phenylketonuria.

Other macrocyclic receptors have been developed for enantioselective sensing in the last decade. Wolf and Isaacs reported that the formation of 1:1 host-guest complexes results in spontaneous induction of circular dichroism signals that can be used for accurate determination of the absolute configuration and enantiomeric composition of chiral amino acids, amines, amino alcohols, alcohols and terpenes based on a simple mix-and-measure protocol by using π -extended acyclic cucurbiturils.^{934,935} A preorganized ureido cavity decorated with chiral alkyl units was developed by Lhoták and co-authors through the introduction of chiral alkyl substituents into the lower rim of

calix[4]arene immobilized in the 1,3-alternate conformation.⁹³⁶ As shown by ¹H NMR titration experiments in dimethylsulfoxide (DMSO)-*d*₆, these compounds can be used as receptors for chiral anions. The chiral recognition ability resulted to be strengthened by the introduction of another chiral moiety directly onto the urea N atoms, with the highest selectivity factor being 3.33 (K_L/K_D) achieved for *N*-acetyl-L-phenylalaninate. Bidermann and co-authors also reported the enantioselective sensing of terpenes, steroids, amino acids, peptides and drugs with acyclic cucurbit[n]urils and molecular tweezers.⁹³⁷ CDs have been used in graphene-based hybrid materials,⁹³⁸ carbon nanofiber composite,^{939,940} and as combined receptor with glutathione⁹⁴¹ for enantioselective sensing.

In the last decades, enantioselective sensors based on homochiral metal-organic frameworks,⁹⁴²⁻⁹⁴⁶ chiral covalent organic frameworks,⁹⁴⁷ homochiral zeolites,^{948,949} and nanoparticles⁹⁵⁰ with chiral geometrical shapes, or functionalized with chiral ligands that confer overall chirality, have been developed for enantioselective sensing of small molecules such as antibiotics, toxins, and chemicals, biomacromolecules such as DNA and protein, and biomarkers in living cells. Very recently, Li and co-authors designed and prepared homochiral self-assembled purely covalent cages through imine formation in water.^{951,952} Enantioselective encapsulation of small chiral compounds was demonstrated for these cages by NMR spectroscopy and circular dichroism analyses paving the way for their utilization for enantiomer sensing and separation.

4.5.2 Chiral analysis by NMR spectroscopy

Since the 1960s NMR spectroscopy has a key role, among spectroscopic methods, to sense the signal of enantiomers of chiral compounds in a diastereomeric environment generated by a chiral auxiliary. Starting from the pioneering Pirkle's alcohol,⁹⁵³ over time three main classes of chiral auxiliaries have been used, namely chiral derivatizing agents (CDAs), chiral solvating agents (CSAs), and chiral lanthanide shift reagents (CLSRs). Although CLSRs still attract interest for enantiomer differentiation by NMR spectroscopy,⁹⁵⁴⁻⁹⁵⁶ currently CSAs have assumed a leading role among other auxiliaries. Indeed, chemical derivatization procedures, which feature CDAs, are not required for CSAs. Meanwhile, the use of diamagnetic CSAs avoids the occurrence of linewidth broadenings as in the case of CLSRs, an effect that may decrease accuracy and reproducibility of the enantiomer quantification. In 2018, comprehensive discussions on differentiation of chiral compounds using NMR spectroscopy, and on CSAs have been reported by Wenzel⁹⁵⁷ and Balzano et al.,⁶⁴⁰ respectively.

In the last decades, researches and applications in the field of enantiodifferentiation of chiral compounds by NMR spectroscopy have been oriented towards the following topics: *a*) design of chiral auxiliaries introducing specific structural elements able to maximize the effectiveness of noncovalent forces, such as ion-pairing, HB, π - π , and dipole-dipole interactions, in terms of directionality and enantioselectivity; *b*) exploitation of inexpensive molecules belonging to the

natural chiral pool as starting materials to prepare more complex auxiliaries through further derivatization; *c*) utilization of multinuclear spectroscopy for chiral recognition, ^{77}Se and ^{125}Te NMR spectroscopy representing the last frontier in this field;^{958,959} *d*) advanced techniques to deconvolute overlapped NMR spectroscopic signals and complex spectra.⁹⁶⁰

Typically, CSAs contain aromatic nuclei as well as HB donor and acceptors (Figure 77). Recently, Zawisza et al. used enantiopure aziridin-2-yl methanols **62-66** as highly effective sensors for enantiodifferentiation of α -racemic carboxylic acids containing tertiary or quaternary stereogenic centers.⁹⁶¹ The authors observed linear correlation between theoretical and observed % *ee* values for **62** and enantiomerically enriched samples of mandelic acid, indicating the possible application of this class of CSAs in the *ee* determination. On the basis of the experimental results, it was assumed the pivotal role of NH and OH groups, and related HBs, for chiral recognition. Bai et al. used actinomycin D for NMR enantiodifferentiation of chiral carboxylic acids.⁹⁶²

The BINOL motif has been widely used in CSAs for NMR spectroscopy, in particular because the large atropisomeric naphthyl ring is able to cause shielding effects through π -stacking stabilization that account for enantiomeric discrimination. On this basis, in the last few years (*R*)- or (*S*)-BINOL, and derivatives, have been used to assign the *ee* of flavanones^{963,964} and chiral drugs.^{965,966} Ema et al. developed bifunctional BINOL-macrocycles containing diacylaminopyridine moieties for the enantiodifferentiation of chiral carboxylic acids.⁹⁶⁷ Chiral BINOL-based CSAs with function of Brønsted acids were selected for determination of indoloquinazoline alkaloid-type tertiary alcohols and 3-arylquinazolinones,^{968,969} and binaphthalene skeleton ureas as sensors for phenylethanol and arylpropanoic acids.^{970,971} The BINOL motif is also contained in the amino alcohol **67** recently reported by Lei et al. as a CSA for the enantiodifferentiation of carboxylic acids.⁹⁷² In this case, the analysis by ^1H NMR spectroscopy demonstrated the excellent enantiodifferentiation ability of **67** toward 14 chiral compounds including both carboxylic acids and non-steroidal anti-inflammatory drugs.

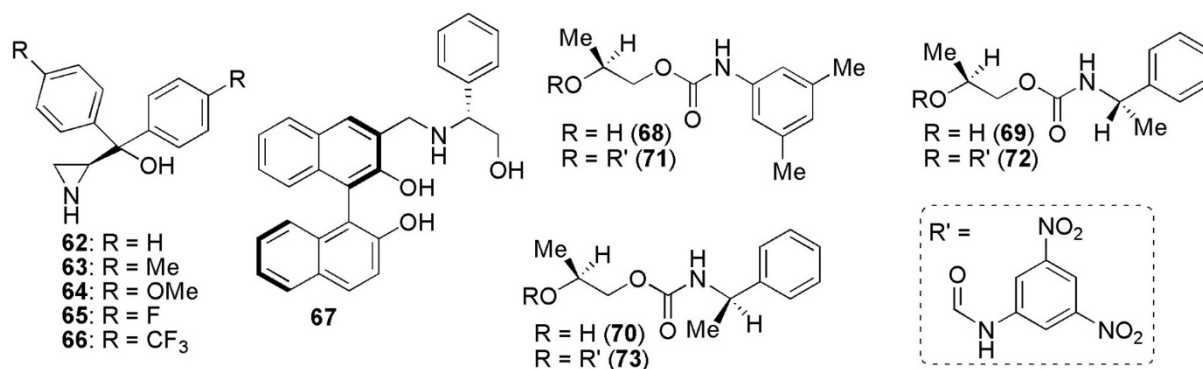


Figure 77. Structures of CSAs **62-73**.

3,5-Disubstituted phenylcarbamate moieties, bearing π -clouds, HB acceptor and HB donor sites, have been introduced in a series of CSAs, this structural element also characterizing some widely used polysaccharide-based CSPs,⁵¹ and other CSs.^{973,974} Focusing on the ethyl lactate scaffold, Balzano and Uccello-Barretta reported the preparation of compound **68**, in which the primary hydroxyl is carbamoylated, compounds **69** and **70**, as diastereomeric derivatives bearing an additional chiral center, and compounds **71-73**, containing an additional π -acid 3,5-dinitrophenyl moiety on the secondary hydroxyl.⁹⁷⁵ The enantioselectivity of these compounds was verified towards *N*-3,5-dinitrobenzoyl derivatives of amino acid methyl esters. Among CSAs **68-70**, the presence of an additional stereogenic center, as in **69** and **70**, makes them more effective as chiral auxiliaries compared to compound **68**. Otherwise, given that the diastereomeric relationship of **69** and **70** did not affect the enantioselectivity efficiency, the lactate moiety was supposed to be mainly involved in the enantioselective interactions contributing to the enantiodifferentiation of the NMR spectroscopy signals. In CSAs **71-73**, the presence of two carbamoyl functions led to better enantioselectivity, CSA **71** showing the best results in terms of enantiodifferentiation. More recently, the same group reported the use of thiourea derivatives as CSAs for amino acids, showing that an achiral base additive (DABCO or DMAP) plays an active role in the chiral discrimination processes, mediating the interaction between the CSA and the enantiomeric mixtures.^{976,977} C_2 -symmetrical bithioureas⁹⁷⁸ and a strong HB donor-selenourea⁹⁷⁹ were also reported for NMR spectroscopic chiral recognition of α -amino acids and tertiary alcohols, respectively.

Various other classes of CSA have been utilized in recent years, among them tetraaza macrocycles for enantiodifferentiation of α -amino acids and small peptides,^{980,981} tyrosine-modified pillar[5]arenes for enantiomeric identification of chiral aromatic amines,⁹⁸² and chiral squaramides⁹⁸³ and Kagan's amides⁹⁸⁴ with high versatility towards different classes of chiral compounds. In recent years, chiral liquid crystals have been also used for NMR enantiotopic discrimination owing to the effect of magnetically induced anisotropic interactions.^{985,986} Indeed, the molecules from a liquid crystalline phase are partially oriented, thus when solute molecules are dissolved in such anisotropic medium, they undergo weak interactions with the molecules from the liquid crystal, which induces their partial alignment. When the liquid crystal is chiral, solute-solvent interactions are diastereoselective, and the anisotropic NMR spectra of each enantiomer are consequently different.⁹⁸⁶

In the last few years, Silva's group studied enantiodifferentiation of chalcogen containing amines⁹⁸⁷ and alcohols⁹⁸⁸ by using ⁷⁷Se and ¹²⁵Te NMR spectroscopy, the diastereomeric environment being provided by enantiopure derivatizing agents in both cases. The use of chalcogen (⁷⁷Se and ¹²⁵Te) NMR spectroscopy in chiral recognition is still in its infancy compared to other nuclides such as ¹⁹F and ³¹P.⁹⁵⁸ The main advantage of chalcogen nuclides is their ability to detect different

structures without the difficulties encountered in ^1H NMR, like signals overlapping, multiplicity and high sensitivity to the analysis conditions. Recently, Silva et al. described chiral discrimination and assignment of the absolute configuration of primary amines, based on a three-component NMR derivatization protocol, involving a racemic primary amine such as **74**, 2-formylphenyl-boronic acid (**75**) and enantiopure (*R*)-3-(phenylchalcogen)-1,2-propanediols **76** and **77**, as CDAs, in CDCl_3 at 25°C (Figure 78a).⁹⁸⁹ In the NMR analysis, the observed chemical shift differences of $^1\text{H}_a$ and $^1\text{H}_b$ of the diastereomeric adducts **78** were 0.015 ppm (7.5 Hz) and 0.044 ppm (22 Hz), respectively (500 MHz frequency) (Figure 78b). For the hydrogen $^1\text{H}_b$, it was possible to measure the integrals without signals overlapping, whereas $^1\text{H}_a$ was affected by the multiplicity of the signals. The enantiopurity could be also evaluated through ^{77}Se - $\{^1\text{H}\}$ (98.5 MHz) NMR spectroscopy, the chemical shift difference of the two diastereoisomers **78** being 0.83 ppm (81.8 Hz) (Figure 78c). In the case of adducts **79**, the split signals of $^1\text{H}_a$ and $^1\text{H}_b$ (0.012 and 0.048 ppm, respectively) were similar to the observed for **78**, the ^{125}Te - $\{^1\text{H}\}$ NMR spectroscopic experiment showing a split signal of 0.43 ppm (56.8 Hz) (Figure 78d).

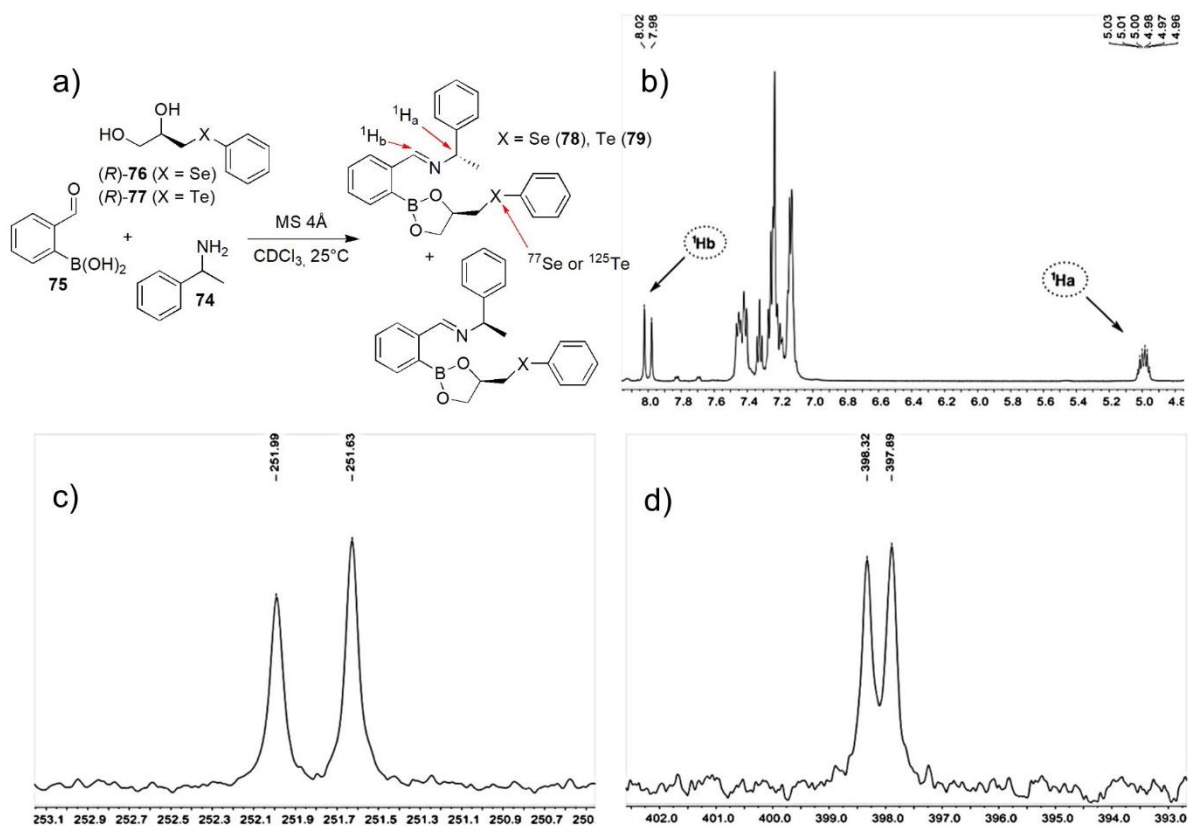


Figure 78. a) Derivatization of racemic primary amine **74** with CDA **76** and **77** by the three-component reaction; b) ^1H , and c) ^{77}Se - $\{^1\text{H}\}$ NMR spectra of diastereomeric mixtures of adducts **78**; d) ^{125}Te - $\{^1\text{H}\}$ NMR spectrum of diastereomeric mixtures of adducts **79** Adapted with permission from ref. 989. Copyright 2019 John Wiley and Sons.

NMR approaches based on self-induced recognition of enantiomers (SIRE) deserves to be mentioned being applicable to a wide range of chiral compounds. This topic has been recently reviewed by Szántay and coauthors.⁹⁹⁰ This self-induced form of recognition, which was first noted by Uskoković and co-authors in 1969,⁹⁹¹ is based on the fact that the presence of HB donor/acceptor, strongly electron-withdrawing groups such as CF₃ and NO₂, and/or π -stacking aromatic moieties in the molecular structure facilitates relatively strong attractive intermolecular interactions, so that homo- and heteroenantiomeric diastereomeric associates may be formed in sufficiently high proportions to achieve signal separation (Figure 79).⁹⁹² Through dynamic equilibria, a chiral compound forms homo- and heterochiral transient associates which may be dimers or higher-order oligomers. This mechanism provides different distributions of the enantiomers in the various associates depending on their concentrations and the values of $K_{\text{Homochiral}}$ and $K_{\text{Heterochiral}}$. Technically, the ability to observe the SIRE-based separation of NMR signals, as a matter of fact in absence of an external chiral auxiliary, depends on the resolution power, and the operational temperature range of the NMR spectrometer.⁹⁹⁰

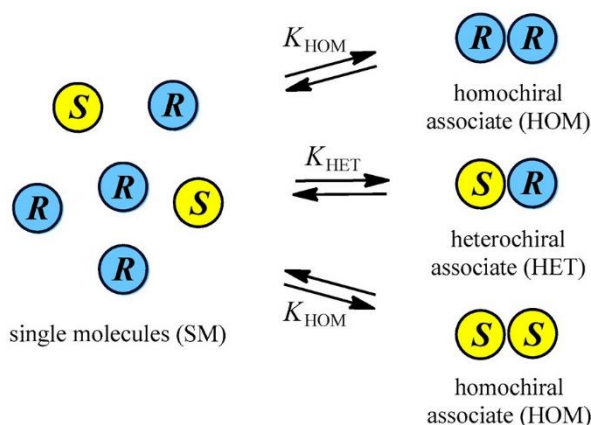


Figure 79. General principle of SIRE. Reproduced with permission from ref. 992. Copyright 2020 MDPI.

It is worth mentioning that over time, SIRE have been reported by using various names such as solute-solute interaction of enantiomers, self-induced anisochrony, statistically controlled association diastereoisomerism, statistically controlled association diastereomeric anisochronism, self-induced nonequivalence, NMR nonequivalence of enantiomers, self-discrimination of enantiomers, and self-induced diastereomeric anisochronism.

4.6 Induced conformational chirality

Helical structures, such as double helix of DNA and α -helix of proteins, play crucial roles in nature, determining biological activities and functions of biological macromolecules. In a biomimetic perspective, over time scientists have made huge efforts to develop artificial helical polymers, supramolecules, and oligomers.^{993,994} Due to the inherent chirality of the helix arrangements,

molecules, supramolecules, oligomers, polymers, and their assemblies can result chiral as effect of the helicity exclusively, even in absence of chiral elements in their structure, with one-handed helical conformation. For this purpose, noncovalent interactions, such as HBs, π - π aromatic stacking, ion-dipolar interactions, charged electrostatic interactions, are of key importance for holding up supramolecular helical architectures, and this function may be modulated by solvent polarity, acidic and basic additive as well as temperature.⁹⁹⁴

In the 1960s, it was known that even if highly isotactic, a vinyl polymer obtained from an achiral monomer of general formula $\text{CH}_2=\text{CXY}$ does not present a measurable optical activity.⁹⁹⁵ The reason is that each asymmetric carbon which is formed in the process of the polymerization becomes “pseudo” asymmetric after the polymer grows to a long chain, with the exception of the carbon atoms located near the ends of the polymer chain.⁹⁹⁶ This also occurred in the vinyl polymers which have asymmetric terminal groups deriving from optically active initiators.⁹⁹⁷ In 1970s, Nolte and co-authors reported the possibility of yielding optically active polyisocyanides when the polymerization proceeds with forming a tightly coiled helix of polymer and the helix is sufficiently stable in solutions.^{998,999} Okamoto and co-authors reported that the copolymer of triphenylmethyl methacrylate (TrMA) with a small amount of (*S*)-1-phenylethyl methacrylate showed a large positive optical rotation which was opposite in sign to that of poly[(*S*)-1-phenylethylmethacrylate].^{1000,1001} This abnormal optical rotation was attributed by the authors to the helical conformation of the isotactic TrMA sequence, preferential in one screw sense, which was formed in the process of the polymerization. Then, the same group successfully prepared optically active polymers of TrMA by using (–)-sparteine-*n*-BuLi complex as a chiral catalyst.⁹⁹⁶ This catalyst provided a polymer which contained no chiral component but had a chirality caused only by helicity. Later, Yashima and co-authors described the induction of helicity in a stereoregular, *cis-transoidal* poly((4-carboxyphenyl)acetylene) (poly-**80**) by an optically active amines (Figure 80).¹⁰⁰² This polymer consisted of a number of short helical units with many helix-reversal points and, consequently, was achiral. However, optically active amines, such as (*R*)-**81** and (*S*)-**82** were able to interact noncovalently with the carboxyl groups of the polymer, inducing a dynamic one-handed macromolecular helicity in the polymer itself, thus originating optical activity. The authors also showed that this helicity could be ‘memorized’ when the amine was replaced by various achiral amines such as **83**.¹⁰⁰³ Various derivatives of aliphatic and aromatic polyacetylenes bearing a functional group were also found to form an induced helix when they are complexed with optically active compounds.^{1004,1005}

The chiral amplification was for the first time observed in synthetic helical polymer systems by Green et al. in the late 1980s.¹⁰⁰⁶⁻¹⁰⁰⁸ They discovered the features of the dynamic macromolecular

helicity of polyisocyanates, and that their right- and left-handed helical conformations are interconvertible from each other by rarely occurring helical reversals owing to very small helix inversion barriers.

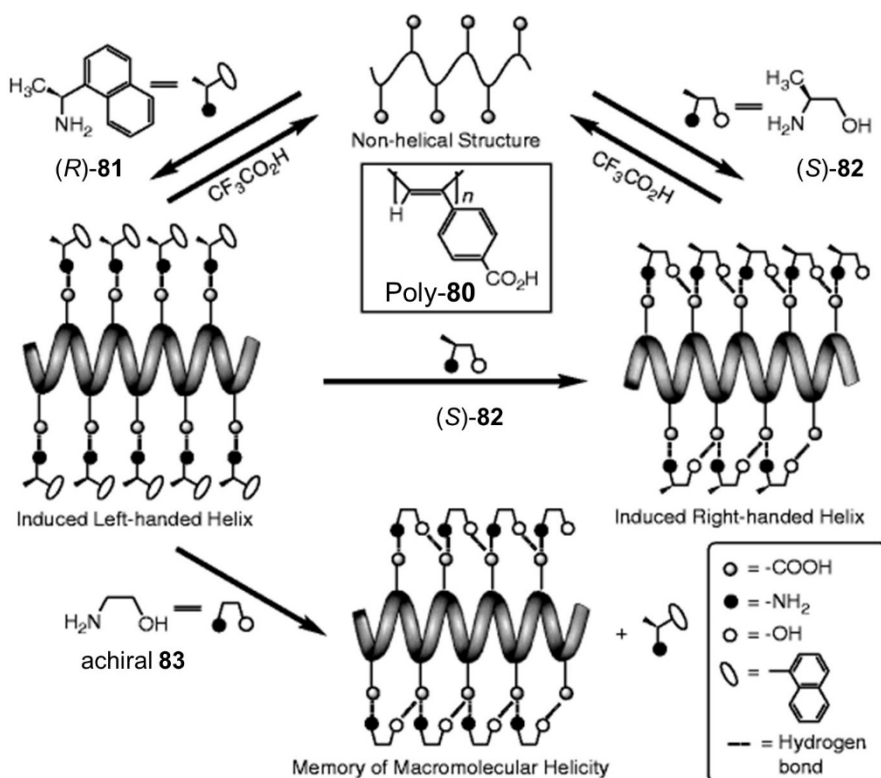


Figure 80. Schematic illustration of induced one-handed helicity in poly-80, and the memory of macromolecular helicity. Adapted with permission from ref. 1003. Copyright 1999 Nature Publishing

Polyamides may also adopt helical conformation.¹⁰⁰⁹ Lu et al. reported the synthesis of a series of polyamides with intramolecular HB motifs via polycondensation reactions.¹⁰¹⁰ These polyamides could fold into helical conformation, which was in sharp contrast to their linear analogs that were unable to form intramolecular HBs. The chirality of helical conformation can further be tuned via acid–base complexation using chiral residues. Yokoyama et al. investigated the effect of the α -substituted chiral side chains on the helical conformation of *N*-substituted poly(*p*-benzamide).¹⁰¹¹ Circular dichroism spectra demonstrated that the poly(*p*-benzamide) has a right-handed helical conformation in protic polar solvents, and a random structure in chloroform, which indicated that solvophobic interactions play a key role in the helical folding of the poly(*p*-benzamide).

The intrinsic chirality of α -amino acids and their HB sites may originate formation of diverse ordered structures beyond molecular-level α -helices or β -sheets to nanoscale chirality, which make chiroptical materials available.⁹⁹⁴ An artificial chiral self-assembly comprising multiple species, which are combined by noncovalent forces, may be challenging to produce.¹⁰¹² Feng and co-authors

explored the influence of bipyridine in tuning the supramolecular chirality of terephthalic phenylalanine derivatives.¹⁰¹³ Liu and co-authors reported a pyrimidine/aryl amino acid HB co-assembly featured by chiral nanostructures and chiroptical properties.¹⁰¹⁴ Recently, Xing et al. observed that in the solid state, alanine and phenylglycine decorated with pyrene segments (PA and PP, respectively) (Figure 81a) self-assembled into a helix-like structures by asymmetrical HBs between carboxylic acid and amide segments (Figure 81b), further inducing supramolecular tilted chirality of the achiral pyrenes.¹⁰¹⁵ Incorporating melamine into the co-assemblies inverted the supramolecular handedness of the aryl amino acids (Figure 81c), resulting in inversion of the handedness of circularly polarized luminescence (CPL). Melamine induced chirality at the nanoscale, generating one-dimensional (1D) helical nanostructures. The introduction of 7,7,8,8-tetracyanoquinodimethane, which is an electron-deficient molecule that forms charge-transfer complexes with pyrene segments, showed the selectivity in the ternary co-assembly towards the amino acids, thus only PP co-assembled with melamine and 7,7,8,8-tetracyanoquinodimethane synergistically, whereas PA adopted binary co-assembly with melamine (Figure 81d).

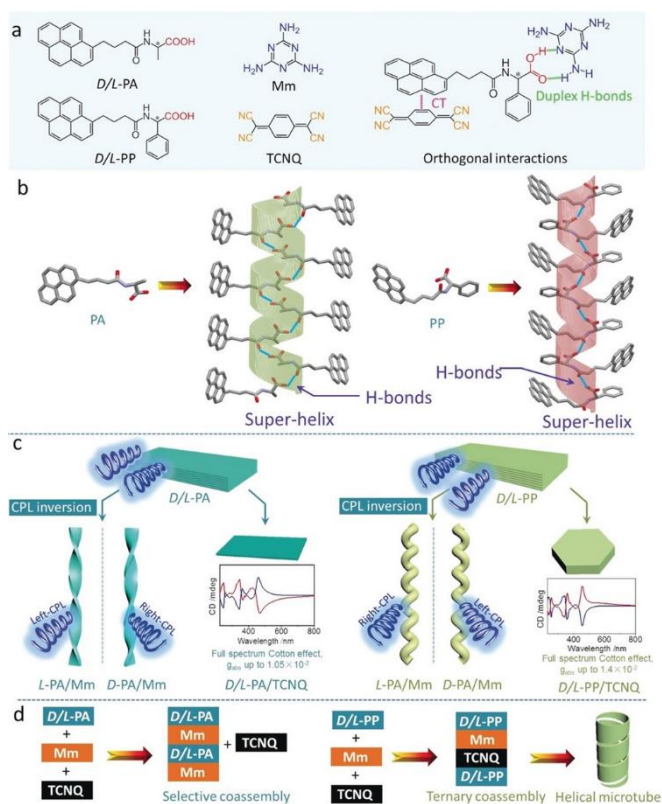


Figure 81. a) Chemical structures of building units and their orthogonal interactions; b) self-assembled helical-structure formation at the molecular-level and nanoscale; c) evolution of self-assembly with various components, as well as their chiroptical responses and supramolecular handedness; d) ternary co-assembly. Reproduced with permission from ref. 1015. Copyright 2020 John Wiley and Sons.

Approaches based on induced chirality have been also exploited for synthesizing homochiral MOFs. Zaworotko and co-authors synthesized Λ -CMOF-5 and Δ -CMOF-5 as chiral variants of MOF-5, ($\text{Zn}_4\text{O}(\text{1,4-benzenedicarboxylic acid})_3$), by preparing MOF-5 in the presence of L- or D-proline, inducing chirality and enabling the growth and isolation of CMOF-5 crystals consisting of helix assemblies (Figure 82).¹⁰¹⁶ An achiral square grid net, [$\text{Zn}(\text{BDC})(\text{NMP})$], forms in the absence of proline. CMOF-5 undergoes a reversible single crystal-to-single crystal phase change to MOF-5 when immersed in organic solvents, while NMP does not induce loss of chirality. In turn, MOF-5 undergoes chiral induction when immersed in NMP, affording racemic conglomerate of CMOF-5.

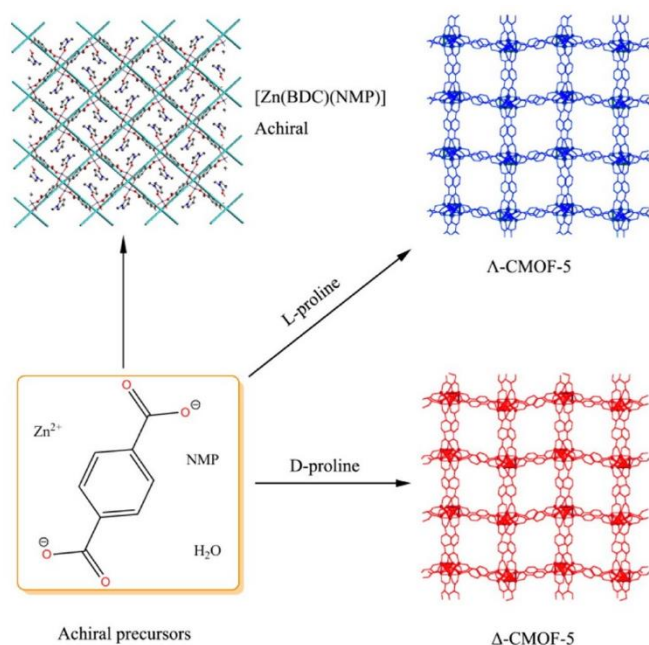


Figure 82. Synthesis of CMOF-5. The presence of L- or D-proline additives induces chirality and enables the growth and isolation of CMOF-5 crystals. An achiral square grid net, [$\text{Zn}(\text{1,4-benzenedicarboxylic acid})(\text{NMP})$], forms in the absence of proline. Reproduced with permission from ref. 1016. Copyright 2015 American Chemical Society.

More recently, Chen, Hong, et al. described that while assembling achiral H_3BTB [BTB = Benzene-1,3,5-tris(4-benzoic acid)] ligands and $\text{Zn}^{\text{II}}/\text{Cd}^{\text{II}}$ clusters leads to a 2D coordination polymer, introduction of pyridine into such assembly system leads to a 3D chiral MOF (M) or (P) (Figure 83).¹⁰¹⁷

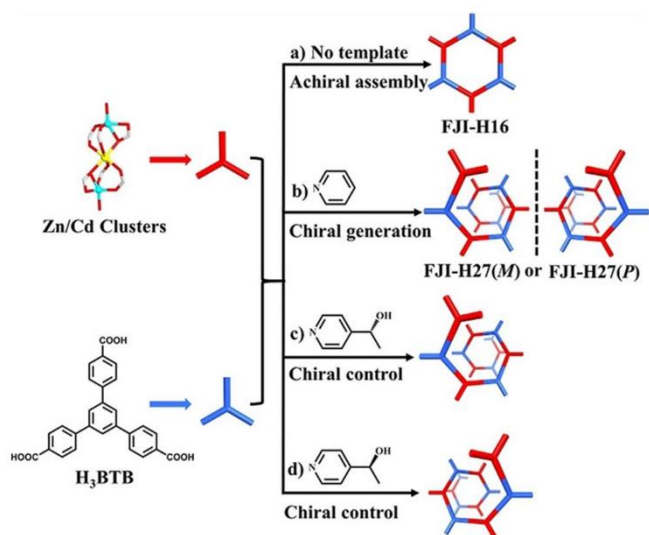


Figure 83. Chiral induction from achiral precursors through template driven self-assembly process: a) achiral self-assembly without template; b) pyridine driven generation of chirality; c), d) controlling chiral orientation and distribution of bulk samples through targeted modification on pyridine. Adapted with permission from ref. 1017. Copyright 2021 John Wiley and Sons.

4.7 Symmetry-breaking and absolute asymmetric synthesis

Spontaneous achiral-to-chiral transformations are mainly related to conglomerate crystallization, Viedma deracemization, supramolecular aggregation of achiral units, induced chirality by adsorption of achiral molecules on surfaces, and the Soai reaction.³⁵ The autocatalytic Soai reaction represents the demonstration of enantioselective autocatalysis able to yield spontaneous mirror symmetry breaking in a homogeneous reaction system. In this process, the authors showed that a chiral product can act as a chiral catalyst for its own formation in the alkylation of pyrimidinyl aldehydes with diisopropyl zinc, where the chiral pyrimidine alkanol accelerates its own formation and promotes the prevalence of its own configuration.^{33,35,1018,1019} In contrast to classical asymmetric synthesis based on the use of chiral starting materials and catalysts, absolute asymmetric synthesis may be based on induced chirality when chiral products crystallize enantioselectively. In this method, in absence of any external asymmetric source, a chiral compound having a chiral center is obtained from a prochiral substrate, and a dynamic preferential crystallization (subsection 4.4.2), along with the racemization of the new chiral center, is performed continuously producing the crystal of the product with high enantiomeric purity. In the last few years, this approach has been applied to diverse reaction systems.^{30,1020-1023} Absolute asymmetric synthesis has been reported to be also promoted by physical chiral forces such as circularly polarized light and chiral magnetic fields.^{35,239,914,1024,1025} Very recently, Sakamoto et al. have performed chiral symmetry breaking from a racemate using optical vortices with orbital angular momentum and a helical wavefront.¹⁰²⁶ This methodology of asymmetric transformation originates by the combination of enantioselective crystal nucleation by

irradiation with optical vortices, and crystallization-induced dynamic optical resolution of conglomerate crystals. Chiral vortices generated using a spiral phase plate with a 532 nm continuous wave-laser were used to irradiate a supersaturated solution of a racemic isoindolinone, leading to crystal nucleation. The handedness of the final crystals was controlled by the winding direction of the chiral optical vortices. Li, Qiu, and co-authors reported an enantioselective porous graphene membrane by mechanical stirring, the front and back of the membrane displaying mirror-image circular dichroism signals.^{1027,1028} The method was presented as advantageous compared to conventional graphene-based membranes *a)* for membrane preparation, given that the chiral environment was provided by simply stirring and no chirality source was needed in the graphene materials, *b)* because chiral induction could be modulated by controlling the mechanical stirring, and *c)* because porous graphene, with stable pores, could be generated in a one-pot process and easily immobilized on the membrane for successful enantioselective separation of racemic amino acids.

In the field of induced chirality, adsorption and organization of intrinsically chiral or prochiral molecules on achiral or chiral surfaces represent hot-topics.¹⁰²⁹ When racemic or achiral molecules form chiral adsorbates, local mirror symmetry breaking in their assemblies may be observed provided that two-dimensional (2D) conglomerates, homochiral clusters, or mirror-related structures are spontaneously formed. For instance, achiral flat molecules may form chiral adsorbates through adsorption on a solid surface. In this regard, Jelínek, Starý et al. showed the enantiofacial adsorption of flat prochiral molecules on an achiral metal surface, this process generating enantioenriched adsorbates (through path A, Figure 84).¹⁰³⁰ This result could be possible due to the chirality transmission from the homochiral helical precursor to the enantiofacially adsorbed prochiral molecules, through on-surface transformations. Otherwise, the formation of enantioenriched adsorbates was not achievable through direct adsorption on the achiral surface (path B, Figure 84). As depicted in Figure 84, while the chiral adsorbates could be formed at temperature T_1 , at temperature $T_2 > T_1$ racemization of the originally homochiral adsorbates took place and the transferred chirality was lost.

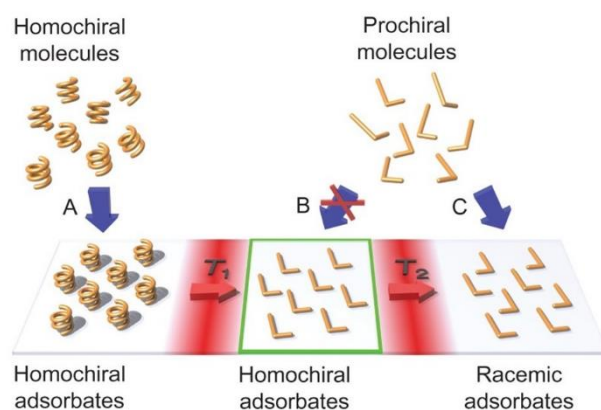


Figure 84. Path A: the vacuum deposition of homochiral molecules (represented here by helices of the same handedness) onto an achiral substrate provides homochiral adsorbates; path B: the vacuum deposition of prochiral molecules (represented here by L-shaped objects) onto an achiral substrate does not lead to homochiral (or enantioenriched) adsorbates as spontaneous global mirror-symmetry breaking is disfavored; path C: vacuum deposition of prochiral molecules onto an achiral substrate delivers racemic adsorbates. Reproduced with permission from ref. 1030. Copyright 2017 Nature Publishing.

Very recently, Zhao et al. reported induced molecular chirality from an achiral stilbazolium dye by encapsulating the dye molecule in the chiral channel of a homochiral Tb^{3+} -containing MOF.¹⁰³¹ In the chiral channel, the *P*- or *M*-enantiomers of the dye was generated through a confinement effect of the MOF, and stabilized by the water molecules in the channel. The induced chirality of the stilbazolium dye was characterized by solid-state CPL. Host-guest interactions between of a polyoxometalate cluster $\text{PMo}_{12}\text{O}_{40}^{3-}$ and CD molecules were found to be involved in the induction of chirality of the inorganic guest (Figure 85).¹⁰³² In this case, the noncovalent inclusion occurring at the primary hydroxyl side of CDs was shown to be a critical factor in modulating the induced chirality. Interestingly, induced chirality reversal could be generated by modulating opening size or adding a competitive guest such as 1-adamantane carboxylic acid (ADCOOH). Host-guest complexation was found to also originate induction of chirality of pillararene host with amplification of chirality to detect cryptochiral compounds.¹⁰³³ Based on this result and computational studies, it was proposed that the guest molecule induces the chirality of pillararene via a chiral match/mismatch effect and causes the amplification of the circular dichroism signals, the extent of the amplification depending on the host-guest interaction affinity.

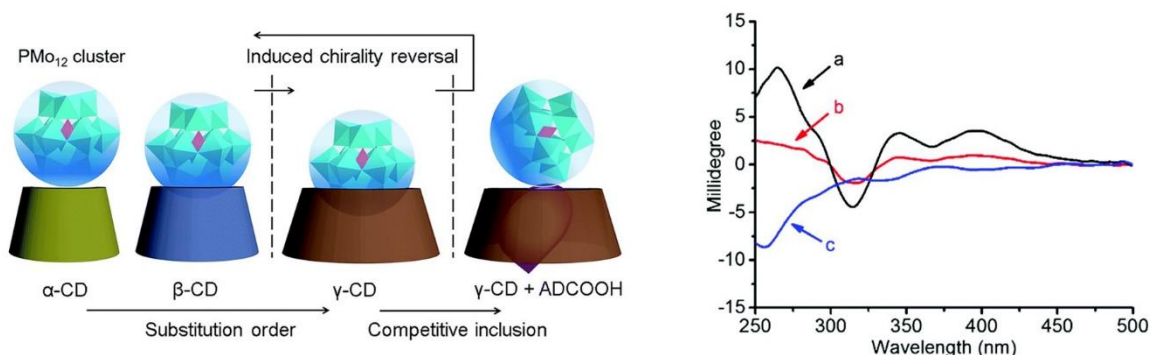


Figure 85. Schematic illustration of the positions of PMo_{12} cluster close to the cavity openings of α -, β - and γ -CD (left) (ADCOOH = 1-adamantane carboxylic acid). The dashed lines indicate the reversals of the induced chirality referring to the position changes. Circular dichroism spectra of PMo_{12} (right) mixing with (a) α -CD, (b) β -CD, and (c) γ -CD in aqueous solution at room temperature. Reproduced with permission from ref. 1032. Copyright 2018 Royal Society of Chemistry.

The chiralization of surfaces through chirality induced by adsorption on the surface itself is an active area with growing applicative perspective for enantioselection. When achiral gas-phase molecules exhibit chirality induced upon adsorption on a surface, these modified surfaces may show enhanced enantioselective adsorption capability. In the last decade, the interaction between the intrinsically chiral propylene oxide and propene, which is made chiral through adsorption on Pt(111)^{1034,1035} and Cu(111)¹⁰³⁶ surfaces, have been explored through scanning tunneling microscopy and DFT calculations, given that the small size of the system allowed to calculate the energies of the interacting systems and evaluate the nature of the interaction modes. More recently, Kurata and Yoshizawa have showed that chirality could be transferred to a polymer film during the polymerization process of achiral reactive monomers on the surface.¹⁰³⁷

Nanoconfinement strategies have been shown to significantly impact chiral induction. De Feyter et al. created and used nanocorrals by scanning probe lithography on covalently modified graphite surfaces to induce chirality in the enantiomorphic assembly of a prochiral molecule at the liquid/graphite interface.¹⁰³⁸ By controlling the orientation of the nanocorrals with respect to the underlying graphite surface, the nanocorral handedness could be chosen, the chiral bias in molecular self-assembly being created at an achiral surface solely by the scanning probe lithography process. Recently, the same group have shown the enantioselective adsorption from a solution of a racemate of chiral molecules in chiral lateral nanoconfinement at the solid/liquid interface.¹⁰³⁹ In this case, chiral symmetry breaking was achieved by the combination of surface symmetry and additional lateral geometric confinement during nucleation, and one enantiomer could be selected simply by choosing the relative orientation between the (achiral) substrate and the square-shaped region where monolayer growth was nanoconfined. Thus, the spatial confinement alone could provide chiral symmetry breaking to achieve enantioseparation in the assembly of chiral molecules based on the following key stages, *a*) the nucleation stage in which the enantioselection takes place, and *b*) the growth from the chiral seed. Given the selective domain adsorption in nanocorrals,¹⁰⁴⁰ the requirements for enantioselective adsorption in nanocorrals were envisaged in the following properties, *a*) anisotropy in the interactions along the unit cell vectors of the self-assembled molecular networks, and *b*) conglomerate formation with different angles of the two enantiomorphs with respect to the underlying graphite lattice.

Noncovalent interactions are an essential tool in designing heterogeneous enantiospecific (and enantioselective) interfaces. In this perspective, HB and π - π interactions play the major role, however other interactions have been considered for the purpose. For instance, Miao, Deng et al. observed the pivotal role of XB in self-assembly of an iodine substituted thienophenanthrene derivative at the 1-octanic acid/graphite interface, identifying three concentration-dependent chiral arrangements and

transitions of 2D molecular assembly:¹⁰⁴¹ *a*) at high concentration the molecules self-assembled into a honeycomb-like chiral network sustained by vdW forces and intermolecular C=O⋯I⋯S XBs; *b*) at moderate concentration, a chiral kite-like nanoarchitecture was observed, which was underlain by the C=O⋯I⋯S and I⋯O=C XBs, and molecule–solvent C=O⋯I⋯H XBs; *c*) at low concentration, the molecules formed a chiral cyclic network originating from the solvent co-adsorption through molecule–molecule C=O⋯I⋯S XBs and molecule–solvent C=O⋯I⋯H XBs.

The chromatographic counterpart of SIRE (subsection 4.5.2), the phenomenon of self-association of enantiomers also underlies self-disproportionation of enantiomers (SDE), yielding fractions of a nonracemic sample enriched and/or depleted in one of the constituent enantiomers under achiral chromatographic conditions.¹⁰⁴²⁻¹⁰⁴⁴ In particular, Soloshonok et al. demonstrated by achiral HPLC that, for a wide range of fluorinated compounds, a CF₃ group attached to a stereogenic carbon strongly promotes self-association.¹⁰⁴⁵ The heteroenantiomeric associates were supposed to be linear oligomers, with the CF₃ groups pointing away from one another to minimize their electrostatic repulsive interactions. Otherwise, steric repulsion between these electronegative groups leads to lower aggregation numbers in the corresponding homoenantiomeric associates. Klika and co-authors explored the molecular basis of molecular self-associations in SDE by NMR spectroscopy and molecular modelling.¹⁰⁴⁶⁻¹⁰⁴⁸

5. Trends in enantioselective recognition in separation science: chromatographic methods

5.1 Major instrumental techniques applied to separation of enantiomers

Just very few, more or less successful, attempts for separation enantiomers have been described in the literature until 1960s.^{88,154-156,1049,1050} Henderson and Rule were the first who, in 1939, reported partial separation of enantiomers on the column packed with the disaccharide lactose.¹⁵⁴ Later, the same lactose was used by Prelog and Wieland to prove the asymmetry of 3-valence nitrogen by separation of the enantiomers of Tröger's base.¹⁵⁵ The planar (paper) chromatography was used for separation of enantiomers by Kotake et al. in 1951.¹⁵⁶ This was the first case of using cellulose-based material as a CS. The article by Dalglish in which he postulated his three-point interaction model in analogy to substrate-enzyme complexes was published in 1952.⁸⁸ The underivatized (native) cellulose was also used for separation of enantiomers of chiral catechins in early 1960s.¹⁰⁴⁹ An amylose-containing natural material was used for partial separation of various racemates by Krebs et al. in the study published in 1956.¹⁰⁵⁰ These studies indicated that the enantiomers could, in principle, be separated based on the chromatographic approach. However, the skepticism was still big in 1960s about realizing this by instrumental techniques such as gas chromatography (GC) or HPLC, as clearly expressed by Gil-Av: "*When we started this work in 1964, this topic was in a "state of frustration". Nobody believed that it could be done. In fact, people were convinced that there could not possibly*

*be a large enough difference in the interaction between the D- and L solute with an asymmetric solvent. This was the feeling people had, even those known as unorthodox thinkers. This view had also some experimental basis, because a number of communications had been published, in which it was claimed that such resolutions could be effected, but nobody was able to reproduce these results, and some of them were shown to be definitely wrong”.*¹⁰⁵¹ Later, experimental, technological, and theoretical advancements fully demonstrated the huge potential of chromatographic technologies for the direct separation of enantiomers.

In direct enantioseparation, the absence of irreversible chemical reactions or phase transitions favors the application of this approach also for preparative purposes, since no efforts are required for releasing of the resolved enantiomers from the transient diastereomeric molecular entities formed in the separation process. Otherwise, indirect methods to separate enantiomers require the formation of a covalent linkage between a chiral auxiliary and the chiral analyte, further separation of formed diastereomeric compounds on achiral adsorbents, and a final reaction step to remove the chiral auxiliary and restore the analyte in its enantiomerically enriched or pure form.

Since 1980s, series of books have been published covering multiple aspects of enantioseparations.^{53,56,1052-1054} In addition, many published review papers and books deal with various specific topics in this field. These include separation of enantiomers in various techniques such as GC,^{1055,1056} HPLC,^{1057,1058} SFC,¹⁰⁵⁹ capillary electrophoresis (CE),^{55,1060,1061} capillary electrochromatography (CEC)¹⁰⁶² and microchip-based platforms.¹⁰⁶³ Another set of review papers are dealing with specific type of CSs such as polysaccharide derivatives,^{50,51} glycopeptide antibiotics,¹⁰⁶⁴⁻¹⁰⁶⁶ CDs,¹⁰⁶⁷⁻¹⁰⁷⁰ Pirkle-type,¹⁰⁷¹ chiral ion-exchangers,¹⁰⁷² and MOFs.^{185,319,833} One more group of review papers deals with high resolution and fast separations,^{1073,1074} chiral recognition mechanisms,^{54,55,1075-1077} and molecular modelling.^{57,58,59,565,1078-1080} There are also review papers published on various aspects of application of enantioseparations, in particular about preparative and product scale separations,¹⁰⁸¹⁻¹⁰⁸⁶ enantioselective pharmaceutical,¹⁰⁸⁷⁻¹⁰⁸⁹ biomedical,^{52,1090-1092} environmental,^{1093,1094} food and beverage analysis.¹⁰⁹⁵ The narrative thread of all above mentioned methods, techniques, and applications is that they are all based on the enantioselective noncovalent interaction between two counterparts of which one is called analyte, selectand, guest, or ligand, and the other one selector, host, or receptor. In brief, noncovalent interactions are the key tool underlying all direct approach to separate enantiomers. Despite that, separation techniques have been often overviewed with a slight emphasis on the noncovalent interactions considered by the inventors and developers of various CSs. On this basis, the aim of this section is not a detailed overview of various enantioseparation techniques as summarized in the list of contents (this has been done in various excellent review papers cited above). Rather, for a better understanding of the chromatographic

enantioseparation at molecular level, trends of chromatographic techniques, various groups of CSs, and enantioseparation medium, are discussed herein by focusing on noncovalent interactions and mechanisms involved in chromatographic enantioseparations and underlying the enantioseparation outcome. The evolution of the chromatographic technologies is also briefly described, with the aim to highlight the technological bases allowing noncovalent interactivity to act in chromatographic terms. Therefore, a complete and updated summary of enantioseparation techniques, or the aspects not directly related to noncovalent selector-selectand interactions (for instance, preparative scale separations, fast separations, etc.), are not the subjects of this section. On the other hand, a general overview of noncovalent interactions is not a direct goal of this text. The aim is viewing noncovalent interactions as a fundamental basis on the molecular level leading to enantioseparations on the macroscopic level. Thus, this section attempts to answer the following questions: 1) How well does current theory classify, differentiate and describe noncovalent interactions involved in molecular recognition responsible among other effects also for enantioseparations in various techniques? 2) How precise can we measure experimentally or compute (theoretically) noncovalent interactions involved in molecular recognition? 3) Is it possible based on the current state of our knowledge about noncovalent interactions, and experimental and theoretical tools available, to at least unambiguously explain, or in the best case predict, enantioseparations we observe experimentally? 4) How can the state of the art enantioseparation processes contribute to the further advancement and refining of theoretical and experimental tools used for describing noncovalent interaction?

The non-chromatographic separation processes shortly described in Section 4 are also based on enantioselective noncovalent interactions between two counterparts, similar to separation processes described in this section. However, there is a major difference between the techniques discussed in sections 4 and 5. This conceptual difference has been highlighted in earlier literature.^{1096,1097} As Davankov stated, the matter is that the chemical transformation or phase transition are “one-step” processes, whereas chromatography is a “multistep” separation method. This means that in instrumental enantioseparation techniques, such as GC, HPLC, SFC, CE and CEC the overall resolution of the solutes originates from a large number of stereoselective “one-step” adsorption-desorption cycles. The cumulative nature of the chromatographic separation is the reason that a free energy difference in interactions of enantiomers with CSs as small as 0.025 kJ/mol may in principle be sufficient for baseline chromatographic enantioseparations, whereas the free energy difference required in “one-step” techniques is several orders higher.¹⁰⁹⁶ This may allow some parallels with noncovalent interactions which may be rather weak individually (as a single interaction), but lead to big (sometimes huge) effects due to their multiplicity (high number of interactions of a given type), as well as multimodality. The chromatographic separation is a time-dependent process because it is

achieved by simultaneous action of multiple noncovalent interactions occurring in the course of the separation process which evolves in time. Several kinds of noncovalent interactions can be engaged in a single adsorption-desorption step, but the major result is achieved due to cumulative repetition of these steps for a certain period of time (defined, for a generic compound “i”, as *retention* and *migration time*, t_i , in chromatography and electromigration techniques, respectively).

The non-chromatographic separation techniques used sometimes for enantiomeric excess determination, such as sensors or NMR spectroscopy are also of non-accumulative nature. These techniques are based on real equilibrium in the system, while in separation science one deals basically with pseudo-equilibria. In theory, due to their cumulative nature, chromatographic separation methods can be more sensitive for detection of weak noncovalent interactions compared to non-chromatographic separation methods. Given the relationship between a chromatographic process and involved noncovalent interactions, useful information may be obtained from the peak parameters (Figure 86): *a) retention factor* (k), a measure of the time which each enantiomer interacts with the CSP, give t_0 as the retention time of a standard non-retained compound (*dead time* or *holdup time*), *b) separation selectivity*, or *selectivity factor* (α), a measure of the retention shift of the second eluted enantiomer compared to the first one, as well as *c) their temperature dependences*.

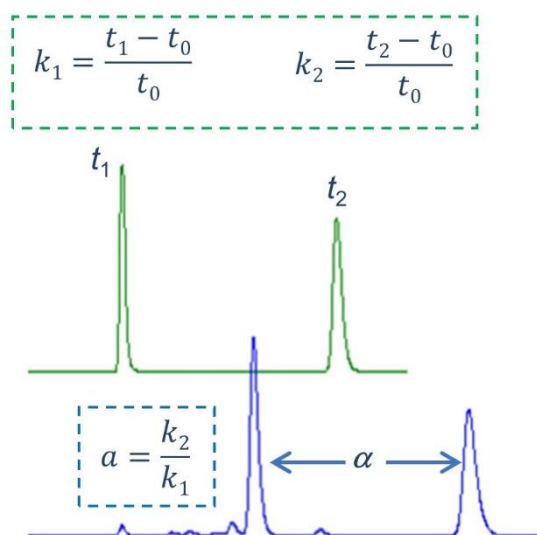


Figure 86. Definition of chromatographic parameters: t_0 , retention time of a standard non-retained compound; t_1 , retention time of the first eluted enantiomer; t_2 , retention time of the first eluted enantiomer; k_1 , retention factor of the first eluted enantiomer; k_2 , retention time of the first elute enantiomer; α , selectivity factor.

These are all macroscopic expressions of the thermodynamics of the process, in other words a sign of noncovalent interactions occurring at molecular level between selector and selectand.

5.1.1 Gas chromatography

In 1966, the very first separation of enantiomers by instrumental techniques was reported in GC by Gil-Av and co-workers.¹⁰⁹⁸ The authors performed the separation of racemic *N*-trifluoroacetyl amino acid alkyl esters on glass capillary columns coated with *N*-trifluoroacetyl L-isoleucine lauryl ester, these enantioseparations being driven by HBs. In this seminal study, the authors recognized that, due to small free energy differences between the noncovalent diastereomeric selectand-selector associates responsible for separation of enantiomers, high efficiency of the separation system was a prerequisite for observing enantioseparation. Therefore, they used capillary GC columns instead of packed columns, as well as selector-selectand pairs which were selected very carefully. The authors noticed that “*The possibility of hydrogen bonding and, in an intuitive way, the remote resemblance of the solute-solvent system to a peptide-enzyme complex, determined the choice of these compounds*”.¹⁰⁹⁸ It is very indicative that careful consideration of noncovalent interactions, specifically HB, became the basis of the success in this pioneering study. This short paper contains at least two other statements which are still actual today. One is about the structural resemblance required for successful enantioselective recognition saying that “*the choice of solute-solvent systems should be made preferentially in a way such that multipoint interactions could take place in the neighbourhood of the asymmetric centers*”.¹⁰⁹⁸ Another interesting statement is that “*The columns described should have interesting analytical applications and might also serve as a tool for the study of stereospecific interactions*”.¹⁰⁹⁸ This last passage clearly states that not only the theory of noncovalent interactions has to be used to explain the observations in enantioselective chromatography but also, *vice versa*, enantioselective chromatography can provide solid real-life experimental results as a basis to tune and refine methods and techniques developed in the domain of theoretical, physical and computational chemistry. Indeed, two main problems are observed in the current literature: *a*) theoretical chemists not always confirm experimentally structures, energies and affinities computed for large systems. Regrettably, this aspect weakens reliability and strength of theoretical approaches which lacks critical evaluation and validation, and gets accepted as it is, slowing down the refining of these approaches; *b*) the accessibility of more friendly computational resources makes computational treatment of molecular systems accessible beyond the domains of theoretical science. As we have already mentioned in section 3, this may be a positive factor for the community of scientists. Nevertheless, scientific “experimental” papers in the field of enantioselective chromatography gets often “diluted” with unreliable computational results. This serious flaw also affects other experimental domain, as recently stressed by Clark et al.: “*I think that the danger is that including calculations (mostly DFT) in good experimental manuscripts is becoming a requirement without the calculations adding anything real to the paper*”.⁴⁶¹

The important advantage of chiral GC over chiral HPLC is the faster diffusion in the gas phase compared to liquid phase mass transfer and, consequently, the plate numbers are commonly higher in GC compared to HPLC separations. This makes possible baseline separation of two enantiomers in GC, with well-prepared columns, even in the case of thermodynamic selectivity of recognition in the range of 1.05-1.10. The difference of free enthalpy (Gibbs free energy) of diastereomeric associates corresponding to the abovementioned thermodynamic selectivity of recognition at 298 K is in the range 0.1208-0.2360 kJ/mol. Otherwise, the thermodynamic selectivity required for baseline separation of two enantiomers with standard well-packed HPLC column commonly exceeds 1.10. It has to be mentioned that some recently developed chiral HPLC columns based on superficially porous and small silica particles bring the column performance in GC and HPLC closer to each other.

As a gas-phase separation technique, chiral GC is mostly used for separation of volatile and thermostable chiral compounds such as essential oils and other volatile natural compounds, flavors, pheromones, fragrances, food additives and few pharmaceutical gases (mostly anesthetics). However, for analysis of these groups of compounds chiral GC cannot be replaced with any other techniques since gaseous samples are not compatible with liquid-phase separation techniques.

At molecular level, direct GC separation of enantiomers requires the rapid and reversible noncovalent intermolecular interaction between the nonracemic chiral stationary phase (selector) and the racemic (or enantiomerically enriched) analyte (selectand). In principle, any chiral compound with an ability to interact noncovalently and enantioselectively with chiral molecules may be used, with more or less success, as CSs in chromatographic enantioseparation techniques. However, there is a set of requirements which a CS has to meet depending on the goal of the separation, as well as the mode and technique used.

The main CSs used in capillary GC columns are amino acid derivatives, chiral metal complexes, and CDs.^{1055,1056} CDs and their derivatives dominate at present as CSs in GC enantioseparations. These CSPs are thermally stable, widely applicable and easy to use.^{1055,1056,1067} New chiral stationary phases for GC, some of which are not yet commercially available, are summarized in recent book chapter by Armstrong and co-authors¹⁰⁵⁶ and in the review paper by Yuan and co-authors.¹⁰⁹⁹ To these groups belong cyclofructan (CF)-based CSPs,^{1056,1099,1100} chiral MOFs,^{1056,1099,1101} POCs^{1056,1099,1102,1103} and chiral ionic liquids.^{1056,1104}

From a mechanistic point of view, it is worth noting that the approach of increasing selector-selectand interactivity by constraining the enantiomers into a confined space (chiral groove, hole-shaped host, chiral cleft, chiral pores), in order to enhance the efficacy of noncovalent interactions, is a rather general approach which, going beyond GC domain and the most recent chemistry of porous materials, also dominates the chemistry of many CSs used in enantioselective chromatography and

in other field of enantiorecognition. For instance, in the GC environment CDs were found to recognize enantiomers through multiple interactions involving inclusion complex formation, dependent on size and shape of the analyte, HBs, dipole-dipole, dispersive, vdW, and steric interactions.¹¹⁰⁵ Most studies reported the impact of derivatization of macrocycle hydroxyls on retention and selectivity compared to the native macrocycles (Figure 87a-c).¹¹⁰⁶⁻¹¹⁰⁸ König et al. showed that the steric effects of the functional groups bearing by the macrocycle play an important role in separations.¹¹⁰⁹ For instance, the derivatization of 6-OH group by bulky substituents may hinder the inclusion interactions and decrease chiral selectivity. Armstrong et al. observed that GC chiral separations can involve either inclusion complexation or external surface interactions.¹¹⁰⁵ The same group compared the enantiorecognition ability of 2,6-di-*O*-pentyl and 2,6-di-*O*-pentyl-3-trifluoroacetyl CDs, showing that the latter had broader enantioselectivity. In this case, the enantioselectivity was improved by increasing dipole–dipole interactions through the introduction of the trifluoroacetyl group in the macrocycle, although the strength of HB interactions was diluted.¹¹¹⁰ CFs consist of 6-8 fructose units connected by β -(1,2) linkages (Figure 87d), differently compared to CDs, their crown ether core is not directly involved in the separation mechanism for most of the analytes. The effect of this feature is a limited enantioselectivity of both per-*O*-methylated CF6 and CF7 compared to α - and β -CDs.¹¹⁰⁰ The accessibility of the central core is reduced due to the intramolecular HBs of 3-OH groups blocking the crown ether core, which can be made accessible by the methylation of these hydroxyl groups. Armstrong et al improved the enantioselectivity of the CF-based CSPs by synthesizing 4,6-di-*O*-pentyl-3-*O*-trifluoroacetyl- (DP-TA-CF6) and 4,6-di-*O*-pentyl-3-*O*-propionyl-CF6. All the hydroxyl groups in both CSs are derivatized and, consequently, the two selectors can only act as HB acceptors. Given the electron-withdrawing character of the trifluoroacetyl moiety, DP-TA-CF6 showed lower retention factors for analytes with HB donating groups and higher retention factors for analytes with permanent dipole moments as compared to DP-PN-CF6.¹¹¹¹

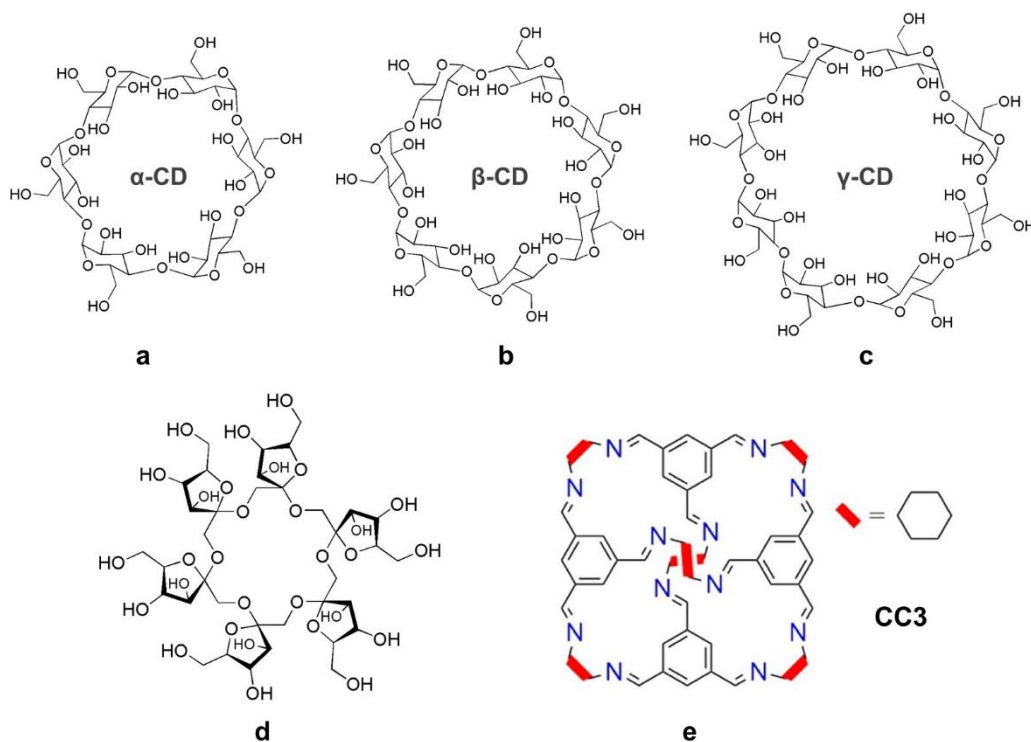


Figure 87. Structures of α - (a), β - (b), and γ -CDs (c), of CF6 (d), and CC3 homochiral POC (e).

In the case of homochiral porous materials such as MOFs and POCs,^{828,1112} the high-ordered pore architecture, ultrahigh specific surface area and well-defined pore size of these materials contribute to the confinement effect and host–guest interaction between enantiomers and chiral pockets of the homochiral material.⁸²⁸ Given the porous structure, the steric hindrance of the analytes has a pivotal role on the separation outcome. Thus, despite the fact that the chirality of the porous framework obviously assists the separation mechanism, the most dominant factor tends to be the perfect match between the guest analyte and the framework size and shape.¹¹¹³ Computational studies supported this model.¹¹¹⁴⁻¹¹¹⁶ On the other hand, if no stereoselective interactions between host and guest are observed, the homochiral framework may adsorb both the enantiomers equally, which in turn, results in no enantioselectivity. Thus, the design of specific interactions proved to improve enantioselectivity. For instance, in 2015 Cooper et al. applied homochiral CC3 (Figure 87e) as CSP in a capillary column for enantioselective GC which exhibited baseline separation toward different chiral molecules.¹¹⁰² Yuan et al. demonstrated that a CC3 packed GC column has good chiral resolution capacity for a wide range of chiral compounds such as alcohols, amines, esters, organic acids, and sulfoxides.¹¹¹⁷ Very recently, Yang et al. proved that the incorporation of hydroxyl groups into the homochiral CC3 nanopores enhanced the HB capability of the material, improving resolution of the chiral alcohols.¹¹¹⁸

In early days of enantioselective GC, all selectors were used as involatile liquids or dissolved in squalane or polysiloxane. Later, the technology was developed for chemically linking selectors to polysiloxanes (Chirasil type stationary phases). The same approach was applied later to complexation GC by the synthesis of Chirasil-Metal and to inclusion GC by the synthesis of Chirasil-Dex. Such combination of CS and polymers offers a combination of the chemical affinity of the selector with the unique coating properties and thermal stability of polysiloxanes, providing capillary columns with high efficiency and extended range of operating temperatures.¹⁰⁵⁶

After the first study of Gil-Av in 1966,¹⁰⁹⁸ several more universal HB CS were developed, and one of them was coupled by Bayer and co-workers to a dimethylsiloxane and (2-carboxypropyl)methylsiloxane copolymers with suitable viscosity to yield currently commercially available Chirasil-Val chiral GC capillary column. The amino function was used for a covalent linkage.¹¹¹⁹ Chirasil-Val exhibits broad separation ability for enantiomers of chiral compounds able to form HB. Commercially availability of the chiral GC columns based on this CS in both enantiomeric forms enables predictable adjustment of enantiomer elution order (EEO). This is a significant advantage. Alternative strategy for synthesis of polymeric CSPs suitable for GC applications is the covalent attachment of CS to commercially available polysiloxanes containing reactive pendant groups (for instance XE-60 or OV-225). This strategy was employed by Sandra and co-workers for linking the diamide CSs to a modified polysiloxane,¹¹²⁰ as well as by König and Benecke¹¹²¹ to develop useful CSPs for GC. Enantiomer separations which are performed by using CSPs containing strong HB donors and acceptors is commonly based on derivatization of the analyte in a way that improves its volatility, as well as its ability to participate in HB-type interactions with a CS. Useful reagents for this purpose are isocyanates and phosgene.¹⁰⁵⁵

In 1997, Schurig proposed CSPs for GC based on coordination. In particular, he demonstrated a suitability of the dicarbonylrhodium(I)-3-trifluoroacetyl-(1*R*)-camphorate having the ability of metal coordination for the GC enantiomer separation of 3-methylcyclopentene.¹¹²² The same principle was later applied to GC separation of enantiomers of oxygen-, nitrogen- and sulfur-containing compounds. The portfolio of CSs was extended by chiral ketoenolate bis-chelates using several divalent transition metal ions, as central ions, and derivatives from terpene ketones such as camphor, menthone, carvone, pulegone and others, as ligands. Manganese(II)- and nickel(II)-(3-(heptafluorobutanoyl)-(1*R*)-camphorate) established as especially useful CSPs for the separation of enantiomers of underivatized cyclic ethers, esters, acetals, aldehydes, ketones and alcohols. Among these were many chiral compounds having a practical importance, such as pheromones, essential oils, metabolites and products of catalytic asymmetric synthesis. The coordination-based CSPs can be used with the maximal temperatures up to 120 °C. This represents a certain limitation.¹⁰⁵⁵ Later, thermal

stability of this CSPs was improved by combining CS with polymers (for instance, Chirasil-Metal).¹¹²³

Kościelski et al reported the first example of GC enantioseparation on a column packed with cyclodextrin-based CSP. In this pioneering study, the chiral analytes were apolar hydrocarbons α - and β -pinene and *cis*- and *trans*-pinane, and α -CD dissolved in formamide was used as a CS.¹¹²⁴ In few years after this study, the potential of alkylated CDs as powerful CS, especially for highly efficient capillary GC, was recognized. Thus, neat heptakis(2,3,6-tri-O-methyl)- β -CD, per-n-pentylated, 3-acyl-2,6-n-pentylated CDs, and several other per-derivatized CD derivatives were used in the undiluted form for the separation of enantiomers of various classes of chiral compounds on deactivated Pyrex glass capillary columns by König and co-workers.¹¹²⁵ Alternatively, Armstrong and co-workers employed more polar CD derivatives containing hydroxypropyl, free hydroxy or trifluoroacetyl groups, coated on the inner surface of fused-silica capillary columns, as useful CSs for GC.¹¹²⁶ In order to combine the enantioselectivity of CDs with the favorable coating properties and high efficiency of polysiloxanes, Schurig and Nowotny dissolved alkylated CDs in moderately polar silicones such as OV-1701. Thus, the CD derivatives were employed for gas chromatographic enantiomer separations irrespective of their melting points and phase transitions.¹¹²⁷ Chemically linking the CD derivatives to the polysiloxane backbone proved to be a useful extension of this approach.¹¹²⁸ Fused-silica columns obtained by dissolution of CD derivatives in polysiloxans possess following favorable properties: *a*) many of CD derivatives cannot be physically mixed with a non-polar polysiloxane matrix but can be chemically attached to it; *b*) such CSP does not retain polar chiral analytes too strongly and they elute at lower temperature; *c*) such CSP has a high degree of inertness, enabling analyses of polar compounds in underivatized form; *d*) higher content of CS, resulting in increased separation factors; *e*) improved long-term stability and absence of droplet formation leading to breakdown of efficiency; *f*) immobilization by cross-linking and/or surface bonding; *g*) and compatibility with all injection techniques.¹⁰⁵⁵

The immobilization of the resulting stationary phases on the fused-silica surface by thermal treatment made it possible to prepare stationary phase that was quite resistant to bleeding, compatible with solvent intake and insensitive to temperature shock and with an extended working temperature range (10-250 °C).¹¹²⁹ Separation factors achievable for enantiomers with CD-type CSs are generally low, but this feature is compensated by the high efficiency of capillary columns. A disadvantage of CD-based CSs is that they are available only in the all-D form. Thus, designed reversal of EEO by using chiral columns with the same chemical composition, but the opposite stereochemical configuration of CSs, is not possible with CD-type CSPs.

Capillary GC commonly offers higher peak performance compared to HPLC and SFC. This opens a potential not only for successful separation of enantiomers of a given compound, but also for separation of contaminants and impurities, simultaneous separation of stereoisomers of chiral compounds possessing more than one element of chirality, separation of various chiral compounds from each other, and simultaneous enantioseparation of individual components of the mixture (e.g., all of natural amino acids).¹⁰⁵⁵ For some complex samples even such advanced technique may not provide a complete solution. In such cases, two-dimensional achiral-chiral or even chiral-chiral GC combination can be used. Additional possibilities for sample detection, component identification and quantification are offered by various coupling techniques. Two dimensional GC can be performed in two different modes: 1) a “heart-cutting technique” involving the use of an achiral polar column in the first dimension and a chiral column (mainly CD-based) in the second dimension,^{1056,1130} 2) comprehensive 2D-GC (GC × GC) in which, in contrast to the above mentioned modus, the entire sample is subjected to analysis in both dimensions. In GC × GC the chiral column is commonly used in the first dimension and a short achiral column in the second dimension.^{1056,1131-1133} The chiral column can also be used in the second dimension, but the use of a short chiral column in the second dimension limits enantioselectivity and temperature control. Also, the second dimension is limited by the prevailing first dimension conditions.^{1056,1132} The use of chiral (enantioselective) columns in the first or second dimension of GC × GC is abbreviated as eGC × GC and GC × eGC, respectively.^{1056,1132} Both enantioselective GC × GC techniques provide effective results and have pros and cons. The interpretation of the GC × eGC chromatogram is easier, while the experimental setup and operation is less tedious with eGC × GC.^{1056,1134}

Thus, from the analytical point of view, chiral GC can provide very useful information. Some of the applications are described in detail in recent review papers and book chapters on this topic.^{1056,1135}

5.1.2 High-performance liquid chromatography

HPLC is a liquid-phase separation technique and, thus, in contrast to GC, the volatility and thermostability of the analyte are not issues. Many detection techniques are available, and there is almost never a need to derivatize the analytes for their better detectability. One of the advantageous factors of chiral HPLC is the availability of a variety of chiral columns. In addition, the mobile phase (MP), as well as MP additives, represent a powerful tool in the hands of the analyst to adjust and optimize separation selectivity in HPLC. Various modes of HPLC, such as so called normal-phase (NP) and reversed-phase (RP), polar organic (PO), and hydrophilic-interaction chromatography (HILIC), are available and strengthening the applicability of this technique to various groups of chiral

analytes in the different matrices. The versatility of MP function is unique in HPLC, more or less similar in CE and CEC, whereas it is not exploitable in GC and SFC.

HPLC separation of enantiomers can be performed in two basic modes: indirect and direct. The indirect mode involves pre-derivatization of enantiomers with chiral reagents in order to form diastereomeric compounds which, due to difference in their free energy of formation, can be separated without using CS (on achiral column). This separation mode does not involve enantioselective noncovalent selector-selectand interactions and, thus, is not within the scope of the present review. In addition, indirect separation of enantiomers is rarely used due to bottlenecks this mode has, as well as due to rapid advancement of the direct enantioseparation field since the 1980s. Direct separation of enantiomers is based on enantioselective noncovalent selector-selectand interactions. This technique offers high speed, precision and sensitivity. In addition, it can be easily automatized and enables analysis of samples containing together with enantiomers also some other chiral and achiral by-products and impurities. Since HPLC is a liquid-phase technique it enables analysis of non-volatile and thermolabile compounds (to this category belong many chiral drugs, agrochemicals and other biologically active compounds). Many different detection principles, among them universal, as well as specific MS detectors, are compatible with HPLC. Sample derivatization for improving its detectability is very rarely (almost never) required. Variety of CSs available for chiral HPLC is much wider than for GC. This represents a certain advantage of this technique since enantiomers cannot be separated based on one universal type of selector-selectand interactions. Variability of a mobile phase (MP) composition and MP additives is additional tool for fine-tuning separation in HPLC. Separation modes such as so-called normal-phase (NP), reversed-phase (RP), polar organic (PO) and hydrophilic interaction chromatography (HILIC) further strengthen the applicability of this technique to various groups of chiral analytes in the different matrices.

5.1.2.1 Chiral stationary phases

Due to multi-step cumulative nature of chromatography less strict requirements apply in this technique for obtaining appreciable enantioselective recognition ability of CSs compared to one-step processes such as adsorption in batch, extraction, etc. This opens the possibility for effective application of a large number of CSs with relatively low chiral recognition ability in chromatographic techniques. Perhaps this is the most likely reason why several hundreds of CSPs are described in the literature, especially for HPLC. Due to their nature, with chromatographic separation methods it is possible to obtain baseline resolved peaks for enantiomers or, in preparative separations, both enantiomers in the enantiomerically pure form, even when the CS has an enantiomeric purity less than 100%.